

Université du Maine
UFR Sciences

Unité de Chimie Organique Moléculaire et
Macromoléculaire-UMR CNRS 6011
LCOM-Chimie des Polymères

THÈSE DE DOCTORAT DE L'UNIVERSITÉ DU MAINE

Spécialité: Chimie et Physicochimie des Polymères

Présentée par

Chuanpit KHAOKONG

Pour obtenir le grade de

Docteur de l'Université du Maine

**Elaboration of electronic conductor composite materials: study of physical
and electronic properties**

Soutenance prévue le 18 Décembre 2008, devant le jury composé de:

M. J.-P. Bazureau	Professeur à l'Université de Rennes I	Rapporteur
M. J.-P. Couvercelle	Professeur à l'Université de Bourgogne	Rapporteur
M. P. Bertus	Professeur à l'Université du Maine	Examineur
M ^{me} V. Tanrattanakul	Assoc. Professeur à l'Université Prince of Songkla Thaïlande	Examinatrice
M ^{me} I. Campistron	Ingénieur CNRS à l'Université du Maine	Encadrante
M. J.-F. Pilard	Professeur à l'Université du Maine	Directeur
M. A. Laguerre	Maître de Conférences à l'Université du Maine	Encadrant

For my grandparent

For my parent

For my brother and sister

For my teachers

Acknowledgement

This thesis was done at the Laboratoire de Chimie Organique Macromoléculaire (LCOM), UCO2M under financial support of Prince of Songkla University, Thailand, and French government. Taking this opportunity, I would like to express my gratitude to people concerning my work and my life during a few past years.

Firstly, I would like to specially thank to my director of thesis, Pr. Jean-François PILARD, for proposing me this work and also for many useful guidance, invaluable advices, discussions, support and encouragement throughout this research. I would also like to thank Dr. Irène CAMPISTRON, Ingénieur d'Etudes CNRS at Université du Maine and Dr. Albert LAGUERRE, Maître de Conférences at Université du Maine, for their availability, patient, invaluable advice and discussion about the result of experiment and also many help in a personal life, especially in my first year in France. I also thank to Dr. Charles COUGNON, Chargé de Recherches CNRS at Université du Maine, for knowledge about electrochemical experiment, his patient and useful advice.

I would like to express gratefulness to Pr. Jean-Pierre BAZUREAU, Professor at Université de Rennes I, Pr. Jean-Pierre COUVERCELLE, Professor at Université de Bourgogne for acceptation to be member of jury as reporter for my work and participant in my thesis defend.

I would like also give appreciation to Pr. Philippe BERTUS, professor at Université du Maine, and Assoc. Pr. Dr. Varaporn TANRATTANAKUL, Lecturer at Faculty of Sciences, Prince of Songkla University, Thailand, for their kindness acceptation to be member of jury in my thesis defend.

I would like also to thank to Dr. Mohamed TABELLOUT, Maître de Conférences at Laboratoire de Physique de l'Etat Condensé (LPEC), Université du Maine and his PhD student, Christele VANGA BOUNGA, for many samples in conductivity measurement. I would like to thank as well Dr. Christian LAUNAY, Maître de Conférences at LPEC, Université du Maine for the thickness measurement of the thin film.

I would like to deeply thank to Pr. Jean-Claude BROSSE, Professor Emérite, who organized the corporation between Thailand and France. He made me interested in the chemical modification of natural rubber by his lecture and gave me the guideline to study in this university. I also thank as well for his kindness.

Acknowledgement

I would like also to give thanks to Dr. Frédéric GOHIER, Maître de Conférences, for his availability, suggestions about organic synthesis and column chromatography.

I would like to thank also to Pr. Laurent FONTAINE, professor of Université du Maine and director of UCO2M, Dr. Daniel DEROUET, Ingénieur de Recherches CNRS, Dr. Jean-Claude SOUTIF, Ingénieur de Recherche, and Dr. Véronique Montembault, Maître de Conférence, Dr. Micheal THOMAS, Ingénieur d'Etudes, for their kindness, Dr. Sagrario PASCUAL, Maître de Conférence, for her kindness advice and availability.

I would like give thanks to Anita LOISEAU, Jean-Luc MONEGER and Aline LAMBERT for their support and help in materials and administration.

I would like deeply thank to Stéphanie PICAN, my best friend, for invaluable advice, availability, and encouragement. I also thank to her family, Cedric and Clément that they always make me smile with their photos.

I would like to thank to all my friends in laboratory during my study, Rachid, Jean-Marc, Faten, Gaëlle, Céline, Ngoc, Nasreddine, Nhung, Christelle, Sandie, Hao, Anuwat, Nitinart, Lapporn, Punyanich, Supinya, Triranart, Ekawit, Ekasit, Freddy, David, Zoubida, Mounia for their kindness and good atmosphere in laboratory. I would like to give special thanks to Charles for his help about the electrochemical experiment and discussion.

I would like also thank to all Thai students at Le Mans for their help and many parties during I stay here.

Finally, I would like to thank to my grandparent, parent, brother and sister for their love, their support and encouragement. I would like to express thanks to COURTEILLE family for their kindness, support, encouragement and many desserts. I would like to say thank you also to my teachers since I was young and everybody that they supported me until I am here and finish my study.

General introduction	1
Chapter 1-Literature Review	7
1.1. Introduction	7
1.2. Telechelic polyisoprene	7
1.2.1. Definition.....	7
1.2.2. Synthesis methods of telechelic polyisoprene	8
1.2.2.1. Oxidation in the presence of redox system	8
1.2.2.2. Oxidation by photochemical method.....	10
1.2.2.3. Oxidation at high temperatures and high pressures.....	12
1.2.2.4. Oxidation by cleavage reagent specific to double bonds.....	13
1.2.2.5. Metathesis degradation	17
1.3. Polyurethanes (PUs).....	20
1.3.1. Classification of polyurethanes.....	21
1.3.1.1. Foams.....	21
1.3.1.2. Solid polyurethanes	22
1.3.2. Method of synthesis of polyurethanes.....	24
1.3.2.1. Classic method of polyurethane synthesis using isocyanates	24
1.3.2.2. Synthesis of polyurethane by pathways without isocyanate.....	31
1.3.2. Application of polyurethanes.....	34
1.4. Ionic liquids.....	36
1.4.1. Definition and properties of ionic liquids.....	36
1.4.2. Applications of ionic liquids.....	38
1.4.2.1. Used in organic synthesis	38
1.4.2.2. Biotransformations in Ionic Liquids.....	41
1.4.2.3. Use of Ionic Liquids in MALDI mass spectroscopy	41
1.4.2.4. Use of Ionic Liquids in materials chemistry	41
1.5. Polymer electrolytes and conducting polymers.....	43
1.5.1. Polymer electrolytes.....	43
1.5.1.1. Types of polyelectrolyte	43
1.5.1.2. Polyurethane based polyelectrolytes	45
1.5.1.3. Polyelectrolyte from rubber.	46
1.5.2. Conducting polymers composites	48
1.5.2.1. Synthesis methods of conducting composites.....	49
1.5.2.2. Polyurethane based conducting polymers.....	53
1.5.2.3. Conducting composite polymers from rubber	56
1.6. Conclusion.....	57
Chapter 2-Synthesis and characterization of telechelic cis-1,4-polyisoprene	65
2.1. Introduction	65
2.2. Oxidative degradation of cis-1,4-polyisoprene	65
2.2.1. Epoxidation of cis-1,4-polyisoprene	66
2.2.2. Cleavage of epoxidized cis-1,4-polyisoprene 2 in organic meduim.....	69
2.3. Synthesis and characterization of hydroxytelechelic polyisoprene precursor of polyurethane	72
2.4. Modification of hydroxytelechelic cis-1,4-polyisoprene precursor of polyurethanes..	74
2.4.1. Hydrogenation of hydroxytelechelic cis-1,4-polyisoprene 4.....	74

Table of contents

2.4.2.	Epoxidation of hydroxytelechelic cis-1,4-polyisoprene 4.....	76
2.5.	Synthesis and characterization of aminotelechelic cis-1,4-polyisoprene precursor of polyurea	79
2.6.	Epoxidation of aminotelechelic polyisoprene polyurea precursor	82
2.7.	Conclusion.....	84

Chapter 3- Synthesis and characterization of polyurethane based conducting composites86

3.1.	Introduction	86
3.2.	Ionic liquid incorporated polyurethanes.....	87
3.2.1.	Synthesis of linear and crosslinked ionic liquid incorporated polyurethanes.....	87
3.2.1.1.	[bmim]PF ₆ incorporated polyurethane films	89
3.2.1.2.	[thtdp]Cl incorporated polyurethane films.....	91
3.2.2.	Thermal properties of ionic liquid incorporated polyurethane films	94
3.2.2.1.	Thermal properties of polyurethane films without ionic liquids.....	94
3.2.2.1.	Thermal properties of [bmim]PF ₆ incorporated polyurethane films.....	97
3.2.2.2.	Thermal properties of [thtdp]Cl incorporated polyurethane films	101
3.2.3.	Conductivity measurement of ionic liquid incorporated polyurethane films.	107
3.2.3.1.	Conductivity measurement of polyurethane films without ionic liquids ...	108
3.2.3.2.	Conductivity measurement of [bmim]PF ₆ incorporated polyurethane films... ..	109
3.2.3.3.	Conductivity measurement of [thtdp]Cl incorporated polyurethane films	114
3.3.	Ionic liquid incorporated polyureas	117
3.3.1.	Synthesis of linear and crosslinked ionic liquid incorporated polyureas	117
3.3.2.	Thermal properties of ionic incorporated polyurea films.....	119
3.3.3.	Conductivity measurement of ionic liquid incorporated polyurea films.....	121
3.4.	Polymerisation of conducting polymers on polyurethane films.....	123
3.4.1.	Chemical polymerization of aniline on polyurethane films and characterization of films.....	123
3.4.2.	Electropolymerization of aniline on polyurethane films	128
3.4.2.1.	Electropolymerization of aniline on polyurethane coated electrode	128
3.4.2.2.	Electropolymerization of aniline on polyurethane casting films	132
3.4.2.3.	Electropolymerization of aniline on polyurethane thin film on ITO plate .	136
3.4.2.4.	Electropolymerization of EDOT and Py on polyurethane film	138
3.5.	Conclusion.....	139

Chapter4- Synthesis and properties of polyurethane using chain extender with pyrrole side group.....143

4.1.	Introduction	143
4.2.	Synthesis and characterization of new chain extender with pyrrole side group.....	145
4.2.1.	Synthesis of 1-(3-bromopropyl)-1 <i>H</i> -pyrrole 9	146
4.2.2.	Synthesis of diethyl 2-(3-(1 <i>H</i> -pyrrol-1-yl)propyl)malonate 10.....	148
4.2.3.	Synthesis of 2-(3-(1 <i>H</i> -pyrrol-1-yl)propyl)propane-1,3-diol 11.....	150
4.3.	Synthesis and properties of polyurethanes using 2-(3-(1 <i>H</i> -pyrrol-1-yl)propyl)propane-1,3-diol as chain extender.....	151
4.3.1.	Linear polyurethane with different amounts of chain extender.....	152
4.3.1.1.	Thermal properties of linear polyurethanes with chain extender.....	153
4.3.2.	Crosslinked polyurethanes with different amounts of chain extender.....	157

Table of contents

4.3.2.1.	Thermal properties of crosslinked polyurethanes with chain extender	158
4.4.	Electrochemical polymerization of pyrrole on polyurethane films.	162
4.4.1.	Electrochemical polymerization of pyrrole on pyrrole-swollen polyurethane films containing chain extender.	162
4.4.2.	Electrochemical polymerization of pyrrole on polyurethane films containing chain extender.	165
4.5.	Conclusion.....	169
General conclusion	172
Experimental part	174
Appendix	194

Abbreviations:

NR	Natural rubber
EPI	Epoxidized cis-1,4-polyisoprene
HTPI	Hydroxytelechelic cis-1,4-polyisoprene
CTPI	Carbonyltelechelic cis-1,4-polyisoprene
EHTPI	Epoxidized hydroxytelechelic cis-1,4-polyisoprene
HHTPI	Hydrogenated hydroxytelechelic cis-1,4-polyisoprene
PINH	Butylaminotelechelic cis-1,4-polyisoprene
EPINH	Epoxidized butylaminotelechelic cis-1,4-polyisoprene
<i>m</i> -CPBA	<i>meta</i> -chloroperbenzoic acid
FTIR	Fourier Transform Infrared Spectroscopy
¹ HNMR	Proton-1 Nuclear Magnetic Resonance spectroscopy
¹³ CNMR	Carbon-13 Nuclear Magnetic Resonance spectroscopy
SEC	Size Exclusion Chromatography
\overline{M}_w	Weight average molecular weight
\overline{M}_n	Number average molecular weight
MS	Mass Spectroscopy
IL	Ionic liquid
[bmim]PF ₆	1-butyl- 3-methylimidazolium hexafluorophosphate
[thtdp]Cl	Trihexyltetradecylphosphonium chloride
PU	Polyurethane
EPU	Epoxidized polyurethane
TDI	Tolylene-2,4-diisocyanate
H12MDI	Dicyclohexylmethane diisocyanate
I-IPDI	Isocyanurate of isophone diisocyanate
DBTL	Dibutyltin dilaurate
PANI	Polyaniline
PPy	Polypyrrole
EDOT	3,4-ethylene dioxathiophene
SEM	Scanning electron microscope
DSC	Differential scanning calorimetry
TGA	Thermogravimetric analysis
DTG	Derivative thermogravimetry
DRS	Dielectric relaxation spectroscopy

General introduction

The polyelectrolyte and conducting polymer composites are widely used in many applications, such as sensors, batteries, anticorrosion coatings, electromagnetic shieldings and so on. Among the wide range host polymers, polyurethanes are one of conventional polymers which are chosen¹⁻⁶ because of their two phases morphology (hard and soft). The soft segments allow ions dissolving and mobility in matrix while hard segments act as physical crosslink to soft segments and so contribute to dimension stability and good mechanical properties.

In polyelectrolyte application, polyurethanes are normally doped with various alkali metal salts^{5,6}. Nowadays, ionic liquids, room temperature molten salts, are become interesting in the polyelectrolyte application because they show many special properties, especially high conductivity, high thermal stability, low volatility and non-flammability. Polyelectrolytes from ionic liquids are prepared by incorporating ionic liquid in a polymer matrix⁷ or by polymerization of ionic liquid containing vinyl groups⁸.

In addition, a combination of conventional polymers with conducting polymers allows the creation of new polymeric materials with interesting characteristic properties, for example an elastomeric material with high conductivity. The composite between conducting polymer and polyurethane were widely synthesized by both chemical and electrochemical techniques¹⁻⁴, the simplest one is the in situ polymerization of conducting monomer on polyurethane matrix. Also, the electrochemical polymerization of conducting monomer in the polyurethane was studies^{9,10}.

Besides from common diols, polyurethanes were also prepared from commercial hydrogenated hydroxyl-terminated polyisoprene (EPOL[®])¹¹⁻¹². Concerning the interest of the renewable source, the development of the natural source products was played attention for used as starting material in the synthesis of other materials. Natural rubber is thus one of the most interesting materials. Controlled degradation of synthetic and natural rubber in both organic and latex phase has been developed in our laboratory^{13,14}. The reduction of carbonyl chain ends groups to alcohol groups was also performed and polyurethanes based on this hydroxytelechelic cis-1,4-polyisoprene have been prepared^{15,16}. Modulation of their structure allowed to obtain higher thermo-mechanical properties than those of polyurethane based on commercial analogue.

The purpose of this work is to elaborate a valuable material from polyisoprene, renewable source, by combining elastomeric polyurethane based on polyisoprene block with high conductive ionic liquids and conducting polymers, such as polyaniline, polypyrrole by incorporating ionic liquid in polyurethane and polymerization of conducting monomer on polyurethane matrix.

The first chapter of this thesis is the literature survey of controlled degradation for preparing the telechelic oligomer from synthetic and natural rubber and of polyurethane, ionic liquid, polyelectrolyte and conducting composites types and applications. Especially usage of polyurethane in those applications was described.

The second chapter concerns the reaction of controlled cleavage of high molecular weight synthetic cis-1,4-polyisoprene using periodic acid in organic medium to obtain carbonyl telechelic cis-1,4-oligoisoprene (CTPI). The chain end modification of carbonyl groups to alcohol groups to obtain hydroxy telechelic cis-1,4-polyisoprene (HTPI) is presented. Also, main chain isoprene unit modifications by hydrogenation and epoxidation of HTPI for preparing different precursors of polyurethane are described. Reductive amination of CTPI to obtained n-butylamino telechelic cis-1,4-polyisoprene is detailed as well.

The third chapter consists of two main parts; in the first part, a preparation of incorporated ionic liquids polyurethanes, their thermal properties and conductivity are stated. The second part describes the preparation of composites of conducting polymers and polyurethanes using chemical polymerization and electrochemical polymerization techniques.

The fourth chapter deals with the synthesis and characterization of a new type chain extender containing pyrrole pendent group. The preparation of polyurethane film using this chain extender, their thermal properties and the electropolymerization of pyrrole group in film is lastly demonstrated.

-
1. P.C. Rodrigues, P.N. Lisboa-Filho, A.S. Mangrich, L. Akcelrud, *Polymer* 46 (2005) 2285.
 2. E. Hrehorova, V.N. Bliznyuk, A.A. Pud, V.V. Shevchenko, K.Y. Fatyeyeva, *Polymer* 48 (2007) 4429.
 3. C.-P. Chwang, C.-D. Liu, S.-W. Huang, D.-Y. Chao, S.-N. Lee, *Synth. Met.* 142 (2004) 275.
 4. L.Y. Chiang, L.Y. Wang, C.S. Kuo, J.G. Lin, L.Y. Huang, *Synth. Met.* 84 (1997) 721.
 5. S.-M. Lee, C.Y. Chen, C.C. Wang, *Electrochimica Acta* (2004) 4907.

6. P. Pissis, A. Kyritsis, G. Georgoussis, V.V. Shilov, V.V. Shevchenko, *Solid State Ionics* 136-137 (2000) 255.
7. J. Fuller, A.C. Breda, R.T. Carlin, *J. Electroanal. Chem.* 459 (1998) 29.
8. H. Ohno, *Electrochim. Acta.* 46 (2001) 1407
9. Q. Pei, X. Bi, *J. Appl. Polym. Sci.* 38 (1989) 1819.
10. Q. Pei, X. Bi, *Synth. Met.* 22 (1987) 145.
11. F. Burel, A. Feldman, C. Bunel, *Polymer* 46 (2004) 15.
12. F. Burel, A. Feldman, C. Bunel, *Polymer* 46 (2004) 483.
13. J.C. Brosse, I. Campistron, D. Derouet, A. El Hamdaoui, S. Houdayer, S. Gillier- Ritoit, *J. Appl. Polym. Sci.*, 78 (2000) 1461.
14. S. Gillier- Ritoit, D. Reyx, I. Campistron, A. Laguerre, R.P. Singh, *J. Appl. Polym. Sci.* 87(1) (2003) 42.
15. N. Kebir, I. Campistron, A. Laguerre, J.-F. Pilard, C. Bunel, J.-P. Couvercelle, C. Gondard, *Polymer*, 46 (2005), 6869.
16. N. Kebir, I. Campistron, A. Laguerre, J.-F. Pilard, C. Bunel, J.-P. Couvercelle, *e-Polymers* 48 (2004).

Chapter 1-Literature Review

1.1. Introduction

According to our framework, we played attention to elaborate materials from the renewable resource, such as natural rubber. Thus, the literature survey of concerning works was done.

In this chapter, firstly, various strategies for preparation of precursors, called telechelic oligomers, from high molecular weight natural and synthetic rubbers via controlled degradation feature are described.

Secondly, due to aim of our study being synthesis of polyurethane based conducting composites, hence, polyurethane types, mode of preparation including starting materials and their applications are then defined. Subsequently, the important role of Ionic Liquids, the new generation salts, is demonstrated in the recent researchs as well as in material chemistry. Their structure, unique properties and applications in many areas are expressed, particularly in polyelectrolytes.

Finally, we write about the polyelectrolytes and conducting composites. Types of polyelectrolytes, also ionic liquids incorporated polyelectrolytes, the preparation of polymer conducting composites, especially the employment of polyurethane and elastomers as polyelectrolytes and conducting matrix are represented.

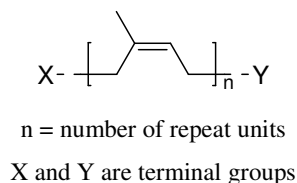
1.2. Telechelic polyisoprene

1.2.1. Definition

The term 'telechelic' was proposed originally by Uraneck, Hsieh and Buck for low molecular weight polymers bearing two functional end groups. Nowadays, this term is also applied to oligomers having two or more terminal groups [1].

Telechelic liquid natural rubber (TLNR) can be defined as a low molecular weight oligomer having number average molecular weight approximately 100-10000 and containing reactive terminal groups capable for using in further chain extension and crosslinking. TLNR still consists of isoprene units, basic structure of natural rubber (NR). The main difference from NR is that TLNR has reactive groups at the chain end, as donated by X and Y. X and Y may, or may not, be similar.

Although research on the production of TLNR began in the early 1970s, commercial TLNR is still not widely available. Most TLNR used in research are prepared especially in the laboratory [1].



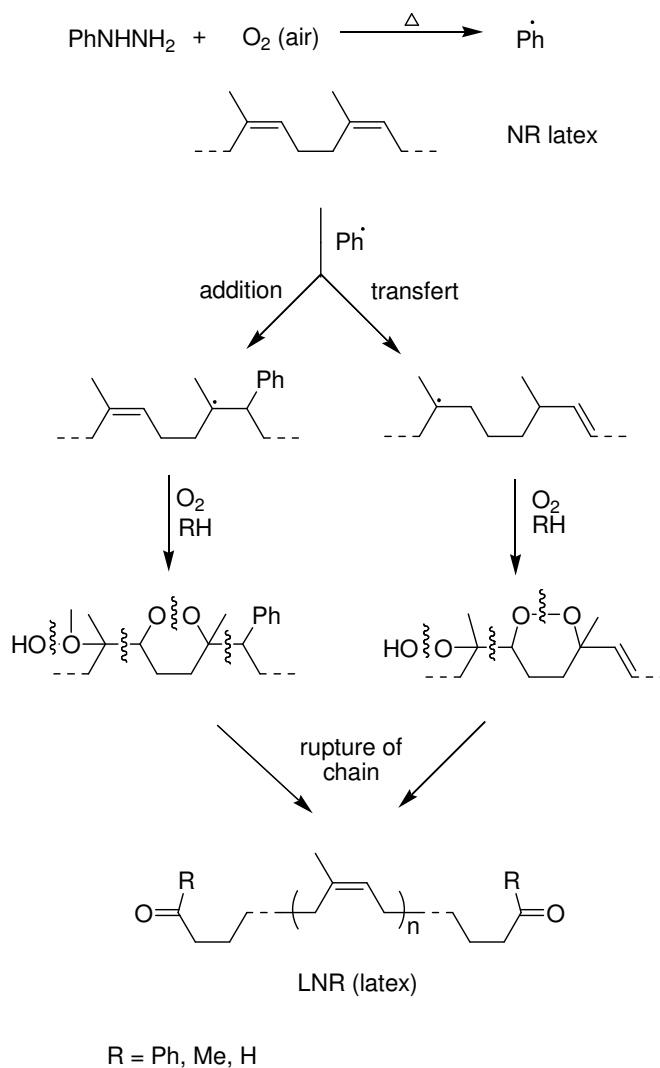
Scheme 1.1 Chemical structure of telechelic liquid natural rubber.

1.2.2. Synthesis methods of telechelic polyisoprene

Basically, the methods involve controlled degradation or depolymerization of the NR backbone via oxidation chain scissions by either chemical or photochemical routes. The methods can be classified into 5 main categories.

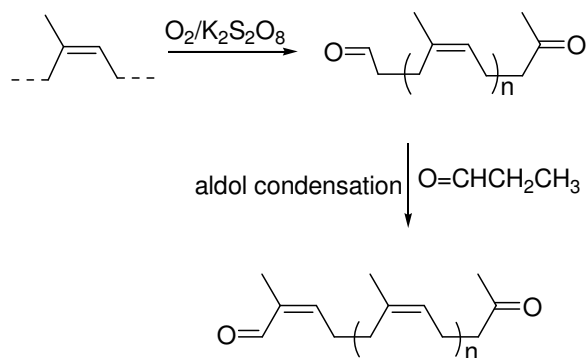
1.2.2.1. Oxidation in the presence of redox system

This method utilizes an appropriate mixture of oxidizing and reducing agents (redox couple). The redox couple can cleave polymer chains with the introduction of reactive terminal groups on the resulting oligomers. Thus, an oxidizing agent such as an organic peroxide, hydrogen peroxide, atmospheric oxygen or ferric chloride-oxygen, coupled with reducing agent such as an aromatic hydrazine or sulphanilic acid were employed to depolymerise NR to yield TLNR bearing phenylhydrazone, carbonyl or hydroxyl terminal groups, depending on the redox system type employed. The depolymerization can be carried out either in an organic solvent or directly in the latex phase. The depolymerization reaction of NR in the latex phase using phenylhydrazine as reducing agent and atmospheric oxygen as an oxidizing agent is more favoured owing to it being economically viable in an industrial scale. A reaction mechanism was proposed by Boccaccio and de Livonniere [2] as shown in Scheme 1.2.



Scheme 1.2 Mechanism of the oxidizing cleavage by atmospheric oxygen in the presence of phenylhydrazine at the carbon-carbon double bond of the natural rubber in latex phase.

Tangpakdee et al. [3] have studied an oxidative degradation reaction of deproteinized natural rubber using different initiators, AIBN, potassium persulfate ($\text{K}_2\text{S}_2\text{O}_8$) and benzoyl peroxide in the presence of a carbonyl product such as acetone formaldehyde or propanal. They demonstrated that $\text{K}_2\text{S}_2\text{O}_8$ /propanal system is most effective for NR degradation at 60°C . The mechanism that they proposed is the oxidation of chain by radical initiator followed by the reaction of propanal with aldehyde end group. The obtained TLNR contained aldehyde and ketone groups.

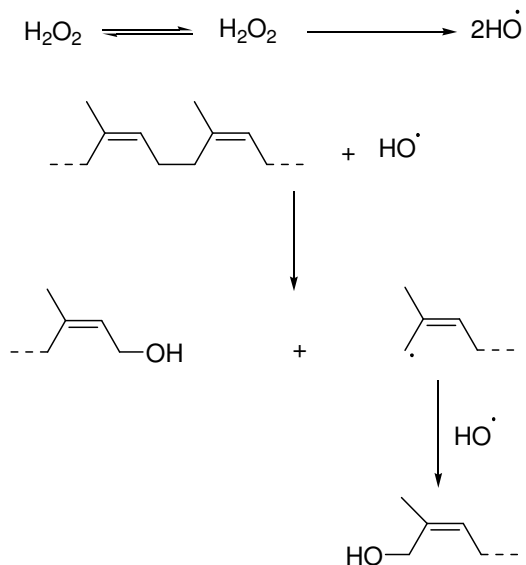


Scheme 1.3 The degradation reaction of deproteinized natural rubber in the presence of $\text{K}_2\text{S}_2\text{O}_8$ and propanal.

1.2.2.2. Oxidation by photochemical method

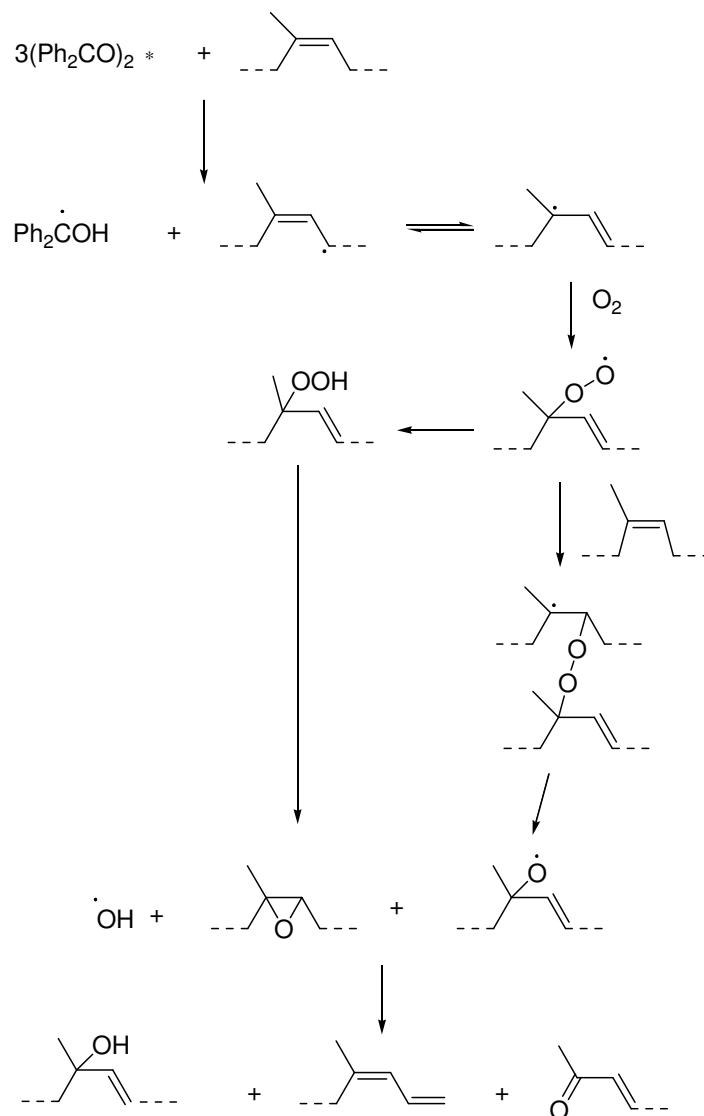
Control degradation of NR by photochemical chain scission for preparation of LNR was first explored by Cunneen [4]. NR was irradiated with UV light in presence of nitrobenzene as a photosensitizer to give carboxy-terminated natural rubber (CTNR) having \overline{M}_n of about 3000. The degradation of NR in solid state was studied but not appears to have further development.

The controlled degradation of NR in solution was also studied by Ravindran et al. [5] NR depolymerization in toluene by UV light in the presence of hydrogen peroxide and methanol or tetrahydrofuran gives HTNR having \overline{M}_n of 8700 or 5000, respectively. They also found that sunlight is almost as effective as UV light in degradation of NR in toluene. However, the concentration of NR in solution is limited at 10%. The mechanism of the degradation has been suggested as shown in Scheme 1.4.



Scheme 1.4 The proposed mechanism of cis-1,4-polyisoprene degradation reaction by hydrogen peroxide/UV radiation.

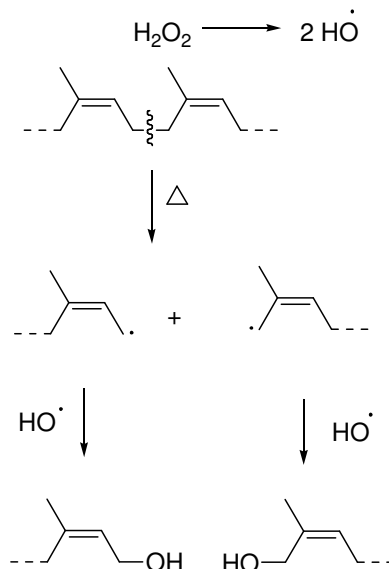
Later, the degradation of NR from fresh latex with 20% DRC (Dry Rubber Content) by sunlight and hydrogen peroxide was also reported but there are no information of type and functionality. In another case, NR was depolymerized by swelled in solution in the presence of benzophenone (photosensitizer) and exposed to sunlight for a day to give TLNR. The mechanism of the reaction believed to be involve in this method is given in Scheme 1.5 leading to chain scission and obtaining hydroxyl, hydroperoxide and ketone end groups [1].



Scheme 1.5 The proposed mechanism of cis-1,4-polyisoprene degradation reaction by benzophenone/UV radiations.

1.2.2.3. Oxidation at high temperatures and high pressures

In this method, masticated NR in toluene containing 30-40% hydrogen peroxide was heated at 150°C in reactor at a pressure of 200-300 psi to yield HTNR having \overline{M}_n between 2500 and 3000 g/mol. Unfortunately, analytical data indicate that the efficiency of functionalization of HTNR by this method is low. This explained as being caused by side reactions. A mechanism of reaction was proposed as shown in Scheme 1.6 [6].



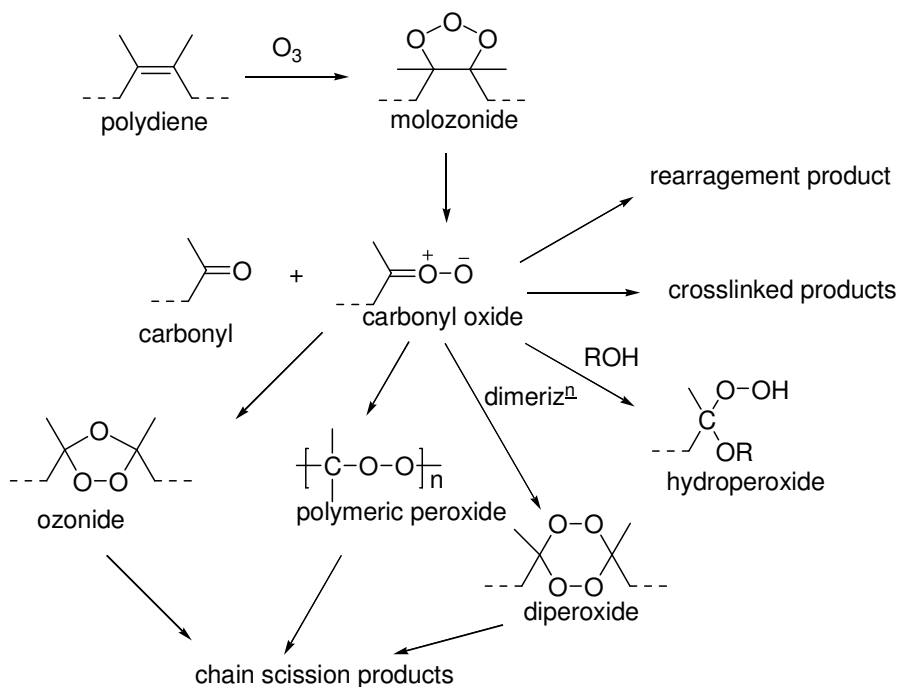
Scheme 1.6 The proposed mechanism of degradation of cis-1,4-polyisoprene by hydrogen peroxide at high temperature and high pressure.

1.2.2.4. Oxidation by cleavage reagent specific to double bonds

- **Ozonolysis**

The term ‘ozonolysis’ refers to the cleavage of bonds by ozone leading to the formation of peroxy or non-peroxy products, whereas the term ‘ozonization’ refers merely to the process of treatment of a compound with ozone.

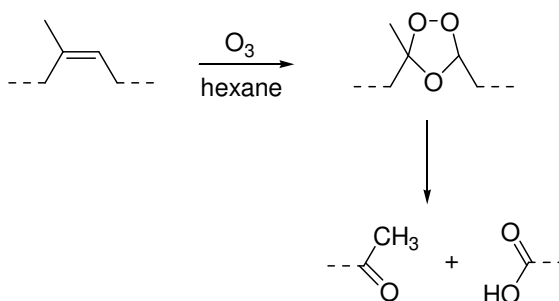
Mechanism of ozone attack on C=C bonds of polydiene rubber backbones, causing chain scission and yielding various peroxidic products was proposed by Criegee (Scheme 1.7) [7]. The reaction between C=C bonds and ozone leads to the unstable molozonide formation. This unstable species can easily cleave to a stable carbonyl compound (aldehyde or ketone) and an unstable carbonyl oxide (zwitterions). The carbonyl oxide then undergoes reaction leading to final, stable products. Degradation of unsaturated rubber by ozone results in a decrease in molecular weight and increase in species containing oxygenated function group (aldehyde, ketone, acid, peroxide, etc).



Scheme 1.7 Mechanism of reaction of ozone at double bond of polydienes.

Tanaka et al. showed that controlled ozonolysis of *trans*- and *cis*-1,4-polyisoprene and 1,4-polybutadiene results in selective chain scission and produces HTNRs having 11 and 10 units and HTBDs having 12 and 13 repeat units with very narrow polydispersities of 1.01-1.06 [8].

Montaudo et al. reported that ozonolysis of *cis*-1,4-polyisoprene in hexane at ice-bath temperature without further treatment with either oxidizing or reducing agents can lead to the formation of telechelic oligomers bearing only ketone and carboxylic acid end groups with no oligomeric ozonides being detected [9]. Whereas, ozonolysis of *cis*-1,4-polyisoprene in carbon tetrachloride reported by Anachkov [10], leads to the basic ozonolysis products: ozonide, ketones and aldehydes.



Scheme 1.8 Ozonolysis of *cis*-1,4-polyisoprene in hexane.

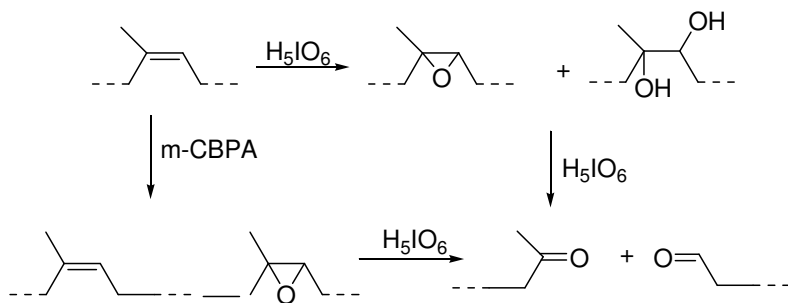
- **Cleavage by periodic acid or transition compounds**

Guizard et al. developed the method of the specifically double bonds cleavage to obtain bifunctional oligomers. Ruthenium tetroxide was used in the presence of peracid as co-oxidant. Chain scission occurs at unsaturated site rather than entirely randomly [11].

Lead tetraacetate, $\text{Pb}(\text{OAc})_4$ and periodic acid (H_5IO_6) are interesting for degradation of polyisoprenic chain. Typically, both reagents cause cleavage of *vic*-glycols to yield carbonyl compounds. Burfield and Gan [12] found that $\text{Pb}(\text{OAc})_4$ causes degradation of hydrolyzed epoxidized synthetic rubber faster than that of epoxidized synthetic rubber. Synthetic polyisoprene sample which presumably contains no 1,2-diols, was also slowly degraded by $\text{Pb}(\text{OAc})_4$. They also found that H_5IO_6 could be used to degrade NR and acid hydrolyzed NR. In the case of NR, it is believed that the chain degradation occurs in the presence of a few 1,2-diol units in the molecular chain.

H_5IO_6 was also used by Reyx and Campistron for preparation of telechelic liquid natural rubber. They found that epoxide content of starting rubber decreased from 25 to 8% after degradation reaction. The NMR spectrum showed the presence of aldehyde and ketone moieties, residual oxiranes, and secondary furanic and cyclic structures [13].

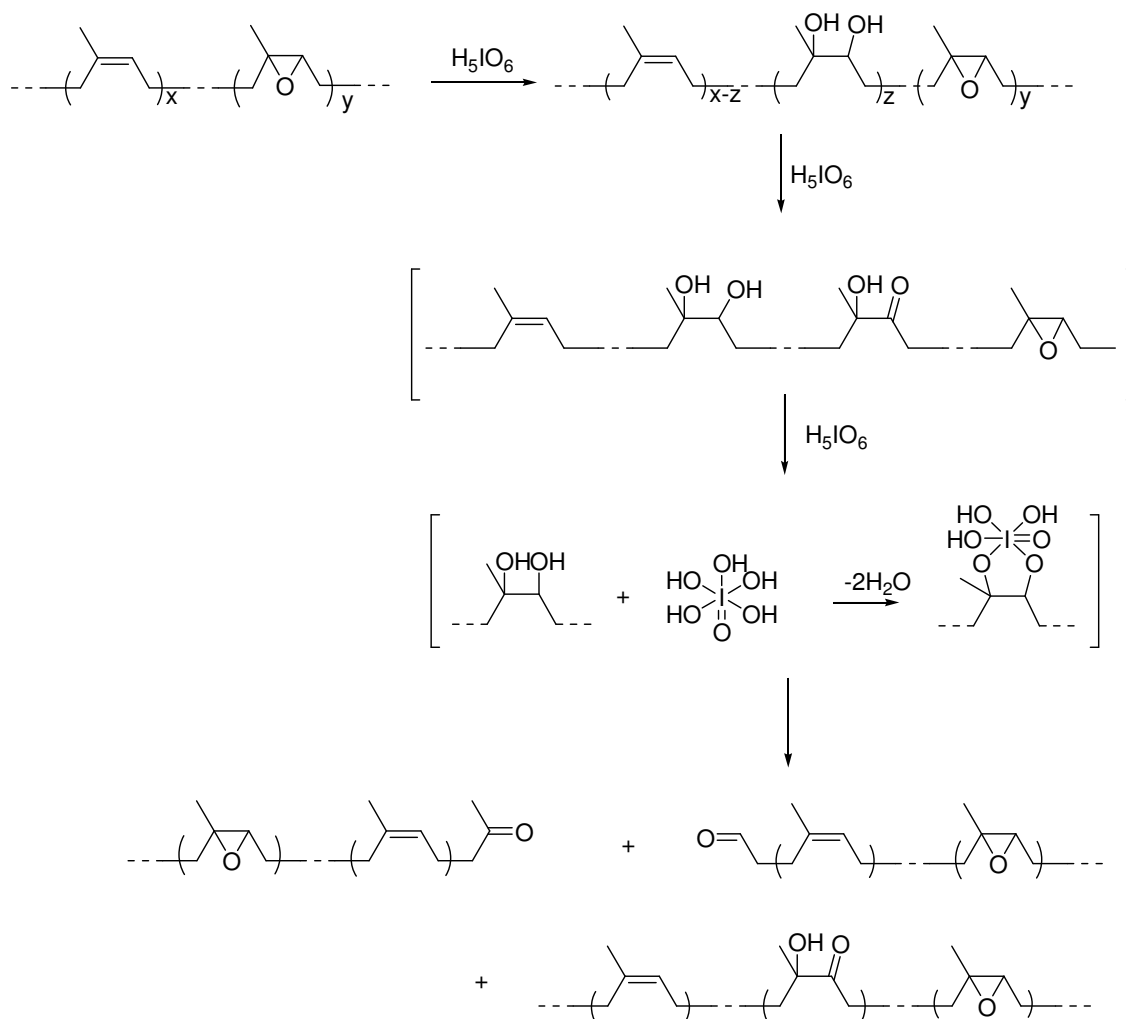
Gillier-Ritoit et al. [14] investigated chain degradation of polyisoprene and epoxidized polyisoprene using H_5IO_6 in organic solvent. The degraded PI gave H-NMR characteristics similar to those of degraded epoxidized polyisoprene. The degraded rubber containing aldehyde and ketone terminal ends, but the reaction is slower than in case of epoxidized polyisoprene. They found that in epoxidized polyisoprene, the H_5IO_6 cleavage of polymer chain occurs nearly instantaneously, while H_5IO_6 cleavage of double bonds of polyisoprene is slower process. It appears that two equivalents of H_5IO_6 are needed for cleavage of double bond in polyisoprene. They proposed that the cleavage result from two steps. Firstly, H_5IO_6 reacts with a double bond to give an epoxide or α -glycol. Secondly, the epoxide or α -glycol is cleaved by reacting with the second equivalent of H_5IO_6 . They proposed the pathway of reaction as shown in Scheme 1.9.



Scheme 1.9 The degradation of cis-1,4-polyisoprene and epoxidized cis-1,4-polyisoprene using H_5IO_6 .

Mauler et al. investigated that degradation of cis-1,4-polyisoprene by using H_5IO_6 /ultrasonic radiation (sonochemical) is more efficient than the use of radiation or chemical degradation alone. The presence of ultrasound irradiation accelerates the chemical degradation process leading to lower molecular weight products [15].

The degradation of deproteinized epoxidized NR using H_5IO_6 was performed by Phinyocheep et al. The epoxidation of deproteinized NR was carried out in latex phase using performic acid formed *in situ* by reaction of hydrogen peroxide and formic acid. The epoxidized NR was then degraded by H_5IO_6 . In all ENR samples obtained, there was no observation of NMR signals corresponding to products of side reactions such as formation of diol and furan, as previous mention. After treatment with H_5IO_6 , they still found epoxides and also the new signals of carbonyl and hydroxyl functional groups and the molecular weight decreased. Therefore, they proposed reaction pathway as shown in the Scheme 1.10 [16].



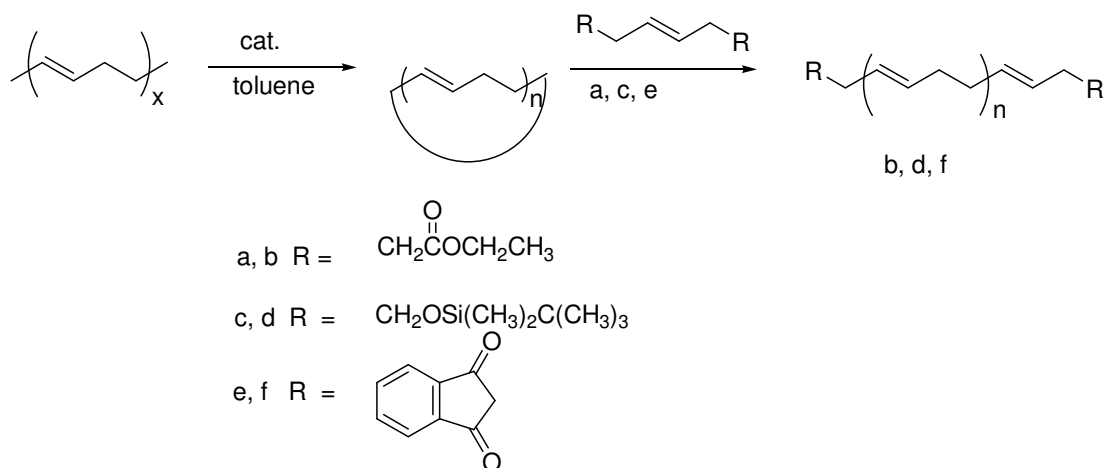
Scheme 1.10 Proposed reaction pathway of oxidative degradation of epoxidized rubber by periodic acid.

1.2.2.5. Metathesis degradation

Depolymerization agents or chain transfer agents and catalysts especially Lewis acid Schrock and Grubbs' are used in metathesis depolymerization of polyalkenamers including polydienes, resulting oligomers and telechelic oligomers [18].

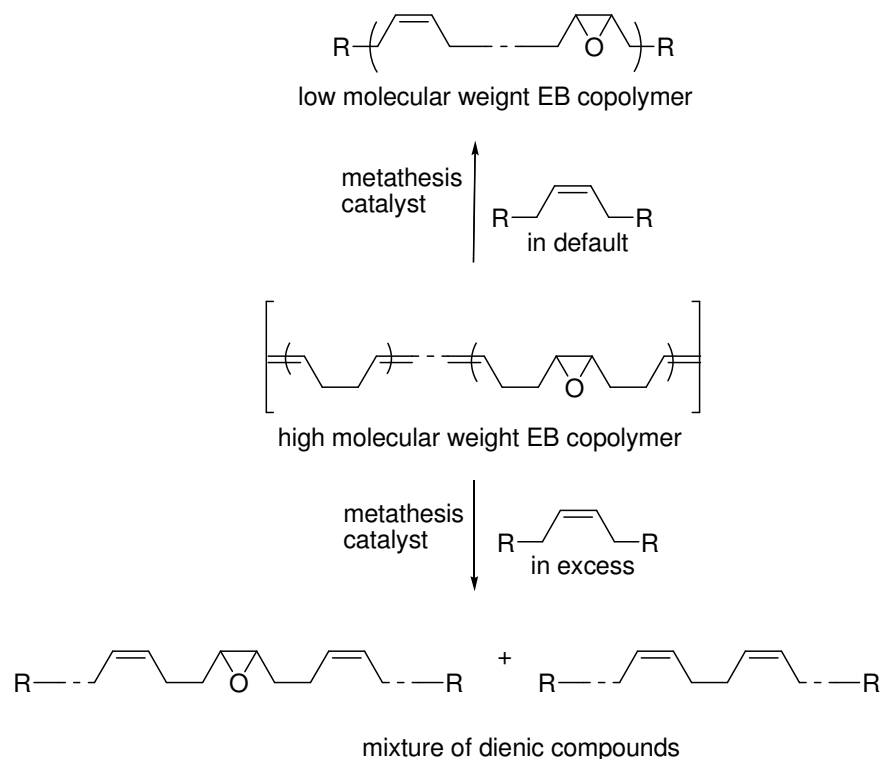
Use of Lewis acid catalyst such as $\text{WCl}_6/\text{Sn}(\text{CH}_3)_4$ can lead to side reactions. Therefore, Marmo et al. reported the synthesis of mass-exact telechelic polybutadiene oligomer by metathesis degradation of cis-1,4-butadiene using allylsilane monoene and alkyldienes complex catalyst [19]. They also synthesized the diester, disilyl ether and diamide telechelic polybutadiene oligomers via cyclic diene metathesis depolymerization. The

characterisation of obtained products shows that these telechelic are perfectly difunctional. The mechanism was described that the first stage proceeds through intermolecular cyclization of 1,4-polybutadiene, then macrocyclic butadiene cross-metathesis with functionalized monoene to form linear difunctional telechelic oligomer [20].



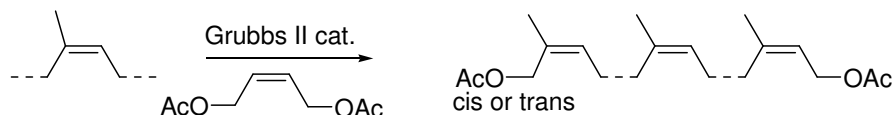
Scheme 1.11 Depolymerization of 1,4-polybutadiene with diethyl 4-octene-1,8-dioate (a), bis(*t*-butyldimethylsilyl)-3-hexene-1,6-diol diether (c), and 2-butene-1,4-diylbis(phthalimide) (e).

However, there is not much work using this technique in degradation of polyisoprene for a present. Our laboratory interested in preparing telechelic polydiene. Thanki et al. was performed metathetic alkenolysis of partially epoxidized *cis*-1,4-polybutadiene using Grubbs' ruthenium benzylidene compound as catalyst and 4-octene as depolymerizing agent as shown Scheme 1.12 They found that when the mol ratio of monomer unit to catalyst decreases, yield of oligomer increases linearly [18].



Scheme 1.12 Metathesis alkenolysis of partially epoxidized polybutadiene.

Recently, Solanky et al. developed a new approach for obtaining end-functionalized acetyloxy polyisoprene in a controlled manner through a metathesis methodology using second generation Grubbs catalyst and chain transfer agent from cis-1,4-polyisoprene. Oligomers of molecular weight range 8000-40000 g/mol were obtained in very good yields, while lower molecular weight was obtained in moderate yields. Moreover, they have prepared telechelic natural rubber with molecular weight 38000 from deproteinized natural rubber in latex phase. [21].

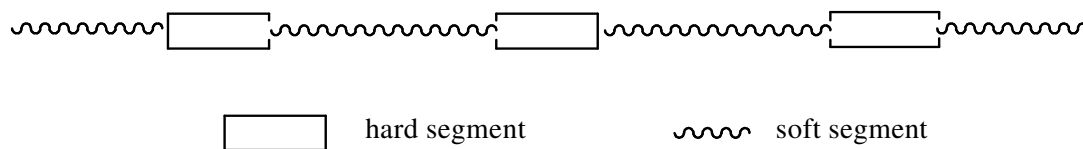


Scheme 1.13 Structure of product by metathesis degradation.

1.3. Polyurethanes (PUs)

The initial step that led to the worldwide interest in polyurethanes was taken by Otto Bayer of I.G. Farbenindustrie, Leverkusen, Germany in 1937. The first materials synthesized by Bayer were prepared via reactions between diamines and aliphatic diisocyanates. These produced polyurea materials that were infusible and strongly hydrophilic could not compete with the polyamides, particularly in fibre applications. Further work with aliphatic diisocyanates and glycol produced material with properties that were more willing for a use in fibrous applications. Synthesis of materials with high molecular weight glycols and aromatic diisocyanates yielded the first polyurethane elastomers [25].

Polyurethanes are employed in a broad range of uses and applications, including machinery transport, furnishings, textiles, paper-making, packaging, adhesives and sealants, and medicine [25]. They are diblock, flexible elastomers consisting of soft segment (polyether or polyester) reinforced by condensation with a hard segment (diisocyanate). The phase separation morphology, in which the hard and soft phases are thermodynamically immiscible, promotes hydrogen bonding in the hard domain involving urethane C=O and N-H moieties on adjacent polymer chain segments [26]. The elastomeric properties of the thermoplastic polyurethane vary with the number of variables, including soft segment molecular weight and hard segment concentration as a consequence of alteration in hydrogen bonding characteristics. The soft segment is typically a low glass transition temperature polyether, polyester or polyalkyldiol, generally of molecular weight 400-5000. The hard segment is usually a high glass transition temperature, possibly semicrystalline aromatic diisocyanate, linked with a low molecular weight chain extender. Polyurethanes are generally synthesized with chain extenders consisting of low molecular weight diols or diamines which produce additional urethane or urethane-urea segments respectively. The properties range from very brittle and hard materials to soft, tacky, viscous ones [25].



Scheme 1.14 Hard segments and soft segments in polyurethanes.

1.3.1. Classification of polyurethanes

Considering the particular properties of polyurethanes and the way in which these are used, we can classify polyurethanes in 2 main types: foams and solid polyurethanes [27].

1.3.1.1. Foams

Foams are made by forming gas bubbles in the polyurethane mixture called 'blowing'. Foam manufacture can be carried out continuously to produce continuous laminates or discontinuously to produce moulded items. There are three foam types [27,28]:

- **Low density flexible foams** are materials of density 10-80 kg/m³, composed of lightly crosslinked, open-cells. It means that air may flow through the structure very easily. Essentially flexible and resilient padding materials, flexible foams are produced as slabstock or individually moulded cushion and pads. Semi-rigid variants also have an open-cell structure but different chemical formulations [27].

- **Low density rigid foams** are highly crosslinked polymers with a closed-cell structure. Each bubble within the material has unbroken wall so that gas movement is impossible. These materials offer good structure strength in relation to their weight, combined with outstanding thermal insulation properties. A chlorofluoromethane gas is usually contained within the cells, and as these substances have a much lower thermal conductivity than air, thus closed-cell foams have a significantly lower thermal conductivity than any open-celled foam. However, if this low thermal conductivity is to be retained, the chlorofluoromethane gas must not leak away. Consequently, rigid polyurethane foams insulation must have at least 90% of closed cells and a density about 30 kg/m³ [27].

- **High density flexible foams** are defined as those having density above 100 kg/m³. The range includes moulded self-skinning foams and microcellular elastomers. Self-skinning systems are used to make moulded parts having a cellular core and a relatively dense, decorative skin. There are two types, those with open-cell core and an overall density in the range up to about 450 kg/m³ and those with a largely closed cell or microcellular core and an overall density above about 500 kg/m³. Microcellular elastomers have a substantially uniform density in the range from 400-800 kg/m³ and mostly closed cells which are so small that they are difficult to see with the naked eye. The biggest applications of self-skinning foams and

microcellular elastomer are moulded parts for upholstery and vehicle trim and foreshore-soling. Microporous elastomers are microcellular foam foils or sheets having a proportion of open, communicating cells [27].

1.3.1.2. Solid polyurethanes

- **Polyurethane elastomers.** Most of PU elastomers have excellent abrasion resistance with good resistance to attack by oil, petrol and many common non-polar solvents. They may be tailored to meet the needs of specific applications as they may be soft or hard, of high or low resilience, solid or cellular.

Types of polyurethane elastomers commercially available include thermoplastic elastomers in form suitable for conventional thermoplastic processing, cast elastomers made by mixing and casting reactive liquid components, elastomeric fibres and various one- and two- component systems for making elastomer coatings on textiles and other flexible substrates. There are also millable polyurethane rubbers which can be processed by traditional methods used in the rubber industry [27].

All most of these polyurethane elastomers are based on segmented block copolymers having alternating soft and hard segments. The soft segments are polyester or polyether chains, the hard segments (rigid or stiff at ambient temperature) are the reaction products of a polyfunctional isocyanate and a diol or a diamine. In general, the fully-cured elastomers are tough, abrasion-resistant materials of high strength having good resistance to many solvents and chemicals [27,28].

Types of polyurethane elastomers:

– *Thermoplastic polyurethane elastomers (TPU)* are supplied as granules or pellets for processing by the well-established thermoplastic processing techniques such as injection moulding and extrusion. By these means, elastomeric mouldings may be mass-produced to precise dimensions. The physical properties and the range of working temperature of TPU fill the gap between conventional moulded rubbers and engineering thermoplastics. The high modulus of TPU is attributable to a two-phase polymer microstructure, result from the physical bonding and aggregation of hard segments of adjacent polymer chains. The resulting hard block domains act as crosslinked, physically-bonded crystalline centres dispersed in the

soft domain of flexible polyether or polyester chains. The hard block domains, therefore, act as molecular reinforcing fillers [27].

TPU are electrical insulating materials with volume resistivities in range from 10^9 to about 10^{13} ohm.cm. Antistatic and electrically conducting TPU may be obtained by the incorporation of graphitic carbon, electrolytes solution or ionic liquids. Furtado et al. prepared the polyurethane electrolytes/carbon black composites. Film is amorphous and flexible. At room temperature, conductivity reaches a value of 5×10^{-6} S/cm [29].

However, polyurethanes are also used in the electrical applications as the matrix of polymer electrolytes [30-33] and polymer conducting composites because they are composed of soft segments that allow the ions mobility with the good mechanical properties from physical reinforced by hard segments [36-40].

– *Cast polyurethane elastomers.* These are elastomers made by mixing and pouring a degassed reactive liquid mixture into mould. The product includes both linear and partially crosslinked materials. The linear cast PU elastomers are chemically and physically similar to TPU [27].

– *Polyurethane fibres (Spandex).* The first commercial PU fibre was developed in Germany during the early 1940s. It was made by reacting 1,6-hexane diisocyanate (HDI) with a slight excess of 1,4-butanediol. The polymer, having a high level of intermolecular physical bonding, gives a stiff fibre. Polyurethane fibre may be broadly subdivided into normal and elastic. Normal polyurethane fibres have the similar properties to those of polyamides [34]. They are obtained from low molecular weight glycols and diisocyanates. The elastic fibres are known as spandex fibres. Spandex fibres are chemically similar to thermoplastic PU elastomers. They are usually made by a continuous two-stage process using isocyanate-terminated prepolymer that is chain-extended with low molecular weight diol, diamine or hydrazine. Several methods of spinning have been used; dry spinning from solution, reaction spinning, wet spinning and hot-melt extrusion [27].

– *Elastomeric Polyurethane coatings.* Elastomeric PU coatings have very high abrasion and soil resistance. They are used as fabric coatings to make simulated leather and other decorative and water resistant materials for clothing and furnishing. Thin layer PU coatings are also widely used to improve the surface finish and furnishing fabrics. Poromeric materials are microporous polyurethane elastomers that are coated onto textiles, often non-woven

materials to make leather-like sheet materials for used in footwear. Poromeric foils are also available for adhesive lamination to leather splits to make a material for composite shoe-uppers. It combined the breathability, abrasion and water-resistance with moisture absorption of leather and its ability to confirm the shape of the foot [27].

- **Adhesive, binders, coatings, sealants and paints.** PU is also used in flexible coatings for textiles and adhesives for film and fabric laminates. PU paints and coatings give the highest wear resistance to surfaces such as floors and the outer skins of aircraft. They are also becoming widely used for high quality finishes on automobiles [27].

PU can be use to join most other materials together. They make tough, vibration-resistant adhesives with a wide range operating temperatures. It was used as binder for both organic and inorganic materials. Polyurethane adhesives polymerize to form strong bonds without the need to use high temperature [27].

1.3.2. Method of synthesis of polyurethanes

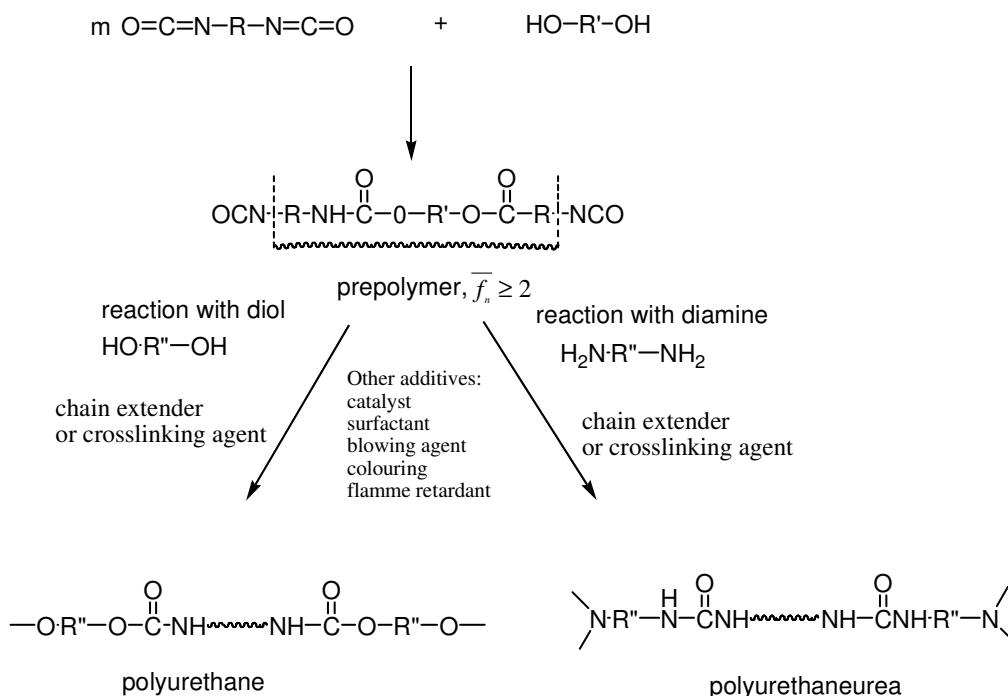
Polyurethane polymerization reaction contains features of both addition and condensation polymerization. Although no small molecule is eliminated during polymerization, the reaction between the diol and the diisocyanate can be classified as a condensation polymerization reaction. The kinetic of the polymerization reaction more closely resembles that of condensation polymerization than addition polymerization.

1.3.2.1. Classic method of polyurethane synthesis using isocyanates

Commercially, polyurethanes can be synthesized via “one-step” process or multistep syntheses.

- **One step method**

The one step process is the quickest and easiest of the manufacturing techniques. A functional or multifunctional liquid isocyanate and liquid diol are mixed in a mould, and allowed to react as shown in Scheme 1.15. A lightly crosslinked structure can be synthesized with careful selection of the precursors. Curing of material from one-step procedure produces an elastomer.



Scheme 1.16 Two steps polyurethane synthesis [25].

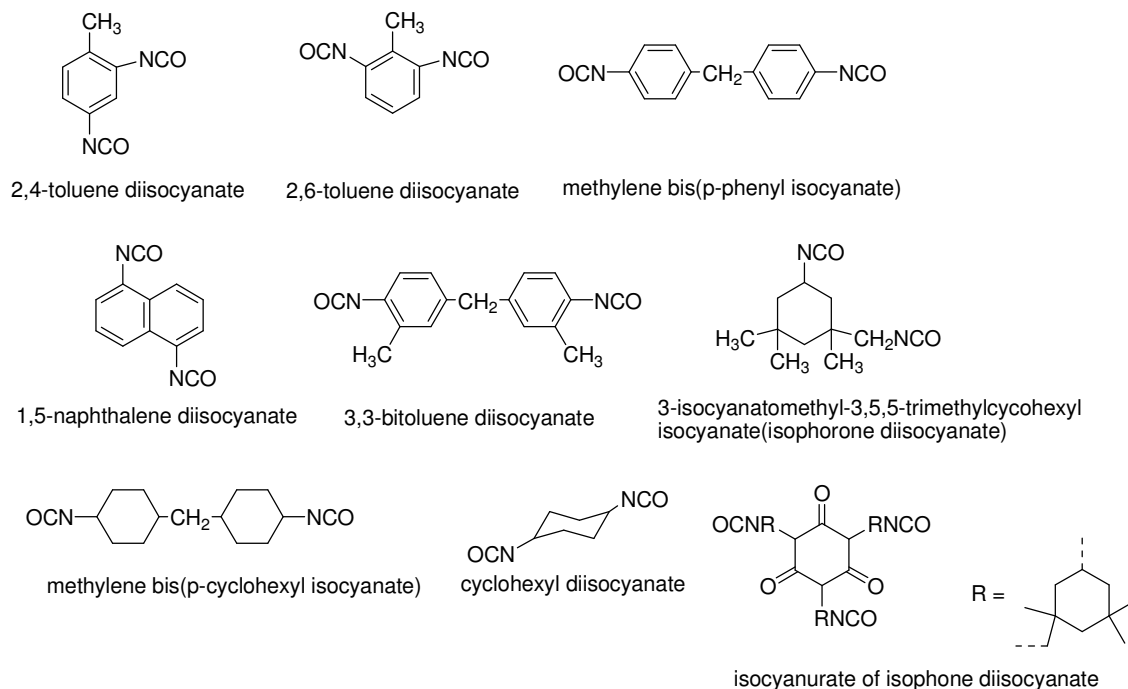
• Raw materials in polyurethane synthesis

A. Isocyanates

Both aliphatic and aromatic isocyanates can be used to synthesize polyurethanes. The presence of an aromatic isocyanate in the hard segment produces a stiffer polymer chain with higher melting point. The two most commonly used isocyanates are toluene diisocyanate (TDI) and 4,4'-diphenylmethane diisocyanate (MDI). TDI is less expensive than MDI, but MDI has superior reactivity, and polymers based on MDI may possess better physical properties. TDI is usually prepared as an isomeric mixture of 2,4-TDI and 2,6-TDI. MDI is crystallisable while 2,4-TDI does not crystallize in the solid state. Other aromatic diisocyanates, such as naphthalene diisocyanate (NDI) and bitoluene diisocyanate (TODI) also can result in high-performance polymers, but at a higher cost than MDI based materials. MDI is available in several forms based on two types of product, purified monomeric MDI and polymeric MDI [25,27].

Typical aliphatic diisocyanates include 1,6-hexane diisocyanate (HDI), isophorone diisocyanate (IPDI) and methylene bis(p-cyclohexyl isocyanate) (H_{12}MDI). Because aromatic diisocyanates and polymers made from them are somewhere unstable toward light and

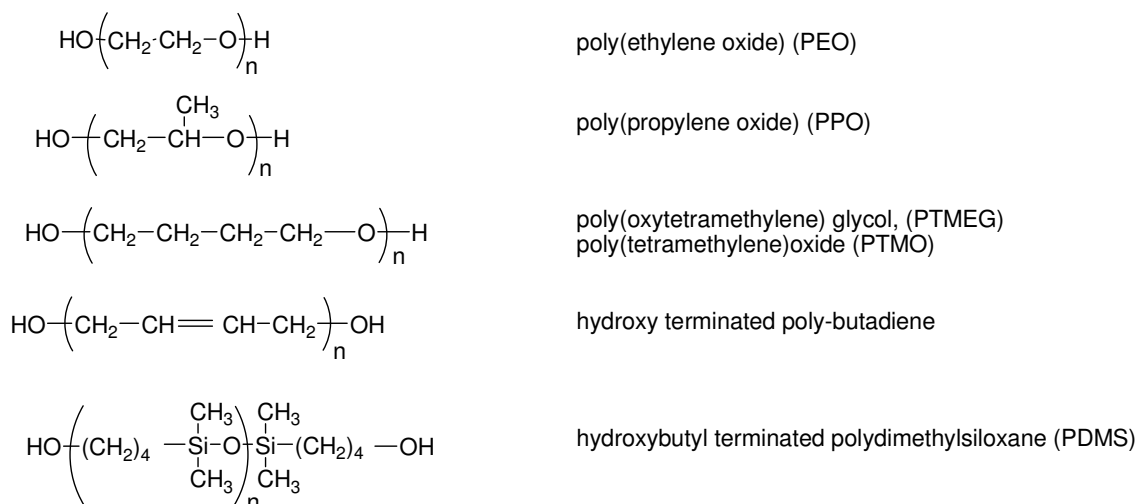
become yellow with time, aliphatic isocyanates have found wider use in coating applications, than aromatic containing materials. In addition to greater light stability, polyurethanes based on aliphatic isocyanates possess increased resistance to hydrolysis and thermal degradation. Unfortunately, this is sometime accompanied by a decrease in the mechanical properties of the material. The chemical structures of commonly used diisocyanates used in polyurethane synthesis are shown below, in Scheme 1.17 [25].



Scheme. 1.17 Some commonly used isocyanates

B. Polyols

Polyols available for elastomer synthesis include polyesters, polyethers, polycarbonates, hydrocarbons and polydimethylsiloxanes. The most commonly used polyols are polyethers or polyesters based compounds [25]. The structure of the polyol plays a part in determining the properties of the final urethane polymer [27]. Commonly used polyols are shown in Scheme 1.18 [25].

**Scheme 1.18** Some commonly used polyols.

Traditionally, polyurethanes have been produced with polyester and polyether soft segments. Polyurethanes synthesized from polyesters possess relatively good physical properties; however, they are susceptible to hydrolytic cleavage of the ester linkage. Polyether-based polyurethanes exhibit a relative high resistance to hydrolytic cleavage, when compared with polyester urethanes, and are favoured for used in applications where hydrolytic stability is required. The polyether that results in polyurethane with the best physical properties is polytetramethylene oxide and polytetramethylene glycol (PTMO and PTMEG) [25,35].

In the present, much attention has been focused on the innovation and development of newer materials from renewable sources because these materials may act as potential raw material for the polymer manufacture in the future in the place of synthetic raw materials for example polyisoprene, we can obtain from natural rubber. Besides, polyurethane was synthesized from common used diol, it is possible to prepare it from hydroxytelechelic polyisoprene. Burel et al. have prepared PU network from commercial hydrogenated hydroxy-terminated polyisoprene (EPOL[®], Atofina) [22]. Furthermore, Kebir et al. successfully prepared PU with polyisoprene backbone and they are able to control and modulate PUs structure to obtain lower or higher thermal-mechanical properties than one of commercial polydiene based PU [23, 24].

C. Additives

In addition to isocyanates and polyols, the basic materials for making polyurethanes, a wide range of auxiliary chemicals may be added to control and modify both the polyurethane reaction and the properties of final polymers.

D. Catalysts.

A number of catalysts can be used for the reaction of isocyanates with water and polyols and these include aliphatic and aromatic tertiary amines, and organometallic compounds, although compounds of mercury or lead are also used. Alkali metal salts of carboxylic acids and phenols, and symmetrical triazine derivatives are used to promote the polymerization of isocyanates. The tertiary amines are the catalyst most widely used in making PU foams. The catalytic activity depends on their structure and basicity. The organometallic catalysts also used to accelerate the urethane reaction. The most popular organometallic catalysts are stannous octoate and dibutyltin dilaurate [27].

E. Chain extenders

Chain extenders can be categorized into general classes of aromatic diol and diamines, and the corresponding aliphatic diols and diamines. Trifunctional or higher functional chain extenders also act as branching or crosslinking agents. Common commercial chain extenders included 1,4-butanediol (BD), ethylene diamine(ED), 4,4'-methylene bis(2-chloroaniline) (MOCA), ethylene glycol (EG) and hexanediol (HD) [25] .

Diamine chain extenders react rapidly and vigorously with isocyanates to produce urea groups, and the resultant urea group can produce a polymer crosslinked with biuret link [25].

F. Crosslinking agents

Crosslinking agents have a functionality of three or more. They are also sometimes known as curing agents. They are used to increase the level of covalent bonding in rigid polyurethane such as some rigid foam and also as additives in many semi-rigid foam systems. The commonly used crosslinking agents are diethanolamine, triethanolamine and glycol [25,27].

G. Others

a) *Blowing agents*. They were used in foam manufacturing to form bubbles during the polymerizing reaction [25]. Flexible polyurethane foams are usually made using the carbon dioxide formed in the reaction of water and diisocyanate either as the sole blowing agent or as the principal blowing agent in association with trichloromonofluoromethane or methyl chloride, or a mixture of both [25,27]. However, because of the toxicity of these chemical and problem in eliminate excess CO₂, nowadays, a directly CO₂ injection in mixture of isocyanate and polyol was used in a foam production.

b) *Surfactants*. Surface-active materials help in mixing immiscible components of the reaction mixture. They are particularly useful in foam making where they help to control the size of the foam cells. Early polyurethane foams system used one or more organic, usually non-ionic surfactants, such as substituted nonyl phenols, fatty acids ethylene oxide condensates and alkylene oxide block copolymers. Most flexible and rigid foams are now made using organosiloxanes or silicone-based surfactants [27].

c) *Fillers*. Particulate and fibrous fillers may each be used in most kinds of polyurethanes. Particulate fillers are used in flexible polyurethane foams to reduce their flammability and to increase the weight of seat cushions for furniture and to increase their resistance to compression. Fibrous fillers are reinforcing; they give increased stiffness and they increase the range of operating temperature of rigid foams, self-skinning foams and flexible reaction injection moulding products [27].

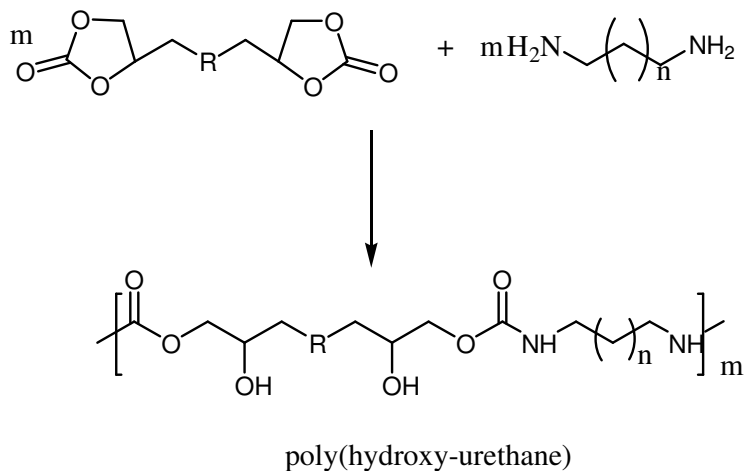
Mineral fillers are sometimes used to reduce coasts and to increase the compressive strength of rigid foams used in composite building panels [25].

d) *Colouring materials*. Organic and inorganic pigments can be used. Dispersion of suitable pigments in polyols or in plasticizers is available from suppliers. The pigment must not react with isocyanate and must be stable at high curing temperatures. The most widely used colouring material is carbon black which gives some protection against surface discoloration caused by UV light [27].

e) *Flame retardants* are added to polyurethane to reduce the flammability as measured by specific test under particular set of controlled standard conditions. The most widely used flame-retardants are chlorinated phosphates esters [27].

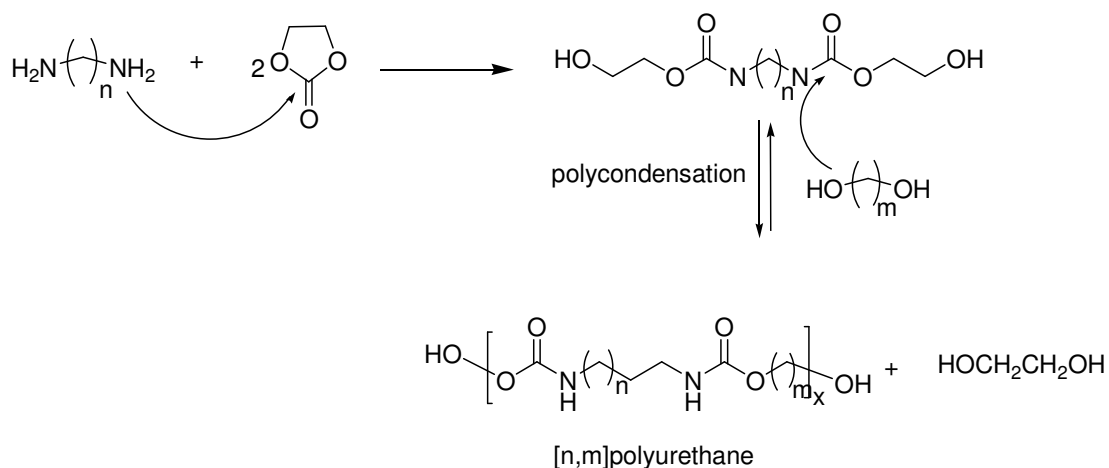
- **Synthesis from carbonate derivatives**

Besides polyesters and polyethers, polycarbonates are used as polyol reagents. Oligomers terminated with five-member cyclic carbonate groups are reacted with diamines to obtain product containing hydroxyl groups in β -position [42-47]



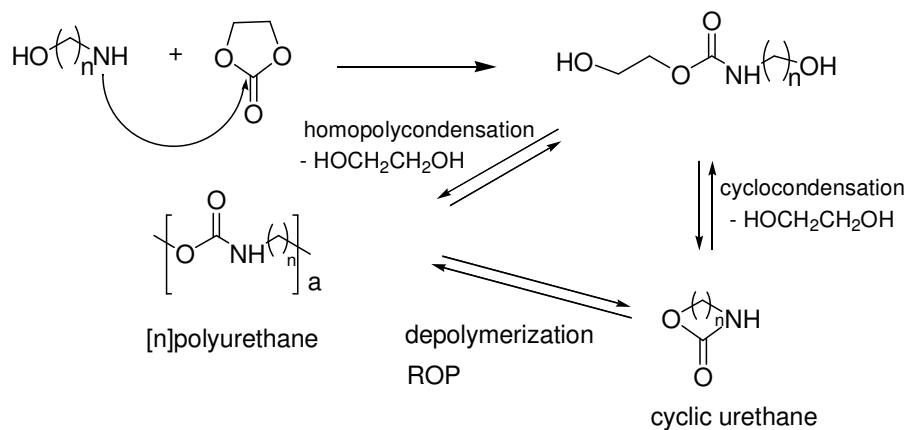
Scheme 1.20 Reaction of cyclic carbonate and diamine.

Rokicki et al. proposed a new method of the synthesis of aliphatic polyurethanes from diamines and diols or alternatively from α,ω -aminoalcohols using ethylene carbonate as a substitute of phosgene. It has been found that bis(2-hydroxyethoxycarbonylamino)alkanes and diols containing six or more carbon atoms in a molecule carried out in the presence of tin coordination catalysts, lead to $[n,m]$ polyurethanes and ethylene glycol formed as a side-product [42] (Scheme 1.21).



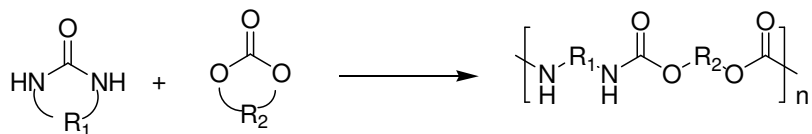
Scheme 1.21 Synthesis of [n,m]polyurethane.

Moreover, the cyclic urethane and [n]polyurethane can also be obtained from the reaction of ethylene carbonate with α,ω -aminoalcohols (Scheme 1.22).



Scheme 1.22 Synthesis of [n]polyurethane from cyclic carbonate and aminoalcohol.

The copolymerization of 2,2-dimethyltrimethylene carbonate and ϵ -caprolactam to result a copolymer with the alternating ester and urethane groups was reported by Wurm et al. First, the polycarbonate is formed and then the insertion of ring-opened lactam moiety into the carbonate group occurs [48]. In the same way, an aliphatic polyurethane can be prepared by copolymerization of trimethylene urea with cyclic carbonate five- or six-members ring [49]. Therefore, the copolymerization of equimolar amounts of 2,2-dimethylene carbonate (DTC) and tetramethylene urea (TeU) was done by Schmitz et al. The microstructure of resulting copolymers depends on the reaction conditions and catalyst.

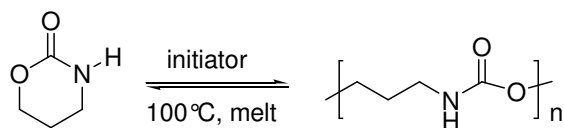


Scheme 1.23 Reaction of cyclic carbonates with cyclic ureas.

- **Synthesis of PU from aliphatic cyclic urethanes.**

Alternatively, aliphatic polyurethanes can be prepared according to a chain growth polymerization method, employing ring opening polymerization of aliphatic cyclic urethanes [50-52].

Cationic ring-opening polymerization of trimethylene urethane at 100°C using methyl trifluoromethane sulfonate (TfOMe), Trifluoromethanesulfonic acid (TfOH) and $\text{BF}_3 \cdot \text{OEt}$ as initiator to obtain poly(trimethylene urethane) was done by Höcker et al. [50]. Hall and Schneider have used NaH and N-acetyl- ϵ -caprolactam as polymerization catalyst [53].



Scheme 1.24 Ring opening polymerization of a cyclic urethane.

1.3.2. Application of polyurethanes

The applications of polyurethanes are summarized in 7 important areas.

- **Automotive.** Polyurethanes have found increasing in this area. Applications include seating, interior padding, exterior body panels, complete soft front ends, component mounted in the engine space and accessories such as mirror surrounds and spoilers [27].

- **Furniture.** This application is dominated by polyurethane flexible foams where strong-tough but decorative- integral-skinned flexible or rigid foam structures are needed, polyurethanes are also ideal. Polyurethane competes with rubber latex foam, cotton, horsehair, polyester fibres, metal springs, wood, expanded polystyrene, polypropylene and PVC [27].

- **Construction.** When sandwiched between metal, paper, plastics or wood, polyurethane rigid foam plays an important role in the construction industry. Such composites can replace conventional structures of brick, cement, wood or metal, particularly when these latter materials are used in combination with other insulating materials such as polystyrene foams, glass fibres or mineral wool [27].

- **Thermal insulation.** Rigid polyurethane foams offer advantage in the thermal insulation of buildings. Refrigerators and other domestic appliances, and refrigerated transport. Competitive materials include cork, wood, glass fibre, mineral wool, foamed polystyrene, urea formaldehyde and phenol formaldehyde [27].

- **Footwear.** Soles and some synthetic uppers for many types of footwear are produced from polyurethanes. These compete with traditional leather and rubber, PVC and poly(ethylene-vinyl acetate). Polyurethane adhesives are widely used in shoe and slipper manufacture. Polyurethane coatings are used to improve the appearance and wear resistance of shoe uppers made from both real leather and from PVC leathercloth [27].

- **Composites in electronic applications.** Recently, thermoplastic polyurethane (TPU) doped with various alkali metal have been studied widely as polymer electrolytes for using in batteries [32,33,54] and electrochromic devices [31].

Moreover, PU are also used as host polymer in conducting composite for enhancing the mechanical properties for various applications such as molecular electronics, sensors [55], light emitting diodes [56], corrosion protection antifouling coatings [57] and electromagnetic interface shielding [58] while lightweight, flexibility and high conductivity materials are required.

- **Biomedical applications.** These materials play a major role in development of many medical devices. The interaction between polyurethane chemistry and body chemistry for improved polyurethane implant products was studied [59]. The application covers cardiovascular devices, artificial organs, tissue replacement and augmentation, enhancing coatings and many others. The associated properties for this application are durability, elasticity, elastomer-like character, fatigue resistance, compliance and acceptance or tolerance in body during the healing [25,60].

The evaluation of sunlight stability of polyurethane elastomers for maxillofacial prosthesis was done by Chu et al. [61]. Furthermore bulk and surface modification via hydrophilic/hydrophobic balance or attachments of biological active species such as anticoagulant or biorecognizable groups are possible via chemical group typical for polyurethane structure [62]. Acharya et al. synthesized -SO₂ and -COOH groups incorporated polyurethane used for metal complexation. It was found resulting polyurethane has retarded the bacterial growth significantly [63].

1.4. Ionic liquids

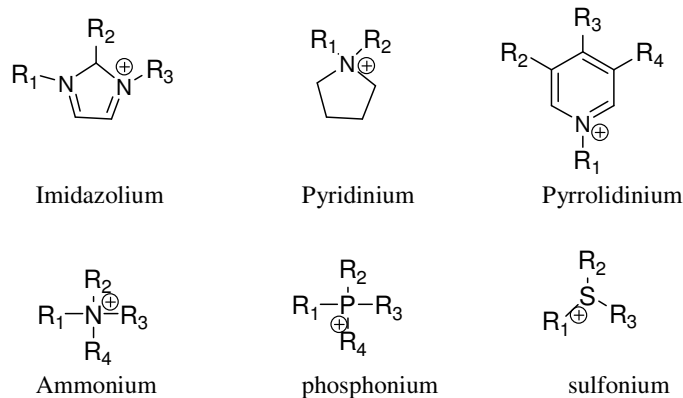
1.4.1. Definition and properties of ionic liquids

The general definition of ionic liquids (ILs) is that they have a melting point lower than 100°C. Furthermore, ILs do not evaporate like volatile organic compounds do, but they will decompose at high temperatures. The decomposition temperature depends on the IL, and particularly on the anion. The low melting point and negligible vapour pressure lead to wide liquid range, often more than 300-400°C.

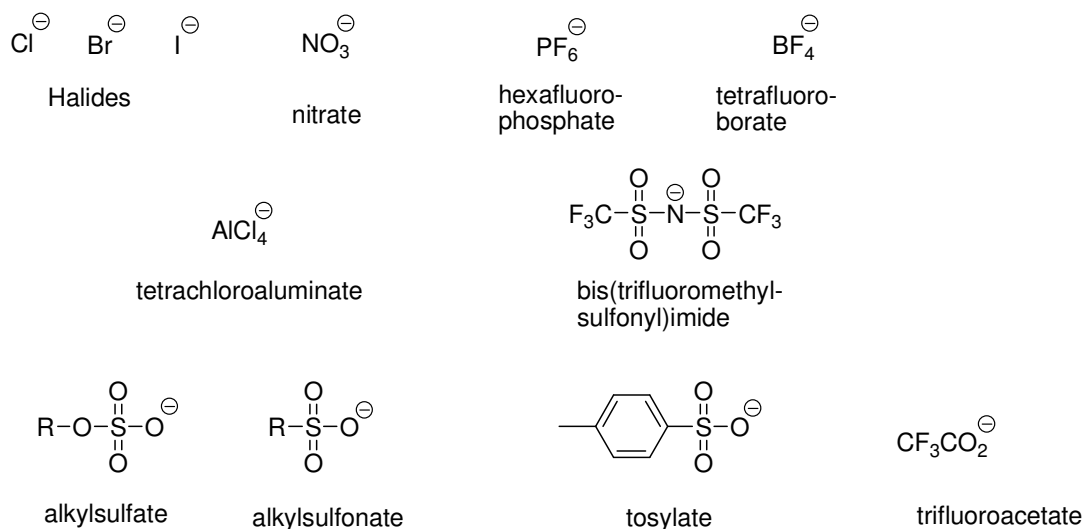
The earliest discovery of an ionic liquid can be dated to the middle of nineteenth century, when some “red oil” was observed in a Friedel-Crafts reaction. In 1914, the first room temperature IL, ethylammonium nitrate, [EtNH₃][NO₃], was synthesized [64]. In 1951 AlCl₃-based ionic liquids were developed by Hurley and Wier at Rice Institute in Texas as a bath solution for electroplating aluminium [65]. In 1963 the US Air force Academy became interested in that work and developed it further with aim of finding new electrolytes for batteries. In the 1970s Osteryoung and Wilkes succeeded in preparing room-temperature liquid chloroaluminate melts. The first organic reaction that was carried out in an acidic tetrachloroaluminate ionic liquid was Friedel-Crafts alkylation [66], and since then ionic liquids have been used as reaction solvents in various organic reactions. The first generations of ionic liquids that contain aluminium are very hygroscopic and air-sensitive, and therefore they are not easy to handle. A few year later this problem was solved when new air- and water-stable anions, such as halides, [PF₆]⁻, [BF₄]⁻ and [CF₃CO₂]⁻, were discovered by Wilkes and Zaworotko [67]. Since then, a wide selection of different ionic liquids has been synthesized.

An ionic liquid is formed from organic cations and inorganic or organic anions. Commonly used cations are large and unsymmetric, e.g. derivatives of imidazolium, pyridinium, pyrrolidinium, ammonium, phosphonium and sulfonium (Scheme1.25). Typical

inorganic anions are e.g. halides, tetrachloroaluminate, hexafluorophosphate, tetrafluoroborate and bis(trifluoromethylsulfonyl)imide and typical organic anions and alkylsulfate, alkylsulfonate, *p*-toluenesulfonate(tosylate) and trifluoroacetate (Scheme 1.26) [68].



Scheme 1.25 Commonly used cations in ionic liquids.



Scheme 1.26 Commonly used anions in ionic liquids.

The chemical and physical properties of ionic liquids can be turned by selecting a certain anion and cation combination. Also different ionic liquids can be mixed together to make binary or ternary ILs.

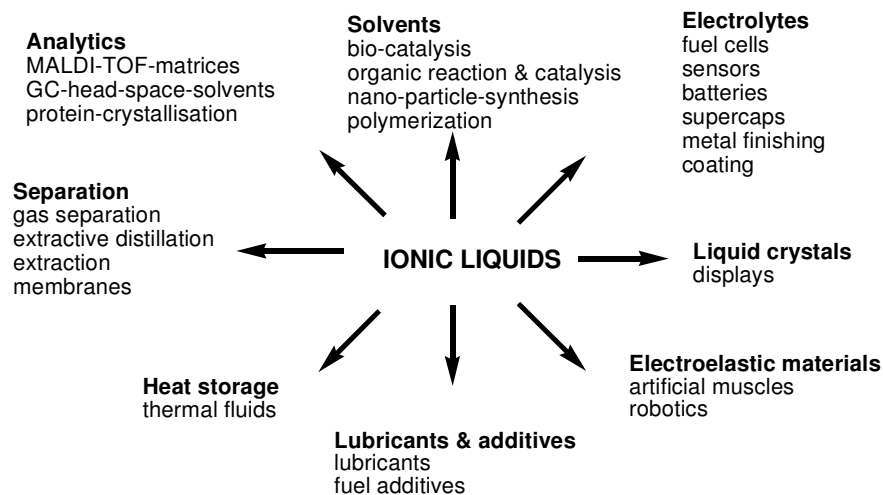
Generally, ILs are miscible into polar solvents, but not into non-polar ones. The anion usually has a larger effect on solubility than the cation, but some fine-tuning can be done with alkyl chain of cation. The longer the alkyl chains are, the more non-polar the IL is. Water

solubility is an important property, and it also varies according to the anion. Halides, tetrafluoroborate and triflate-containing ILs commonly are miscible with water, and hexafluorophosphate and bis(trifluoromethylsulfonyl)imide-containing ILs are immiscible.

The most important properties of ionic liquids are:

- thermal stability
- Low vapour pressure
- Electric conductivity
- Tunable solubility (possibility for biphasic systems)
- Liquid crystal structures
- High electroelasticity
- High capacity
- Non-flammability

These properties enable the use of ionic liquids in a wide application range as shown in Scheme 1.27 [69].



Scheme 1.27 Selection of applications where ionic liquids have been used [68].

1.4.2. Applications of ionic liquids

1.4.2.1. Used in organic synthesis

Applications of ionic liquids in organic synthesis as alternatives to conventional media are concentrated in two directions. One is to take place of organic solvents due to their unique

solvent properties and the other is to take place of liquid acids due to their variable acidity [69].

- **Transition metal-catalyzed reactions in ionic liquids.**

Ionic Liquids are used as immobilising agents for transition metal catalyst and their precursors. In the most case, catalyst precursors are immobilised in ionic liquid.

The separation of products from the reaction mixture and the recovery of catalyst are the major disadvantage in the homogeneous catalytic process. Among the various approaches to overcome these problems, ionic liquid biphasic catalysis is one of the most important alternatives. These biphasic systems might combine the advantage of both homogeneous catalysis, such as greater catalytic efficiency and mild reaction condition and heterogeneous catalysis such as ease to recycling and separation of products. Therefore, it is good reason to study well-known transition metal-catalysis in ionic liquids as alternative solvents [69-70].

The Suzuki cross-coupling reaction using a Pd catalyst in 1-butyl-3-methylimidazolium hexafluorophosphate, [bmim][BF₄], as solvent has been reported to give an excellent yield [71,72].

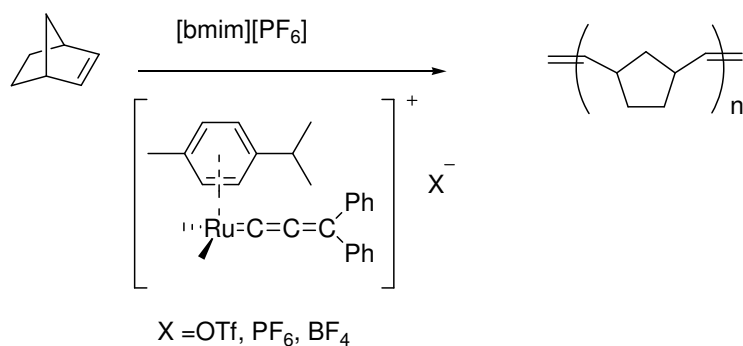
A series of Still coupling reactions with Pd catalyst precursor associated with Ph₃As in presence of Cu(II) has been demonstrated in [bmim][BF₄]. This procedure permitted extensive recycling of solvent and catalyst without a significant loss in activity [73].

Palladium-catalysed alkoxy carbonylation of aryl halides in [bmim][BF₄] and [bmim][PF₆] was done by Mizushima et al.[74].

- **Olefin metathesis.**

Olefin metathesis has become a powerful tool for cleavage, as well as the formation of C=C bonds in fine chemicals, polymers and in natural products. [75]. Buijsman and co-workers [76] reported that the Grubbs ruthenium catalyst precursor dissolved in [bmim][PF₆] promoted the Ring-Closing Metathesis (RCM) of several dienes for at least three cycles. The ruthenium allenylidene catalyst was employed in the Ring-Opening Metathesis polymerisation of cyclic olefins in the ionic liquid [bmim][PF₆] and showed a remarkable recyclability [77]. The best results were obtained by using a biphasic system comprising [bmim][PF₆] and toluene. The ionic liquid could be re-used after the sixth recycling for the

same polymerization reaction without any treatment simply by reloading a new portion of the cationic allenylidene complex [69].



Scheme 1.28 Ring-opening Metathesis Polymerization (ROMP) of norbornene [76].

- **Atom Transfer Radical Polymerization (ATRP)**

Haddle et al. first reported Atom Transfer Radical Polymerization (ATRP) of MMA in 1-butyl-3-methylimidazolium hexafluorophosphate, a frequently used room temperature ionic liquid. It was found that the reaction rate was lower in IL than those in bulk or other organic solvents. In addition, the Cu(II) contamination of resultant polymer was reduced due to the good solubility of catalyst in ionic liquid. They also found that the ionic liquid containing catalysts were easily separated from the resultant polymer and unreacted monomer and could be reused without affecting ‘living’ nature of the subsequent ATRP of MMA in it [78]. Vijayaraghavan et al. also reported the successful charge transfer polymerization of MMA by using IL as solvent. The reaction rate and polymer yields at short reaction time are enhanced compared to in conventional solvents [79].

- **C-C cleavage reactions**

The catalytic cracking of polyethylene to give light alkanes is one of the most important plastics recycling processes. The commonly used methods include pyrolysis, catalytic cracking with acidic materials and reactions in supercritical water. The wide range of products obtained is a problem in each case. A new method using acidic chloroaluminate (III) ionic liquids to crack polyethylene has been developed. It has been shown that this method is quite selective toward low molecular weight feedstock. Another advantage of this method is

that the products are very easily separated from ionic liquids by solvent extraction or other physical separation processes [70].

1.4.2.2. Biotransformations in Ionic Liquids.

The use of enzymes in organic solvents rather than in aqueous media greatly enhances their technology application. Biocatalysis in organic solvents often suffers from the disadvantage of reduced activity, selectivity or stability of enzymes, as compared to aqueous media [80]. ILs are used in three different methods in the enzyme system, as a co-solvent in aqueous phase, as a pure solvent and as a two-phases system with solvent. The use of IL in the biocatalytic transformations has solved some problems encountered in their application in aqueous and organic solvent. In lipase-catalysed reaction, the use of ILs has increased the solubility of substrate by 3-fold, and the yield has been doubled by minimising the side reactions [81].

1.4.2.3. Use of Ionic Liquids in MALDI mass spectroscopy

Room temperature Ionic Liquids with high solubilising power, negligible vapour pressure, a broad liquid range and the ability to absorb laser light have been designed for use as MALDI matrices.

They have found applications in peptide and protein quantification as well as analysis of phospholipids. The resolving power, reproducibility and ability to quantify were found to be improved by using ionic liquid matrices in MALDI [82].

1.4.2.4. Use of Ionic Liquids in materials chemistry

ILs have been used as electrolytes in electromechanical actuator systems based on conducting polymers [69] and p-conjugated polymer electrochemical devices [83].

Trialkylimidazolium-based ILs have been developed as novel, thermally stable treatment for layered silicates and graphite for the purpose of preparing high quality polymer nanocomposites by Aida and co-worker[84].

Especially, the Ionic Liquids are expected to be stable and excellent electrolyte solutions. However, most of small and light weight electronic devices require film-like electrolyte materials so-called polymer electrolytes. Polymer electrolytes from Ionic Liquid can be prepared in two ways:

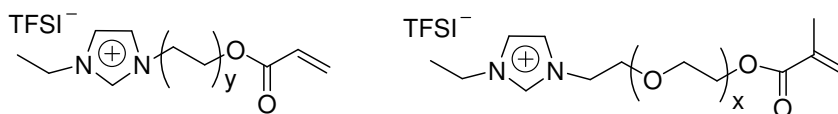
• Incorporate Ionic Liquids with polymer matrix

Room temperature ILs can be blended to form gels that may be used to make novel electronic devices, coating materials and antistatic materials.

Sigh et al. synthesized Ionic Liquids containing 2,3-dimethyl-1-octylimidazolium cation and BF_4^- , PF_6^- , CF_3SO_3^- , $\text{N}(\text{CF}_3\text{SO}_2)_2^-$ anions and incorporated in different polymers to obtain polymers which show conductivity over a wide range (10^{-3} - 10^{-6} S/cm) [85].

Gel polymer electrolytes (GPEs) of *N*-butyl-*N*-methylmorpholinium bis(trifluoromethanesulfonyl)imide ($\text{Mor}_{1,4}\text{TFSI}$) and poly(vinylidene fluoride)-hexafluoropropylene copolymer (PVdF(HFP)) were prepared by Kim et al. [86]. Ionic conductivity of GPEs containing 2 and 3 weight ratio of $\text{Mor}_{1,4}\text{TFSI}$ reached 2×10^{-3} S/cm at 60°C . GPEs containing propylene carbonate (PC) has higher ionic conductivity (10^{-2} S/cm at 60°C) than GPEs without PC because of plasticizing effect.

Ohno et al. prepared new class of GPEs by prepared the switterionic liquid and then mixed with PVdF(HFP). The conductivity of the polymer gel electrolyte is about 10^{-5} S/cm at 50°C [87].



Scheme 1.29 Structure of ionic liquid monomers tethering imidazolium cation.

• Synthesis of polymers from polymerizable Ionic Liquids

Ohno et al. have prepared polymerizable ILs and their polymers as stable polymer electrolytes [88-92]. Vinylimidazole was quaternized with alkyl halide, and then halide anion was substituted with suitable anion such as tetrafluoroborate anion. Thus obtained polymerizable ILs were polymerized to be ion conductive films. However, the ionic conductivity was extremely lowered after polymerization in spite of excellent ionic conductivity before polymerization [88]. This decreasing conductivity was explained by the decrease in the segment mobility of ions. Binding of ions through covalent bonds reduced thermal motion of the ion unit and accordingly increased the glass transition temperature. Since the ionic conductivity depends on T_g , it is essentially important to lower T_g for improvement of ionic conductivity in the polymerized ILs.

1.5. Polymer electrolytes and conducting polymers

1.5.1. Polymer electrolytes

Polymer electrolytes are prepared by dissolving electrolytes in polymers, while the polymer acts as a macromolecular solvent which solvates the electrolyte ions [93]. Polymer electrolytes have been widely investigated in recent decade since the discovery of poly(ethylene oxide) (PEO) electrolytes by Wright et al. [94]. Most of the ionic conductive polymers have been developed as mixtures of inorganic salts and PEO derivatives [95]. PEO can dissolve large amount of inorganic salts, which is attributed to the association of the ether oxygen atom with lithium (in Li battery), and can subsequently transport the dissociated ions by the segmental motion of main chain.

Polymer electrolytes have been widely studied due to their applicability for variety of solid state and electrochemical device applications including batteries [32,33,54], fuel cells [96], supercapacitors [97], electrochromic devices and chemical sensors. After a successful technical feasibility conducted by Armand et al., polymer electrolytes started to play an important role in developing new types of rechargeable lithium or lithium-ion batteries [98].

The application of polymer electrolytes in the place of liquid ones avoids the problem of electrolyte leakage from devices and also enables the design of devices with large surfaces and any shape. It has been found that polymer electrolytes based on host polymer metrics that have oxyethylene chains yield higher ionic conductivities only at elevated temperatures [94,95]. The semi-crystalline character and high glass transition temperature are the reasons for the low conductivity at ambient temperature. On the other hand, polymer electrolytes based on polyacrylonitrile, poly(vinylidene fluoride) and poly(methyl methacrylate) display higher ionic conductivity in the order of mS/cm at room temperature [99].

1.5.1.1. Types of polyelectrolyte

The polyelectrolytes are used widely in two ways:

- **Solid polymer electrolytes (SPE)**

Solid polymer electrolytes (SPEs) are formed by complexing a polymer with alkali metal salts. The ionic conductivity is due to the motion of dissolved ionic species in a polymeric matrix. The ionic mobility is promoted by segmental motion of polymer host and the conduction take places in the amorphous phase of the SPEs [100]. Since the early work of

Wright [101] and Armand et al., solid polymer electrolytes have been studied with much interest for their applications in solid state electrochemical devices [102].

From the studies of the ionic conduction mechanism for PEO+LiX electrolytes, it was found that the ionic transport take place in the amorphous phase [94,95,103] and conductivity depends on several factors, such as the mobility of flexible chain, the degree of dissociation of salts and the anion radius. Since the linear PEO chain demonstrated a very high solvating power and high flexibility at high temperature, the earliest lithium polymer electrolytes were proposed using a linear PEO polymer. However, at ambient temperature, PEO+LiX system exhibited low conductivity due to high crystallinity. In order to overcome this drawback of high crystallinity at ambient temperature, several approaches were undertaken via modifying the polymer chain to reduce T_g , increase the amorphous character of PEO-type polymers and improve the conductivity at ambient temperature [104-107]. Random copolymers [108], block copolymers [109-110] and comb-branched block copolymers were used to increase the conductivity of polymer electrolytes due to the increase in the amorphous character of PEO portion.

Hong et al. prepared three polyurethane electrolytes with a linear polyurethane an hybrid of linear and hyperbranched polyurethanes and a low crosslinked copolymer of a linear and hyperbranched polyurethanes complex with LiClO_4 . Ionic conductivities are 10^{-5} - 10^{-7} S/cm [100].

Santhosh et al. prepared solid polymer electrolytes by mixing LiClO_4 in DMF with crosslinked polyurethane acrylates with polyurethane acrylate (PUA) solutions in the presence of initiators, thermal crosslinked performed through the acrylate end groups [111].

Besides using alkali metal salts to complex with polymers in preparing polymer electrolytes, recently, ILs are also used to incorporate with polymers. They can act as plasticizers and ions carriers in polymer electrolytes [85,112-114].

Composite solid electrolytes based on polyacrylonitrile (PAN), poly(ethylene oxide) (PEO) and poly(vinyl alcohol) (PVA) and ionic liquids as well using plasticizers were prepared. The polymer electrolytes showed a rubber like characteristic. The electrochemical stability window of electrolytes, determined at the glassy carbon electrode was about 3 V [115].

In addition, Ohno et al. [88-92] have prepared new type polyelectrolyte from polymerizable ionic liquid PEO derivatives which have imidazolium salts and vinyl end

groups in structure. The ionic conductivity is increased as ethylene oxide (EO) unit number increases but ionic conductivity of polymers decreased compared with monomers. It is suggested that the distance between vinyl polymer and terminal imidazolium cation is an important factor with respect to high ionic conductivity for these molten salt-type polymers.

• Gelled polymer electrolytes (GPE)

Recently, high permittivity molecules, ethylene carbonate (EC) and propylene carbonate (PC) have been added to the polymer host as plasticizer to form gel-type electrolytes [116,117]. In this case, the main role of polymer is to serve as the matrix of film, which provides mechanical strength. The conductivities of gel electrolytes were improved to 10^{-3} to 10^{-4} S/cm at room temperature due to the solvating power and mobility of plasticizers.

Polymeric gel electrolyte films consisting of poly(ethylene oxide)-based polyurethane containing lithium salt (LiClO_4 and LiPF_6) dissolved in propylene carbonate have been prepared by Yoshimoto et al. [32] and Wen et al. [54]. Films are self-standing, transparent and flexible with high mechanical strength and high conductivity. The highest conductivity, 1.5 mS/cm at 60°C , was obtained for the polymeric gel containing 50% of $1.5 \text{ ml/dm}^3 \text{ LiClO}_4/\text{PC}$.

A composite polyelectrolyte of TPU/PPy in LiClO_4/PC was prepared by Wen et al. [118]. The composite shows higher ionic conductivity than pure TPU at the same amount of LiClO_4/PC .

Gel polyelectrolytes were also prepared by incorporating ionic liquid and polymer in the presence of PC [86]. A new class of GPE was prepared by mixing the switterionic liquid and then mixed with PVdF(HFP) [87]. These GPE were obtained as films with switterionic liquid up to 80 wt%.

1.5.1.2. Polyurethane based polyelectrolytes

The researchers have focused their attention on the synthesis of novel polymeric materials possessing high ionic conductivity, mechanical strength, and thermal stability which could ultimately be used for practical applications. Extensive research on uses of PEO revealed that ionic conduction occurs in the amorphous region of electrolytes. In the research for producing amorphous, mechanically stable polyether host matrices for polymer electrolytes, different approaches such as synthesis of polymer blends, composite polymer electrolytes, and polymer networks with physical and chemical crosslinked have been made. Thermoplastic polyurethanes (TPUs) have also been studied as a matrix of polymer electrolytes [119].

Recent reports have noted that polyurethane (PU)-based polymers can be used as polymer electrolytes for rechargeable lithium-ion batteries [31-33]. The interest in using PU as a matrix for polymer electrolytes is related to the possibility of increasing the mechanical properties of linear polyethers. Furthermore, the low glass transition temperature (T_g) hences higher mobility of the dissolved ions. The hard segment domains, which are in the glassy state and either distributed or interconnected throughout the rubbery phase of the soft segment, act as reinforcing filler and hence contribute to the dimensional stability of the polymer electrolyte.

Cheng et al. [102] proposed a series of polymer-based electrolytes from water-borne polyurethanes. They show good results for both single-ion conductors without adding any salt and gel-type electrolytes.

Lee et al. [120] studied the effect of the oxyethylene chain on the conductivity of a polyurethaneurea electrolyte synthesized from 4,4'-diphenylmethane diisocyanate (MDI), poly(ethylene glycol) (PEG), and 3,5-diaminobenzoic acid using LiClO_4 as dopant. The increasing of T_g and shift of carbonyl and ether bands with salt concentration show the Li^+ ions coordinate of the urethane and urea groups of PUU with ether oxygen of PEG. DSC shows the lower T_g of soft segment as longer length of oxyethylene chain is.

Heumen et al. [26] used $\text{NH}_4\text{CF}_3\text{SO}_4$ as dopant for PU with the soft segments of poly(tetramethylene glycol) (PTMG) and poly(propylene glycol) (PPG). The conductivity of PPG-based TPU/ $\text{NH}_4\text{CF}_3\text{SO}_3$ at 100°C is about 10^{-5} mS/cm. They have also prepared TPU from polytetramethylene oxide (PTMO), MDI and using 1,4-butanediol as chain extender.

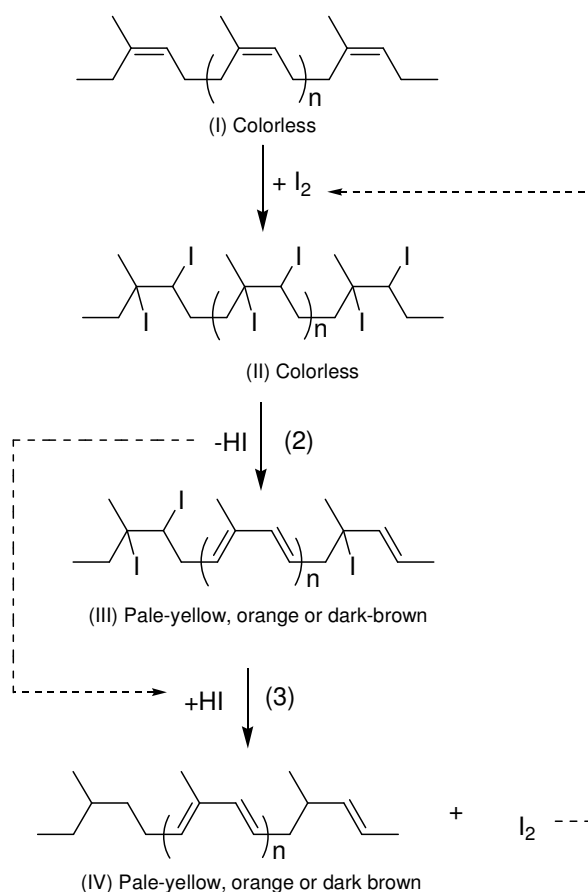
Shibata et al. [121] found that the ionic conductivity of poly(etherurethane)-based electrolyte increased up to 10^{-5} S/cm at room temperature by blending with polysiloxane or polyether-modified polysiloxane. The improvement of conductivity is attributed to increase of ion mobility and decrease of ion density.

1.5.1.3. Polyelectrolyte from rubber.

Marwanta et al. [122] prepared polyelectrolyte with high ionic conductivity (1.2×10^{-5} S/cm at 50%wt ionic liquid) and good elasticity by mixing nitrile rubber (poly(acrylonitrile-co-butadiene) rubber; NBR) with ionic liquid, *N*-ethylimidazolium bis(trifluoromethanesulfonyl)imide (EImTFSI). Films are transparent at ionic liquid content less than 60%wt.

Klinklai et al. [123,124] investigated the conductivity of deproteinized and highly deproteinized liquid natural rubber having epoxy group (LEDPNR) mixed with alkali metal salts. It found that ionic conductivity of resulting LEDPNR was dependent upon the alkali metal salts.

Dai [125] reported that a I_2 -doping of 1,4-polyisoprene yields soluble conjugated conducting polymers through double bonds shifting reactions. The formation of conjugated sequences of unsaturated double bonds in the polyisoprene backbone is followed by ultraviolet/visible and nuclear magnetic resonance spectroscopies. The sequences are stable and, resembling polyacetylene, they are probably responsible for the high conductivity of 'I₂-doped' polyisoprene (Scheme 1.30).



Scheme 1.30 Reaction of polyisoprene with I_2 leading to the formation of conjugated sequences.

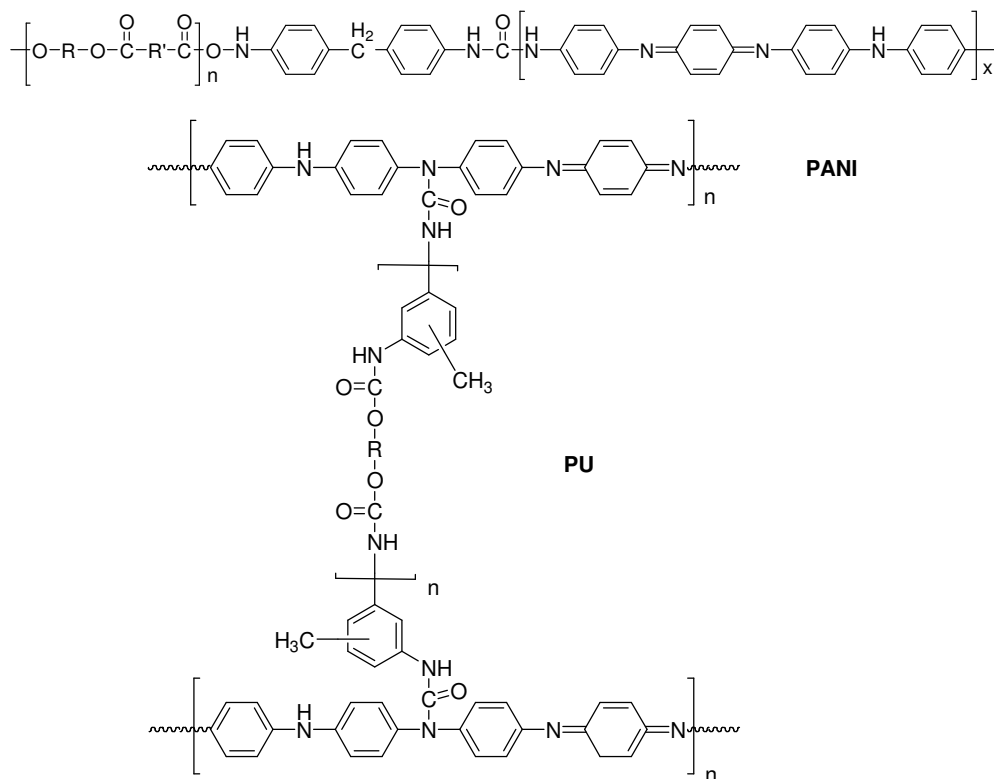
1.5.2. Conducting polymers composites

Electroconductive polymers have attracted a great deal of attention, mainly due to their potential application in a variety of new technologies, such as electronic devices, electrochromic displays [126], rechargeable batteries [32], electromagnetic interference shieldings [58,127] and anticorrosion and antistatic primer layers [128,129]

Conducting polymers which are the focus of considerable current research can be classified: (a) polyacetylene, (b) poly(p-phenylene), (c) polyaniline and (d) polyheterocycles. Classes (a) and (b) exhibit high electrical conductivity which can reach to $10^{-5} - 10^{-7}$ S/cm but their poor stability restricted the wide application. Polypyrrole (PPy), polyaniline (PANI) and polythiophene in class (c) and (d) not only feature relatively high electroconductivity up to 10^{-3} S/cm but also is much more stable than polyacetylene and poly(p-phenylene). In addition, PPy, PANI and polythiophene can be much more easily prepared by an oxidative polymerization. Considering much higher cost of thiophene than pyrrole and aniline, PPy PANI should be the most attracted conducting materials with brilliant industrial background [130].

However, many potential applications of conducting polymers have been limited because of its poor mechanical properties and processability [131]. They are both insoluble in common solvents and infusible as well as their films are hard and usually brittle [130]. Due to these reasons, considerable research has been undertaken in improving its stability and mechanical properties. They have been often block copolymerized or blended with other polymers such as polyurethane (PU) [36-40], nitrile rubber (NBR) [132], poly(vinylidene fluoride) (PVDF) [133], poly(ethylene terephthalate) (PET) [134] for obtaining composites with conductivity of conducting polymer and mechanical properties of the matrix polymer.

Copolymer and polymer networks of polyurethane and polyaniline from isocyanate-terminated polyurethane prepolymer and the amine-terminated or amine group in polyaniline were prepared and studied by Wang [135] and Rodrigues [136]. Conductivity was in the 10^{-4} S/cm range.



Scheme 1.31 Polyurethane/polyaniline copolymer and Polyurethane/polyaniline network structure.

A combination of conventional polymers with conductive polymers allows the creation of new polymeric materials with interesting characteristic properties. Various methods are being followed for making composites of conducting polymers with conventional polymers.

1.5.2.1. Synthesis methods of conducting composites

One way of making composites involves synthesizing the conducting polymers inside the matrices of conventional polymers. Conducting polymer blends and composites are prepared via two routes; chemical and electrochemical method.

A. Chemical synthesis

There are many synthesis routes for the polymerization of conducting polymers by chemical methods.

a) *In situ* polymerization. This is simple and widely used in preparing the conducting composites. Conducting monomer has been polymerized in the presence of host matrix and oxidation-acid solution or initiator.

Highly transparent conducting polyaniline-nylon-6 and polyaniline-polyurethane composite films can be obtained by immersing polymer films containing aniline into an oxidant solution such as $(\text{NH}_4)_2\text{S}_2\text{O}_8$ containing HCl [133] and aqueous FeCl_3 [135].

Conductive surfaces of polyurethane were prepared by chemical polymerization of 3-methylthiophene in the PU film by immersing PU containing 3-methylthiophene in organic solution of ferric chloride [136]. Chiang et al. also used this method to prepare polyaniline-interpenetrated networks of fulleranol-polyurethanes [137].

It is also possible to incorporate oxidant or initiator into conventional polymer matrix and then exposed to the conducting monomer solution or vapour. Conductive polyurethane was prepared by impregnating PU foams with oxidant (I_2 or $\text{Fe}(\text{CF}_3\text{SO}_3)_3$) from supercritical CO_2 and then exposing to the pyrrole vapour at room temperature [138-141]. PPy-TPU composite film was synthesis by immersing TPU film in FeCl_3 /propylene carbonate solution and then film was dipped into PPy/propylene carbonate solution [142].

Another way, conducting polyaniline-coated fabric was prepared by dropwising oxidant $(\text{NH}_4)_2\text{S}_2\text{O}_8$ into solution of aniline-protonic acid containing substrate [143], while polypyrrole-coated fabric was prepared by exposing pyrrole-dipping fabrics to FeCl_3 [144,145].

b) Emulsion polymerization. The reaction is carried out in heterogeneous system, usually with both aqueous and non-aqueous phases. The monomer as well as the polymer usually dissolved in the non-aqueous phase. In other hand , in inverse system, water-soluble monomers are dispersed in a non-aqueous medium. Rucken and Yang have reported this method in preparation of PANI-PS composite. A gel-like emulsion of PS and aniline in benzene is dispersed phase and an aqueous solution of sodium dodecylsulphate is continuous phase. The oxidant dissolved in an aqueous solution of HCl was dropwised to the emulsion solution with vigorous stirring. A green to dark blue solid material was obtained [146].

c) Dispersion polymerization. The polymerization of a monomer dissolved in an organic liquid or water produces an insoluble polymer in the form of a stable colloidal dispersion. Gill et al. [147] have used a dispersion polymerization method to prepare stable polyaniline-silica colloid composites. Banerjee et al. [148] have prepared blends of HCl-doped polyaniline nanoparticles with poly(vinyl chloride), polystyrene, poly(methyl

methacrylate), poly(vinyl acetate) and poly(vinyl alcohol) by suspending polyaniline-HCl particles in solution of matrix polymer and sonicated.

d) Solution blending. Conducting and insulating polymers can be dissolved in a common solvent and afterwards processed in to thin films. A miscible conductive PANI/ PU film has been prepared by using THF as solvent. The blends were coated on the glass substrate. It showed preferable electrical properties [149]. PANI-PVC composites were prepared in the same manner [150]. Dodecylbenzenesulfonic acid doped PANI/TPU blend was prepared through casting after dissolution of both components in THF [151].

e) Dry blending. This method consists of a preparation by blending the powder of conducting and host polymer in mixer. Polyaniline-poly(methyl methacrylate and polyaniline-polystyrene blends have all been prepared by this method [152].

f) Melt processing. The conducting polymer is dispersed in a thermoplastic polymer matrix by mechanical mixing and then compression moulded in a hot press. A major requirement for this process is that thermal stability of conducting polymer should be sufficient to withstanding compound in the melt of chosen host polymer. For this purpose, the host polymer should possess a low melting temperature. Polyaniline-Poly(vinyl chloride), polyaniline-polyethylene terephthalate glycol and polyaniline-nylon-12 blends have been prepared using this method [153].

B. Electrochemical synthesis

By electro-oxidatively polymerization of conducting monomer on insulating, mechanically superior polymer film, a composite film having a high conductivity and the good mechanical properties may be obtained [152,154-156].

In the electrochemical synthesis, the monomer, the solvent and the electrolyte anion diffuse into the insulating polymer coating. As a result, polymerization starts in the interface between the electrode surface and the polymer insulating film. The electrochemical synthesis is generally accomplished by potentiostatic or galvanostatic polarization. Alternatively, the synthesis may also be carried out by cyclic voltammetry, driving the electrode potential between the limits of monomer oxidation and reduction of the synthesized electroactive polymer conducting.

The electrochemical cell consists of one, two or three compartments. Three electrodes are commonly employed: a working electrode, a reference electrode and a counter electrode. Electrochemical synthesis is carried out in aqueous or non-aqueous system and in inert atmosphere.

a) Potentiostatic polymerization

For this technique, the voltage is maintained constant. Polyaniline-polyurethane composite films with high flexibilities and mechanical strength similar to pure polyurethane and conductivity close to that of pure polyaniline have been obtained by electropolymerizing aniline on a PU-coated Pt electrode in a water/acetonitrile/ethylene glycol electrolyte solution [154,155]. A constant potential of 2.0 V was applied. In the composite films, polyaniline was dispersed in the particulate form inside and on the inner surface of the polyurethane.

Using potentiostatic polymerization method, synthesis of polyaniline-polycarbonate composites has been carried out in aqueous and non-aqueous media. The working was coated with polycarbonate by dip-coating from solution in CHCl_3 . The conductivity of composite was of the same order than that of pure PANI obtained under the same condition [157].

Polyurethane/polythiophene conducting copolymers were prepared on PU film coated Pt electrode by electrochemical polymerization of thiophene at the constant potential. They found the chemical bonds between polythiophene and polyurethane. The copolymer shows better thermal stability than polythiophene [158].

b) Galvanostatic polymerization. Composite films of polyaniline and copolyamide, poly-p-phenylene terephthalamide/diphenlyether (PPDTA) have been prepared by galvanostatic polymerization of aniline on a PPDTA/Pt working electrode in water or a mixture electrolyte solution [159]. Tungsten trioxide based polyaniline films were prepared by galvanostatic polymerization of aniline in an aqueous HCl solution containing suspended tungsten particles [152]

c) Cyclic voltammetry. Polyaniline-nitrile rubber composites were prepared by cyclic voltammetry polymerization (0-2.0 V vs Ag/AgCl) of aniline on a rubber-coated Pt working electrode using an acetonitrile solution of trifluoroacetic acid and electrolyte [160]. The increase in the anodic and cathodic peak currents was found to be proportional to the thickness of the resulting conducting film.

The chemical method of synthesis is relatively simple and cheap compared to the electrochemical synthesis. However, the electrochemical approach has several advantages in that the electrical properties of the composite can be modified by simply varying the conditions of electrolyte [158]. The electrochemical is clean. However, it limit in the size of composite films prepared that depends on the size of the electrode.

1.5.2.2. Polyurethane based conducting polymers

Polyurethane offers the elasticity of rubber combined with the toughness and durability. Owing to such interactions, interconnected or isolated hard segments remain distributed in the soft segments matrix, through the soft domain may contain some hard segments dissolved in it [38]. The recent technological interest concerns the studies on composites containing conductive polymers and inert polymer matrix. In the case of conducting polymers, the objective is the preparation of polymeric materials with good mechanical properties and processability associated with high conductivity.

- **Synthesis of TPU-PANI composites**

Polyaniline is only conducting polymer whose electrical properties can be controlled suitably by charge-transfer doping and/or protonation due to its reversible electrochemical response during anodic oxidation and cathodic reduction. However, two major limitations of polyaniline is an unprocessability by conventional methods and its poor mechanical properties. These limitations can be overcome by preparing conducting PANI blends and composites, which possess the mechanical properties of the insulating host matrix and electrical properties of conducting PANI.

Recently, incorporation of conductive PANI into a host polymer forming interpenetrated network (IPN) has been a newly adopted method as an approach to combine electrical conductivity of PANI with desirable mechanical strength of insulating polymers.

Pei and Bi [154,155] used potentiostatic polymerization technique to prepare polyaniline-polyurethane composite films with high flexibility and mechanical properties similar to those of pure polyurethane and conductivities close to that of pure PANI. PANI was dispersed inside the inner surface substrates.

Wang et al. [161] prepared PANI-PU IPN using chemical oxidative process in HCl solution. The resulting products were washed with water and THF for remove excess aniline monomer.

Hrehorava et al. [36] reported electrical properties of polyurethane elastomer/polyaniline composite films under tensile deformation. Surface modification of PU was performed by swelling the parent film in aniline followed by its contact with acidified oxidant solution to polymerize aniline and form PANI-HCl distributed inside surface/subsurface layer of the film. Volume modified PU was prepared by mixing PU and PANI-HCl solution in dimethylformamide and then casting on PVC substrate. Nonlinear current-voltage characteristics were obtained in the surface modified PU and linear characteristic were obtained in case or volume modification samples.

Flexible and freestanding films from polyurethane based on castor oil were synthesized by Malmonge et al. [162]. The polyurethane based on castor oil was prepared by pre-polymer method while PANI dissolved in N-methyl-2-pyrrolidinone (NMP) was separately prepared. The PANI solution was mixed with polyol and then the polyurethane at the desired proportions was added. Films were prepared by casting solution on glass surface.

Electrically anisotropic polyaniline–polyurethane composites were prepared by applied electric field in liquid medium for induce orientation of polyaniline particles and subsequently polymerized into polyurethane network [163].

Liao et al. [164] reported a series of novel conducting IPN prepared by sequential polymerization of maleimide-terminated polyurethane (UBMI) and polyaniline (PANI) which were doped with dodecylbenzenesulfonic acid (PANIDB). The solution of PANIDB and UBMI was stirred for 48 h for approaching the equilibrium conditions. Then, benzoyl peroxide, 1% wt based on the weight of UBMI was added into solution and stirred well at room temperature. The mixture was later casted into mould.

Polyaniline-dodecylbenzenesulfonic acid/Polyurethane (PANI-DBSA) blends were prepared by in situ polymerization of aniline in a well-dispersed aqueous solution of PU ISP-blend) and by simple solution mixing method (SM-blend).The ISM-blend shows the homogeneous structure and high dielectric constant. [37]. Wang et al. reported that *p*-dodecylbenzenesulfonic acid doped Polyaniline/Polyurethane displayed good antifouling property [57]. PU with *m*-phenylene 4-diaminosulfonic acid (PDSA) as chain extender blending with (DBSA) doped polyaniline was prepared by Ho et al. [40]. They reported that

chain extender can influence the properties of blends. The sulfonic chain extender PDSA provides an additional probability of creating H-bonding with DBSA.

- **Synthesis of TPU-PPy composites**

Polypyrrole like many conductive polymers is insoluble in most organic solvents and infusible because of its decomposition before melt. As thus result, the conventional methods for polymer processing may not usually be applied.

Due to this reasons, several attempt has been made to improve the poor mechanical properties and conductive polymer making blends or composites with other conventional polymers.

The effect of conducting PPy on the morphology and ionic conductivity of thermoplastic polyurethane doped LiClO_4 has been described by Wen et al. [118]. They used polyether-based PU that has ether linkages in the main chain. The polyurethane has the advantage to coordinate alkali metal ions and can be used as polymer electrolyte in Li batteries. PU was coated on polypropylene plates, after dried, films were immersed in FeCl_3/PC solution and then dipped into pyrrole/PC solution. After remove unreacted component, the composite films were thus obtained and dried.

The composite synthesis of PU-PPy by electrochemical polymerization of pyrrole inside PU films was reported by Bi and Pei [165].

The conductive elastomeric polyurethane foams were developed by Fu et al. [166]. The FeCl_3 in methanol solution was diffused into PU foam and then the PU/oxidant composite was exposed to the pyrrole monomers vapours. A deficiency of this method is that rather large amounts of solvent were used. In later work, they prepared this composite via a Supercritical carbon dioxide method. The solvent was avoided by using Supercritical carbon dioxide (scCO_2) as solvent. Shenoy et al. [136,137] used ferric trifluoromethane sulfonate ($\text{Fe}(\text{CF}_3\text{SO}_2)_3$) and I_2 in scCO_2 and ethanol cosolvent.

- **Synthesis of TPU-PT composites**

Recently, Seri et al. synthesized polyurethane/polythiophene (PU/PT) conducting copolymer using PU as matrix by electrochemical method [167]. In dropping coating method, PU-Pt bipolymer film in acetonitrile and benzonitrile medium using LiClO_4 and tetraethylammonium tetrafluoroborate as electrolyte respectively, were prepared in presence of thiophene. The PU film was coated on the cleaned electrode surface of working electrode.

The PU-coated electrode was placed into the electrolysis cell and the electrolysis was run in a given potential. The amounts of insulating and conducting polymers were determined gravimetrically.

For the suspension method [167], the PU/PT bipolymer films were synthesized onto a platinum electrode surface using mixture of 0.1 M thiophene + 0.2 M LiClO₄ + PU solution in each half-cell in an acetonitrile medium. Prior to electrosynthesis, the mixture was thoroughly stirred to disperse PU solution. PU/PT bipolymer film in benzonitrile medium was also achieved using a mixture of 0.1 M thiophene+0.2 M Et₄NBF₄+PU solution in each half-cell under the same conditions.

Urethane-substituted polythiophene exhibits good solubility and improves processability. The polyurethane-substituted polythiophene in β -position (P3UT) that was chemically synthesized by solution polymerization using FeCl₃ as the oxidant in chloroform, is not only soluble in common solvent, but also in strong polar solvents such as N,N-dimethylformamide, N,N-dimethylacetamide and NMP. The blends of P3UT with PU were prepared by dissolving each component in THF. The films were cast from solution into glass plates [168].

Ruckenstein and Sun [136] prepared PU films containing 3-methylthiophene by condensation of poly(propylene glycol) diol, poly(propylene glycol) triol and TDI in the presence of catalyst.

1.5.2.3. Conducting composite polymers from rubber

Yildirim et al. polymerized pyrrole on cis-1,4-polybutadiene-coated Pt-electrode. The insulating polymer film was dip-coated from cis-1,4-polybutadiene (PB) solution. PPy-cis-1,4-polybutadiene composites were prepared by electrochemical oxidation of pyrrole onto cis-1,4-polybutadiene coated Pt-electrode. It was observed that the amount of coated PPy changes as function of the time of electrolysis. Rate of PPy polymerization is dependent on the thickness of cis-1,4-polybutadiene coating. They found that the covalent bonds may be formed between PPy and cis-1,4-PB because there are no weight change when washed film with chloroform which it is the solvent of PB. SEM image shows that PPy grows uniformly in the insulating cis-1,4-PB [169].

Yigit and coworkers synthesized conducting polymer composites of polythiophene using synthetic and natural rubbers as the insulating matrices. The composites were prepared

by electrochemical polymerization of thiophene onto a synthetic or natural rubber-coated PT electrode [170].

1.6. Conclusion

The literature survey allows us to review various methods and properties of telechelic polyisoprene synthesis. The oxidative degradation by periodic acid shows the simple way and controlled feature. Therefore, we have chosen this method in the degradation of cis-1,4-polyisoprene in this work.

In addition, in this survey, we have remarked the various applications of polyurethanes in our daily life. Because of the unique properties of the phase separation in their structure, the properties are varied from soft, flexible to hard materials. Polyurethane meets the requirement that is necessary for the electronic applications. It can be used as the matrix in polyelectrolytes, conducting composite and other applications. The soft segments mobility allows an ion transfer in the matrix while hard segments give the good mechanical properties in the polyelectrolytes and conducting composite applications.

In this study, we also found that the new generation salts, ionic liquids, were recently used in numerous applications. They show many special properties, especially high conductivity, low volatility and non-flammability that are suitable for being employed in the polyelectrolyte application. The incorporation of these salts in polyelectrolyte instead of common alkali salts, such as LiClO_4 , LiPF_6 permits the synthesis of a new class of polyelectrolytes. It also can avoid an migration problem as presented for the organic electrolytes incorporation. This brings us the idea of their incorporation in the polyisoprene based polyurethane in our case.

Furthermore, the survey of the conducting polymer composites literature confirmed us that polyurethanes are widely use as well as the host material in conducting composites to obtain elastomeric materials with good conductivity. Also, the employment of rubber in polymer electrolytes and conductive composites pointed out the possibility of ion transfer along polyisoprene chains. The elasticity properties of elastomer enhance ion mobility and ion transfer in the matrix. This exposed the potential for using polyisoprene based polyurethane as matrix in polyelectrolytes and conducting composites.

This survey also let us to choose method for preparing the composites. The *in situ* polymerization of conducting monomers on polymer matrix is simple and cheap , while the electropolymerization technique is clean and leads an easier control of the reaction by potential application.

References

1. H.M. Nor, J.R. Ebdon, Prog. Sci. 23 (1998) 143.
2. G. Boccaccio, H. de Livonnier, Actual. Chim. 2 (1991) 100.
3. J. Tangpakdee, M. Mizokoski, A. Endo, Y. Tanaka, Rubber Chem. Technol. 71 (1998) 795.
4. J.I. Cunneen, NR Technol. 4 (1973) 65.
5. T. Ravindran, M.R. Gopinathan, J.D. Francis, Makromol. Chem. Rapid Commun. 7 (1986) 159.
6. S.K. Gupta, M.R. Kurup, E. Devadoss, R. Muthiah, S. Thomas, J. Appl. Polym. Sci. 30 (1985) 1095.
7. R. Criegée, Angew. Chem. Internat. Edit 14 (1975) 745.
8. Y. Tanaka, Y. Shimizu, P. Boochthum, M. Shimizu, R. Mita, Polymer 34 (1993) 1098.
9. G. Montaudo, E. Scamporrino, D. Vitalini, R. Rapisardi, J. Polym. Sci. Polym. Chem.; Part A 30 (1992) 525.
10. M.P. Anachkov, S.K. Rakovski, R.V. Stefanova, Polym. Degrad. Stab. 67 (2000) 355.
11. D. Burfield, S.N. Gan, Polymer 18 (1977) 607.
12. D. Reyx, I. Campistron, Die Angew. Makromol. Chem. 247 (1997) 197.
13. S. Gillier-Ritoit, D. Reyx, A. Laguerre, I. Campistron, R.P. Singh, J. Appl. Polym. Sci. 87 (2003) 42.
14. R.S. Mauler, F.M. Guaragna, D.L. Gobbi, D. Samios, Eur. Polym. J. 33 (1997) 399.
15. P. Phinyocheep, C.W. Phetphaisit, D. Derouet, J.C. Brosse, J. Appl. Polym Sci 95 (2005) 6.
16. C. Guizard, H. Cheradamme, Eur. Polym. J. 17 (1981) 121.
17. D.C. Dragunski, A.R. Freitas, A.F. Rubira, E.C. Muniz, Polym. Degrad. Stab. 67 (2000) 239.
18. P.N. Thanki, D. Reyx, I. Campistron, A. Laguerre, R. P. Singh, Eur. Polym. J. 40 (2004) 2611.

19. J.C. Marmo, K.B. Wagener *Macromolecules* 26 (1993) 2137.
20. J.C. Marmo, K.B. Wagener, *Macromolecules* 28 (1995) 2602.
21. S. S. Solanky, I. Campistron, A. Laguerre, J.-P. Pilard, *Macromol. Chem. Phys.* 206 (2005) 1057.
22. F. Burel, A. Feldman, C. Bunel, *Polymer* 46 (2005) 483.
23. N. Kebir, G. Morandi, I. Campistron, A. Laguerre, J.-F. Pilard, *Polymer*, 46 (2005), 6844.
24. N. Kebir, I. Campistron, A. Laguerre, J.-F. Pilard, C. Bunel, J.-P. Couvercelle, C. Gondard, *Polymer*, 46 (2005), 6869.
25. N.M.K. Lamba, K. A. Woodhouse, *Polyurethane in biomedical applications*, CRC Press, Florida, 1998.
26. J. van Heumen, W. Wieczorek, M. Siekierski, J.R. Stevens, *J. Phys Chem* 99(1995) 15142.
27. G. Woods, *The ICI polyurethane book*, 2nd ed., ICI Polyurethane and John Wiley & Sons, Netherland, 1990.
28. B.A. Dombrow, *Polyurethanes*, 2nd ed., Chapman and Hall, London, 1965.
29. C.A. Furtado, P.P. de Souza, G. Goulart Silva, T. Matencio, J.M. Pernaut, *Electrochim. Acta* 46 (2001) 1629.
30. F. Groce, F. Gerace, G. Dautzemberg, S. Passerini, G.B. Appetecchi, B. Scrosati, *Electrochim. Acta* 39 (1994) 2187.
31. J.D.van Heumen, J.R. Stevens, *Macromolecule* 28 (1995) 4268.
32. N. Yoshimoto, H. Nomura, T. Shirai, M. Ishikawa, M. Wakihara, *Electrochim. Acta* 50 (2004) 275.
33. T.-T. Cheng, T.-C. Wen, *J. Electroanal. Chem.* 459 (1998) 99.
34. Z. Wirpsza, *Polyurethanes : Chemistry, Technology and Applications*, Ellis Horwood Limited, New York, 1993.
35. M. Seki, K. Sato, *Makromol. Chem* 193 (1992) 2971.
36. E. Hrehorova, V.N. Bliznyuk, A.A. Pud, V.V. Shevchenko, K.Y. Fatyeyeva, *Polymer* 48 (2007) 4429.
37. C.-P. Chwang, C.-D. Liu, S.-W. Huang, D.-Y. Chao, S.-N. Lee, *Synth. Met.* 142 (2004) 275.
38. Y.Z. Wang, Y.C. Hsu, R.R. Wu, H.M. Kao, *Synth. Met.* 132 (2003) 151.
39. L.Y. Chiang, L.Y. Wang, C.S. Kuo, J.G. Lin, L.Y. Huang, *Synth. Met.* 84 (1997) 721.
40. K.S. Ho, K.H. Hsieh, S.K. Huang, T.H. Hsieh, *Synth. Met.* 107 (1999) 65.

41. A. Nathan, D. Balikal, N. Vyavahare, S. Zalipsky, J. Kohn, *Macromolecules*, 25 (1992) 4476.
42. G. Rokicki, A. Piotrowska, *Polymer* 43 (2002) 2927.
43. B.Ochiai, Y. Satoh, T. Endo, *Green Chem.*, 7 (2005) 765.
44. N. Kihara, Y.Kushida, T. Endo, *J. Polym. Sci, Part A : Polym. Chem.*,34 (1996) 2173.
45. N. Kihara, T. Endo *J. Polym. Sci, Part A : Polym. Chem* 31 (1993) 2765.
46. H. Tomita, F. Sanda, T. Endo, *J. Polym. Sci, Part A : Polym. Chem* 39 (2001) 851.
47. H. Tomita, F. Sanda, T. Endo, *J. Polym. Sci, part A : Polym. Chem* 39 (2001) 860.
48. B.W. Wurm, H. Keul, H. Höcker, *Macromolecules* 25 (1992) 2977.
49. F. Schitz, H. Keul, H. Höcker, *Polymer* 39 (1998) 3179.
50. S. Neffgen, H. Keul, H. Höcker, *Macromolecule* 30 (1997) 1289.
51. H.K. Hall, Jr, *J. Am Chem. Soc* 80 (1980) 6412.
52. J. Kusan, H. Keul, H. Höcker, *Macromolecules* 34 (2001) 389.
53. H.K. Hall, Jr. A.K. Schneider, *J. Am Chem Soc.* 80 (1958) 6409.
54. T.-C. Wen, W.-C. Chen, *J. Power Sources* 92 (2001) 139.
55. S. Brady, K.T. Lau, W. Megill, G.G. Wallace, D. Diamond, *Synth. Met.* 154 (2005) 25
56. C.-H. Kuo, K.-C. Peng, L.-C. Kuo, K.-H. Yang, J.-H. Lee, M.-K. Leung, K.-H. Hsieh, *Chem. Mater.* 18 (2006) 4121.
57. X.-H. Wang, J. Li, J.-Y. Zhang, Z.-C. Sun, L. Yu, X.-B. Jing, F.-S. Wang, Z.-X. Sun, Z.-J. Ye, *Synth. Met.* 102 (1999) 1377.
58. O. Yavuz, M.K. Ram, M. Aldissi, P. Poddar, H. Srikanth, *Synth. Met.* 151 (2005) 211.
59. R.E. Philips, M.C. Smith, R.J. Thomas, *J. Biomaterials Applications*, 3 (1988) 207.
60. R.J. Zdrahala, I.J. Zdrahala, *J. Biomaterials Applications* 14 (1999) 67.
61. C.C. Chu, T.E. Fisher, *J. Biomat. Res.* 12 (1978) 347.
62. J.N. Baumgartner, C.Z. Yang, S.L. Cooper, *Biomaterials* 18 (1997) 831.
63. V. Archaya, C.R. Prabha, C. Narayanamurthy, *Biomaterials* 25 (2004) 4555.
64. T. Wilton, *Chem. Rev.* 99 (1999) 2071.
65. Hurley FH & Wier TP, *J. Electrochem. Soc.* 98 (1951) 203, in J. Kärkkäinen, Preparation and characterization of some ionic liquids and their use in the dimerization reaction of 2-methylpropene, Dissertation of University of Oulu, Finland, *Acta Univ. Oul.* A480 2007.
66. J.A. Boon, J.A. Levisky, J.L. Pflug, J.S. Wilkes, *J. Org. Chem.* 51(1986) 480.
67. J.S. Wilkes, M.J. Zaworotko, *J. Chem Soc., Chem. Commun.* (1992) 965.

68. J. Kärkkäinen, Preparation and characterization of some ionic liquids and their use in the dimerization reaction of 2-methylpropene, Dissertation of University of Oulu, Finland, Acta Univ. Oul. A480 2007.
69. N. Jain, A. Kumar, S. Chauhan, S.M.S. Chauhan, Tetrahedron 61(2005) 1015.
70. D. Zhao, M. Wu, Y. Kou, E. Min, Catalysis Today 74 (2002) 157.
71. C.J. Methew, P.J. Smith, T. Welton, Chem. Commun (2000) 1249.
72. W. Miao, T.H. Chan, Org. Lett. 5 (2003) 5003.
73. S.T. Handy, X. Zhang, Org. Lett. 3 (2001) 233.
74. E. Mizushi, T. Hayashi, T. Tanaka, Green Chem 3 (2001) 76.
75. M. R. Buchmeiser, Chem Review 100 (2000) 1565.
76. R.C. Buijsman, E. Vanueran, J.G. Sterrenburg, Org. Lett. 2001, 3, 3785.
77. S. Csihony, C. Fischeister, C. Bruneau, I.T. Horvath, P.H. Dixneuf, New J. Chem. 26 (2002) 1667.
78. H. Ma, X. Wan, X. Chen, Q-F. Zhou, Polymer 44 (2003) 5311.
79. L. Schwarz, M.C. Bowyer, C.I. Holdsworth, A. McCluskey, Australian Journal of Chemistry 59(2) (2006) 129.
80. A.M. Klibanow, Trends Biotechnol. 15 (1997) 97.
81. N. Kaftzik, P. Wasserscheid, U. Kragl, Org. Process Res. Dev. 6 (2002) 553.
82. D.W. Armstrong, L-K. Zhang, L. He, M.L. Gross, Anal Chem. 73 (2001) 3679
83. W; Lu, A.G. Faduv, B. Qi, B.R. Mattes, G. Wallace, J. Ding, G. Spink, J. Mazurkiewicz, D.R. MacFarlane, S. Forsyth, M. Forsyth, Science 297 (2002) 983.
84. T. Fukushima, A. Kosaka, Y. Ishimura, T. Yamamoto, T. Takigawa, T. Aida, Science 300 (2003) 2072.
85. B. Singh, S.S. Sekhon, Chemical Physics Lett. 414 (2005) 34.
86. K-S. Kim, S-Y. Park, S-H. Yeon, H. Lee, Electrochim. Acta 50 (2005) 5673.
87. H. Ohno, M. Yoshizawa, W. Ogihara, Electrochim. Acta 48 (2003) 2079.
88. H. Ohno, Electrochim. Acta. 46 (2001) 1407.
89. M. Yoshizawa, H. Ohno, Electrochim. Acta 46 (2001) 1723.
90. H. Ohno, M. Yoshizawa, W. Ogihara, Electrochim. Acta 50 (2004) 255.
91. S. Washiro, M. Yoshizawa, H. Nakajima, H. Ohno, Polymer 45 (2004) 1577.
92. W. Ogihara, S. Washiro, H. Nakajima, H. Ohno, Electrochim. Acta 51 (2006) 2614.
93. Solid State Ionics 169 (2004) 21.
94. Polymer 14 (1973) 589 in Reactive & Functional Polymers 67 (2007), 19.

95. D. Golodnitsky, E. Livshits, A. Ulus, Z. Barkay, I. Lapides, E. Peled, S.H. Chung, S. Greenbaum, *J. Phys. Chem. A* 105 (2001) 10098.
96. K. Suzuki, M. Yamaguchi, S. Hotta, N. Tanabe, S. Yanagida, *J. Photochem. And Photobiol. A : Chem.* 164 (2004) 81.
97. A. Lewandowski, A. Swiderska, *Solid State Ionics* 161 (2003) 243.
98. P. Santhosh, T. Vasudevan, A. Gopalan, K-P. Lee, *J. Power Source* 160 (2006) 609.
99. P. Santhosh, A. Gopalan, T. Vasudevan, K-P. Lee, *Material Research Bulletin* 41 (2006) 1023.
100. L. Hong, L.Y. Shi, X. Z. Tang, *Macromolecules* 36 (2003) 4989.
101. P.V. Wright, *Br. Polym J.* 7 (1975) 319.
102. T.-T. Cheng, T.-C. Wen, *J. Electroanal. Chem.* 459 (1998) 99.
103. T. Himba, *Solid State Ionics* 9-10 (1983) 1101.
104. W. Baochen, F. Li, P. Xinsheng, *Solid State Ionics* 48 (1991) 203.
105. J. F. Le Nest, S. Callens, A. Gandini, M. Armand, *Electrochim. Acta* 37, (1992) 1585.
106. X. Andrieu, J. P. Boeue, T. Vicédo, *J. Power Sources* 43-44 (1993) 445.
107. H. Bischoff, D. Rahner, K. Wiesener, T. Steurich and, R. Sandner, *J. Power Sources* 43-44 (1993) 473.
108. J. R. M. Giles, *Solid State Ionics* 24 (1987) 155.
109. M. Watanabe, S. Oohashi, K. Samui, N. Ogata, T. Kobayashi, *Macromolecules* 18 (1985) 889.
110. F.M. Gray, J.R. MacCallum, C.A. Vincent, J.M.R. Giles, *Macromolecules* 20 (1987) 392.
111. P. Santhosh, T. Vasudevan, A. Gopalan, Kwang-Pill Lee, *J. Power Source* 160 (2006) 609.
112. A. Lewandowski, A. Swiderski, *Solid State Ionics* 169 (2004) 21.
113. J. Sun, D.R. MacFarlane, M. Forsyth, *Solid State Ionics* 147 (2007) 333.
114. W. Ogata, K. Sanui, M. Rikukawa, S. Yamada, M. Watanabe, *Synth. Met.* 69 (1995) 521.
115. A. Lewandowski, A. Swiderska, *Solid State Ionics*, 169 (2004), 21.
116. H. Hong, C. Liquan, H. Xuejie, X. Rongjian, *Electrochim. Acta* 37 (1992) 1671.
117. F. Groce, F. Gerace, G. Dautzemberg, S. Passerini, G. B. Appetecchi, B. Scrosati, *Electrochim. Acta* 39 (1994) 2187.
118. T-C. Wen, S-L. Hung, M. Digar, *Synth. Met.* 118 (2001) 11.
119. W. Wieczorek, K. Such, Z. Florjanczyk, J.R. Stevens, *J. Phys. Chem.* 98 (1994) 6840

120. S.-M. Lee, C.-Y. Chen, C.-C. Wang, *Electrochim. Acta* 49 (2004) 4907.
121. M. Shibata, T. Kobayashi, R. Yosomiya, M. Seki, *Eur. Polym. J.* 36 (2000) 485.
122. E. Marwanta, T. Mizumo, N. Nakamura, H. Ohno, *Polymer* 46 (2005) 3795
123. W. Klinklai, S. Kawahara, T. Mizumo, M. Yoshizawa, Y. Isono, H. Ohno, *Solid State Ionics* 168 (2004) 131.
124. W. Klinklai, S. Kawahara, T. Mizumo, M. Yoshizawa, J. T. Sakdapipanich, Y. Isono, H. Ohno, *Eur Polymer J.* 39 (2003) 1707.
125. L. Dai, J.W. White, *Polymer* 32 (1991) 2120.
126. K.-R. Lin, C.-H. Kuo, L.-C. Kuo, K.-H. Yang, M.-K. Leung, K.-H. Hsieh, *Eur. Polym. J.* 43 (2007) 4279.
127. E. Hakansson, A. Amiet, S. Nahavandi, A. Kaynak, *Eur. Polym. J.* 43 (2007) 205.
128. A.J. Dominis, G.M. Spinks, G.G. Wallace, *Progr. Org. Coat.* 48 (2003) 43.
129. E. Hür, G. Bereket, Y. Şahin, *Current applied physics* 7 (2007) 597.
130. X.-G. Li, M.-R. Huang, M.-F. Zhu, Y.-M. Chen, *Polymer* 45 (2004) 385.
131. C. Shi, H. Xue, Z. Shen, Y. Li, C. Yang, *J. Appl. Polym. Sci* 86 (2003) 2624.
132. M.S. Cho, H.J. Seo, J.D. Nam, H.R. Choi, J.C. Koo, K.G. Song, Y. Lee, *Sens. Actuators B : Chem.* 119 (2006) 621.
133. V.N. Bliznyuk, A. Baig, S. Singamaneni, A.A. Pud, K.Y. Fatyeyeva, G. S. Shapoval, *Polymer* 46 (2005) 11728.
134. A.A. Pud, S.P. Rogalsky, G.S. Shapoval, A.A. Korzhenko, *Synth. Met.* 99(1999) 175.
135. Y.H. Park, S.H. Choi, S.K. Song, S. Miyata, *J. Appl. Polym. Sci.* 41 (1990) 1073.
136. E. Ruckenstein, Y. Sun, *Synth. Met.* 75 (1995) 79.
137. L.Y. Chiang, L.Y. Wang, C.S. Kuo, J.G. Lin, C.Y. Huang, *Synth. Met.* 84 (1997) 721.
138. S.L. Shenoy, C. Daneil, R.A. Weiss, C. Erkey, *J. Supercrit. Fluids* 4 (1991) 47.
139. Y. Fu, D. R. Palo, C.K. Erkey, R.A. Weiss, *Macromolecules* 30 (1997) 7611.
140. S.L. Shenoy, C. Daneil, C. Erkey, R.A. Weiss, *Ind. Eng. Chem. Res.* 41 (2002) 1484.
141. S.L. Shenoy, C. Daneil, R.A. Weiss, C. Erkey, *Synth. Met* 123 (2001) 509.
142. S. K. Dhawan, N. Singh, S. Venkatachalam, *Synth. Met.* 129 (2002) 261.
143. T-C. Wen, S-L. Hung, M. Digar, *Synth. Met.* 118 (2001) 11.
144. S.K. Dhawan, N. Singh, S. Venkatachalam, *Synth. Met.* 129 (2002) 261.
145. H.H. Kuhn, A.D. Child, W.C. Kimbrell, *Synth. Met.* 71 (1995) 2139.
146. E. Ruckenstein, S. Yang, *Synth. Met.* 3 (1993) 223, S. Yang, E. Ruckenstein, *Synth. Met.* 59 (1993) 1.

147. M. Gill, S.P. Armes, D. Fairhurst, S.N. Emmett, G. Idzorek, T. Pigott, *Langmuir*, 8, (1992) 2178.
148. P. B. Banerjee, B.M. Mandal, *Macromolecules*, 28 (1995) 3940.
149. H. Yashikawa, T. Hino, N. Kuramoto, *Synth. Met.* 156 (2006) 1187.
150. A.K. Tripathi, T.C. Goel, I.K. Varma, *J. Appl. Polym. Sci.* 51 (1994) 1347.
151. D.S. Vicentini, G.M.O. Barra, J.R. Bertolino, A.T.N. Pires, *Eur Polym. J.* 43 (2007) 45657.
152. J. Anand, S.S. Palaniappan, D.N.S. Thyandarayana, *Prog. Polym. Sci.* 23 (1998) 993.
153. L.W. Shacklette, C.C. Han, M.H. Luly, *Synth. Met.* 57 (1993) 3532.
154. Q. Pei, X. Bi, *J. Appl. Polym. Sci.* 38 (1989) 1819.
155. Q. Pei, X. Bi, *Synth. Met.* 30 (1989) 351.
156. C. Shi, H. Xue, Z. Shen, Y. Li, C. Yang, *J. Appl. Polym. Sci.* 89 (2003) 2624.
157. S. Dogan, U. Akbulut and L. Toppare, *Synth. Met.* 53 (1992) 29.
158. B. Sarie, M. Talu, F. Yildirim, E. K. Balci, *Applied Surface Sci.* 9493 (2002) 1.
159. Z. Xue, X.T. Bi, *J. Appl. Polym. Sci.* 47 (1993) 2073.
160. E.L. Tassi, M.A. DePaoli, *J. Chem. Soc., Chem. Commun.*, (1990) 155.
161. L.Y. Wang, S.C. Kuo, L.Y. Chiang, *Synth. Met.* 84 (1997) 587.
162. J. A. Malmonge, C. S. Campoli, L. F. Malmonge, D. H. F. Kanda, L. H. C. Mattoso, G. O. Chierice, *Synth. Met.* 119 (2001) 87.
163. M. Špírková, J. Stejskal, O. Quadrat, *Synth. Met.* 87 (1997) 1264.
164. D.C. Liao, K.H. Hsieh, Y.C. Chern, K.S. Ho, *Synth. Met.* 87 (1997) 61.
165. X. Bi, Q. Pei, *Synth. Met.* 22 (1987) 145.
166. X. Bi, Q. Pei, *Synth. Met.* 22 (1987) 145.
167. B. Seri, M. Talu, F. Yildirim and E.K. Balci, *J. Appl. Surf. Sci.* 205 (2003) 27.
168. R.V. Gregory, M. Liu, *Synth. Met.* 69 (1995) 349.
169. P. Yildirim, Z. Küçükyavuz, *Synth. Met.* 95 (1998) 17.
170. S. Yigit, J. Hacaloglu, U. Akbulut, L. Toppare, *Synth. Met.* 79 (1996) 11.

*Chapter 2-Synthesis and characterization of
telechelic cis-1,4-polyisoprene*

2.1. Introduction

Telechelic oligomers with terminal carbonyl and/or carboxylic groups can be obtained by specific oxidative double bond cleavage of 1,4-butadiene, 1,4-polyisoprene or other unsaturated units in polymers. Epoxidized polymers can also lead to heterotelechelic or homotelechelic oligomers by selective cleavage of epoxide units with suitable oxidative reagent [1].

In this chapter, we present the preparation of telechelic cis-1,4-polyisoprene by oxidative degradation of epoxidized cis-1,4-polyisoprene using periodic acid as selective oxidizing. The cleavage leads to oligomers with aldehyde and ketone chain ends and with polydispersity index near 2. This method has been developed in our laboratory [1-7].

Firstly, epoxidized cis-1,4-polyisoprene was prepared using epoxidizing agent, *m*-chloroperbenzoic acid, subsequently chain cleavage with periodic acid was performed. Secondly, the functional groups modification of carbonyltelechelic cis-1,4-polyisoprene to hydroxytelechelic and butylaminotelechelic cis-1,4-polyisoprene for using as precursor for polyurethane and polyurea synthesis was accomplished.

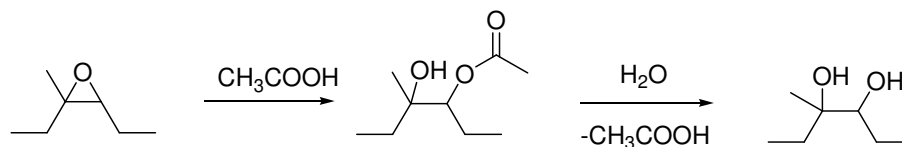
The modification of isoprene unit of hydroxytelechelic and butylaminotelechelic oligomers by epoxidation and hydrogenation was also carried out.

Products in each step were characterized by Fourier Transform Infrared Spectroscopy (FTIR), Nuclear Magnetic Resonance spectroscopy (^1H -, ^{13}C - NMR). The average molecular weights and polydispersity index of telechelic cis-1,4-polyisoprene were determined by Size Exclusion Chromatography (SEC).

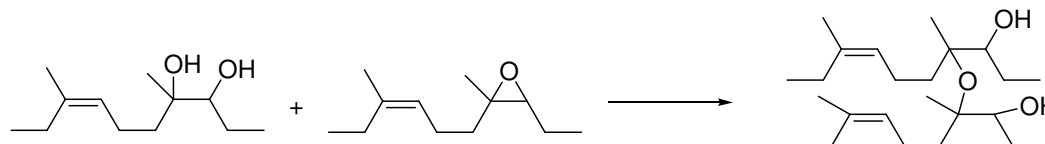
2.2. Oxidative degradation of cis-1,4-polyisoprene

The controlled degradation of cis-1,4-polyisoprene consists of two steps. Firstly, oxidation of carbon-carbon double bonds is performed using *m*-chloroperbenzoic acid. Secondly, a selective cleavage at the oxirane ring in epoxidized product is carried out by periodic acid as shown in Scheme 2.1.

- Formation of ester alcohol and diol in acid medium:



- Crosslinked reaction : formation of ether linkage between chains



In the epoxidation reaction, the reagent were added dropwise to cis-1,4-polyisoprene **1** solution in dichloromethane and control temperature at 0°C. This method allows us to obtain the amount of epoxidation following the proportion of isoprene unit and *m*-CPBA with the satisfying yield (93-97%).

The characterization of the epoxidized product by ¹H-NMR was shown in Fig 2.1, the presence of methylenic and methylic protons at the epoxide ring was indicated by a triplet peak at 2.68 ppm and a singlet peak at 1.29 ppm, respectively. However, in this case, we did not observe the signal of OH group, the product of the oxirane ring opening secondary reaction, at chemical shift about 3 and 4 ppm. By ¹³C NMR characterisation (Fig 2.2), peaks at 60.88 and 64.57 correspond to carbon of epoxide ring.

The percentage of epoxidation can be estimated from the ratio of integration peaks of proton at the epoxide ring ($\delta = 2.68$ ppm) (I_{epoxide}) and ethylenic proton ($\delta = 5.12$ ppm) ($I_{\text{C=CH}}$) of isoprene unit following equation:

$$\tau = I_{\text{epoxide}} * 100 / (I_{\text{epoxide}} + I_{\text{C=CH}})$$

The percentage of epoxidation of product obtained is nearly the same as the calculation (~5%).

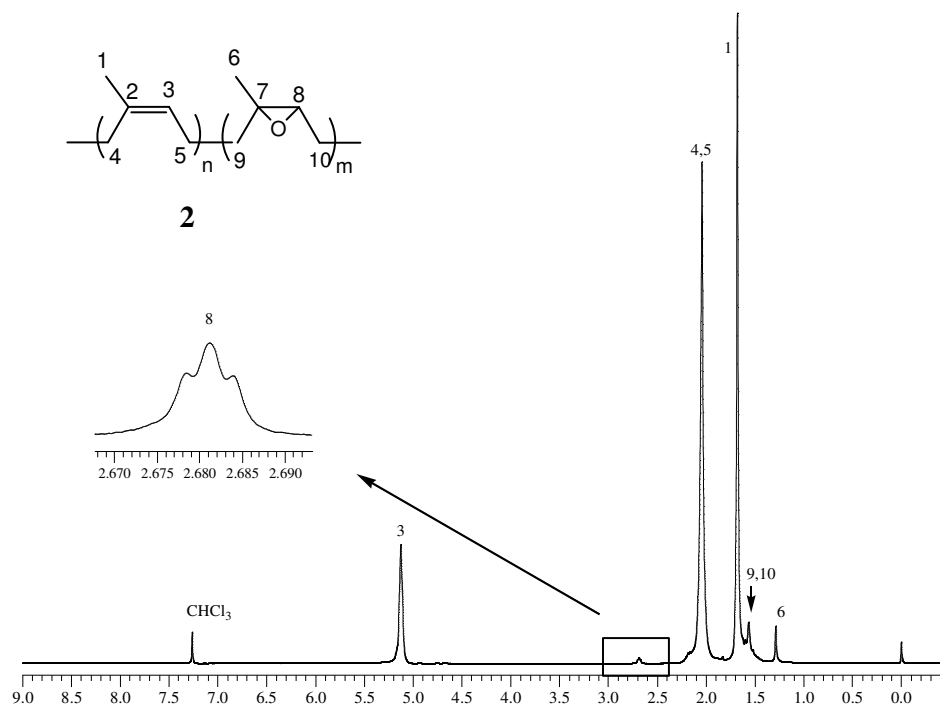


Fig 2.1 ¹H-NMR spectrum of epoxidized cis-1,4-polyisoprene 2.

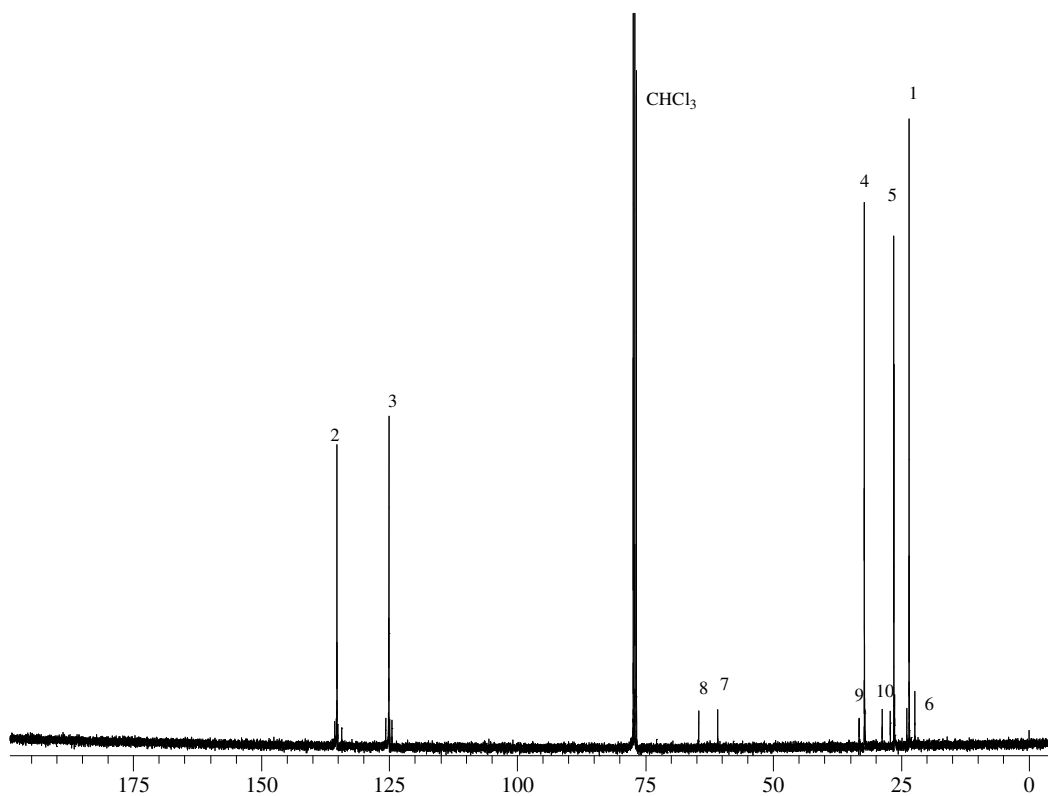


Fig 2.2 ¹³C-NMR spectrum of epoxidized cis-1,4-polyisoprene 2.

2.2.2. Cleavage of epoxidized cis-1,4-polyisoprene 2 in organic medium

The oxirane rings are very reactive toward chemical reactions involving hydrogen donor molecules, thus many chemical modifications can be done from this site, especially cleavage. The cleavage of polyisoprene in organic phase and latex phase using periodic acid has been studied in our laboratory [1-7]. Periodic acid causes the cleavage of the carbon-carbon bond of the oxirane ring forming shorter chain with the formation of aldehyde and ketone functional groups at the chain ends.

Periodic acid was added dropwising into the solution of epoxidized cis-1,4-polyisoprene 2 in THF. The reaction was performed at 30°C during 6 hours. The degradation product is yellow viscous liquid with yielding 88-94%.

The characterization of the product by ¹H-NMR shows the disappearing of the oxirane unit signals at 2.68 and 1.29 ppm. There are the new peaks at 9.78, 2.49 and 2.35 ppm corresponding to protons at the aldehyde group and CH₂ at α and β positions next to the aldehyde end group, respectively. A peak representing methylic protons at ketonic group appears at 2.13 ppm, and CH₂ at α and β positions next to ketonic end group at 2.43 and 2.26 respectively.

The integration of peak of proton at aldehyde function at 9.78 ppm (I_{CHO}) or of those of methylenic protons between 2.26 and 2.49 ppm near carbonyl end groups compared with ethylenic proton in isoprene repeat unit (I_{C=CH}) permits us to calculate number average molecular weight of telechelic cis-1,4-oligoisoprene according to the following equation;

$$\overline{M}_n (\text{CTPI}) = [I_{\text{C=CH}} / I_{\text{CHO}}] \times 68 + 100$$

The \overline{M}_n calculated from ¹H NMR is 1700 g/mol for the degradation of 5% epoxidized cis-1,4-polyisoprene.

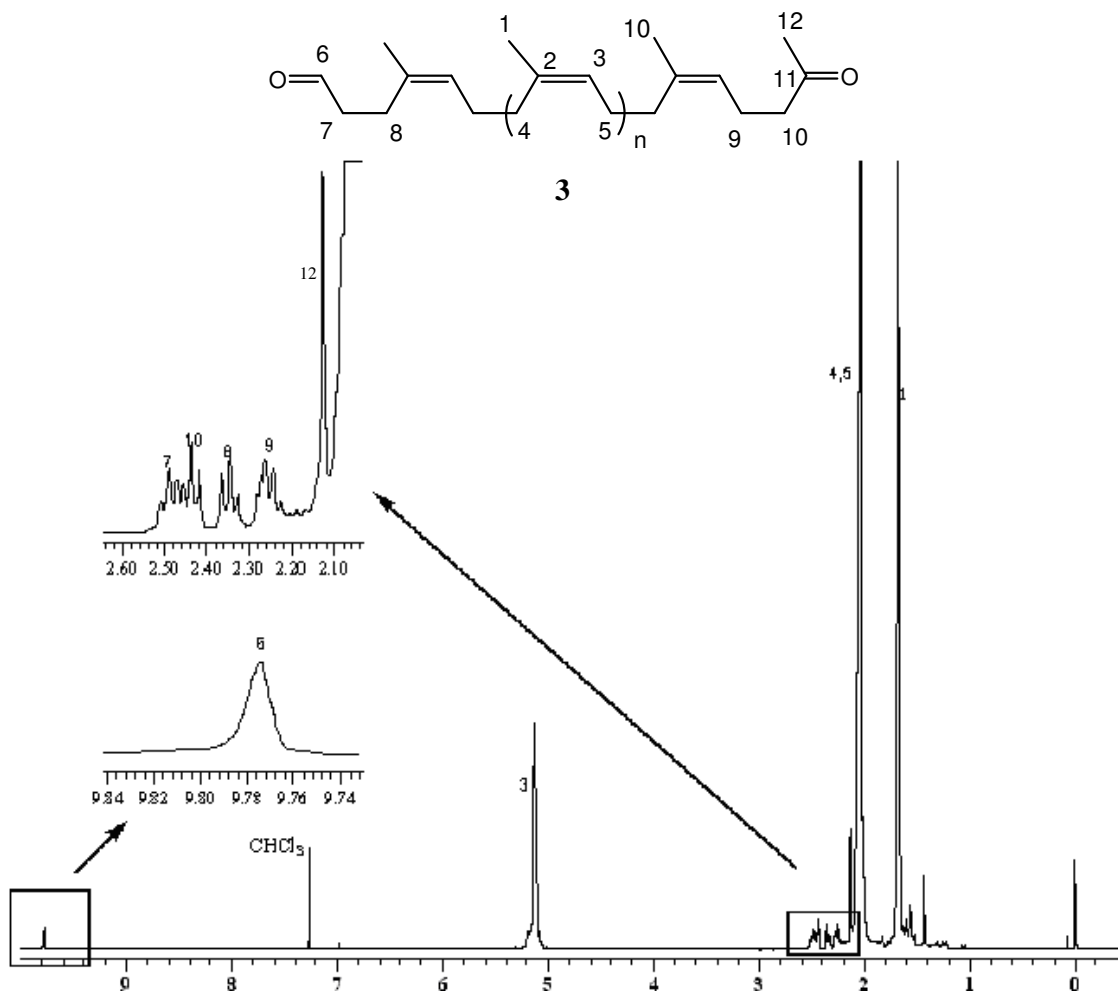


Fig 2.3 ¹H-NMR spectrum of carbonyltelechelic cis-1,4-polyisoprene (CTPI) **3**.

The ¹³C NMR analysis shows the disappearing of carbon signals at epoxide unit (60.88 and 64.57 ppm) and appearing of peaks corresponding to aldehyde and ketone carbons at 202.17 and 208.72 ppm respectively.

From FTIR spectra, we observed the characteristic stretching peak of carbonyl group at 1720 cm⁻¹ (Appendix 1.2).

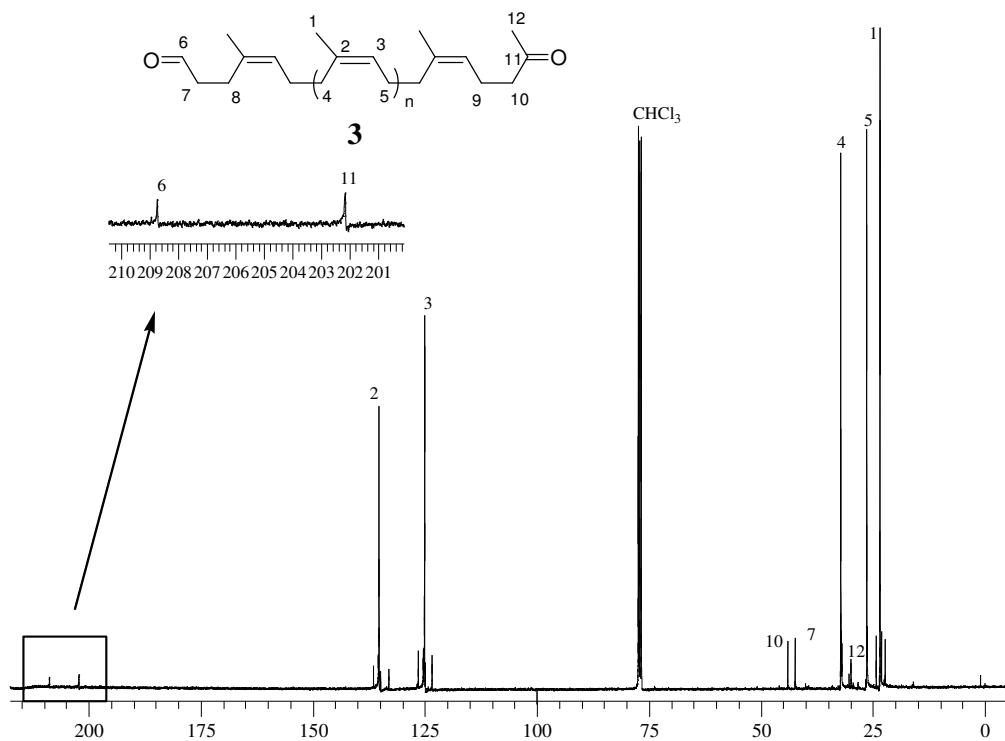
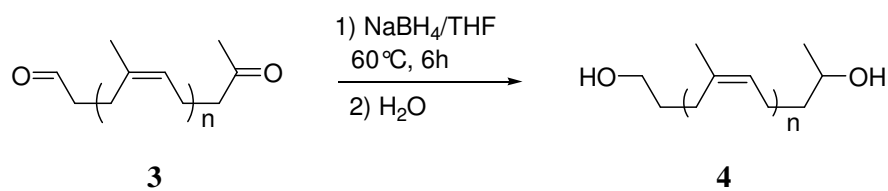


Fig 2.4 ^{13}C -NMR spectrum of carbonyltelechelic cis-1,4-polyisoprene (CTPI) **3**.

Average molecular weights (\overline{M}_n and \overline{M}_w) and polydispersity index of product was determined by Size Exclusion Chromatography (SEC) using polystyrene standard calibration. The value of \overline{M}_n obtained directly from this technique (2500 g/mol) is much higher than value calculated from NMR. The actual \overline{M}_n value for polyisoprene is converted from average molecular weight value obtained from SEC (polystyrene standard calibration) using Benoît factor, 0.67 [10]. The relationship is; $\overline{M}_n(\text{PI}) = 0.67 \overline{M}_n(\text{PS})$, where $\overline{M}_n(\text{PS})$ is the real average molecular weight from standard polystyrene and $\overline{M}_n(\text{PI})$ is real average molecular weight of cis-1,4-polyisoprene corresponding. The value obtained from this equation (1690 g/mol) is close to value obtained from ^1H -NMR (1700 g/mol).

2.3. Synthesis and characterization of hydroxytelechelic polyisoprene precursor of polyurethane

Synthesis of hydroxytelechelic cis-1,4-polyisoprene **4** from carbonyltelechelic cis-1,4-polyisoprene **3** was achieved using sodium borohydride as the specific reduction agent at 60°C for 6 hours. The metal hydride reduces carbonyl function groups into alcohol groups without effect on the carbon-carbon double bond. The reaction pathway was shown in Scheme 2.3.



Scheme 2.3 Synthesis reaction of hydroxytelechelic cis-1,4-polyisoprene **4**.

The $^1\text{H-NMR}$ spectrum (Fig 2.5), allows observing that the characteristic peaks of aldehyde and methylketone protons at 9.78 and 2.13 ppm respectively, and those of the methylenic protons in α and β positions from carbonyl end groups have disappeared. The triplet and multiplet peaks corresponding to $\underline{\text{CH}_2}$ and $\underline{\text{CH}}$ next to hydroxyl groups at the chain ends were noted at 3.63 and 3.80 ppm, respectively. Moreover, a doublet peak of methyl protons of secondary alcohol was remarked at 1.18 ppm.

Number average molecular weight of hydroxytelechelic cis-1,4-polyisoprene can be calculated from following equation;

$$\overline{M}_n = [\text{I}_{\underline{\text{C=CH}}} / \text{I}_{\underline{\text{CHOH}}}] \times 68 + 104$$

where $\text{I}_{\underline{\text{C=CH}}}$ = signal integration of ethylenic proton

$\text{I}_{\underline{\text{CHOH}}}$ = signal integration of CH proton in α -position of hydroxyl unit

The number average molecular weight calculates from $^1\text{H-NMR}$ is 1900 g/mol which corresponds to the value obtained from SEC.

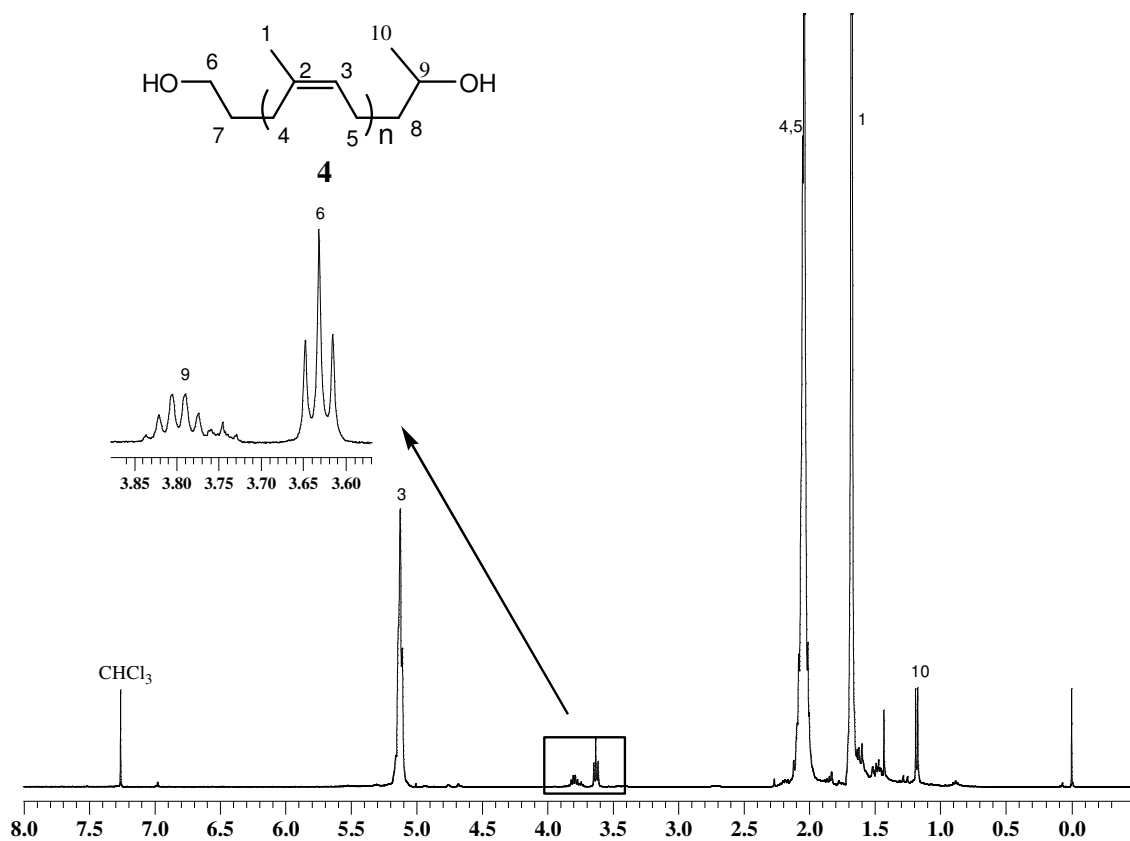


Fig 2.5 $^1\text{H-NMR}$ spectrum of hydroxytelechelic cis-1,4-polyisoprene (HTPI) **4**.

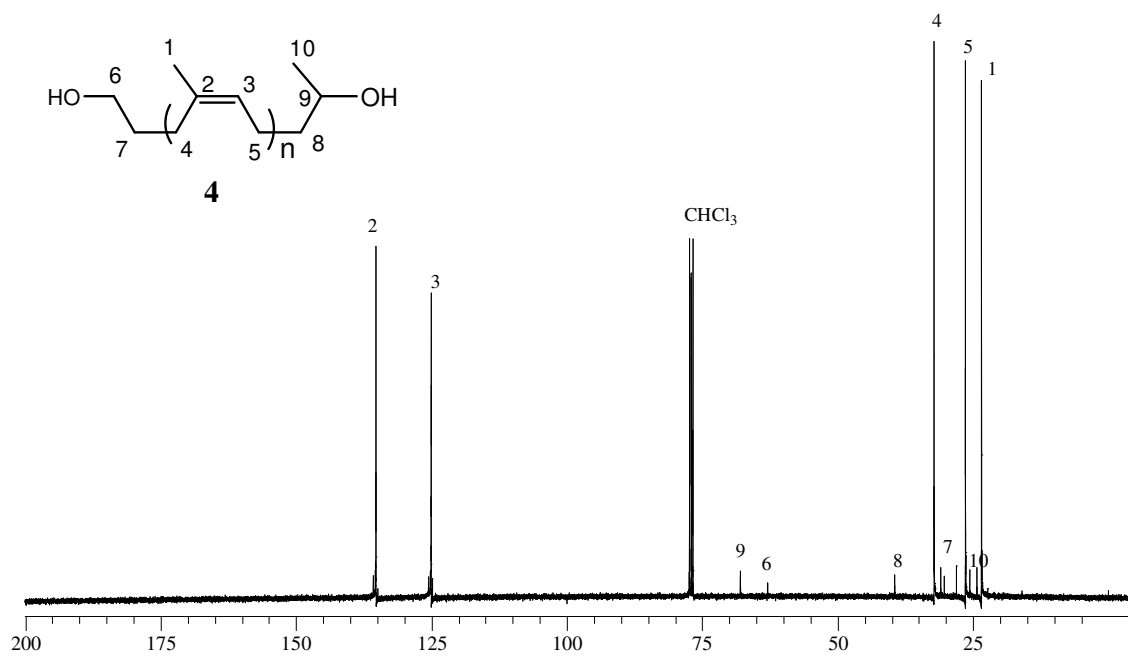


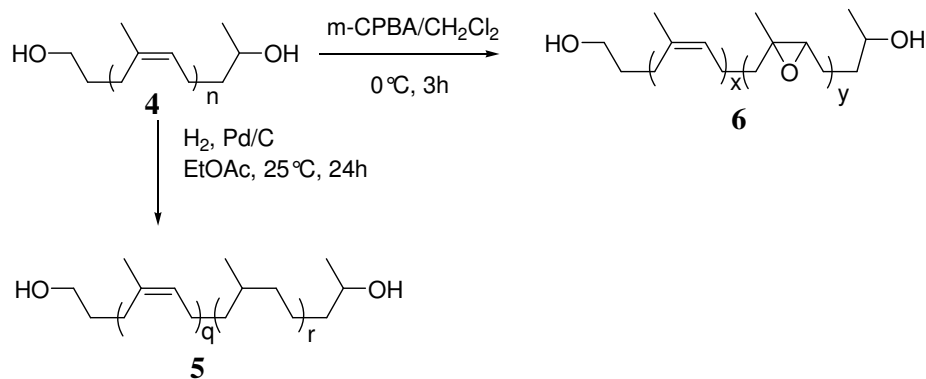
Fig 2.6 $^{13}\text{C-NMR}$ spectrum of hydroxytelechelic cis-1,4-polyisoprene **4**.

By ^{13}C -NMR characterization (Fig 2.6), we observed appearing of peaks at 62.93 and 67.96 ppm corresponding respectively to CH_2 and CH of primary and secondary alcohols. Also, peak of methylic carbon at secondary alcohol appears at 24.24 ppm.

From FTIR spectra, we perceived the disappearing of $\text{C}=\text{O}$ stretching band at 1720 cm^{-1} and appearing of $\text{O}-\text{H}$ stretching at 3350 cm^{-1} (appendix 1.2).

2.4. Modification of hydroxytelechelic cis-1,4-polyisoprene precursor of polyurethanes.

The modifications of hydroxytelechelic cis-1,4-polyisoprene main chain were carried out into 2 ways, epoxidation and hydrogenation, as shown in Scheme 2.4.



Scheme 2.4 Main chain modifications of hydroxytelechelic cis-1,4-polyisoprene **4**.

2.4.1. Hydrogenation of hydroxytelechelic cis-1,4-polyisoprene **4**

Hydrogenation of carbon-carbon double in isoprene units of hydroxytelechelic cis-1,4-polyisoprene **4** was done under hydrogen pressure at 4.0 bar, during 24 hours at 25°C using palladium on activated carbon as catalyst (Scheme 2.4).

From ^1H -NMR characterization, intensity of characteristic signals of isoprene unit at 5.12, 2.04 and 1.67 ppm decreases, while signals between chemical shift 0.84 and 1.37 ppm corresponding to hydrogenated isoprene units were noticed.

The integrations of methylic protons at isoprene unit ($\delta = 1.67\text{ ppm}$) ($I_{\text{CH}_3\text{C}=\text{C}}$) and hydrogenated isoprene unit ($\delta = 0.84\text{ ppm}$) ($I_{\text{CH}_3\text{C}-\text{C}}$) provided a calculation of percentage of hydrogenation and number average molecular weight. In our case, we obtained the

hydrogenated hydroxytelechelic cis-1,4-polyisoprene with 83% hydrogenation. Number average molecular weight was estimated from following equation:

$$\overline{M}_n = [I_{\text{C=CH}}/I_{\text{CHOH}}] \times 68 + [I_{\text{CH}_3\text{C-C}}/3I_{\text{CHOH}}] \times 70 + 104$$

The number average molecular weight calculates from $^1\text{H-NMR}$ is 1790 g/mol which is close to value obtained from SEC (1800 g/mol).

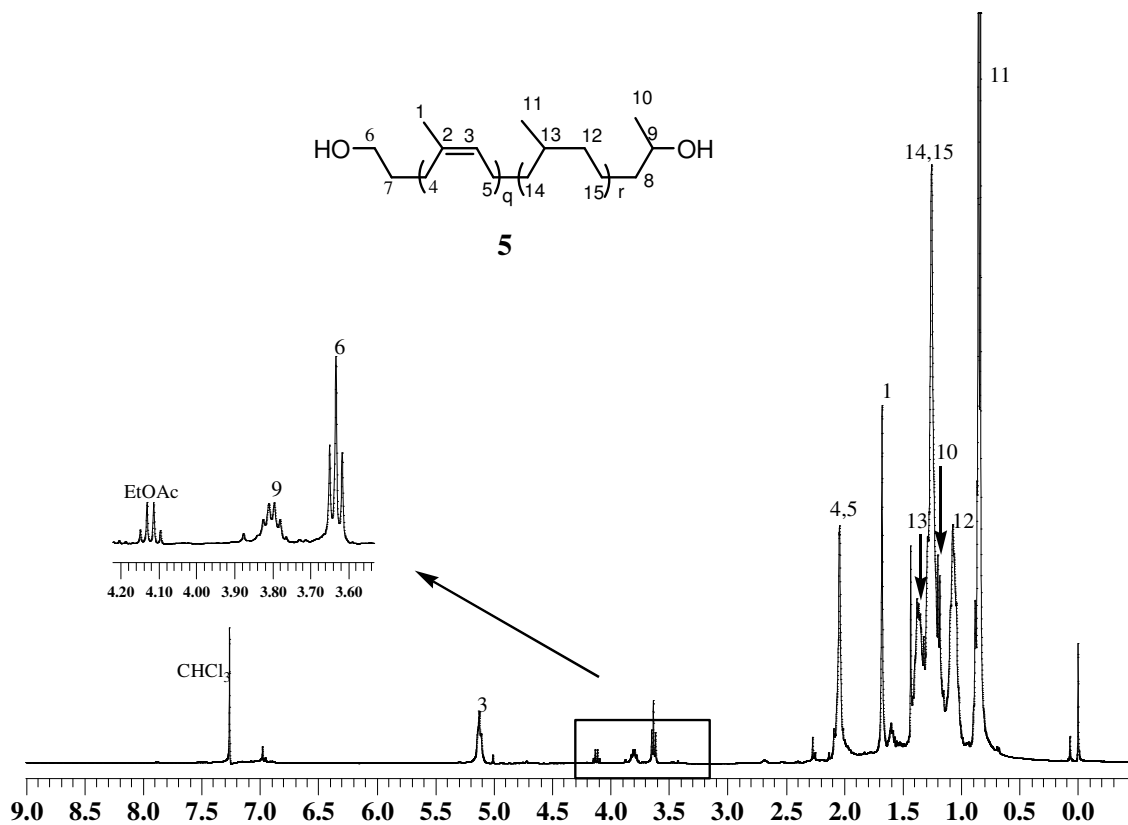


Fig 2.7 $^1\text{H-NMR}$ spectrum of hydrogenated hydroxytelechelic cis-1,4-polyisoprene 5.

^{13}C NMR investigation shows the signal of hydrogenated isoprene units at 18.65 ppm ($\underline{\text{C}}\text{H}_3\text{CH}-\text{CH}_2$), 36.30 ppm($\text{CH}_3\text{CH}-\underline{\text{C}}\text{H}_2$) and 31.17 ppm($\text{CH}_3\text{C}\underline{\text{H}}-\text{CH}_2$).

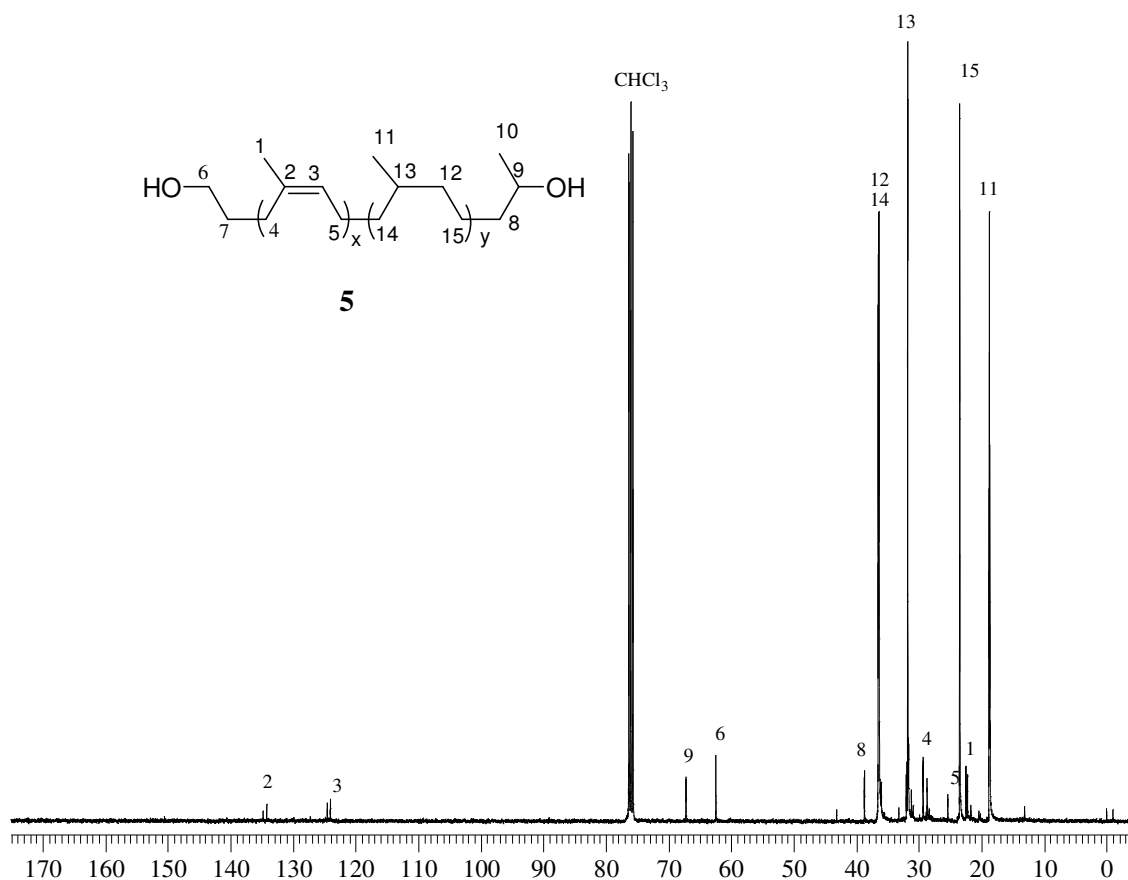


Fig 2.8 ^{13}C -NMR spectrum of hydrogenated hydroxytelechelic cis-1,4-polyisoprene **5**.

FTIR analysis shows the decreasing of intensity of characteristic bands of the carbon-carbon double bond of isoprene units at 3035 ($\nu_{=\text{CH}_2}$) 1664 ($\nu_{\text{C}=\text{C}}$) and 837 cm^{-1} ($\delta_{=\text{C}-\text{H}}$) (Appendix 1.2) which points out the hydrogenated units formation.

2.4.2. Epoxidation of hydroxytelechelic cis-1,4-polyisoprene **4**

Different percentages of epoxidized hydroxytelechelic cis-1,4-polyisoprene **6** corresponding to a proportion of isoprene unit and epoxidizing reagent were performed at 0°C in CH_2Cl_2 for 3 h using *m*-CPBA as the epoxidizing agent.

From ^1H -NMR spectrum, peaks of protons at the epoxidized isoprene units were detected at 2.68 ($\underline{\text{C}}\text{H}_{\text{oxirane ring}}$) and 1.29 ppm ($\underline{\text{C}}\text{H}_3\text{C}_{\text{oxirane ring}}$). Intensity of signal at 2.68 ppm

increases as percentage of epoxidation increases while intensity of ethylenic protons at 5.12 ppm decreases.

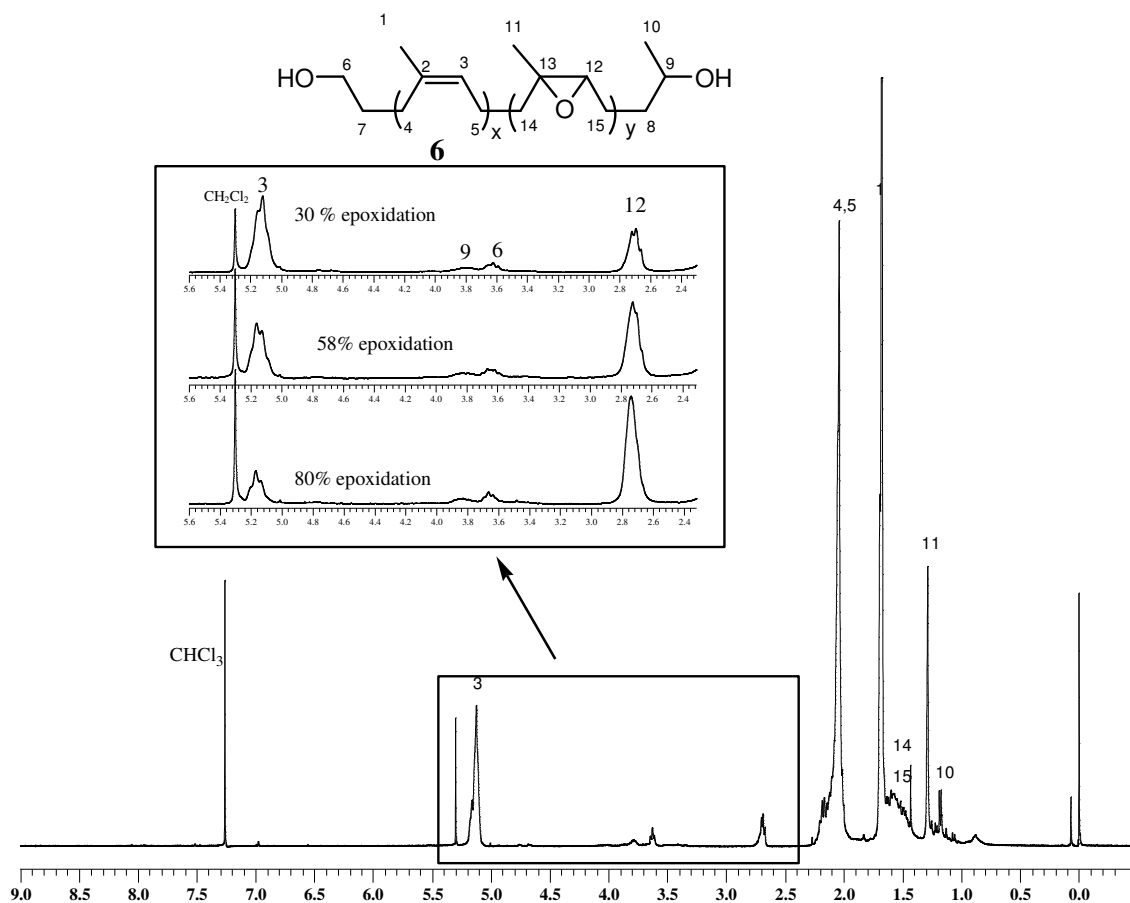


Fig 2.9 ¹H-NMR spectrum of 30 % epoxidized hydroxytelechelic cis-1,4-polyisoprene compared to those of 58% and 80% epoxidized oligomers.

In addition, ¹³C-NMR spectrum confirmed the presence of peaks corresponding to carbons at oxirane ring at chemical shift 59.77 ppm ($\text{CH}_3\text{C}_{\text{oxirane ring}}$) and 63.47 ppm ($\text{C}_{\text{oxirane ring}}$).

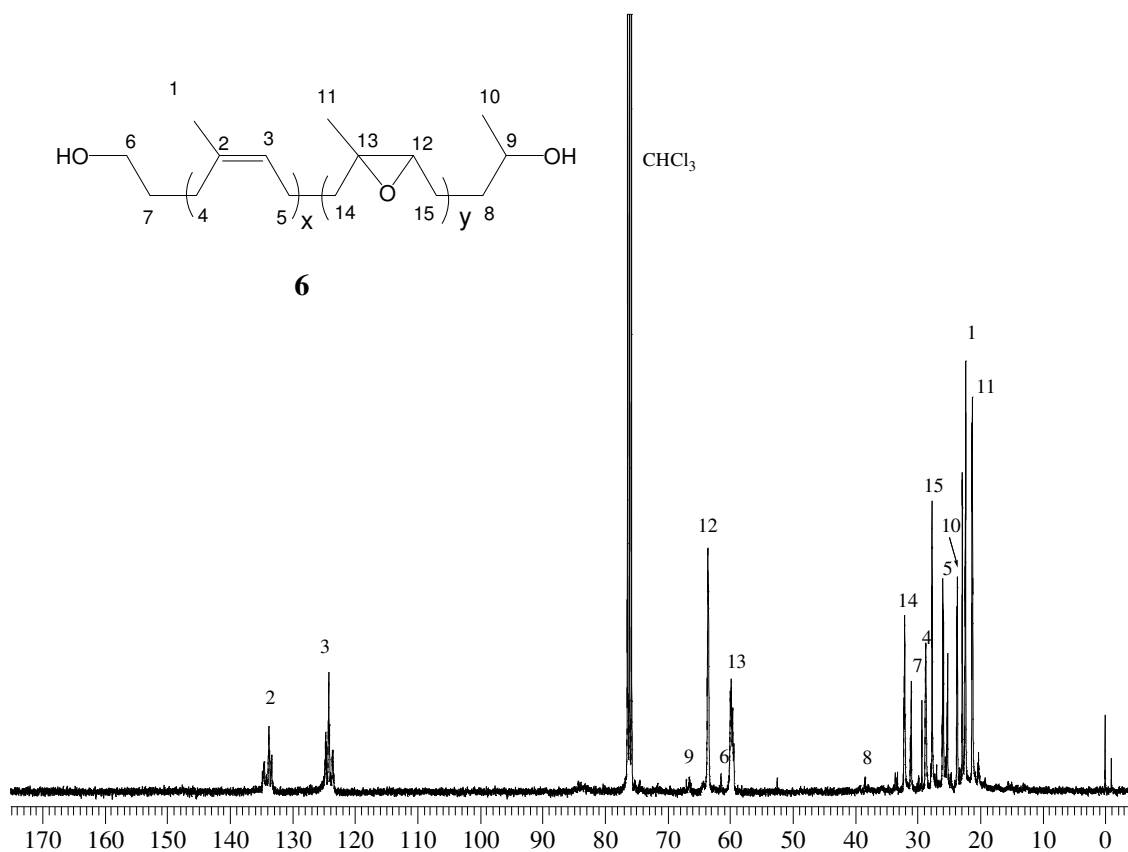


Fig 2.10 ^{13}C -NMR spectrum of epoxidized hydroxytelechelic cis-1,4-polyisoprene **6**.

From FTIR spectra (Fig 2.11), intensity of $\delta_{\text{C-O(epoxide)}} (872 \text{ cm}^{-1})$ band increases as percentage of epoxidation increases, in the other hand, intensity of $\nu_{\text{C=C}}$ and $\delta_{\text{C-H}}$ bands at 1664 and 837 cm^{-1} decreases.

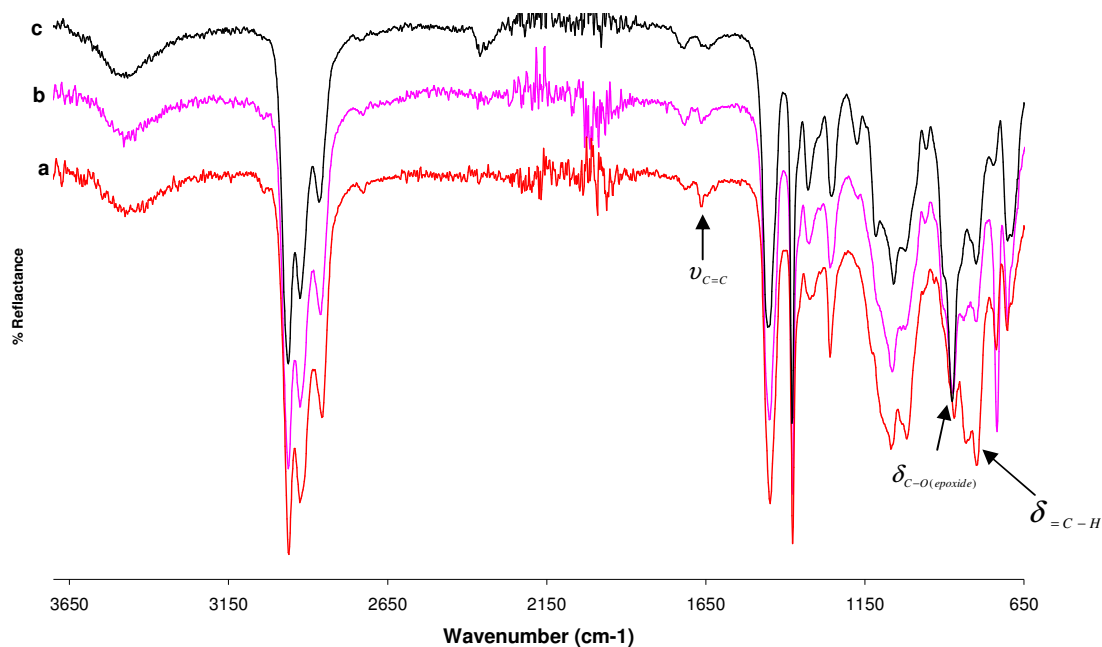


Fig 2.11 FTIR of epoxidized hydroxytelechelic cis-1,4-polyisoprene **6**; a) 30%; b) 58%; c) 80% .

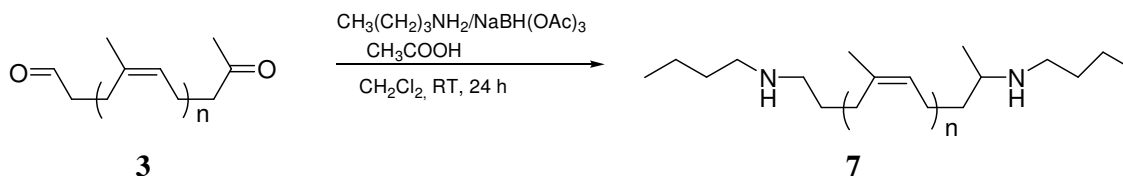
2.5. Synthesis and characterization of aminotelechelic cis-1,4-polyisoprene precursor of polyurea

The reaction of aldehyde or ketone with ammonia, primary amine or secondary amine in the presence of reducing agents to give primary, secondary or tertiary amine, respectively, is known as reductive aminations (of carbonyl compounds). The reductive amination reaction is described as a *direct* reaction when the carbonyl compound and the amine are mixed with the suitable reducing agent without prior formation of the intermediate imine or iminium salt. A *stepwise* or *indirect* reaction involves the preformation of the intermediate imine followed by reduction in a separate step [11].

Direct reductive amination of carbonyl compounds, which allows a one step synthesis of amine from aldehyde and ketone, is a well known reaction [11-15]. The two most commonly used direct reductive amination methods differ in the nature of the reducing agent. The first method is catalytic reduction with platinum, palladium, or nickel catalysts [11]. This is an economical and effective reductive amination method. However, the reaction may give a mixture of products and low yields depending on the molar ratio and the structure of the reactants. Furthermore, reduction has limited use with compounds containing carbon-carbon

multibonds and in the presence of reducible functional groups [16]. The second method utilizes hydride reducing agents particularly sodium cyanoborohydride (NaBH_3CN) for reduction. The successful use of this compound is due to its stability and its different selectivity at different pH values, but this reagent is highly toxic. For this reason, Abdel-Magid et al. [11] have changed to used sodium triacetoxyborohydride ($\text{NaBH}(\text{OAc})_3$) as a general reducing agent for the reductive amination of aliphatic and aromatic aldehydes, aliphatic acyclic and cyclic ketones, with primary and secondary amines. In the comparison with other reductive amination procedures such as $\text{NaBH}_3\text{CN}/\text{MeOH}$, borane-pyridine, and catalytic reduction, $\text{NaBH}(\text{OAc})_3$ gave consistently higher yields and fewer side products. The procedure is carried out effectively in the presence of acid sensitive functional groups and also reducible functional groups such as C-C double bonds.

In our study, we have performed the reductive amination of carbonyltelechelic cis-1,4-polyisoprene **3** with primary amine (n-BuNH_2) in the presence of $\text{NaBH}(\text{OAc})_3$ to provide the oligoisoprene with secondary amine functional groups at the chain ends (Scheme 2.5).



Scheme 2.5 Synthesis of butylaminotelechelic cis-1,4-polyisoprene **7**.

$^1\text{H-NMR}$ (Fig 2;12) shows the disappearing of the characteristic signals of carbonyl end groups and the appearing of signals of butyl at the end chain ($\delta=0.91$ ppm, CH_3 ; $\delta=1.2$ - 1.4 ppm, CH_2 ; $\delta=2.6$ ppm CH_2 and CH at α -position from NH).

By $^{13}\text{C-NMR}$ analysis (Fig 2.13), we observed the appearing of peaks at 46.95 ppm and 53.01 ppm corresponding to CH_2 and CH at the amino chain ends respectively. We observed also peaks of β -methyl group from NH at 20.49 ppm. FTIR spectrum confirmed the transformation of carbonyl end group to butylamino end group. Disappearing of C=O stretching at 1720 cm^{-1} was remarked (appendix 1.3).

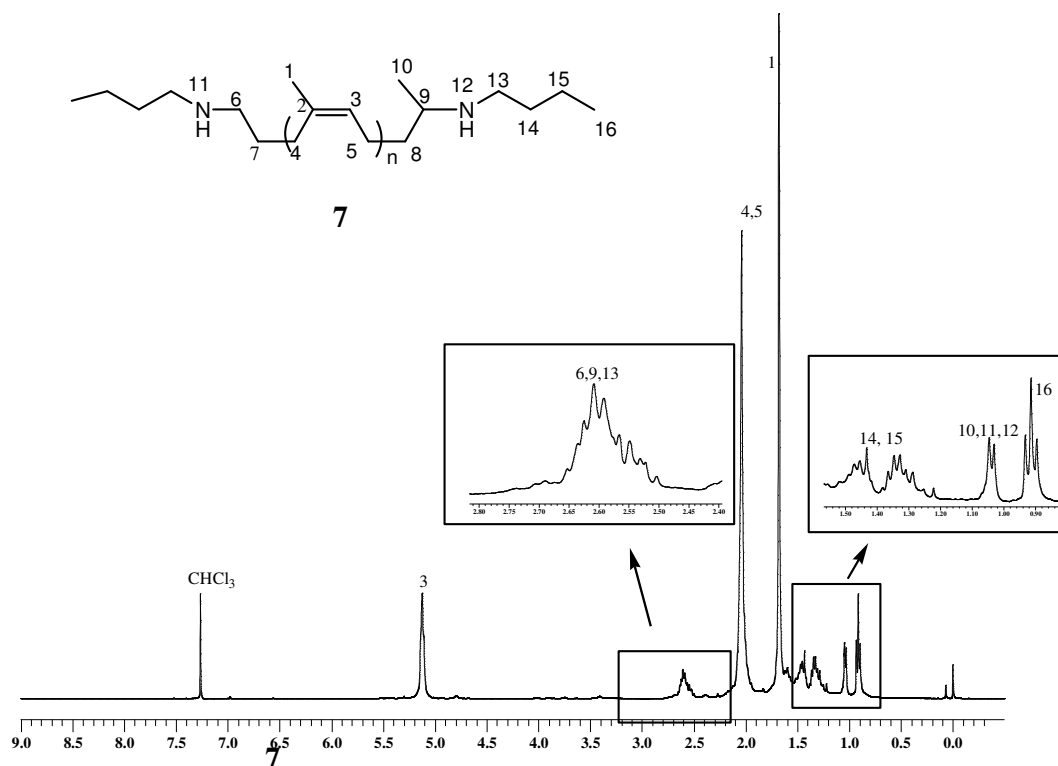


Fig 2.12 $^1\text{H-NMR}$ spectrum of butylaminotelechelic cis-1,4-polyisoprene 7.

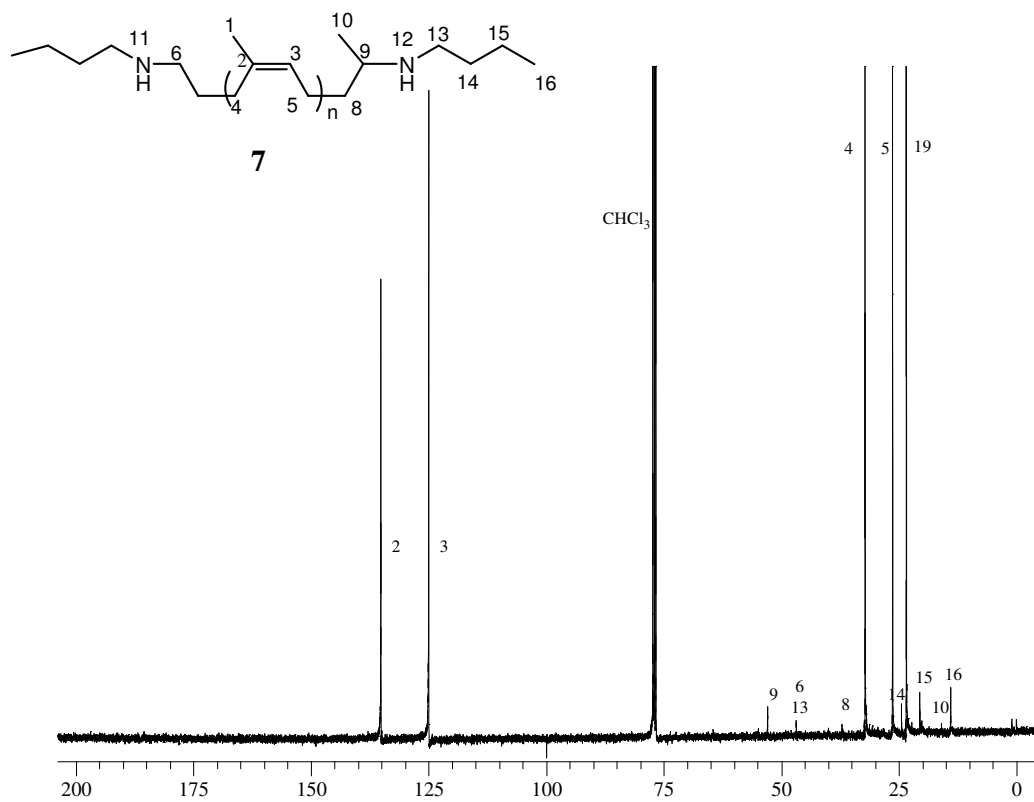
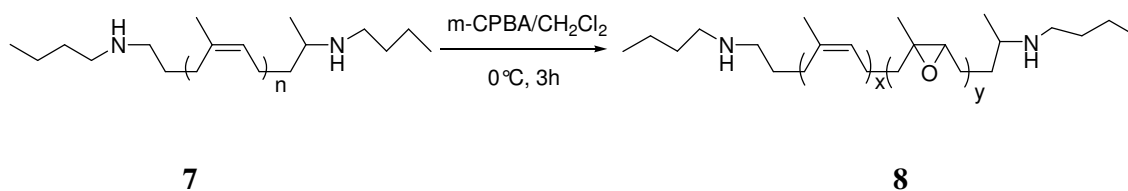


Fig 2.13 $^{13}\text{C-NMR}$ spectrum of butylaminotelechelic cis-1,4-polyisoprene 7.

2.6. Epoxidation of aminotelechelic polyisoprene polyurea precursor

Epoxidation of butylaminotelechelic cis-1,4-polyisoprene was carried out as same as in hydroxytelechelic cis-1,4-polyisoprene by using *m*-chloroperbenzoic acid as epoxidizing agent.

m-CPBA in dichloromethane was added dropwise to butylaminotelechelic cis-1,4-polyisoprene **7** solution. The reaction was performed at 0°C during 3 hours.



Scheme 2.6 Synthesis of epoxidized butylaminotelechelic cis-1,4-polyisoprene **8**.

By ¹H-NMR characterization, we observed the signal of epoxidized isoprene unit at chemical shift 2.70 ppm and 1.30 ppm corresponding to a proton at oxirane ring and methylic protons connected to oxirane ring, respectively.

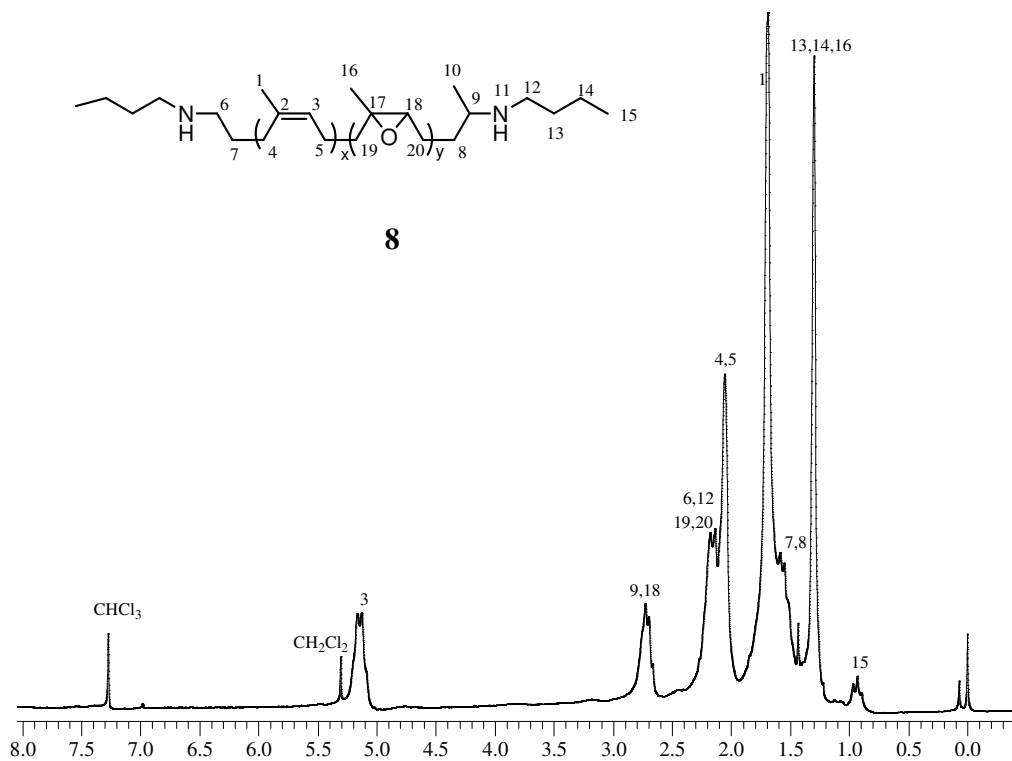


Fig 2.14 ¹H-NMR spectrum of epoxidized butylaminotelechelic cis-1,4-polyisoprene **8**.

^{13}C -NMR spectrum shows signal of the carbon at an oxirane ring at 64.37 and 61.18 ppm (Fig 2.15).

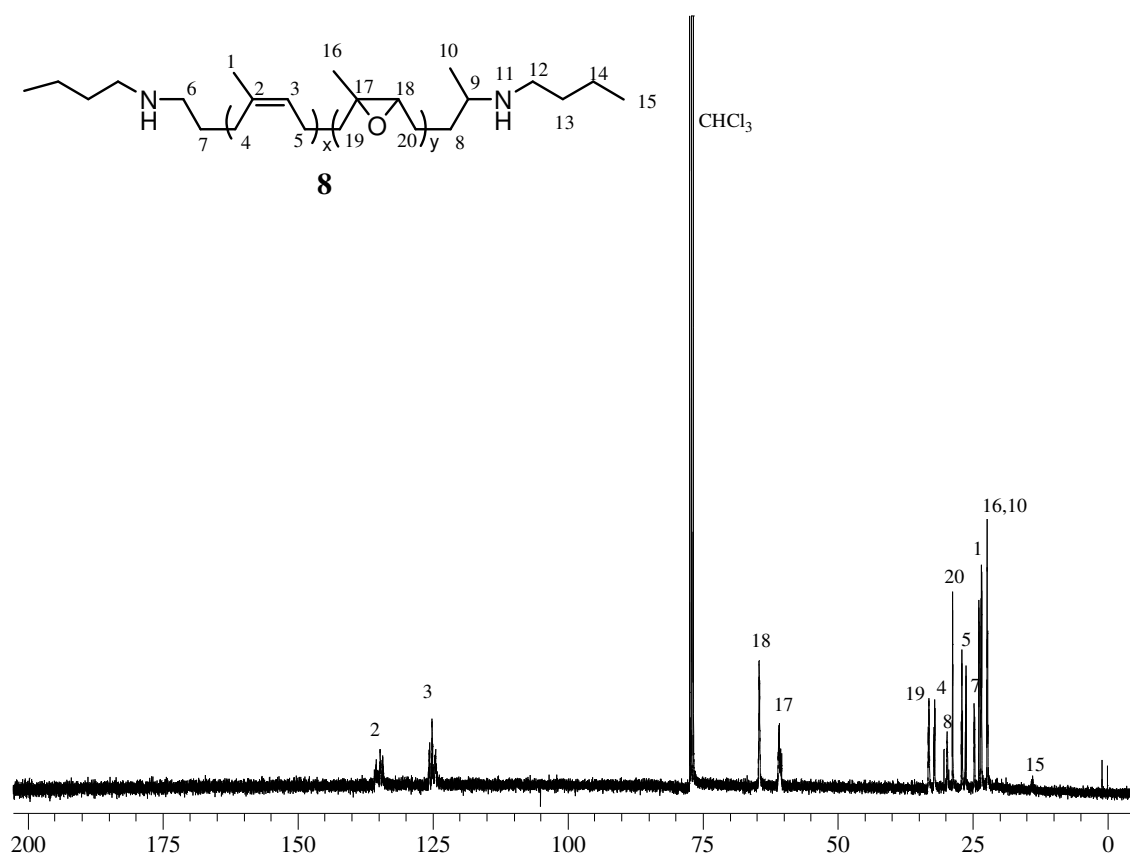


Fig 2.15 ^{13}C -NMR spectrum of epoxidized butylaminotelechelic cis-1,4-polyisoprene **8**.

2.7. Conclusion

The controlled degradation of high molecular weight cis-1,4-polyisoprene was successfully performed by epoxidation and then followed by selective oxidation of epoxidized products to obtain an oligomer with aldehyde and carbonyl functional groups at the chain ends. Carbonyltelechelic cis-1,4-isoprene with the molecular weight in order 2000 and polydispersity index about 1.9 was obtained from the degradation of a 5% epoxidized cis-1,4-polyisoprene. The microstructure study by ^1H and ^{13}C NMR analysis confirmed that the cleavage of polyisoprene chain is controlled and we did not observed signals of secondary reaction products.

The reduction of carbonyl groups to hydroxyl groups using sodium borohydride allows us to obtain hydroxytelechelic cis-1,4-polyisoprene, a precursor for further polyurethane synthesis, with a polydispersity index 1.7 and molecular weight around 2000 g/mol. From this product, chain modification of polyisoprene unit was done by catalytic hydrogenation and different percentages of epoxidation for using as starting materials in polyurethane synthesis.

Furthermore, the carbonyltelechelic cis-1,4-polyisoprene was also reduced by sodium triacetoxyborohydride in the presence of butylamine to attain butylaminotelechelic cis-1,4-polyisoprene. Further main chain modification by epoxidation of this product permits preparing precursor for next step polyurea synthesis.

References

1. J.C. Brosse, I. Campistron, D. Derouet, A. El Hamdaoui, S. Houdayer, S. Gillier- Ritoit, J. Appl. Polym. Sci., 78 (2000) 1461.
2. S. Gillier-Ritoit, Réactions de coupure de chaînes pour la valorisation des polyisoprènes sous forme de cis-1,4-oligoisoprènes téléchéliques ; Application au latex de caoutchouc naturel, thèse de l'Université du Maine, Le Mans, 2001.
3. S. Gillier- Ritoit, D. Reyx, I. Campistron, A. Laguerre, R.P. Singh, J. Appl. Polym. Sci. 87(1) (2003) 42.
4. N. Kebir, Elaboration de nouveaux polyuréthanes à partir de cis-1,4-oligoisoprènes hétérocarbonyltéléchéliques issus de la dégradation contrôlée du cis-1,4-polyisoprène de haute masse. Etude de leurs propriétés mécaniques, thermiques et biocides, thèse de l'Université du Maine, Le Mans, 2005.
5. N. Kebir, G. Morandi, I. Campistron, A. Laguerre, J.-F. Pilard, Polymer, 46 (2005), 6844.
6. N. Kebir, I. Campistron, A. Laguerre, J.-F. Pilard, C. Bunel, J.-P. Couvercelle, C. Gondard, Polymer, 46 (2005), 6869.
7. P. Phinyocheep, C.W. Phetphaisit, D. Derouet, I. Campistron, J.C. Brosse, J. Appl. Polym. Sci. 95 (2005) 6.
8. P. Dreyfuss, J.P. Kennedy, Anal. Chem. 47 (1975) 771.
9. M.C.S. Perera, J.A. Elix, J.H. Bradbury, J. Polym. Sci., Part A 26(2) 1988 637.
10. J.P. Busnel, Polymer 23 (1982) 139.
11. A. F. Abdel-Magid, K. G. Carson, B. D. Harris, C.A. Maryanoff, R. D. Shan, J. Org. Chem. 61 (1996) 3849.
12. G. Morandi, N. Kebir, I. Campistron, F. Gohier, A. Laguerre, J.-F. Pilard, Tetrahedron Lett. 48 (2007) 7726.
13. A.F. Abdel-Magid, S.J. Mehrman, Org. pro. Res. Dev. 10 (2006) 971.
14. R.I. Storrer, D.E. Carrera, Y. Ni, D.W. Macmillan, J. Am. Chem. Soc. 128 (2006) 84.
15. D. Menche, S. Böhm, S. Rudolph, V. Zander, Tetrahedron Lett. 48 (2007) 365.
16. A. Roe, J.A. Montgomery, J. Am. Chem. Soc. 75 (1953) 910.

***Chapter 3- Synthesis and characterization of
polyurethane based conducting composites***

3.1. Introduction

For polyelectrolyte and conducting application, researchers have focused their attention on the synthesis of novel polymeric materials possessing high ionic conductivity, mechanical strength, and thermal stability which could ultimately be used for practical applications.

Recent reports [1-4] have documented that polyurethane can be used as a polymer electrolyte and conducting composite matrix. The interest in using polyurethane as a matrix for this application is related to the possibility of increasing the mechanical strength of composite material. Furthermore, the low glass transition temperature giving higher segment motion of soft segments leads to higher mobility of dissolved ions. Complexes of polyurethane with various alkali metal salts such as LiClO₄ and LiPF₆ for preparing the solid polymer electrolytes (SPEs) have been reported [5,6]. The ionic conductivity is due to the motion of dissolved ionic species in a polymeric matrix. The ionic mobility is promoted by segmental motion of polymer host and the conduction take place in the amorphous phase in the SPEs [7].

Nowadays, ionic liquid have received a great attention to use as electrolyte in polyelectrolyte due to the unique properties, low volatility, thermal stability, high ionic conductivity and so on. Singh et al. [8] have synthesized ionic liquids containing imidazolium cation with different kinds of anions and incorporated in different polymers to obtain polymers which show conductivity over a wide range (10^{-3} - 10^{-6} S/cm). Composite solid electrolytes based on polyacrylonitrile (PAN), poly(ethylene oxide) (PEO) and poly(vinyl alcohol) (PVA) and ionic liquids as well using plasticizers, were prepared. The polymer electrolytes showed a rubber like characteristic [9]. Moreover, polyelectrolyte with high ionic conductivity and good elasticity by mixing nitrile rubber with ionic liquid, *N*-ethylimidazolium bis(trifluoromethanesulfonyl)imide (EImTFSI) (1.2×10^{-5} S/cm at 50%wt ionic liquid) have been reported by Marwanta [10]. Films are transparent at ionic liquid content less than 60%wt.

In this chapter, we describe the synthesis of ionic liquid incorporated polyurethanes, based on polyisoprene, and conducting polymer/polyurethane composites. Firstly, ionic liquid incorporated polyurethanes were prepared by using hydroxytelechelic cis-1,4-polyisoprene (HTPI) and epoxidized hydroxytelechelic cis-1,4-polyisoprene (EHTPI) as precursors

incorporated with two kinds of ionic liquids, 1-butyl-3-methylimidazolium hexafluorophosphate, and trihexyltetradecylphosphonium chloride. Films were characterized with Fourier Transform Infrared Spectroscopy (FTIR). Thermal properties, glass transition properties and thermal decomposition, were investigated by differential scanning calorimetry (DSC) and thermogravimetric analysis (TGA). Conductivity of films was measured by means of dielectric relaxation spectroscopy (DRS). Secondly, conducting polymer/polyurethane composites of polyaniline (PANI), polypyrrole (PPy) and poly(3,4-ethylene dioxathiophene) (PEDOT) were synthesized and characterized by electrochemical technique.

3.2. Ionic liquid incorporated polyurethanes

Ionic liquid was interested to incorporate in the polymer to obtain the polyelectrolyte with high conductivity and good mechanical properties. In our case, we were interested in incorporating ionic liquid in the polyurethane film that is well known as matrix polymer in polyelectrolyte application.

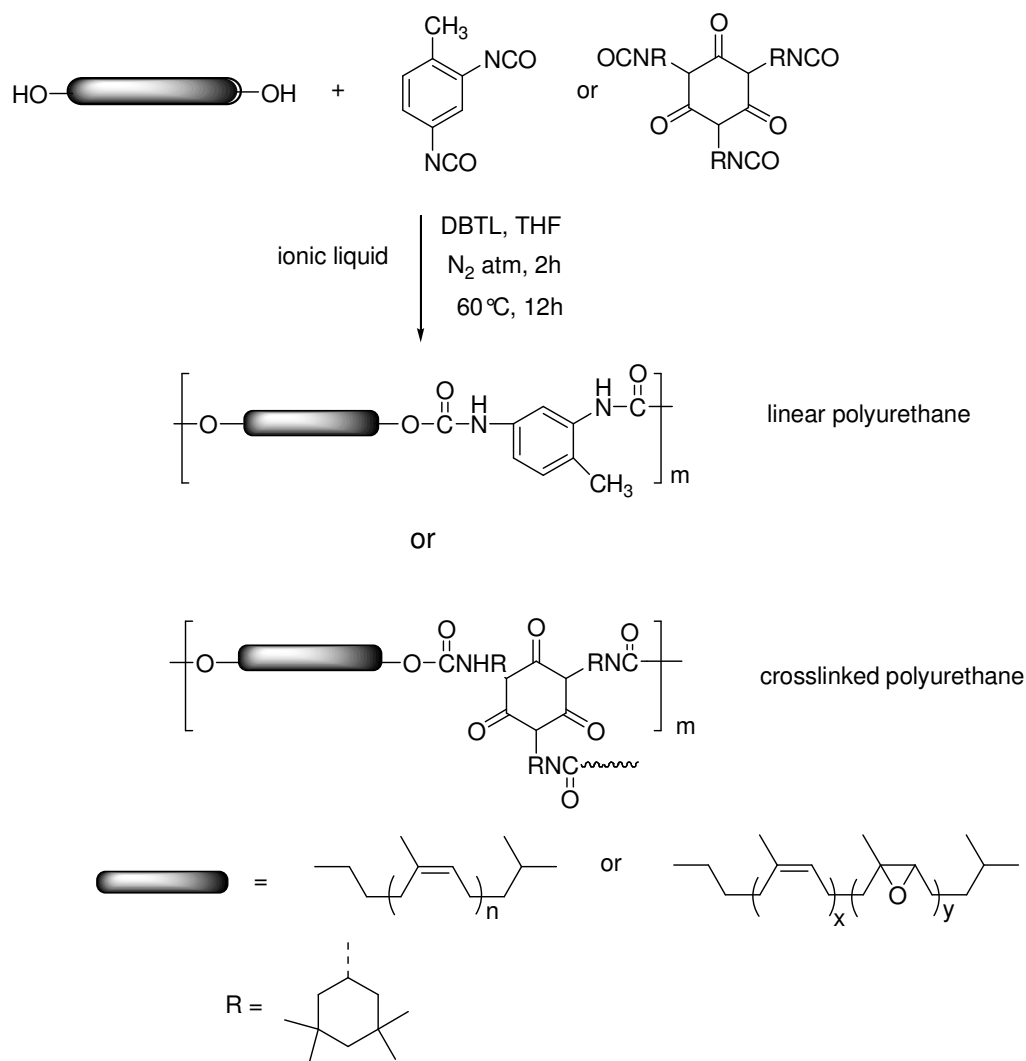
3.2.1. Synthesis of linear and crosslinked ionic liquid incorporated polyurethanes

The synthesis of polyurethanes involves the classical one-shot polyaddition reaction of alcohol groups of telechelic oligomers with isocyanate groups in the presence of a catalyst [11]. In our study, we have prepared also ionic liquid incorporated polyurethane films in the same procedure. Hydroxytelechelic cis-1,4-polyisoprene, **4**, or epoxidized hydroxytelechelic cis-1,4-polyisoprene, **5**, and different proportions of ionic liquid were dissolved in THF. Catalyst and isocyanate (TDI or I-IPDI) were then added into reaction solution. Films were obtained by casting technique under nitrogen atmosphere at room temperature and subsequently cured at 60°C for 12 h (Scheme 3.1).

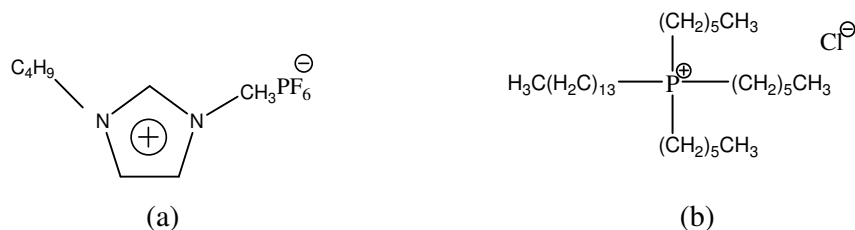
Two kinds of ionic liquids used in this synthesis are 1-butyl-3-methylimidazolium hexafluorophosphate, [bmim]PF₆ and trihexyltetradecylphosphonium chloride, [tthdp]Cl (Scheme 3.2). In order to eliminate unincorporated ionic liquid, films were rinsed with acetone or acetonitrile and the exactly percentage of incorporated ionic liquid was calculated.

Because films are not soluble in solvent for NMR analysis, the characterization by that technique was limited. Films were characterized by FTIR, DSC and TGA. Conductivity of

ionic liquid incorporated films was then measured by dielectric relaxation spectroscopy (DRS).



Scheme 3.1 Synthesis of linear and crosslinked polyurethane and epoxidized polyurethane



Scheme 3.2 Ionic liquid used in this work: a) 1-butyl- 3-methylimidazolium hexafluorophosphate, [bmim]PF₆; b) trihexyltetradecylphosphonium chloride, [thtdp]Cl

3.2.1.1. [bmim]PF₆ incorporated polyurethane films

The composition of [bmim]PF₆ incorporated polyurethane films and observation are summarized in Table 3.1. Films are pale yellow, flexible and transparent, especially, crosslinked polyurethane films are more transparent than linear polyurethane films. In non-epoxidized polyurethane films, ionic liquid incorporated are limited at 10 %wt., when we added more ionic liquid, we observed the phase separation in film and drops of ionic liquid at the films surface. This was attributed to immiscibility between ionic liquid and polyisoprene based polyurethanes. The miscibility of ionic liquid and polyurethane is low because the polyurethane containing mostly hydrocarbon structure (non-polar) is linked with the short urethane unit, while [bmim]PF₆ has a high polarity.

At high epoxidation ratio, polyurethane films are stiff. With the epoxidized films, we can add more amount of ionic liquid in films.

Table 3.1 Composition and appearance of linear and crosslinked polyurethanes with different percentages of [bmim]PF₆.

Polymer code	Diol	Isocyanate	[bmim]PF ₆ (%wt)	Appearance
PU1	HTPI	TDI	0	Yellow, soft, transparent
PU2	HTPI	TDI	10	Yellow, soft, transparent
PU3	HTPI	I-IPDI	0	Yellow, soft, clear
PU4	HTPI	I-IPDI	1	Yellow, soft, clear
PU5	HTPI	I-IPDI	6	Yellow, soft, clear
PU6	HTPI	I-IPDI	10	Yellow, soft, clear
PU7	EHTPI (34%)	I-IPDI	0	Yellow, soft, transparent
PU8	EHTPI (34%)	I-IPDI	10	Yellow, soft, transparent
PU9	EHTPI (34%)	I-IPDI	20	Yellow, soft, transparent
PU10	EHTPI (58%)	I-IPDI	0	Yellow, soft, transparent
PU11	EHTPI (58%)	I-IPDI	12	Yellow, soft, transparent
PU12	EHTPI (58%)	I-IPDI	23	Yellow, soft, transparent
PU13	EHTPI (80%)	I-IPDI	0	Yellow, stiff, transparent
PU14	EHTPI (80%)	I-IPDI	12	Yellow, stiff, transparent
PU15	EHTPI (80%)	I-IPDI	20	Yellow, stiff, transparent
PU16	EHTPI (80%)	I-IPDI	27	Yellow, stiff, transparent
PU17	EHTPI (80%)	I-IPDI	30	Yellow, stiff, transparent

The FTIR spectra of all polyurethane films exhibited absorptions at approximately 3300, 1500 and 1700 cm^{-1} corresponding to N-H stretching, combination of C-N stretching and N-H out of plane bending and C=O stretching of urethane function. C-O stretching presented at 1062 and 1220 cm^{-1} and no NCO absorption was observed at 2270 cm^{-1} showing that the reaction was complete. Comparing FTIR spectra of films with and without [bmim]PF₆, the higher peak intensity at 831 cm^{-1} and an appearance of peak at 557 cm^{-1} in crosslinked (Fig 3.1) and linear (Fig 3.2) films containing [bmim]PF₆ due to P-F bond in PF₆ anion. Appearance of peaks at 1580 1170 and 752 cm^{-1} in crosslinked film represent C=C, C-N and C-H vibration of cyclic [bmim] cation as reported by Wu et al. [12], while in linear films these peaks overlap with peaks of PU structure.

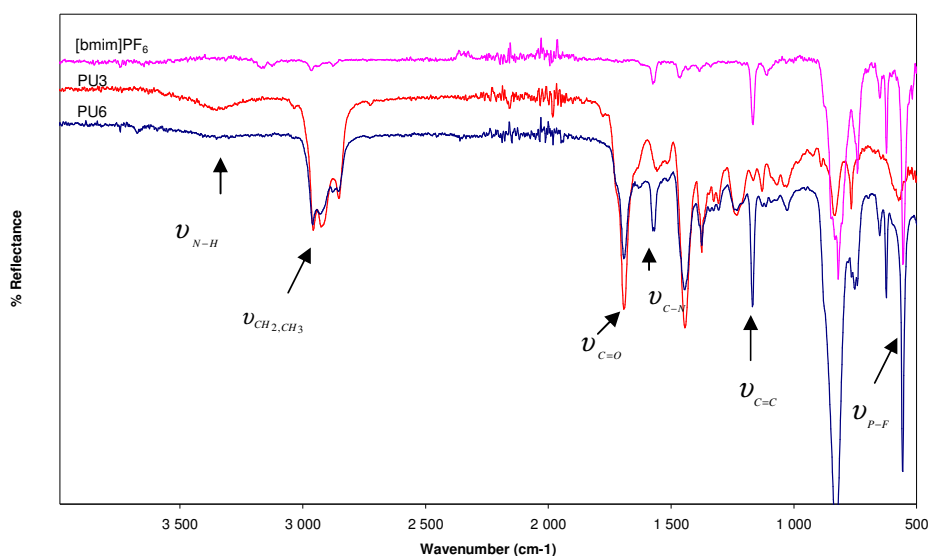


Fig 3.1 FTIR spectra of [bmim]PF₆, crosslinked polyurethane with (PU6) and without [bmim]PF₆ (PU3).

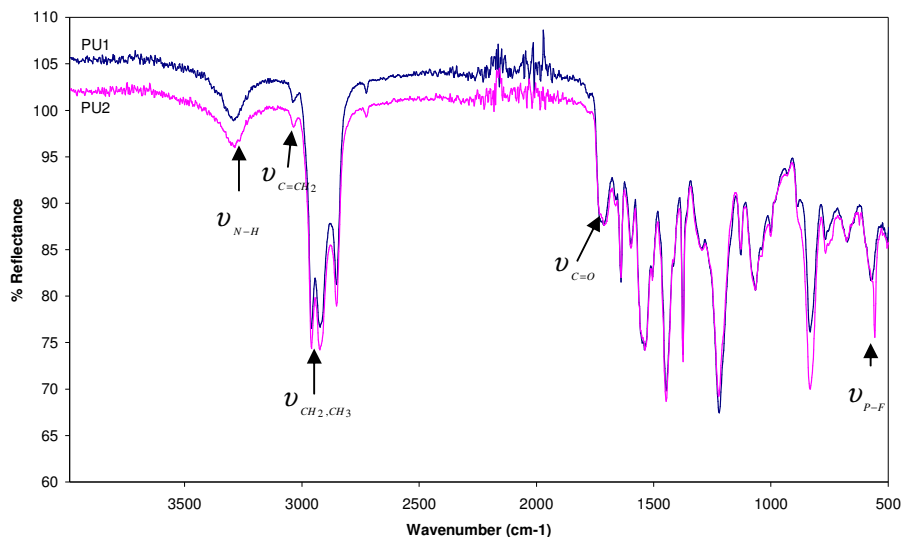


Fig 3.2 FTIR spectra of linear polyurethane with (PU2) and without [bmim]PF₆ (PU1).

Also, in epoxidized polyurethane films, we remarked the higher peak intensity at 831 cm^{-1} and an appearance of peak at 557 cm^{-1} (appendix 2.1)

3.2.1.2. [thtdp]Cl incorporated polyurethane films

In order to improve miscibility of polyisoprene-based polyurethane and ionic liquid, the ionic liquid containing long chain hydrocarbon, trihexyltetradecylphosphonium chloride, [thtdp]Cl, was used to blend with the polyurethane. The composition and appearance of films are shown in Table 3.2. Films are brown, flexible and transparent. We found that this ionic liquid is more miscible with the polyurethane, the migration of ionic liquid at high percentage blending was not observed. Moreover, [thtdp]Cl acts as a plasticizer for polyurethane, films containing [thtdp]Cl are softer. At high percentage incorporated [thtdp]Cl, films are very soft, weak and become sticky. In the epoxidized films, because film is stiffer, we can incorporate [thtdp]Cl up to 59 %wt (in 80% epoxidized film). However, the limitation of the incorporating of this kind of ionic liquid on account to bad mechanical properties at high percentages of ionic liquids is a failure

Table 3.2 Composition and appearance of linear and crosslinked polyurethanes with different percentages of [thtdp]Cl.

Polymer code	Diol	Isocyanate	[thtdp]Cl (%wt)	Appearance
PU18	HTPI	TDI	10	Brown, weak*, transparent
PU19	HTPI	I-IPDI	10	Brown, soft, transparent
PU20	HTPI	I-IPDI	19	Brown, soft, transparent
PU21	HTPI	I-IPDI	30	Brown, soft, transparent
PU22	HTPI	I-IPDI	38	Brown, soft, transparent, sticky
PU23	EHTPI (30%)	I-IPDI	0	Brown, soft, transparent
PU24	EHTPI (30%)	I-IPDI	11	Brown, soft, transparent
PU25	EHTPI (30%)	I-IPDI	20	Brown, soft, transparent
PU26	EHTPI (30%)	I-IPDI	30	Brown, soft, transparent
PU27	EHTPI (30%)	I-IPDI	36	Brown, soft, transparent, sticky
PU28	EHTPI (58%)	I-IPDI	0	Brown, soft, transparent
PU29	EHTPI (58%)	I-IPDI	10	Brown, soft, transparent
PU30	EHTPI (58%)	I-IPDI	18	Brown, soft, transparent
PU31	EHTPI (58%)	I-IPDI	28	Brown, soft, transparent
PU32	EHTPI (58%)	I-IPDI	35	Brown, very soft, transparent
PU33	EHTPI (58%)	I-IPDI	43	Brown, very soft, transparent, sticky
PU34	EHTPI (80%)	I-IPDI	0	Brown, stiff, transparent
PU35	EHTPI (80%)	I-IPDI	9	Brown, soft, transparent
PU36	EHTPI (80%)	I-IPDI	18	Brown, soft, transparent
PU37	EHTPI (80%)	I-IPDI	23	Brown, soft, transparent
PU38	EHTPI (80%)	I-IPDI	32	Brown, soft, transparent
PU39	EHTPI (80%)	I-IPDI	47	Brown, soft, transparent
PU40	EHTPI (80%)	I-IPDI	50	Brown, soft, transparent, sticky
PU41	EHTPI (80%)	I-IPDI	59	Brown, soft, transparent, sticky
PU42	EHTPI (80%)	TDI	0	Brown, stiff, transparent
PU43	EHTPI (80%)	TDI	10	Brown, weak*, transparent

* Film can't be taken off from mould

The FTIR spectra of all polyurethane films exhibited absorptions at approximately 3300, 1500 and 1700 cm^{-1} corresponding to N-H stretching, combination of C-N stretching and N-H out of plane bending and C=O stretching of urethane function. C-O stretching presented at 1062 and 1220 cm^{-1} . In crosslinked films containing [thtdp]Cl, we noted the new peak at 720 cm^{-1} corresponding to peak in [thtdp]Cl, while in epoxidized polyurethane this peak overlaps with peaks of polyurethane (Fig3.3, 3.4 and appendix 2.2). However, the higher incorporation ratio of ionic liquid led to the softer films (PU22, PU27, PU40, PU41) and we did not observed phase separation or drops of [thtdp]Cl in/at films surface.

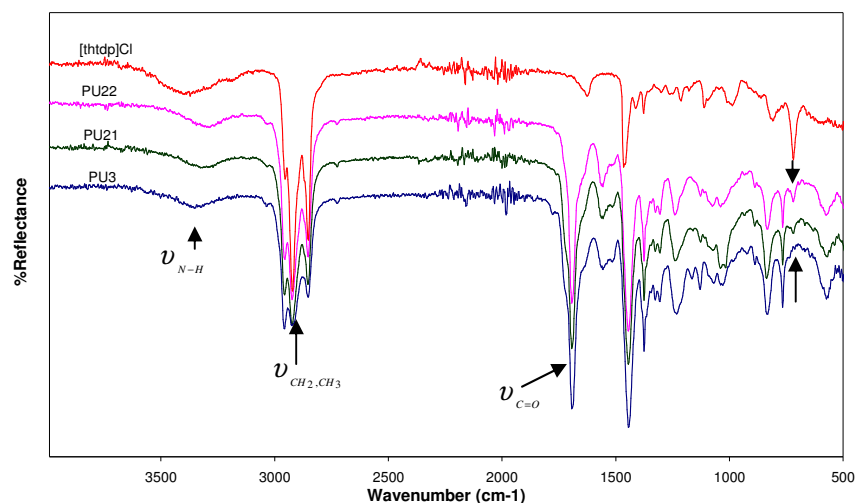


Fig 3.3 FTIR of [thtdp]Cl, crosslinked polyurethane without ionic liquid (PU3), crosslinked polyurethane incorporated with 30% (PU21) and 38% [thtdp]Cl (PU22).

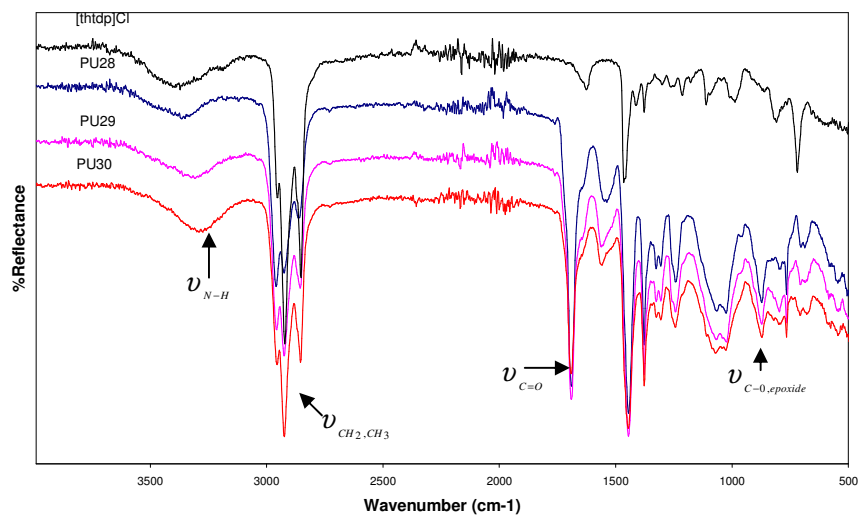


Fig 3.4 FTIR of [thtdp]Cl, crosslinked 58% epoxidized polyurethane without ionic liquid (PU28), linear polyurethane incorporated with 10% (PU29) and 20% [thtdp]Cl (PU30).

3.2.2. Thermal properties of ionic liquid incorporated polyurethane films

Glass transition temperature (T_g) of films was measured by using differential scanning calorimetry. Each sample was scanned from -80°C to 150°C with heating rate $10^{\circ}\text{C}/\text{min}$ under inert atmosphere. Thermal stability of films was investigated up to 600°C under thermogravimetric nitrogen atmosphere using thermogravimetric analysis. The thermal decomposition values of different kinds of films and ionic liquids ([bmim]PF₆, [thtdp]Cl) included different percentages of ionic liquids are reported in Table 3.3 and Table 3.4.

3.2.2.1. Thermal properties of polyurethane films without ionic liquids

T_g of polyurethane films without ionic liquids increases linearly with the increasing percentage of epoxidation as shown in Fig 3.7. This is due to the bulky effect of oxirane rings in the polyurethane main chain; hence higher energy was needed for chain mobility.

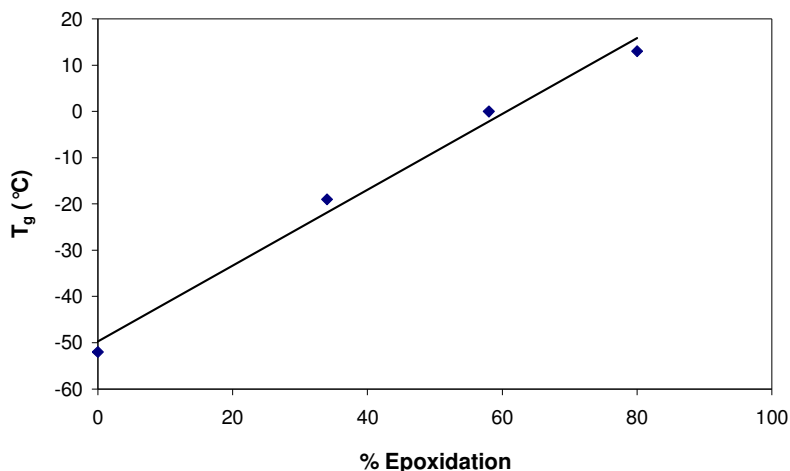


Fig 3.5 The relationship of T_g and percentages of epoxidation of crosslinked epoxidized polyurethane films;

From TGA thermograms (Fig 3.6), the thermal stability of epoxidized film is higher than that of non-epoxidized one. Initial degradation temperature and maximum degradation rate temperature (T_{max}) are higher whereas the degradation rate is lower. At the beginning of degradation, crosslinked polyurethanes have lower degradation rate than linear polyurethanes. DTG curves were analysed comparatively (Fig 3.7), the linear polyurethane (PU1) shows a little weight loss between 150 to 300°C . This corresponds to the degradation of urethane groups of hard segments [13]. The second degradation peak represents the degradation of the

soft segments. This reflects to the phase separation, while crosslinked polyurethane films gave only one step degradation. This is attributed to phase mixing, hard segments act as crosslinkers between the soft segments phases. Thus degradation of hard segments is delayed compared with linear structures.

DTG curves of crosslinked epoxidized polyurethanes (PU23, 28, 34) show the two steps degradation whereas that of in crosslinked non-epoxidized film (PU3) consists of only one step. The first step degradation that was not observed in crosslinked non-epoxidized films could be caused by epoxidized isoprene units. However, this first step degradation is insignificantly different comparing the thermal decomposition data of films with different percentage epoxidation as shown in Fig 3.8. This may be due to the crosslinked structure which “protects” the epoxide structure inside the crosslinking, and thus delays their degradation. The first step degradation is clearer in linear epoxidized film (PU42) compared with linear non-epoxidized (PU1). This first step degradation caused by the both hard segments and epoxidized units which has no effect of crosslinked connection with non-epoxidized isoprene unit.

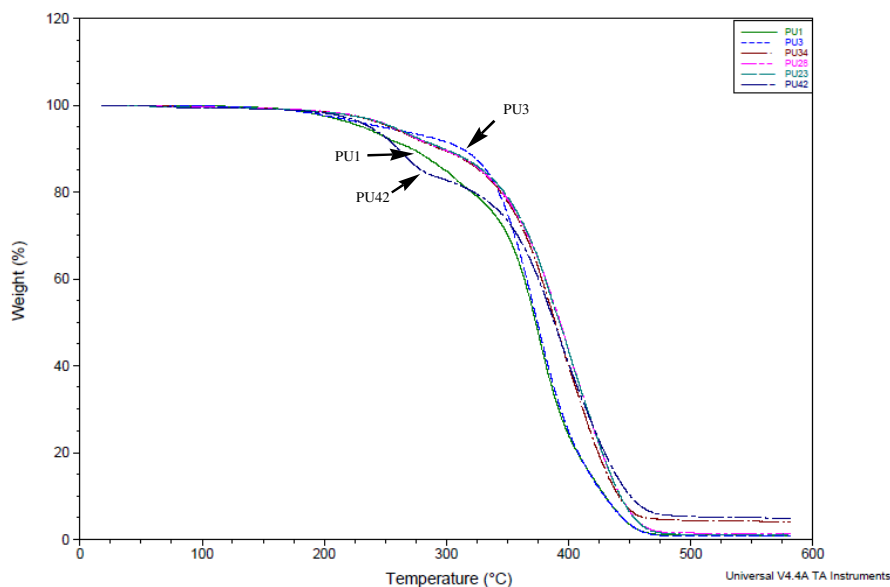


Fig 3.6 TGA thermogram of linear PU (PU1), linear 80% epoxidized PU (PU42), crosslinked PU (PU3), crosslinked 30% epoxidized PU (PU23), 58% epoxidized PU (PU28) and 80% epoxidized PU (PU34).

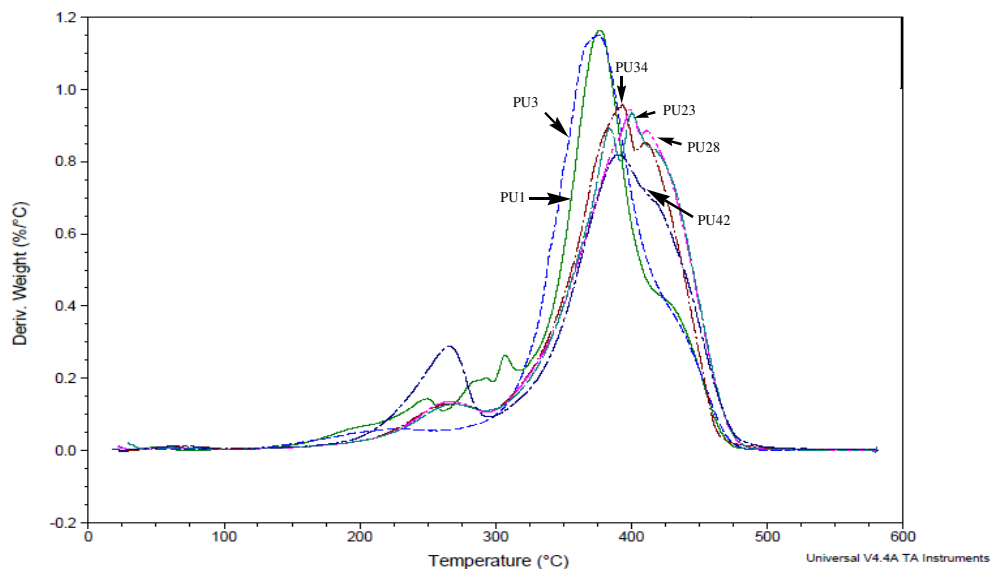


Fig 3.7 DTG curves of linear PU (PU1), linear 80% epoxidized PU (PU42), crosslinked PU (PU3), crosslinked 30% epoxidized PU (PU23), 58% epoxidized PU (PU28) and 80% epoxidized PU (PU34).

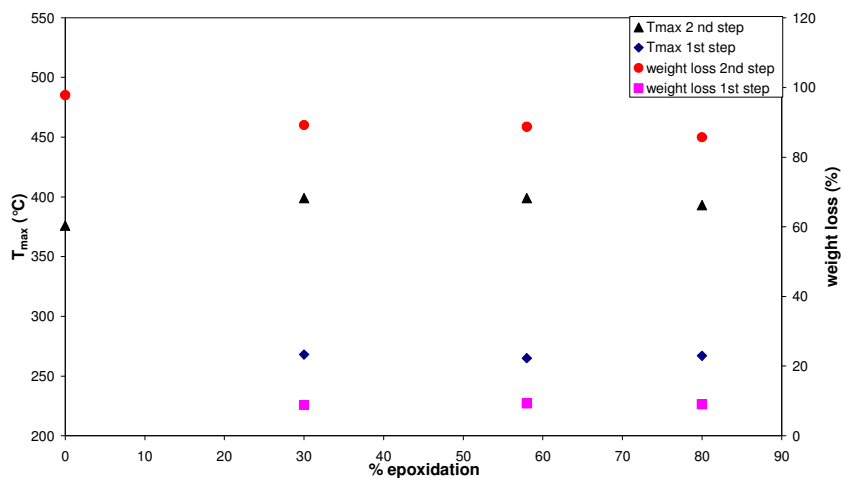


Fig 3.8 Relationship of percentages of epoxidation and thermal decomposition data (T_{max} and weight loss) of different percentage epoxidation films without ionic liquid.

3.2.2.1. Thermal properties of [bmim]PF₆ incorporated polyurethane films

Data of glass transition temperature and thermal decomposition of different percentages of [bmim]PF₆ incorporated polyurethanes and epoxidized polyurethane films are given in Table 3.3.

Table 3.3 Glass transition temperature and thermal degradation value of [bmim]PF₆ incorporated polyurethane films.

polymer code	T _g (°C)	Thermal degradation step					
		1st step		2nd step		3rd step	
		T _{max} (°C)	wt loss (%)	T _{max} (°C)	wt loss (%)	T _{max} (°C)	wt loss (%)
PU1	-58	377	98.2	-	-	-	-
PU2	-58	372	98.4	-	-	-	-
PU3	-52	376	97.8	-	-	-	-
PU4	-51	377	97.9	-	-	-	-
PU5	-53	383	97.4	-	-	-	-
PU6	-53	374	98.6	-	-	-	-
PU7	-19	401	98.3	-	-	-	-
PU8	-19	388	97.7	-	-	-	-
PU9	-17	365	97.9	-	-	-	-
PU10	0	399	98.2	-	-	-	-
PU11	3	395	97.5	-	-	-	-
PU12	-2	392	97.6	-	-	-	-
PU13	13	283	7.7	-	-	402	88.0
PU14	17	269	8.7	331	33.13	394	53.6
PU15	17	260	8.3	332	35.5	392	50.4
PU16	16	268	8.2	332	34.1	392	52.9
PU17	19	273	9.2	338	37.7	391	48.42

Glass transition temperature of linear and crosslinked polyurethane films containing [bmim]PF₆ are not different from that of films without ionic liquid. The relationship between percentages of [bmim]PF₆ in different kinds of films and T_g are shown in Fig 3.9. T_g values are not modified as the amount of [bmim]PF₆ increases. This perhaps because of the immiscibility of [bmim]PF₆ and polyurethane, the amount of ionic liquid in films thus has no effect on films property. On the other hand, T_g increases as the percentage of epoxidation in film increases which might be caused by the increasing of bulky effect from oxirane rings.

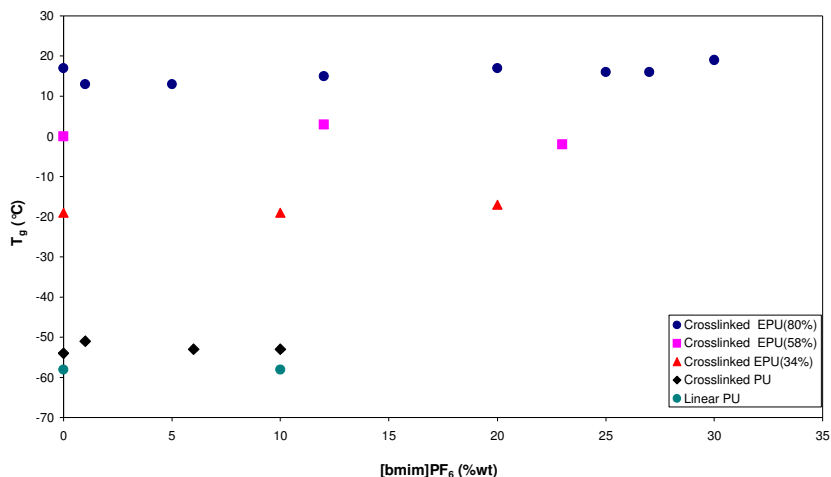


Fig 3.9 The relationship of percentages by weight of incorporated [bmim]PF₆ and T_g of polyurethane films.

[bmim]PF₆ is stable up to 330°C. T_{max} and percentages of weight loss of [bmim]PF₆ incorporated PU films are shown in Table 3.3. It has no difference of thermal stability of films with and without ionic liquid in linear and crosslinked polyurethanes (appendix 2.3). On the other hand, the [bmim]PF₆ incorporated 34% epoxidized polyurethanes (PU8, PU9) show a little decrease in thermal stability compared with films without ionic liquid (PU7) as demonstrated in DTG curve (Fig 3.10). Same observation can be made in Fig 3.12 concerning the 80% epoxidized polyurethanes with (PU14, PU15, PU16, PU17) and without ionic liquid (PU13). The DTG curves for [bmim]PF₆ incorporated crosslinked 34% epoxidized polyurethane films (PU8, PU9) present slightly weight loss of epoxidized unit between 200 to 300°C and two loops overlapped peak between 300 to 490°C. In the same way, in film without [bmim]PF₆, only one peak is noticed between 300 to 490°C. The second peak of degradation is in the same position than that of film without ionic liquid. This second peak is

smaller as percentage of ionic liquid increases. In [bmim]PF₆ incorporated crosslinked non-epoxidized polyurethane films (PU6) (appendix2.3b), we also observe only one peak in this range. This might be caused by the presence of ionic liquid which can activate the reactivity of epoxide ring by acidic nature of the imidazole moiety. Due to the acidity of C2 proton (between two N atoms) of the imidazolium cation, [14,15], the hydrogen bond interaction of imidazolium with epoxide may make easier the cleavage of C-O bond of epoxides [16,17]. Furthermore, the degradation temperature in this step decreases as the percentage of ionic liquid incorporated increases (Fig 3.11).

At more percentage epoxidation, crosslinked 80% epoxidized polyurethane, the degradation peak around 320°C is more clear (Fig 3.12). The degradation rate is slower as percentages of ionic liquid incorporated increase; however, degradation temperature and weight loss are not change. The relationship between T_{max} and percentage incorporated [bmim]PF₆ of step degradation of crosslinked 80% epoxidized polyurethane was presented in Fig 3.13.

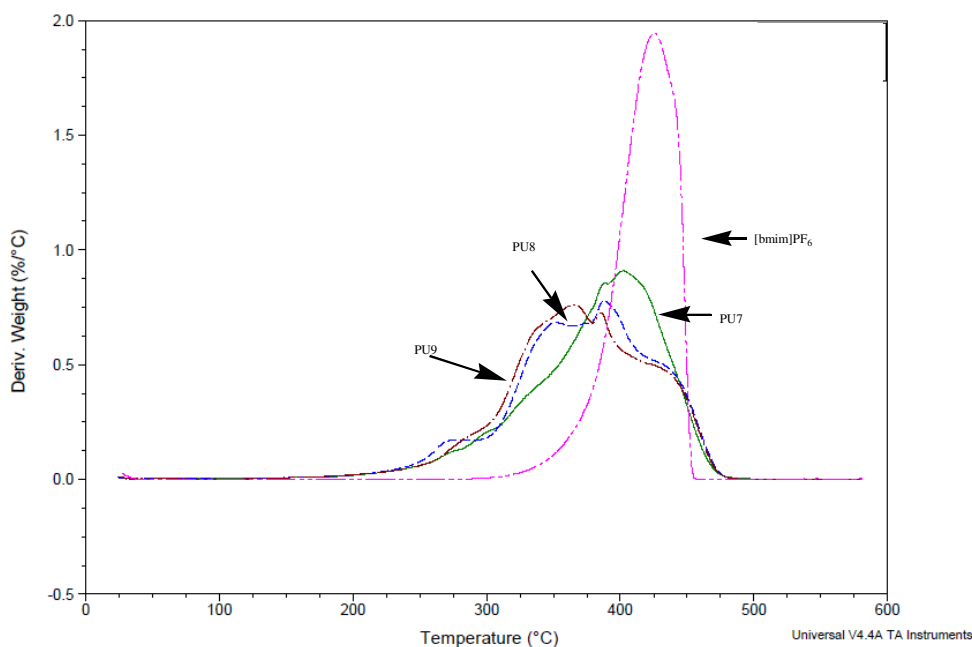


Fig 3.10 DTG curve of 10 %wt (PU8) and 20%wt (PU9) [bmim]PF₆ incorporated and without [bmim]PF₆ (PU7) crosslinked 34% epoxidized polyurethane.

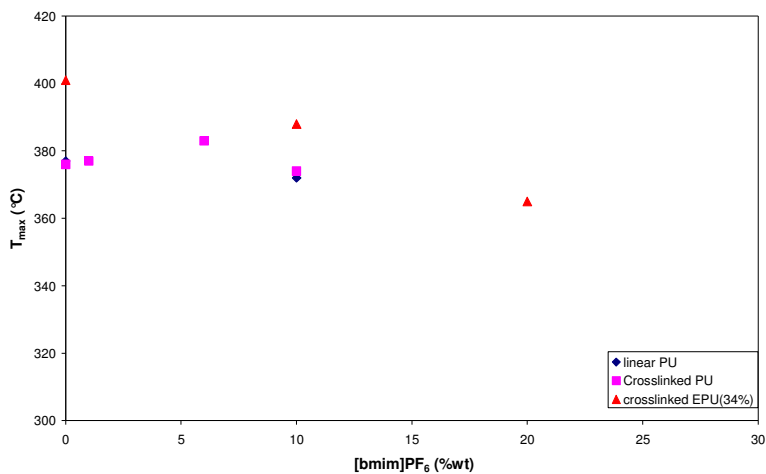


Fig 3.11 The relationship of percentage by weight of incorporated [bmim]PF₆ and T_{max} of polyurethane films.

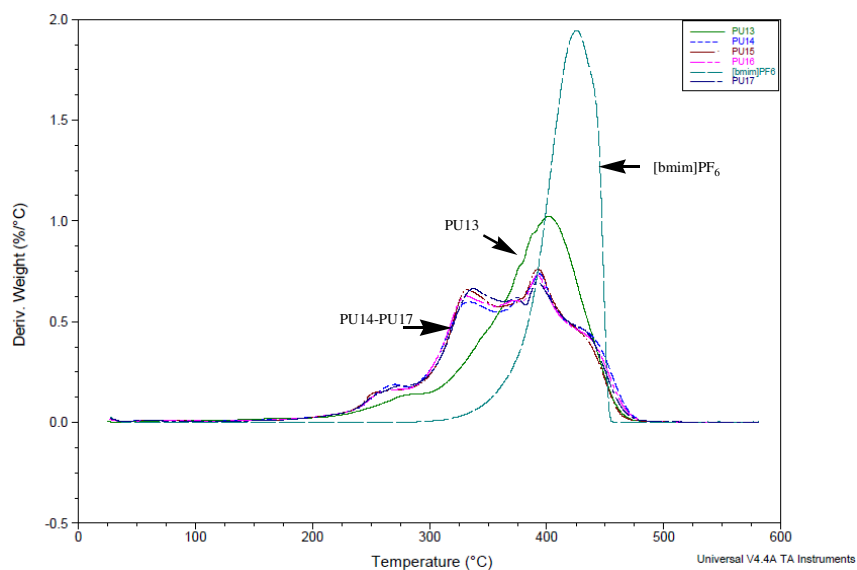


Fig 3.12 DTG curve of 0%wt (PU13), 12%wt (PU14), 20%wt (PU15), 27%wt (PU16) and 30%wt (PU17) [bmim]PF₆ incorporated crosslinked 80% epoxidized polyurethane.

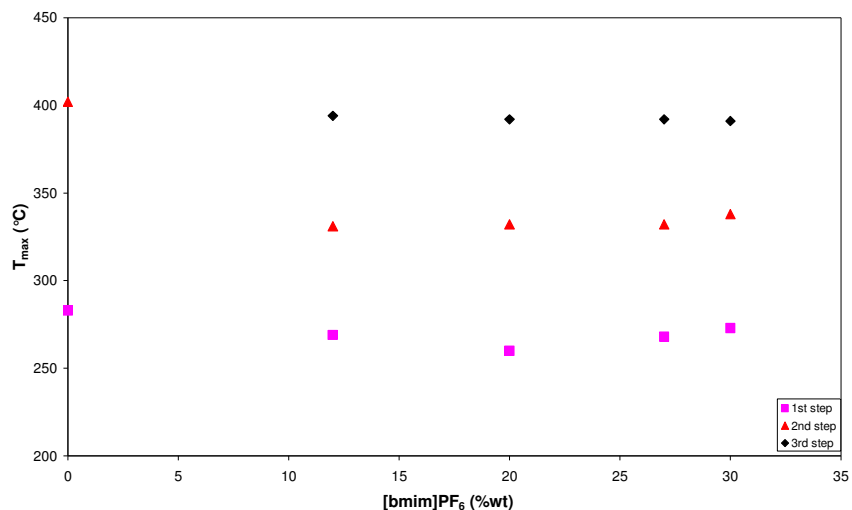


Fig 3.13 The relationship of percentages by weight of incorporated [bmim]PF₆ and T_{max} in each step degradation of 80% epoxidized polyurethane films.

3.2.2.2. Thermal properties of [thtdp]Cl incorporated polyurethane films

Thermal properties of different percentages of [thtdp]Cl incorporated films are summarized in Table 3.4.

Glass transition temperature of [thtdp]Cl incorporated linear non-epoxidized polyurethane film (PU18) is not modified compared with T_g of linear polyurethane film without ionic liquid (PU1) while T_g of crosslinked polyurethane (PU19-22) and crosslink epoxidized polyurethanes (30% epoxidized PU23-27, 58% epoxidized PU28-33 and 80% epoxidized PU34-41) significantly linearly decreases as amount of ionic liquid incorporated increases as shown in Fig 3.14. This probably due to the fact that [thtdp]Cl consists of a long chain hydrocarbon, thus it is well miscible with polyisoprene based polyurethane and it thus can act as plasticizer for films. The softening of film was remarked as the amount of ionic liquid in film was increased.

Table 3.4 Glass transition temperature and thermal degradation values of [thtdp]Cl incorporated polyurethane films.

polymer code	T _g (°C)	Thermal degradation step			
		1st step		2nd step	
		T _{max} (°C)	% wt loss	T _{max} (°C)	% wt loss
PU18	-58	253	19.4	372	70.0
PU19	-55	405	93.9	-	-
PU20	-57	402	92.2	-	-
PU21	-61	392	92.9	-	-
PU22	-62	386	93.1	-	-
PU23	-17	268	8.8	399	89.2
PU24	-21	389	98.2	-	-
PU25	-26	390	97.9	-	-
PU26	-32	367	97.0	-	-
PU27	-39	370	96.8	-	-
PU28	-1	265	9.3	399	88.7
PU29	-3	387	98.6	-	-
PU30	-11	369	98.0	-	-
PU31	-14	369	98.1	-	-
PU32	-18	372	98.1	-	-
PU33	-23	378	98.4	-	-
PU34	14	267	9.0	393	85.7
PU35	11	385	96.2	-	-
PU36	2	370	97.5	-	-
PU37	-4	369	97.6	-	-
PU38	-8	371	96.8	-	-
PU39	-9	371	95.4	-	-
PU40	-14	367	96.3	-	-
PU41	-17	379	97.2	-	-
PU42	6	267	15.8	392	78.3
PU43	3	252	11.7	386	81.8

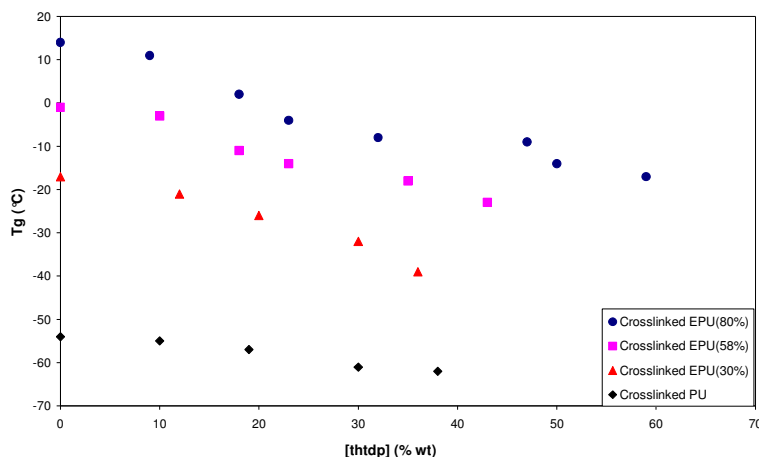


Fig 3.14 Relationship between glass transition temperature and percentage [thtdp]Cl incorporated in crosslinked PU, crosslinked 30%, 58% and 80% epoxidized PU.

From Fig 3.15, all [thtdp]Cl incorporated polyurethane films show a decreasing of thermal stability as the percentage of ionic liquid in film increases. Thermogram of [thtdp]Cl shows a little weight loss before 100°C, this may be due to moisture in the ionic liquid because this kind of ionic liquid is hygroscopic. It is stable up to 320°C, however, when their incorporation in the polyurethane films, decreases their thermal stability. This might be plasticizing effect of ionic liquid makes polymer weaker.

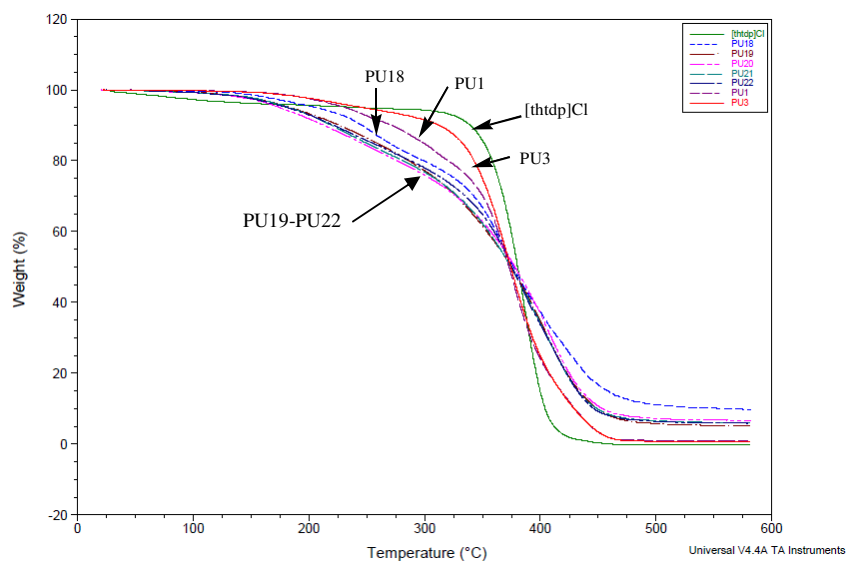


Fig 3.15 TGA thermogram of [thtdp]Cl, linear polyurethane without (PU1) and 10% wt [thtdp]Cl (PU18), crosslinked polyurethane without [thtdp]Cl (PU3), 9% wt (PU19), 19%wt (PU20), 30%wt (PU21) and 38%wt (PU22) [thtdp]Cl.

34% epoxidized polyurethane films containing small amount (10%wt. PU24, 20%wt. PU25) of ionic liquid show slightly higher initial degradation temperature, however at higher percentage of liquid ionic (36% wt PU27), film becomes to degrade at lower temperature than film without ionic liquid. However, T_{max} of all films decreases as the percentage of ionic liquid increases. This may be caused by the plasticizer effect of ionic liquid. Crosslinked 58% and 80 % epoxidized polyurethane films give the same trend (appendix 2.4 and 2.5). Crosslinked 80% epoxidized films without ionic liquid (PU34) show the highest T_{max} .

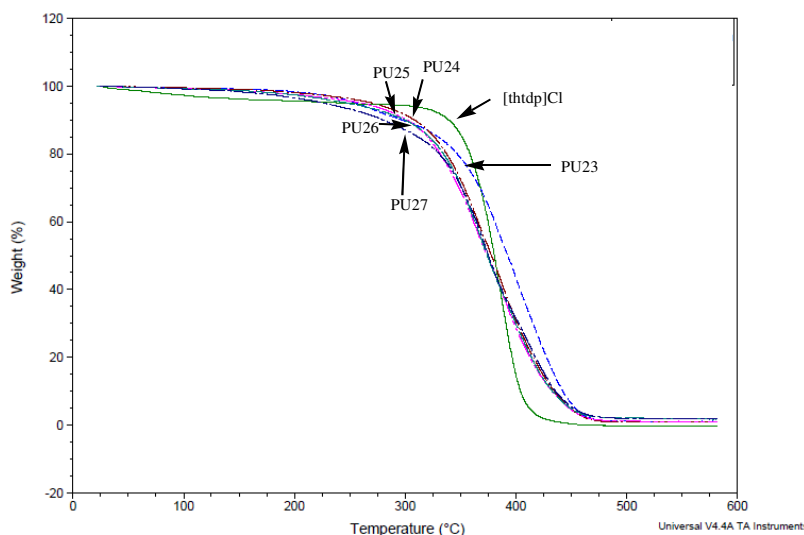


Fig 3.16 TGA thermogram of [thtdp]Cl, crosslinked 34% epoxidized polyurethanes without [thtdp]Cl (PU23), 11% wt. (PU24), 20% wt (PU25), 30% wt. (PU26) and 36%wt. (PU27) [thtdp]Cl.

In all films, T_{max} decreases non-linearly as the percentage of ionic liquid in films increases (Fig 3.17).

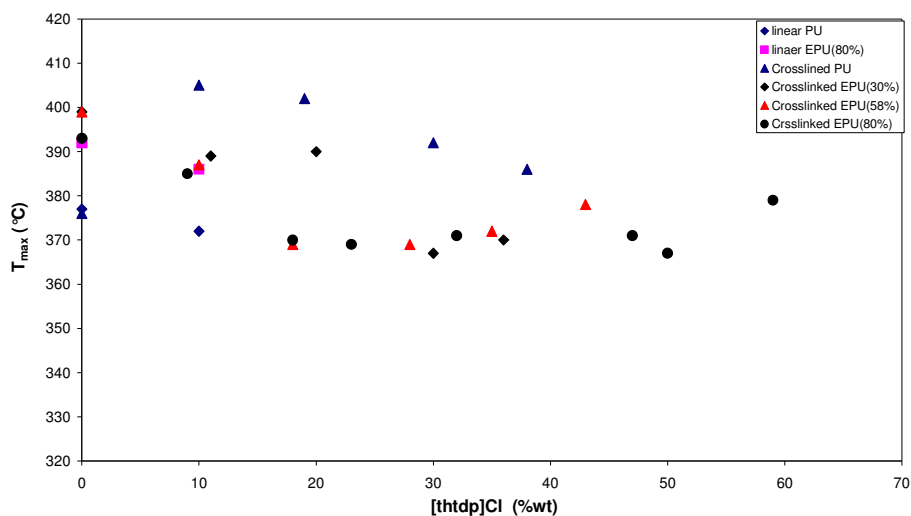


Fig 3.17 Relationship of percentage of [thtdp]Cl incorporated and T_{max} of different polyurethanes.

Weight loss of crosslinked polyurethane films slightly decreases as the percentage of ionic liquid in film increase, while in epoxidation polyurethanes the weight loss nearly not change as amount of ionic liquid in film increases (Fig 3.18).

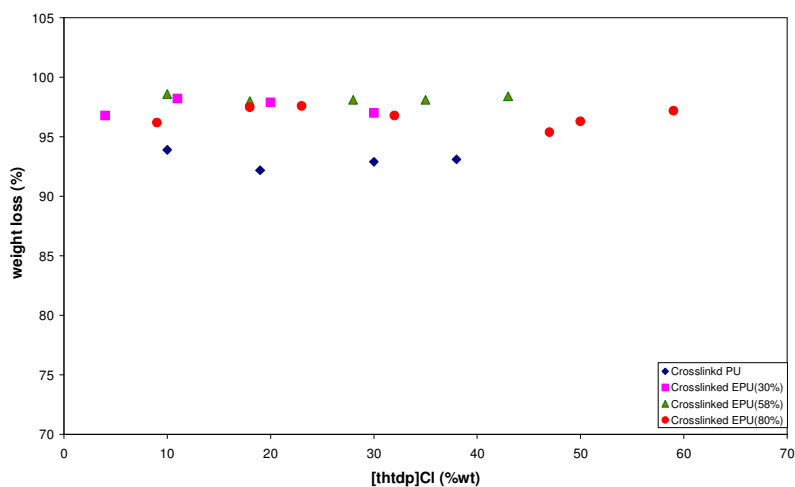


Fig 3.18 Relationship of percentage of [thtdp]Cl and weight loss in crosslinked polyurethanes and crosslinked epoxidized polyurethanes.

Linear 80% epoxidized polyurethane containing ionic liquid (PU43) shows slightly decrease of thermal degradation temperature in the first step compared with film without ionic

liquid (PU42) as given in Fig 3.19. It is probably due to the acceleration degradation effect of [thtdp] cation at epoxide unit.

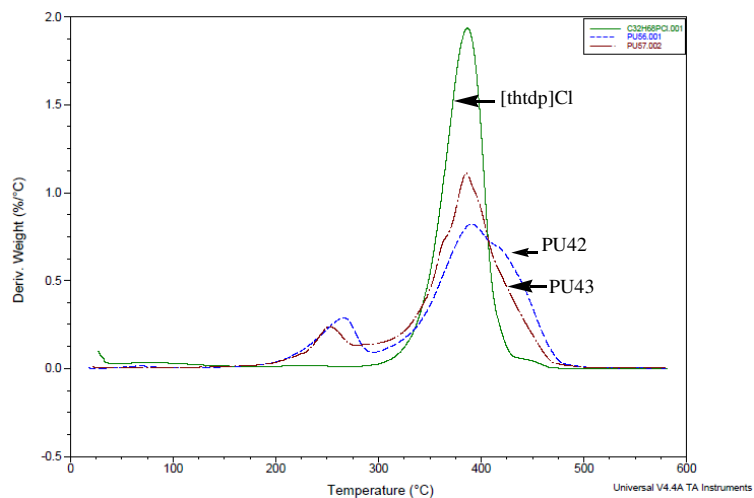


Fig 3.19 DTG curve of [thtdp]Cl, linear 80% epoxidized polyurethane without (PU42) and with 10%wt [thtdp]Cl (PU43).

3.2.3. Conductivity measurement of ionic liquid incorporated polyurethane films.

Conductivity is a bulk parameter which represents the ability of a material to conduct electricity. The units of conductivity are siemens per centimetre (S/cm). A siemen is equal to 1/ohm. Conductivity is represented by the variable "sigma" (σ). The relation between conductivity and resistivity is: $\sigma = 1/\text{resistivity}$ [18].

Resistivity is a bulk parameter which represents a material's tendency to resist the flow of electrical charge. The relation between resistivity(ρ) and resistance(R) is; $R = \rho \cdot L/A$, where L is the length parallel to the moving electrical charge and A is the cross-sectional area through which the charge is flowing.

The conductivity depends on the temperature and frequency. The real part conductivity plot exhibits a low-frequency plateau corresponding to ionic conductivity of samples.

Conductivity of polyurethane films was determined using dielectric spectroscopy between frequencies 0.1 to 10^7 Hz at room temperature. The sample was mounted between two gold parallel electrodes and placed in the seal cell at atmospheric pressure. Obtained conductivity is called ac conductivity.

The frequency dependence of the absolute conductivity [$\sigma = (\sigma'^2 + \sigma''^2)^{1/2}$] of all samples are studied here at room temperature. This conductivity was extracted from the measured real and imaginary parts of the complex dielectric permittivity ϵ^* ($= \epsilon' - i\epsilon''$) using the following relation [19]:

$$\sigma = \sigma' - i\sigma'' = i2\pi f \epsilon_0(\epsilon^* - 1)$$

Where f is the frequency, $i = (-1)^{1/2}$ and ϵ_0 is the permittivity in vacuum.

This procedure was applied for all samples. Conductivity, ac conductivity, values were calculated by mean of WinFit 2.4(1996) software GmbH (Germany).

3.2.3.1. Conductivity measurement of polyurethane films without ionic liquids

Frequency dependence ac conductivities of non-epoxidized (PU1, PU3) and epoxidized polyurethane (PU23, PU28, PU34, PU42) films without ionic liquid are given in Fig 3.20. The conductivity values at low frequency are presented in Table 3.5. Temperature dependence of conductivity of polyurethane was investigated in linear polyurethane as shown in Fig 3.21.

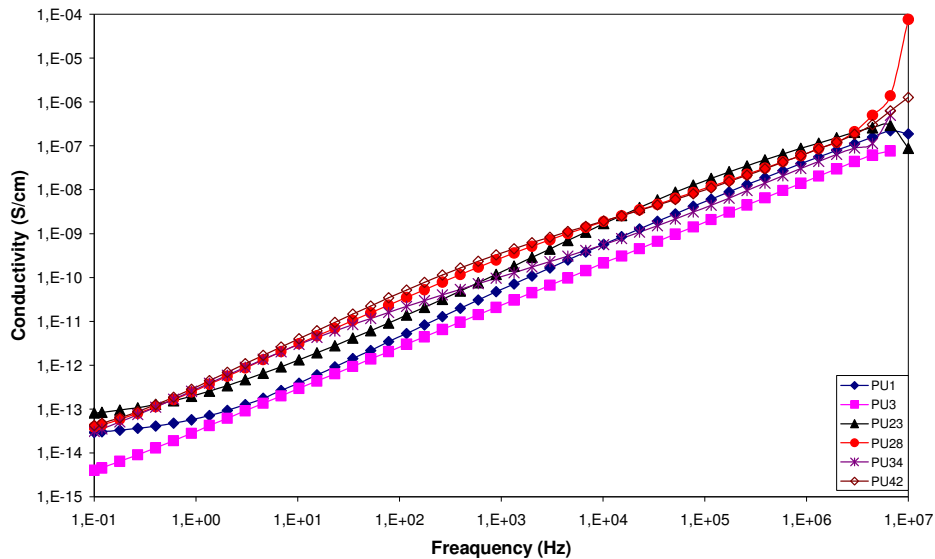


Fig 3.20 Frequency dependence of the conductivity of linear polyurethane (PU1) crosslink polyurethane (PU3), crosslinked 30% (PU23), 58% (PU28) and 80% (PU34) epoxidized polyurethanes without [bmim]PF₆ at room temperature.

The linear polyurethane films without ionic liquid give slightly higher conductivity than crosslinked films at low frequency. This might be caused by the greater flexibility of chain, thus the ion mobility and ion transport are easier as reported in many works [20-22] because charges carriers transport is governed by the mobility of the polymeric chains.

34% epoxidized polyurethane (PU7) show slightly higher conductivity than non-epoxidized films, this can be explained in term of increasing of polar sites amount causing by the oxirane ring that was explained in work of Klinklai et al. [21]. They showed that the conductivity depends on the epoxide groups content. The conductivity increases as the increasing of epoxy content because polar site amount increases until a maximum and then conductivity decreases due to the competitive two factors, chain mobility and polarity site ion carriers. At high epoxide group content, chain mobility is restrained, even polar site ion carrier amount increases, this make the ion mobility in polymer matrix decreases. Thus, the conductivity decreases. Polyurethane films without ionic liquid from two times preparation (PU7, PU10, PU13, PU23, PU28, PU34) have a little different of conductivity. This may be come from the error in the experiment, the different of films thickness.

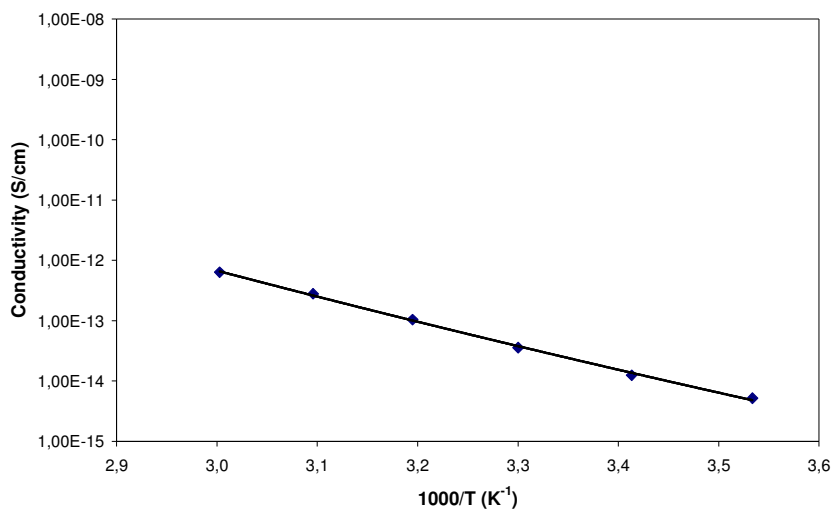


Fig 3.21 Temperature dependence of ionic conductivity in linear polyurethane (PU1).

Conductivity in Fig 3.21 increases gradually with decreasing $1/T$. The trend line is fittings of the Vogel-Tammann-Fulcher-Hesse (VTFH) equation [20,22];

$$\sigma(T) = A \exp\left(-\frac{B}{T - T_0}\right)$$

Where A, B and T_0 are temperature-independent empirical constants. The good fitting of the VTFH equation to conductivity data reflects that conductivity is a function of the mobility of polymer chains [20, 21].

3.2.3.2. Conductivity measurement of [bmim]PF₆ incorporated polyurethane films.

Conductivity of [bmim]PF₆ incorporated films exhibits a low-frequency plateau (Fig 3.22) while this is not noted in films without ionic liquid. Conductivity of films can be estimated from plateau values of frequency versus conductivity curves. At low frequencies, ac conductivity becomes frequency independent, the plateau values giving dc conductivity [10,20,22]. In addition, films with ionic liquid incorporation give higher conductivity than films without ionic liquid. Ionic liquid acts as the electrolyte and it increases ions concentration in the films.

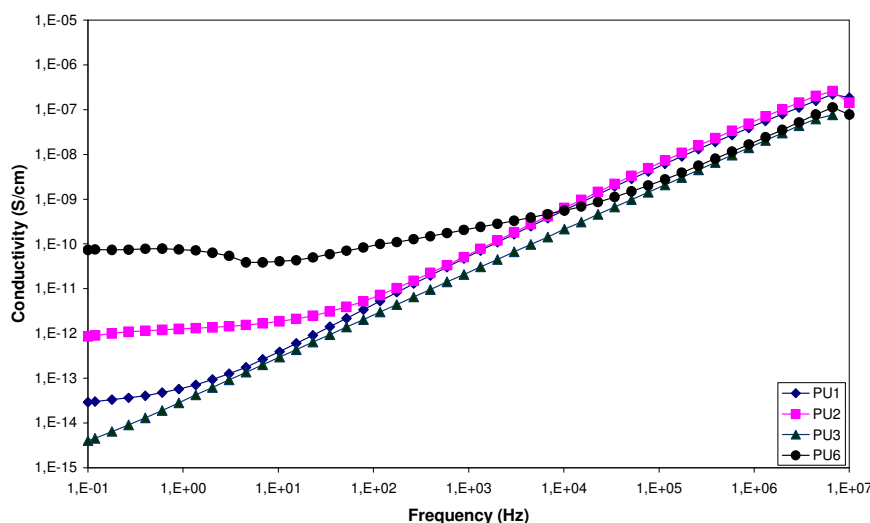


Fig 3.22 Frequency dependence of the ac conductivity of linear polyurethane without (PU1) and 10% wt. [bmim]PF₆ (PU2) and crosslink polyurethane without (PU3) and 10% wt. [bmim]PF₆ (PU6) at room temperature.

Fig 3.22 shows that conductivities of linear and crosslinked non-epoxidized polyurethane films containing 10% wt. [bmim]PF₆ increase compared with those of films without [bmim]PF₆. However, because of the partially miscibility of ionic liquid and polymer, we can not add higher proportion of ionic liquid. There is phase separation and migration of ionic liquid to films surface at amount of [bmim]PF₆ more than 10% wt. At the same percentage of ionic liquid, conductivity is higher for crosslinked films than for linear films.

The dc conductivities of [bmim]PF₆ incorporated polyurethane films are presented in Table 3.5.

Table 3.5 Composition and dc conductivity of [bmim]PF₆ incorporated polyurethane films.

polymer code	Diol	Isocyanate	[bmim]PF ₆ (%wt)	Conductivity (S/cm)
PU1	HTPI	TDI	0	2.92×10^{-14}
PU2	HTPI	TDI	10	8.61×10^{-13}
PU3	HTPI	I-IPDI	0	4.00×10^{-15}
PU4	HTPI	I-IPDI	1	8.08×10^{-15}
PU5	HTPI	I-IPDI	6	1.88×10^{-10}
PU6	HTPI	I-IPDI	10	7.31×10^{-11}
PU7	EHTPI (34%)	I-IPDI	0	1.37×10^{-14}
PU8	EHTPI (34%)	I-IPDI	10	3.25×10^{-13}
PU9	EHTPI (34%)	I-IPDI	20	2.36×10^{-13}
PU10	EHTPI (58%)	I-IPDI	0	1.59×10^{-13}
PU11	EHTPI (58%)	I-IPDI	12	1.67×10^{-12}
PU12	EHTPI (58%)	I-IPDI	23	1.72×10^{-10}
PU13	EHTPI (80%)	I-IPDI	0	2.35×10^{-15}
PU14	EHTPI (80%)	I-IPDI	12	6.20×10^{-14}
PU15	EHTPI (80%)	I-IPDI	20	1.66×10^{-12}
PU16	EHTPI (80%)	I-IPDI	27	2.53×10^{-10}
PU17	EHTPI (80%)	I-IPDI	30	4.15×10^{-9}

In films prepared from epoxidized hydroxytelechelic cis-1,4-polyisoprene, [bmim]PF₆ can be more incorporated in films, because the polarity of polyurethanes increases with the increasing amount of apoxide group. In addition, hydrogen interaction between [bmim]PF₆ and oxygen of oxirane ring can form [12]. The result is that in 80% epoxidation films, ionic liquid can be incorporated up to 30% wt.

The curves of ac conductivity of films scan from frequency 0.1 to 10^7 Hz, are shown in Fig 3.22 and 3.23.

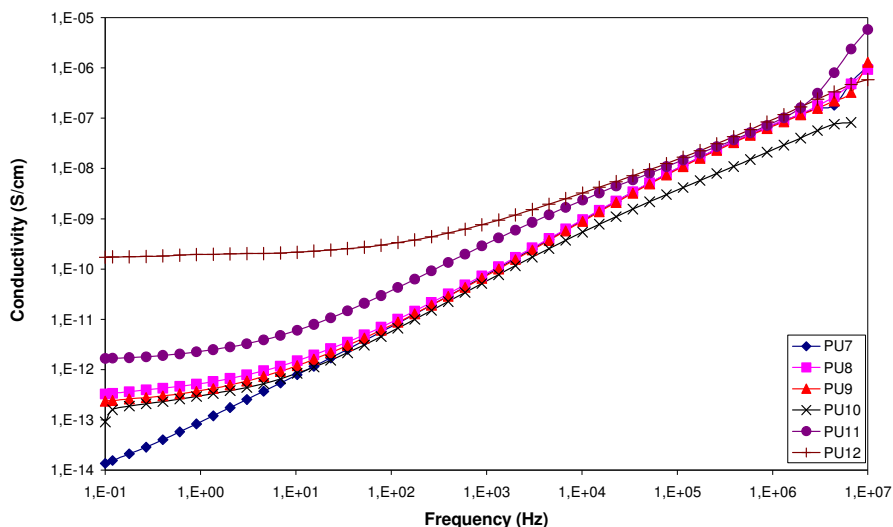


Fig 3.22 Frequency dependence of the ac conductivity of crosslinked 34% epoxidized PU without (PU7), 10% wt. (PU8) and 20%wt [bmim]PF₆ (PU9), crosslink 58% epoxidized PU without (PU10) and 12% wt. (PU11) and 23% wt [bmim]PF₆ (PU12) at room temperature.

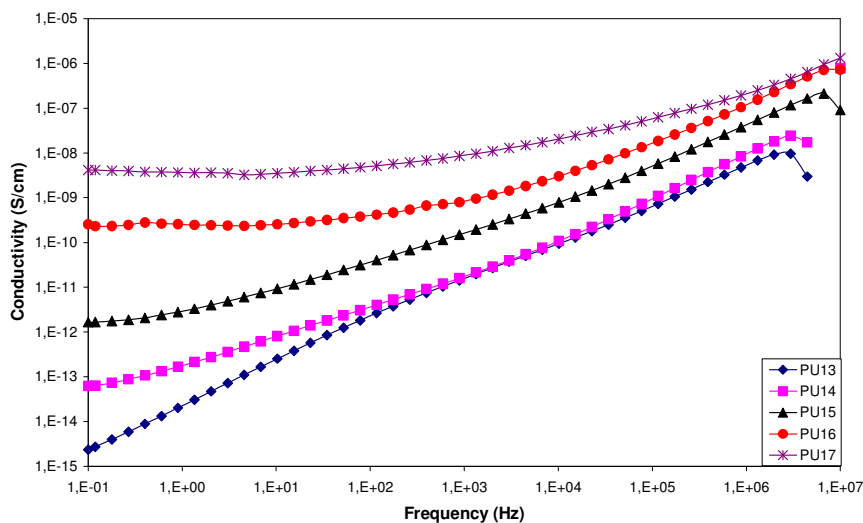


Fig 3.23 Frequency dependence of the ac conductivity of crosslinked 80% epoxidized polyurethane without (PU13), 12% wt. (PU14), 20%wt (PU15), 27%wt. (PU16) and 30%wt. [bmim]PF₆ (PU17) at room temperature.

In crosslinked 34% epoxidized polyurethane, the conductivity is increased by incorporated [bmim]PF₆, but the conductivity does not increase as percentage of ionic liquid in film increases. This might be caused by at low amount of epoxide groups, the ion carriers amount is low, even with increase of ions concentration (from ionic liquid), the conductivity did not increase. On the other hand, in higher epoxidized polyurethanes, the increasing of the epoxide groups make amount of polar sites or ion carriers increases, the conductivity increase when ion concentration increases. This result was observed also in 80% epoxidized film, the conductivity is higher as percentage of ionic liquid in films increases. However, owing to low miscibility of this type of ionic liquid and polyurethane film, the amount of [bmim]PF₆ incorporated limited at 30% wt.

Fig 3.24 presents the increasing of conductivity as the percentages of [bmim]PF₆ in films is increased. This can be explained by the increasing of ions concentration from ionic liquid molecules. At the same percentage of ionic liquid, non-epoxidized polyurethane film give higher conductivity than epoxidized films. Because chain mobility of epoxidized polymers is restricted, ion transport is more difficult compared with in non-epoxidized films.

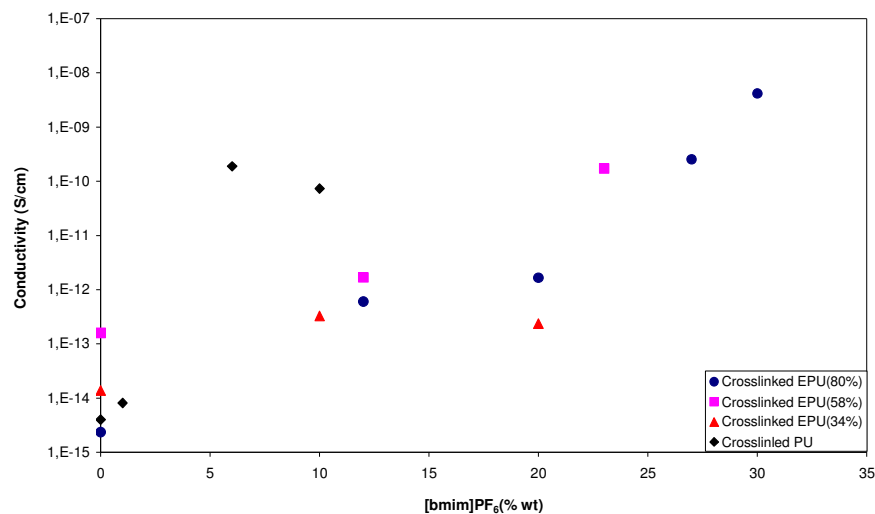


Fig 3.24 Relationship of percentage by weight incorporated [bmim]PF₆ and conductivity of crosslinked polyurethane films at room temperature.

3.2.3.3. Conductivity measurement of [thtdp]Cl incorporated polyurethane films

Frequency dependence of ac conductivity of non-epoxidized polyurethanes is presented in Fig 3.25. [thtdp]Cl incorporated polyurethanes give significantly higher conductivity compared with films without ionic liquid and conductivity increases as higher content of ionic liquid was incorporated in films. This can be explained by the plasticizing effect of this ionic liquid on films. T_g decrease and films are more flexible as ionic liquid is incorporated. Owing to the fact that conductivity of polymer depends on the chain mobility and ion concentration [20-22], the conductivity increases as ionic liquid incorporation in films increases. The relationship between conductivity and percentages of ionic liquid incorporation is given in Fig 3.26. The same result is also observed in epoxidized films (appendix 2.6-2.8). The composition and dc conductivity of polyurethane films are presented in Table 3.6.

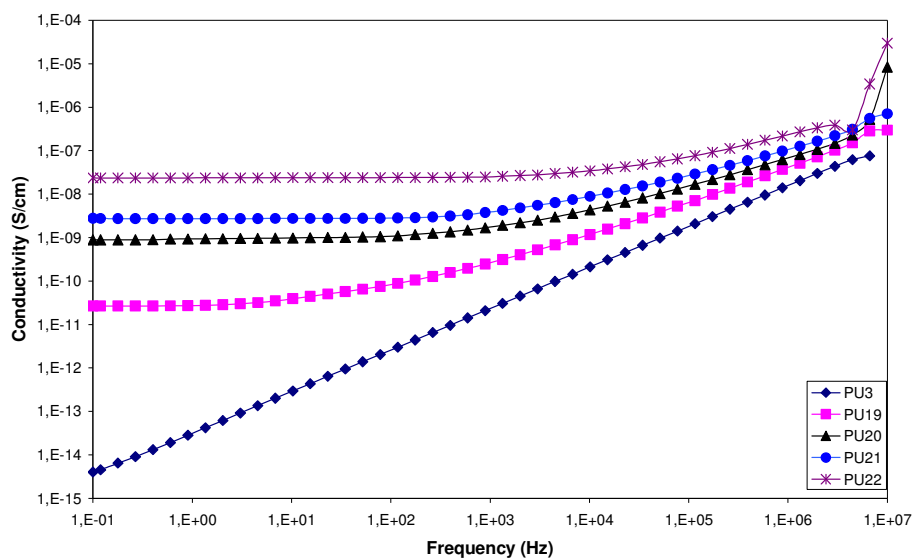


Fig 3.25 Frequency dependence of the ac conductivity of crosslinked polyurethane films with 0% wt (PU3), 10% wt. (PU19), 19%wt (PU20), 30%wt. (PU21) and 38%wt. [thtdp]Cl (PU22) at room temperature.

Table 3.6 Composition and conductivity of [thtdp]Cl incorporated polyurethane films.

Polymer code	Diol	Isocyanate	[thtdp]Cl (%wt)	Conductivity (S/cm)
PU18	HTPI	TDI	10	Nm
PU19	HTPI	I-IPDI	10	2.68×10^{-11}
PU20	HTPI	I-IPDI	19	8.91×10^{-10}
PU21	HTPI	I-IPDI	30	2.77×10^{-9}
PU22	HTPI	I-IPDI	38	2.39×10^{-8}
PU23	EHTPI (30%)	I-IPDI	0	8.14×10^{-14}
PU24	EHTPI (30%)	I-IPDI	11	8.96×10^{-11}
PU25	EHTPI (30%)	I-IPDI	20	8.88×10^{-10}
PU26	EHTPI (30%)	I-IPDI	30	4.31×10^{-9}
PU27	EHTPI (30%)	I-IPDI	36	1.56×10^{-8}
PU28	EHTPI (58%)	I-IPDI	0	3.87×10^{-14}
PU29	EHTPI (58%)	I-IPDI	10	3.09×10^{-11}
PU30	EHTPI (58%)	I-IPDI	18	5.40×10^{-10}
PU31	EHTPI (58%)	I-IPDI	28	1.87×10^{-9}
PU32	EHTPI (58%)	I-IPDI	35	8.38×10^{-9}
PU33	EHTPI (58%)	I-IPDI	43	2.25×10^{-8}
PU34	EHTPI (80%)	I-IPDI	0	3.07×10^{-14}
PU35	EHTPI (80%)	I-IPDI	9	4.39×10^{-12}
PU36	EHTPI (80%)	I-IPDI	18	8.33×10^{-11}
PU37	EHTPI (80%)	I-IPDI	23	5.05×10^{-10}
PU38	EHTPI (80%)	I-IPDI	32	9.04×10^{-11}
PU39	EHTPI (80%)	I-IPDI	47	6.86×10^{-10}
PU40	EHTPI (80%)	I-IPDI	50	1.64×10^{-9}
PU41	EHTPI (80%)	I-IPDI	59	3.70×10^{-8}
PU42	EHTPI (80%)	TDI	0	4.24×10^{-14}
PU43	EHTPI (80%)	TDI	10	Nm

nm = not measure

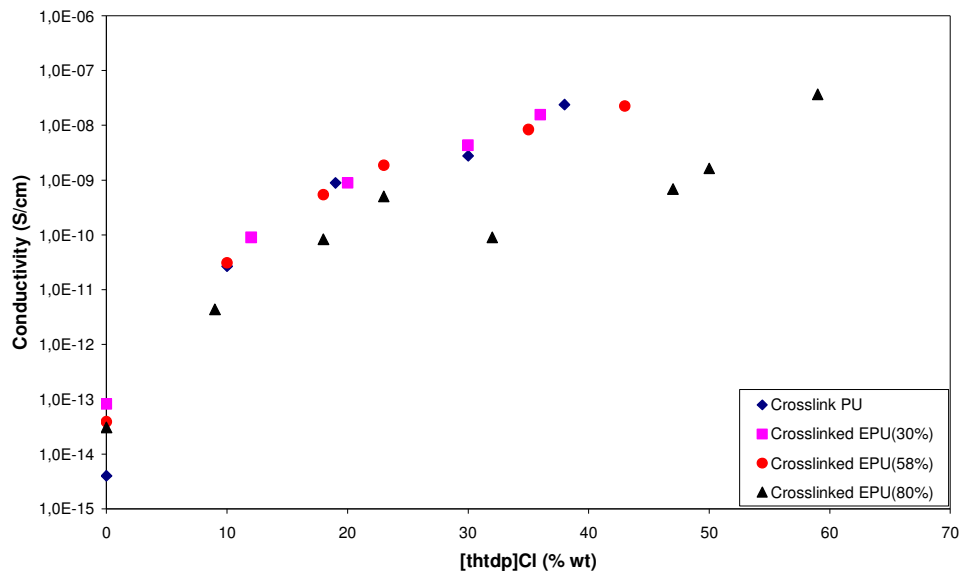


Fig 3.26 Relationship of percentages weight of [thtdp]Cl and conductivity of crosslinked non-epoxidized polyurethane, 30%epoxidized, 58%epoxidized and 80%epoxidized polyurethane.

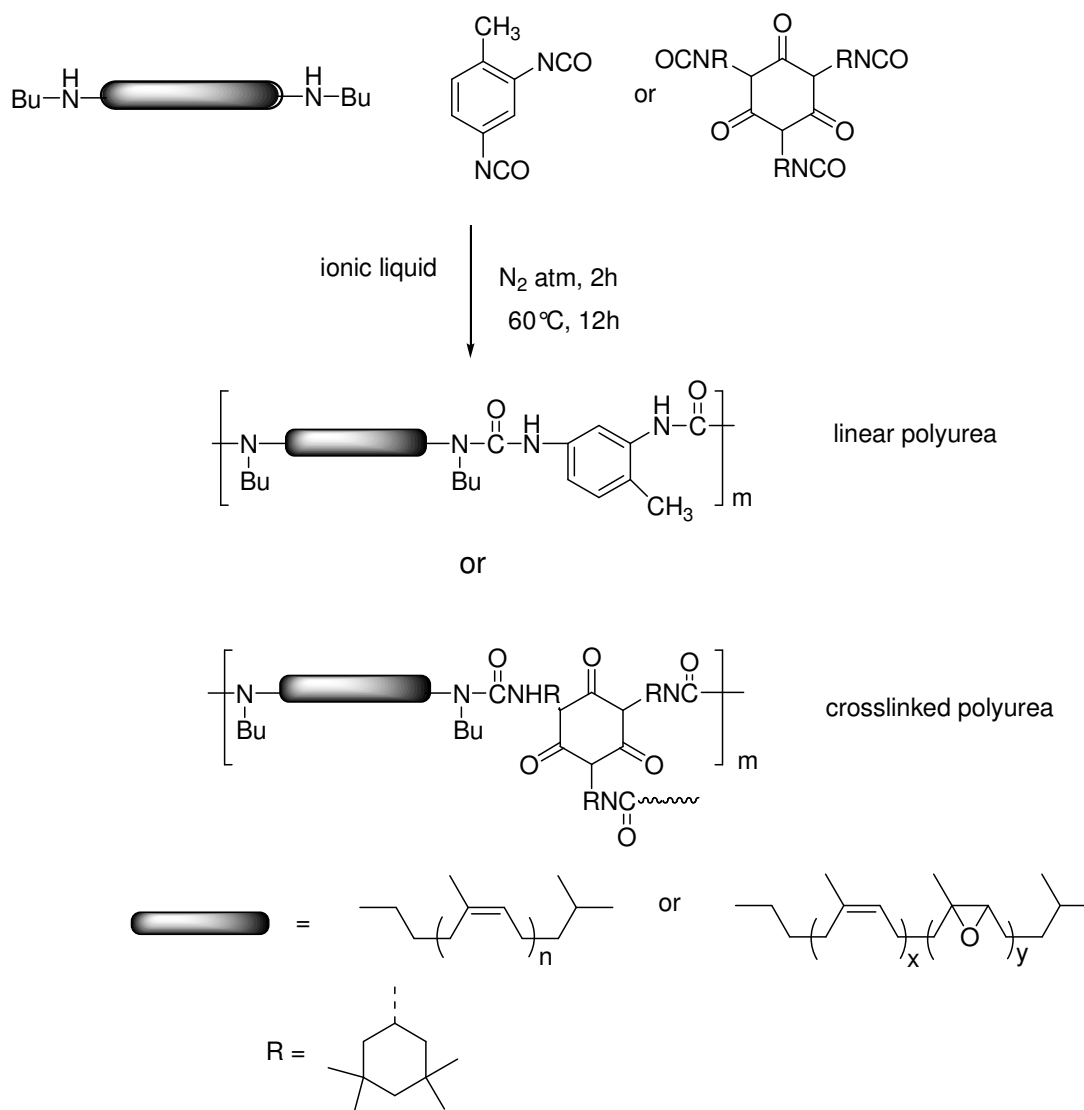
In Fig 3.26, we can see that conductivity of polyurethane films increases non-linearly with the percentage of ionic liquid in films. At the same incorporation percentage of [thtdp]Cl, epoxidized polyurethane films have higher conductivity than non-epoxidized polyurethane film. This can be justified by the increasing amount of the polar site in polymer. Moreover, this ionic liquid acts as plasticizer for films, therefore chain mobility of film is high, too. With the combination effect of chain mobility and increasing ion carriers, the conductivity in epoxidized films is higher than non-epoxidized films.

In contrast, because of the low miscibility of ionic liquid and polymer in [bmim]PF₆ incorporated films, ionic liquid have no plasticizer effect on polymers. Therefore, the conductivity of [bmim]PF₆ incorporated epoxidized polyurethane films is lower than non-epoxidized films.

3.3. Ionic liquid incorporated polyureas

3.3.1. Synthesis of linear and crosslinked ionic liquid incorporated polyureas

The synthesis of linear and crosslinked polyureas and epoxidized polyureas was performed by addition reaction of amine groups of butylaminotelechelic oligomers or epoxidized butylaminotelechelic oligomers with isocyanate groups of TDI or I-IPDI in the presence of catalyst [11]. The reaction occurred instantaneously, films were formed in few minutes after adding isocyanate. Polyureas and ionic liquid incorporated polyureas were prepared in the same procedure; hydroxytelechelic cis-1,4-polyisoprene, **7**, or epoxidized hydroxytelechelic cis-1,4-polyisoprene, **8**, and different proportions of [bmim]PF₆ were dissolved in THF. Catalyst (DBTL) and isocyanate (TDI or I-IPDI) were then introduced into the reaction solution. Films were obtained by casting technique under nitrogen atmosphere at room temperature and subsequently dried at 60°C for 12 h (Scheme 3.3). Films were characterized with FTIR. Thermal properties were investigated by DSC and TGA. Finally, conductivity was determined by means of DRS.



Scheme 3.3 Synthesis of linear and crosslinked polyureas and epoxidized polyureas.

Composition and appearance of polyurea and epoxidized polyurea films with and without [bmim]PF₆ are presented in Table 3.7. Films are brown translucent, homogeneous and flexible. Because of the presence of epoxide units, 54% epoxidized films are stiffer compared with non-epoxidized films.

From ATR mode FTIR analysis, we can observed vibration signals of NH and C=O of urea group at 3340 and 1600 cm⁻¹. Peak at wavenumber 2300 cm⁻¹ corresponding to the absorption band of NCO functional group is observed in linear polyurea, this because we added a large excess of TDI (1.4 mol equivalent). We do not observe this band in other films

(with 1.2 mol equivalent of isocyanate). In [bmim]PF₆ incorporated films (PUR2-PUR5, PUR7), we observed the higher peak intensity at 831 cm⁻¹ and an appearance of peak at 557 cm⁻¹ due to P-F bond in PF₆ anion. This peak is not noted in films without ionic liquid (PUR1, PUR6) (appendix 2.9-2.11).

Table 3.7 Composition and appearance of non-epoxidized and 54% epoxidized polyurea films with and without [bmim]PF₆.

Polymer code	Diamine	Isocyanate	[bmim]PF ₆ (%wt)	appearance
PUR1	PINH	TDI	0	brown, transparent, flexible
PUR2	PINH	TDI	10	brown, translucent, flexible
PUR3	PINH	I-IPDI	10	brown, translucent, flexible
PUR4	PINH	I-IPDI	20	brown, translucent, flexible
PUR5	PINH	I-IPDI	25	brown, translucent, flexible
PUR6	EPINH(54%)	I-IPDI	0	brown, transparent, flexible
PUR7	EPINH(54%)	I-IPDI	20	brown, translucent, flexible

3.3.2. Thermal properties of ionic incorporated polyurea films

Well-defined glass transition temperature of linear non-epoxidized polyurethane with are not modified as [bmim]PF₆ incorporation (T_g = -57°C) (DSC thermograms are presented in appendix 2.12). Thermal properties data of crosslinked polureas are summarized in Table 3.8.

Table 3.8 T_g and thermal decomposition data of crosslinked non-epoxidized and 54% epoxidized polyureas.

Polymer code	thermal degradation step		
	T _g (°C)	T _{max} (°C)	wt. Loss (%)
PUR3	-21 and 28	369	96.8
PUR4	-26 and 29	366	96.6
PUR5	-28 and 28	365	97.3
PUR6	-4	396	93.61
PUR7	-3	394	93.6

T_g value of crosslinked non-epoxidized polyureas is not well-defined. It seems that it shows two values of T_g . We expected that the crosslinked structure makes delay of soft segment movement, thus we observed on higher T_g (around -26°C) than in linear structure, and the transition temperature is not really clear. The second T_g value may be caused by the hard segment movement. Whatever, the second value T_g does not be observed in epoxidized films. By the effect of chain movement restriction due to epoxide groups, crosslinked epoxidized polyurea shows a higher T_g than non-epoxidized films. As the reason of the miscibility limitation of $[\text{bmim}]\text{PF}_6$ and polyisoprene based polymers, T_g of all films are not modified with the ionic liquid incorporation.

DTG curves of the crosslinked polyureas degradation are shown in Fig 3.27. The small weight loss at the beginning of degradation shifted to higher temperature as the proportion of ionic liquid was increased. Initial degradation temperature of film with 25%wt is higher than that film with 10 and 20% wt ionic liquid. This reflects that ionic liquid slightly enhances thermal stability of films. Nevertheless, the main degradation caused by polyisoprene segments degradation does not be modified.

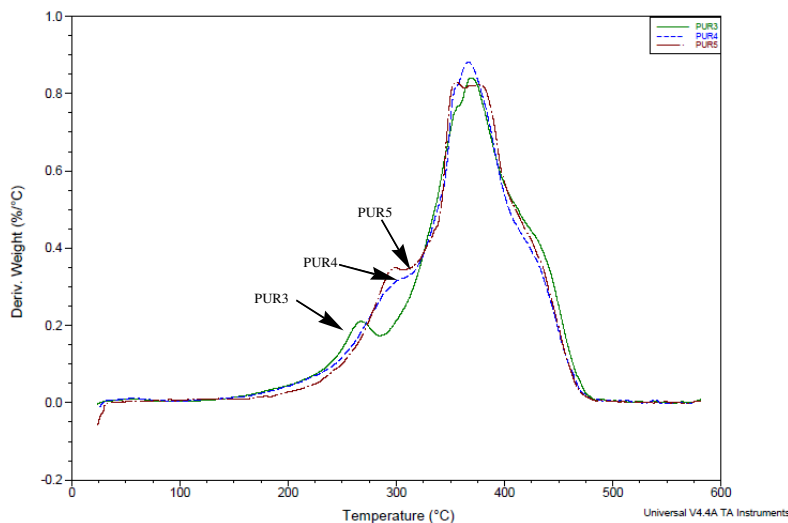


Fig 3.27 DTG curve of crosslinked non-epoxidized polyurea films containing 10%wt (PUR3), 20%wt (PUR4) and 25%wt $[\text{bmim}]\text{PF}_6$ (PUR5).

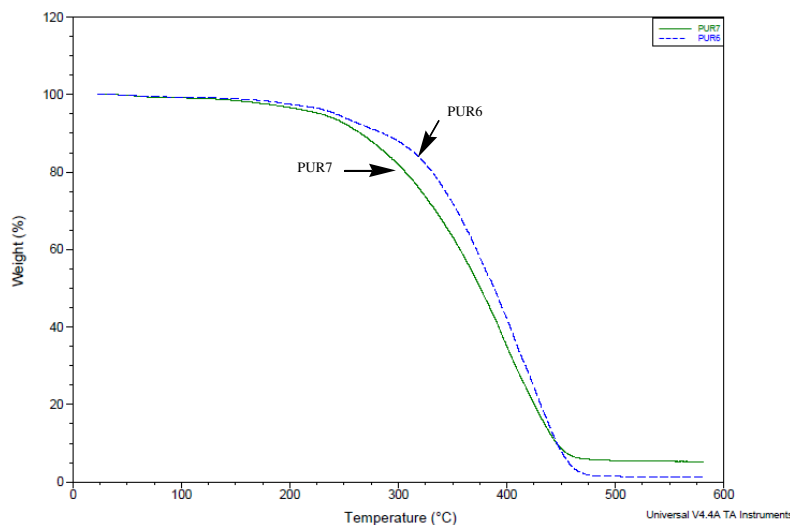


Fig 3.28 TGA thermograms of crosslinked 54% epoxidized polyurea film containing 0%wt (PUR6) and 20%wt [bmim]PF₆ (PUR7).

Fig 3.28 shows the thermal degradation of epoxidized polyurea films with and without [bmim]PF₆. It was found that thermal stability of epoxidized films decreased by ionic liquid incorporation. This can be explained by the activation in C-O cleavage of [bmim]PF₆ via hydrogen bonding formation of cation with epoxide groups [16,17].

3.3.3. Conductivity measurement of ionic liquid incorporated polyurea films

Frequency dependence of ac conductivity of polyurea films measured in frequency range 0.1 to 10⁷ Hz is shown in Fig 3.29. At low frequency, polyurea films with ionic liquid display the plateau value. Furthermore, the conductivity increases as the proportion of [bmim]PF₆ incorporation in films was increased. This can be explained in term of the increasing of ion concentration in films.

In crosslinked epoxidized films without ionic liquid, at low frequency, plateau is not well defined and linear non-epoxidized films presents non-plateau curve.

In films with ionic liquid, an epoxidized film presents higher conductivity than a non-epoxidized film at the same percentage of ionic liquid. This is caused by the presence of polar sites from epoxide groups which act as ions carriers, it enhancing ions transport in films.

dc conductivity of all polyurea films are given in Table 3.9.

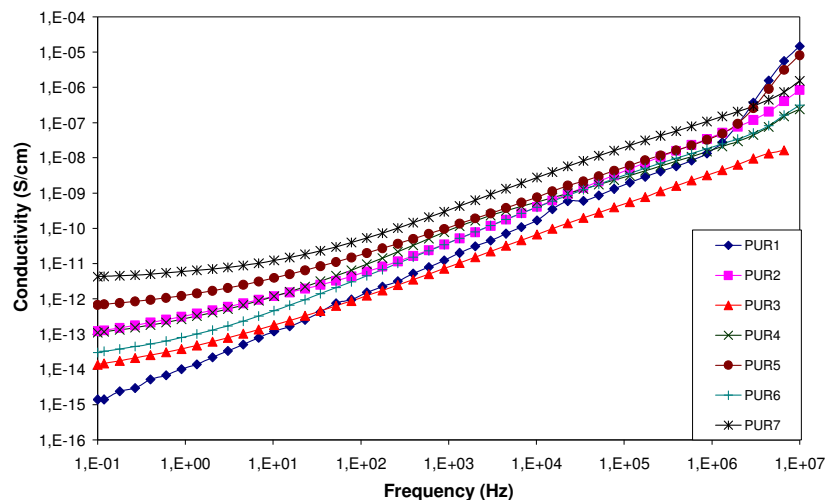


Fig 3.29 Frequency dependence of the ac conductivity of linear non-epoxidized polyureas with 0% wt (PUR1), 10% wt. [bmim]PF₆ (PUR2) and crosslinked non-epoxidized polyureas with 10%wt (PUR3), 20%wt. (PUR4), 25%wt. [bmim]PF₆ (PUR5) and crosslinked 54% epoxidized polyureas with 0%wt (PUR6) and 20%wt [bmim]PF₆ (PUR7) at room temperature.

Table 3.9 Conductivity of non-epoxidized and epoxidized polyureas.

Polymer code	Diamine	Isocyanate	[bmim]PF ₆ (%wt)	conductivity (S/cm)
PUR1	PINH	TDI	0	1.41×10^{-15}
PUR2	PINH	TDI	10	1.21×10^{-13}
PUR3	PINH	I-IPDI	10	1.37×10^{-14}
PUR4	PINH	I-IPDI	20	1.09×10^{-13}
PUR5	PINH	I-IPDI	24	6.76×10^{-13}
PUR6	EPINH(54%)	I-IPDI	0	3.03×10^{-14}
PUR7	EPINH(54%)	I-IPDI	20	4.30×10^{-12}

Conductivity of polyureas is quite less than that of polyurethane at the same percentage incorporation of ionic liquid. This may be due to the fact that chain mobility in these polyureas is more difficult than in polyurethanes because of the bulky effect of butyl group.

3.4. Polymerisation of conducting polymers on polyurethane films

A combination of conventional polymers with conductive polymers allows the creation of new polymeric materials with interesting characteristic properties.

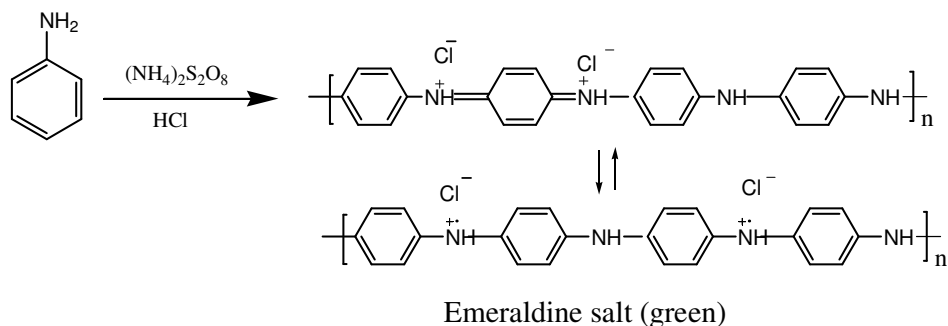
Conducting polymer composites are mainly prepared via two routes; chemical and electrochemical method.

3.4.1. Chemical polymerization of aniline on polyurethane films and characterization of films

We chose aniline as conducting monomers in this study considering the ease of preparation, low cost and environment stability. The chemical methods of the polymerization of aniline are based on the oxidation using suitable oxidants such as ammonium persulphate (APS), sodium chlorate, potassium dichromate, etc. in solution containing mineral or organic acid [23,25].

Chemical polymerization of aniline at the surface of polyurethane was performed using 0.1 M $(\text{NH}_4)_2\text{S}_2\text{O}_8$ in 1.0 M HCl as oxidant. The polymerization was noticed by colour change to be dark green. Finally, a polyurethane film with the dark green surface was obtained as the polymer composite.

The PANI on PU/PANI film by this synthesis method is in doped form, namely emeraldine salt. During the polymerization, the polyaniline was protonated with HCl, called dopant. The reaction is shown in Scheme 3.4.



Scheme 3.4 Chemical polymerization of polyaniline using $(\text{NH}_4)_2\text{S}_2\text{O}_8$ as oxidant in acid condition.

The composite films were characterized with FTIR spectroscopy and Scanning Electron Microscope (SEM). Thermal properties were studied by DSC and TGA.

The images of linear polyurethane film (PU1) and polyurethane/polyaniline composite surface attained from scanning electron microscope are presented in Fig 3.30. The image (Fig 3.30b)) shows the irregularly morphology structure of PANI on PU film with both large and small grain.

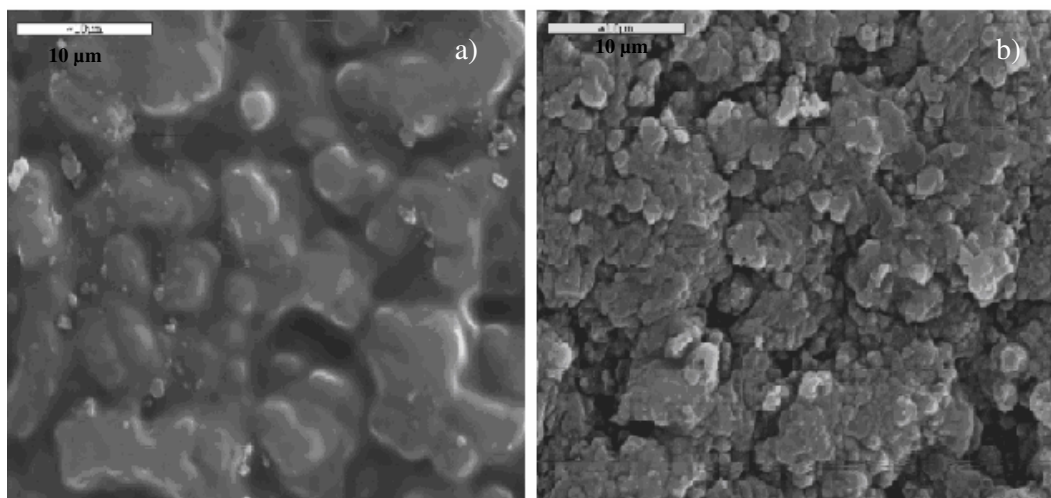
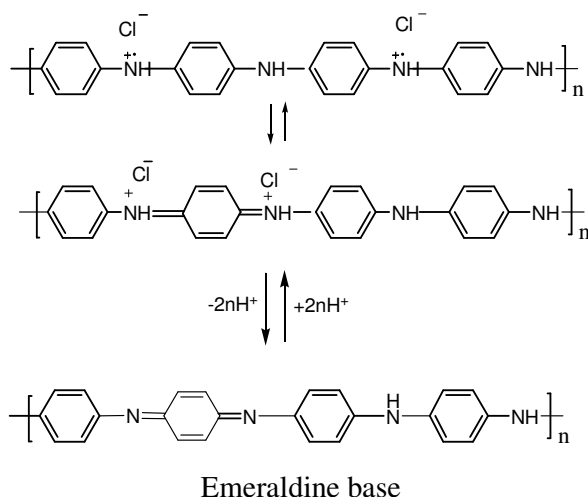


Fig 3.30 SEM images of; a) PU1; b) PU1/PANI composite

The doped form of PANI can be dedoped by deprotonation in basic solution (5% NH_4OH) overnight. A transformation of the protonated form and basic form are presented in Scheme 3.5 [26,27].



Scheme 3.5 Transformation between salt and basic state of polyaniline.

FTIR spectrums of PU/PANI doped and dedoped film compared with pure PU are given in Fig 3.31 and appendix 2.16. In the doped state, a broad spectrum is detected, whereas FTIR spectrum of dedoped state is clearer. This result was also observed by Wen et al. [28]. This phenomenon demonstrates the doping of films by HCl, which gives emeraldine salt, influences the delocalization of electrons and changes the intermolecular vibrations. Thus, only small peaks are observed [29]. Signal at 1310 cm^{-1} corresponds to C-N stretching that attributed to the presence of aromatic amine. Peak at 1510 cm^{-1} is related to C=N bonds stretching of quinoid. In the dedoped films, band of -B-NH-Q in polyaniline was noticed at 1170 cm^{-1} , where B and Q are benzene ring and quinoid respectively. Those appear signals corresponding to PANI structure were reported previously. [30,31].

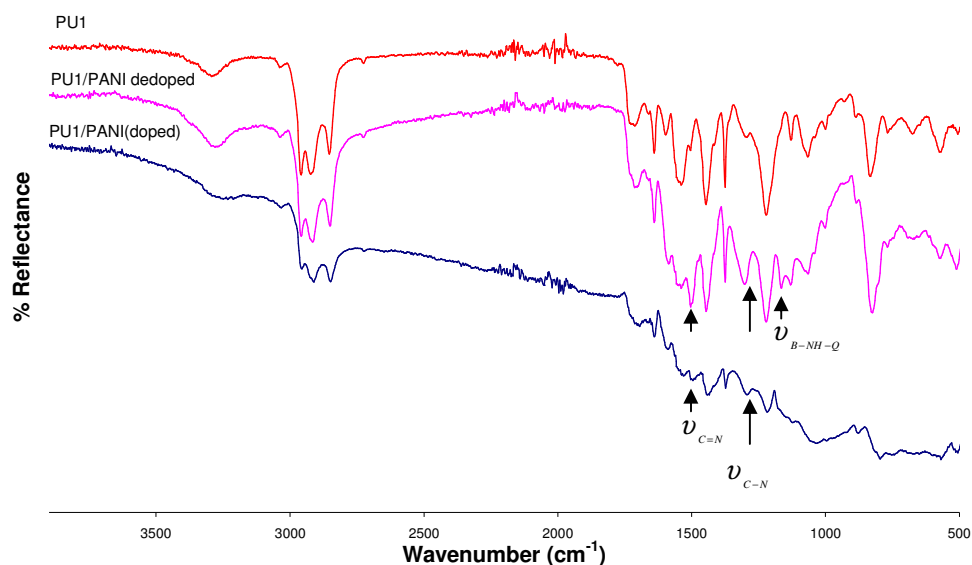


Fig 3.31 FTIR spectrums of PU1/PANI composite prepared by oxidation polymerization with 0.1 M $(\text{NH}_4)_2\text{S}_2\text{O}_8$ in 1.0 M HCl.

From DSC analysis, we did not observed any new phase transition of PANI in composite between temperature scan ranges -80°C to 150°C . Only well defined T_g of soft segment of polyurethane was noted and it was not modified by the presence of PANI. In work of Campos et al., describing the preparation of polyaniline doped with HCl, T_g of PANI is not noticed and degradation of polyaniline become at above 200°C . [31].

Thermal stability of composites was investigated by TGA. Some thermograms and thermal decomposition data are given in Fig 3.32, Fig 3.33 and Table 3.10.

Table 3.10 Thermale decomposition data of polyurethane/ Polyaniline composites prepared by chemical polymerization.

Composites	Thermal degradation	
	T_{max} ($^\circ\text{C}$)	% weight loss
PU1/PANI	351	90.5
PU2/PANI	374	90.3
PU3/PANI	363	95.8
PU6/PANI	379	98.6

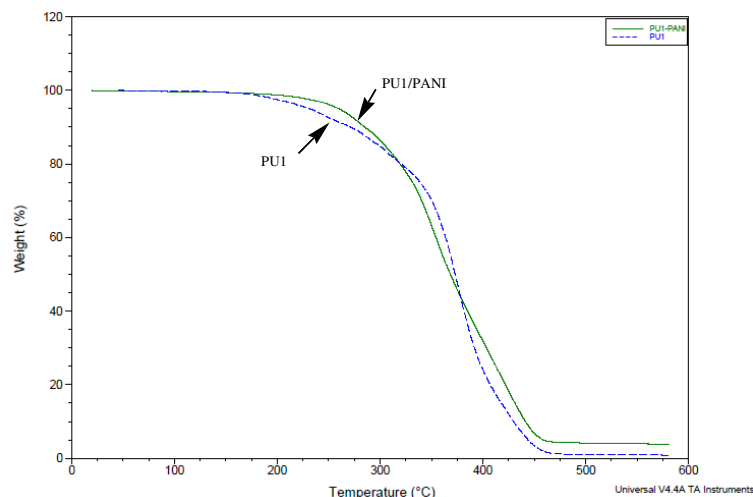


Fig 3.32 TGA thermograms of linear polyurethane (PU1) and linear PU/PANI composites (PU1/PANI).

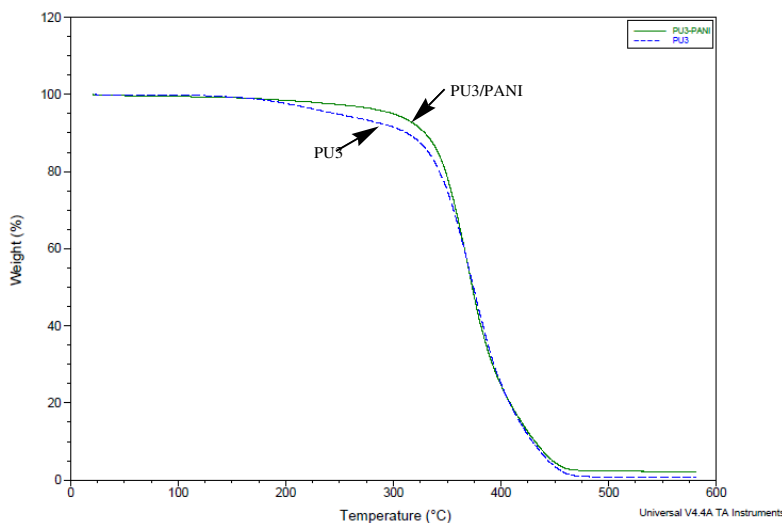


Fig 3.33 TGA thermograms of crosslinked polyurethane (PU3) and linear PU3/PANI composite

Fig 3.32 and Fig 3.33 present thermal degradation curve of linear and crosslinked PU/PANI composites compared with pure PU films. It was found that thermal properties of composites are better than those of polyurethane alone, in both [bmim]PF₆ incorporated (appendix 2.17) and non-incorporated films, especially in linear polyurethane films. The improving of thermal stability in composites can show the mixing of the two polymers.

3.4.2. Electropolymerization of aniline on polyurethane films

The aniline was electropolymerized using cyclic voltammetry in a three-electrode cell compartments. The cell was equipped with Ag/0.1 M AgNO₃ in acetonitrile as reference electrode and platinum wire as a counter electrode. Platinum discs of 1 mm or 10 μm diameters were used as working electrodes.

3.4.2.1. Electropolymerization of aniline on polyurethane coated electrode

Different kinds of polyurethane were coated on the working electrode by drop coating and used for the experiments. The solution of precursors was prepared as the same way as for self-standing casting films. Next, the solution was drop onto Pt-electrode. The film coated electrode was formed under nitrogen atmosphere during 2 hours, and the trace of solvent was then evaporated at 60°C overnight.

Electropolymerization of films coated on the electrode was carried out in dichloromethane solution containing 0.2 M Bu₄NBF₄ used as supported electrolyte and 10mM aniline by applying potential from -1.0 V to 1.0 V with the scan rate of 20 mV/s. Typical cyclic voltammograms obtained for PU film deposited onto a platinum substrate are given in Fig 3.34.

At the first cycle, we observed the oxidation peak of aniline (termed A_{ox}) at 0.85 V [1] to form the corresponding cation radical. Current peak is high in the first cycle and it then drastically decreases in the second cycle and slightly decreases in later cycles. This reflects to the consumption of aniline in films. In the solution, film was swelled with monomer and electrolyte. In the first cycle, there still are a lot of monomers in the film, therefore, high oxidation current peak was observed. After monomer consumption in the first cycle, monomer concentration of monomer in film decreased. Hence, in later cycle, the amount of monomers depends on diffusion of monomer from solution into films. The decreasing of concentration of aniline in film in later cycles leads to the decreasing of oxidation peak. This also shows that the diffusion of aniline into film is slower than the polymerization rate. The formation of polyaniline (PANI) in polyurethane films can be indicated from the appearance of oxidation (or anodic) peak at 0.15 V and reduction (cathodic) peak at -0.04 V, named B_{ox} and B_{red} respectively, in the third cycle. Subsequently, the current peak increased in each cycle. The presence of B_{ox} and B_{red} corresponds to the p-doping and dedoping processes of

polyaniline. This demonstrates the formation and the growth of polyaniline within the polyurethane film.

During the aniline polymerization process, the oxidation peak of polyaniline shifts to the higher potential in each cycle in accordance with a high electron transfer rate constant. The electron transfer between aniline and electrode has to pass the PANI layer. Finally, B_{ox} shift to 0.24 V in the 10th cycle. At the end of polymerization, we noticed the dark green spot at the films coated electrode.

PANI in polyurethane was characterized by p-doping and p-dedoping procedure ranging from -1V to +0.6V. Owing to thin polyurethane film, we can not peel off coated film.

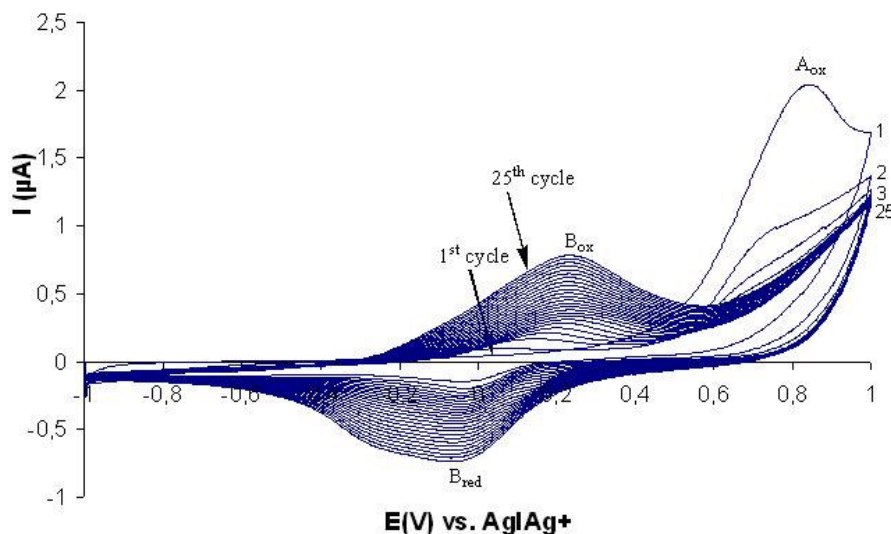


Fig 3.34 Typical cyclic voltammograms of 10 mM aniline + 0.2 M Bu_4NBF_4/CH_2Cl_2 on linear PU coated electrode (LPU(TDI)) recorded on Pt electrode ($\varnothing = 1$ mm) with scan rate 20 mV/s.

The doping-dedoping characterisation of conducting polymer was performed. This type of characterization of conducting polymer reflects the oxidation and reduction of polymer inducing counter ion transfer in and out of film. This phenomenon is called doping and dedoping of conducting polymer [2]. Typical doping and dedoping cyclic voltammogram recorded for polyaniline are shown in Fig 3.35.

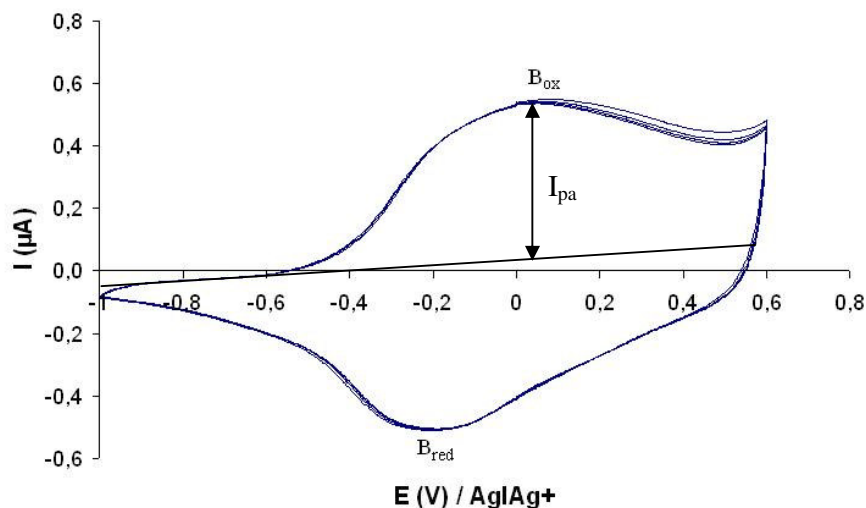


Fig 3.35 Typical cyclic voltammograms of PANI on linear PU (PU(TDI)/PANI) in 0.2 M $\text{Bu}_4\text{NBF}_4/\text{CH}_2\text{Cl}_2$ recorded on Pt electrode ($\varnothing = 1$ mm) with scan rate 20 mV/s.

In Fig 3.35, B_{ox} and B_{red} are identical to that we observed in the Fig 3.34. It confirms that there is formation of PANI in polyurethane coated electrode. Moreover, the cyclic voltammogram in each cycle are identical, that attests the stability of the composite film prepared in these conditions.

P-doping levels of polyaniline on PU films can be calculated by the following equation;

$$\% \text{ doped of PANI, } S_p = [(2 \cdot Q_p) / Q_s] \cdot 100$$

Where Q_p = anodic charge consumed during the oxidation of polymer chains

Q_s = anodic charge consumed during the oxidation of monomer

The p-doping level of PANI in different kind of polyurethane substrates is given in Table 3.11.

Table 3.11 Percentage of dopage of polyaniline in different kinds of polyurethane substrates.

Polymer code	S_p (%)
LPU(TDI)/PANI	6.6
CLPU/PANI	4.5
LEPU(58%)/PANI	6.3
LPU(H12MDI)/PANI	4.7

Percentage of dopage of polyaniline in different polyurethane is not significantly different. Polyurethane type has no effect on dopage of polyaniline in films.

Doping and dedoping of PANI on polyurethane film was done in different scanning rates (10 to 200 mV/s), an anodic peak in cyclic voltammogram increases with scan rate increase as shown in Fig 3.36.

The anodic current peak (I_{pa}), was plotted with the sweep rate (Fig 3.37), all kinds of films present that an anodic current peak increases linearly with scan rate in range 10 to 200 mV/s. This suggests that in this range of scan rate, the redox process is confined to the surface and the oxidation is a diffusionless-controlled process [3,4]. The process of counter ion transfer to the polymer film and back to solution during oxidation-reduction of PANI take place practically inside the PANI layer [8].

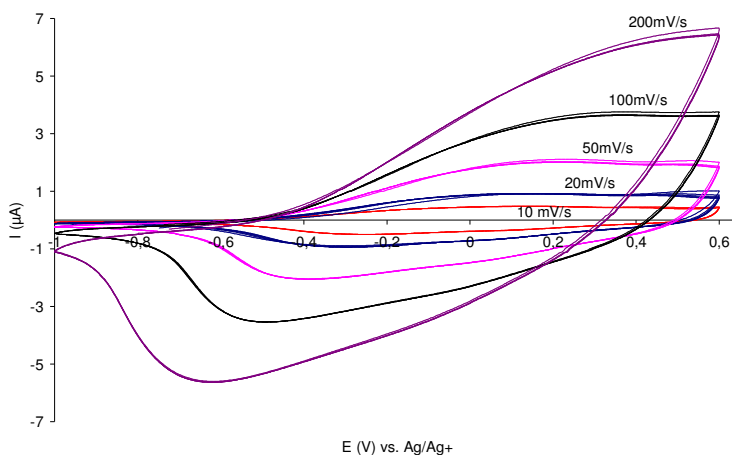


Fig 3.36 Typical cyclic voltammograms of PANI on linear PU (LPU(TDI)) in 0.2 M $\text{Bu}_4\text{NBF}_4/\text{CH}_2\text{Cl}_2$ recorded on Pt electrode ($\varnothing = 1$ mm) with scan rate 10 to 200 mV/s.

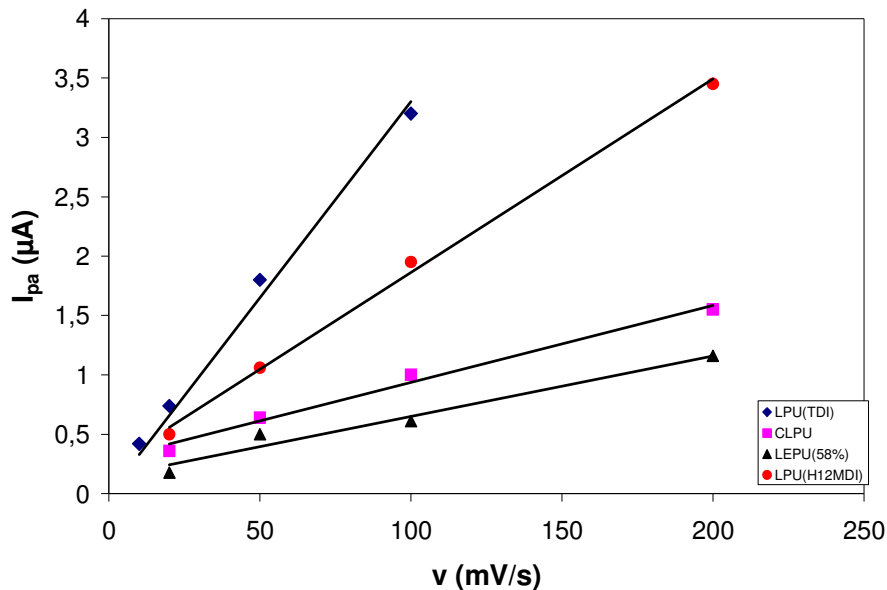


Fig 3.37 Typical relationship between the scan rate (v) and anodic current peak (I_{pa}) of PU/PANI composite.

3.4.2.2. Electropolymerization of aniline on polyurethane casting films

a) In organic medium

Fig 3.38 is the cyclic voltammograms of polyaniline growth on linear polyurethane film during electrolysis in the solution containing 0.2 M Bu_4NBF_4 /dichloromethane and 10mM aniline. The scan potential was controlled between -1.0 V and +1.0 V referred to $Ag/AgNO_3$ /acetonitrile reference electrode. The anodic peak for oxidation of aniline at 0.9 V is not clear, but the current peak is high and it then decreased in later cycle. In the second cycle, an anodic peak (B_{ox}) and a cathodic peak (B_{red}) appear at +0.14 V and -0.08 V corresponding to oxidation and reduction peak of PANI, respectively. The current peaks increase with increasing the number of cycles. The anodic peak potential also continuously shifted to more positive values. This result is similar to the general electrochemical polymerization of aniline on polyurethane coated films. We also performed the polymerization using Pt microelectrode. The optical microscopic images of film using both electrodes were given in Fig 3.39.

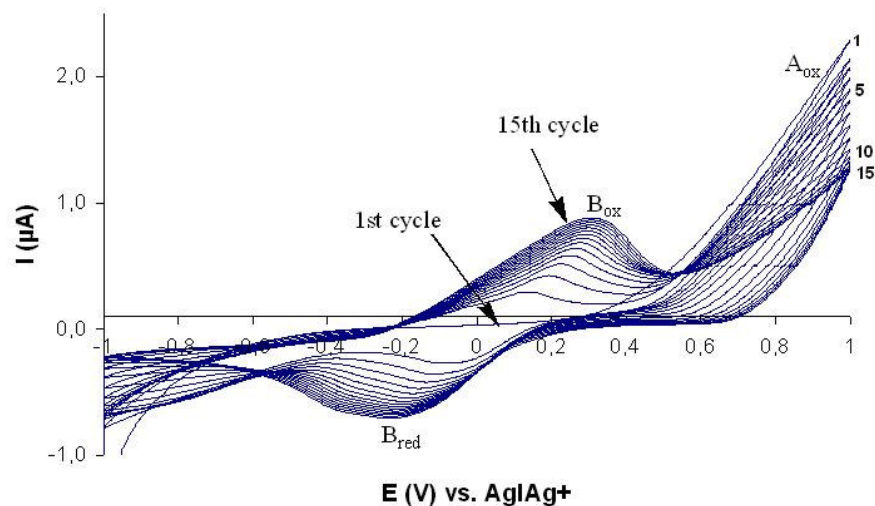


Fig 3.38 Cyclic voltammograms of 10 mM aniline + 0.2 M $\text{Bu}_4\text{NBF}_4/\text{CH}_2\text{Cl}_2$ solution in linear PU (PU1) film recorded on Pt electrode ($\varnothing = 1$ mm). Scan rate 20 mV/s.

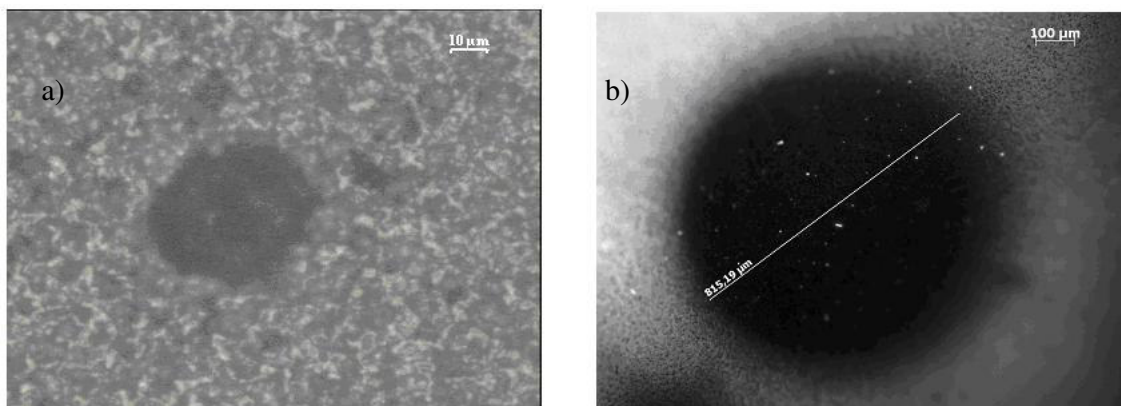


Fig 3.39 Optical microscopic image of PANI on linear polyurethane film prepared in 0.2 M $\text{Bu}_4\text{NBF}_4/\text{CH}_2\text{Cl}_2$ by using a) Pt ($\varnothing = 10$ μm); b) Pt ($\varnothing = 1$ mm) electrode.

Both films were characterized with Scanning Electron Microscope, but we did not observe the difference of surface between non-modified polyurethane part and polyurethane containing polyaniline spot part. This can indicate that polyaniline formed inside polyurethane film.

b) In acid medium

Linear polyurethane prepared by casting technique was swollen in aniline for 10 mins. Electropolymerization of aniline in linear polyurethane, containing 12.4%wt aniline, was carried out in 1.0 M HCl using saturated calomel as reference electrode in the potential required for the polymerization of aniline (from 0 V to + 1 V) in acid medium [1,5-7]. The cyclic voltammograms of the PANI film growth is presented in Fig 3.40.

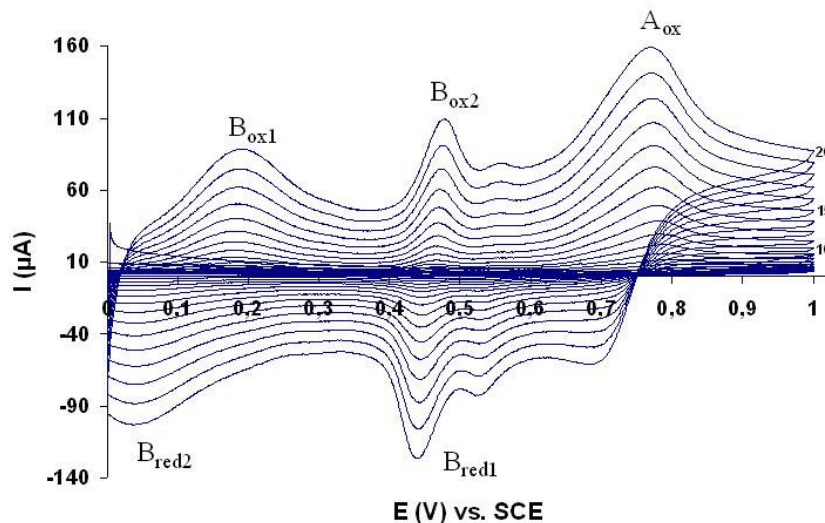


Fig 3.40 Cyclic voltammograms of 12.4 % aniline incorporated in linear PU film (PU1) in 1.0 M HCl recorded on Pt electrode ($\varnothing = 1$ mm). Scan rate 20 mV/s.

An oxidation peak of aniline was observed around +0.94 V in the first cycle and then the current peak of oxidation decreased. At the beginning of electropolymerization anodic peak were not well observed, and then three anodic peaks (named A_{ox} , B_{ox1} , B_{ox2}) and two cathodic peaks (B_{red1} , B_{red2}) appear for the fourth cycle. The currents increase as the number of potential cycles increases. This result is similar to that of the general electropolymerization of aniline [1,5-7]. The increasing of current peaks in this case is much higher and faster than in that when aniline is added in solution. It can be explained by the higher concentration of aniline in film. In addition, the cyclic voltammograms are different from the former case. This is caused by the effect of pH and electrolyte solution on the cyclic voltammograms of polyaniline which reported by Shan and Huang [3,4]. At the end of polymerization, polyurethane film containing dark green spot of polyaniline was observed as shown in Fig 3.42.

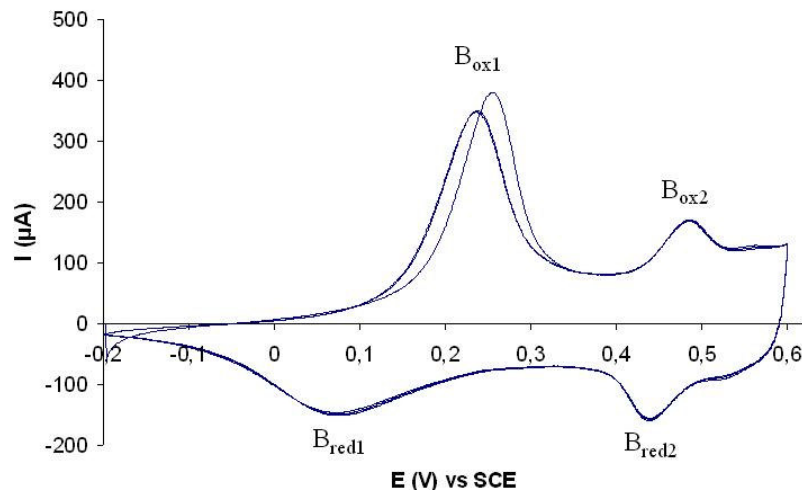


Fig 3.41 Cyclic voltammograms of PANI on linear PU film in 1.0 M HCl recorded on Pt electrode ($\varnothing = 1$ mm) with scan rate 20 mV/s.

Fig 3.41 is the doping and dedoping curve of PANI on linear polyurethane film in 1.0 M HCl. It shows that the formed PANI is stable in the acid condition over this potential window.

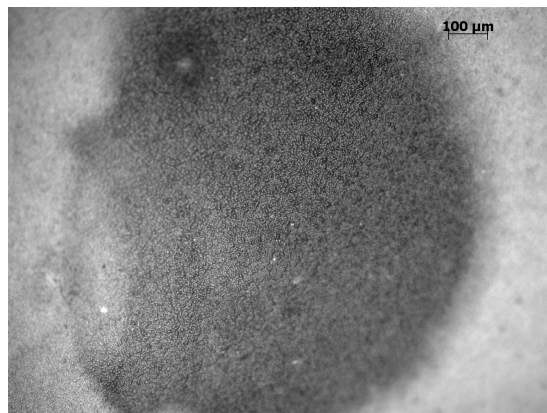


Fig 3.42 Optical microscopic image of PANI on linear PU prepared in 1 M HCl solution using Pt ($\varnothing = 10$ μm) electrode.

From optical microscopic image of film prepared in organic and acid medium (Fig 3.39 and 3.42), polyaniline size that formed in polyurethane film is nearly the same as an electrode size. Hence this method, a precise conducting part can be imprinted on the polymer matrix.

3.4.2.3. Electropolymerization of aniline on polyurethane thin film on ITO plate

In order to form polyaniline in the bulk of polyurethane film, the thickness controlled homogeneous polyurethane thin films deposited on indium tin oxide glass (ITO) were prepared by spin coating technique to obtain thin films in micron scale. Films were formed under nitrogen atmosphere for 2 hours and the trace of solvent was evaporated at 60°C overnight. The thickness of film was measured by mean of reflection index under white light using micro-Raman configuration.

Electropolymerization of aniline in the PU thin film on ITO plate was done in the previously described. The polyurethane coated ITO plate with thickness 1.70 μm was installed in the electrochemical cell containing 25 mM aniline and 1.0 M HCl. The potential range for polymerization, -0.2V to +1.0 V was applied. Cyclic voltammograms for PANI electropolymerization were shown in Fig. 3.37.

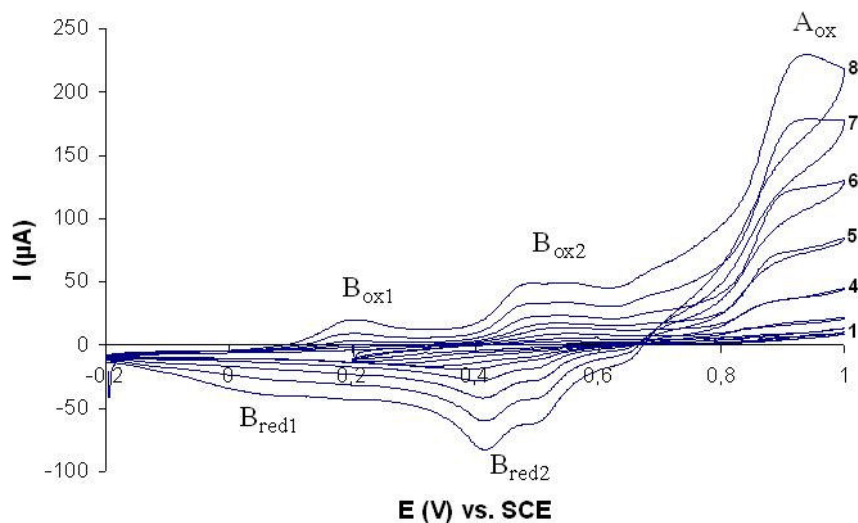


Fig 3.43 Cyclic voltammograms of 25 mM aniline + 1.0 M HCl on linear PU thin film on ITO plate ($e = 1.70 \mu\text{m}$) recorded on Pt electrode ($\varnothing = 1 \text{ mm}$). Scan rate 20 mV/s.

Fig 3.43, at the beginning (1-4 cycles), the voltammogram was quite plateau, without the oxidation peak of aniline. After 5th cycles, the oxidation peak at 0.9 V can be seen well and peak size increased. The increasing of anodic peak at 0.2 and 0.5 V and cathodic at 0.4 V showed the formation of PANI layer. After 5th cycles, peak current drastically increased

because the PANI formation transverses PU film to touch ITO plate owing to very thin polyurethane coating. Consequently, the conducting area increases suddenly and all of plate can induce the polymerization of aniline in the solution, leading to highly increase of current peak. At the end of 8th cycles, we saw also the green film on ITO plate, even in the part where there is no PU film coating.

For investigating if there is formation of PANI everywhere on ITO plate, we used ITO plate as working electrode and cyclic voltammetry from -0.2 V to 0.8 V was performed. The voltammograms were shown in Fig. 3.44. Fig. 3.44b shows the voltammograms when the position that applied electrode was immersed in solution, they show the oxidation and reduction peak of PANI. Fig. 3.44a are the voltammograms when the PANI spot was above solution. However, there are also the oxidations and reduction curves of PANI, even it is smaller than Fig. 3.44b. Therefore, it means that there is PANI formed on this part of ITO plate, too. In Fig. 3.44c nearly all of plate was in solution, the current peak is very high. Hence, it can conclude that PANI was everywhere on ITO plate. Therefore, the formation of polyaniline in all thickness of polyurethane is possible by this technique.

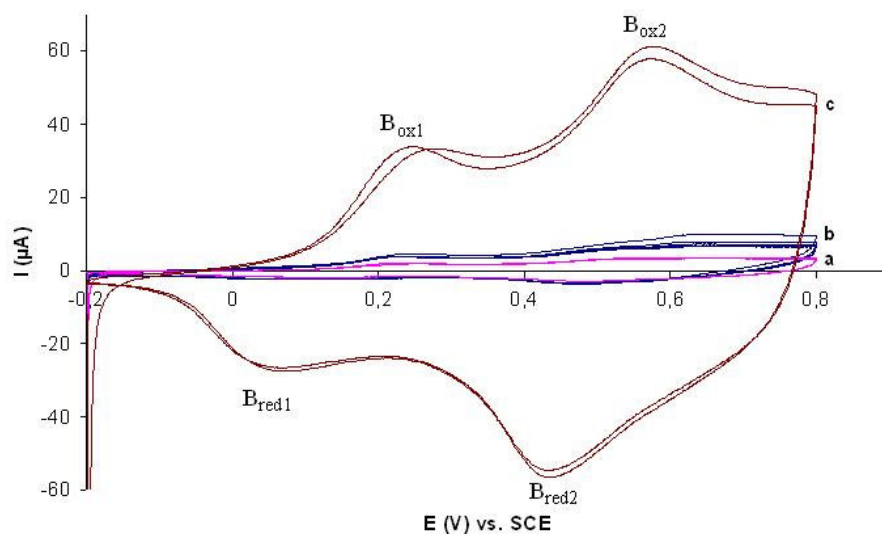


Fig 3.44 Cyclic voltammograms of PANI on linear PU film recorded on ITO plate (area = 4 cm²); a) PANI spot in the solution; b) PANI above solution; c) all ITO plate in solution. Scan rate 20 mV/s.

3.4.2.4. Electropolymerization of EDOT and Py on polyurethane film

Beside aniline, electropolymerization of 3,4-ethylene dioxythiophene (EDOT) and pyrrole (Py) on polyurethane film was also attempt to perform.

Linear polyurethane was swelled in EDOT for 10 mins and electropolymerization of EDOT in polyurethane film, containing 35% wt. of EDOT, was run in 0.5 M LiClO₄ electrolyte solution using saturated calomel as reference electrode in potential range -1.0 V to +1.0 V. Cyclic voltammograms were recorded on Pt disc with diameter 1 mm.

Electrochemical polymerization of Py on polyurethane containing 35% wt. Py was carried out in the same way.

Cyclic voltammograms (appendix 2.19 and 2.20) show the growth of conducting polymer film by increasing of oxidation-reduction current (at B_{ox} and B_{red}) as the number of cycle increase (Appendix 2.19 and 2.20), However, when electrode was taken off from film, we found that PEDOT and PPy deposited at the surface electrode. From optical microscopic image of films after polymerization, only small remaining traces of conducting polymer was observed.

This result was obtained, even glassy carbon was used as working electrode or the polymerization was performed in dichloromethane containing 0.2 M Bu₄NBF₄ solution.

3.5. Conclusion

The study of ionic liquids incorporation in polyurethanes shows the possibility to incorporate ionic liquids in polyisoprene based polyurethanes and to increase conductivity of composite films. An appearance of signal of ionic liquid in FTIR spectra basically confirms an incorporation of ionic liquid in polyurethane films. Miscibility of ionic liquid and polymer is influenced by the structure of ionic liquid. In this study, the ionic liquid containing long chain hydrocarbon, [thtdp]Cl, is more miscible with polyisoprene based polyurethanes than imidazolium type ionic liquid, [bmim]PF₆.

In polyurethanes without ionic liquid incorporation, T_g of polyurethane films increase with the percentages of epoxidation increase. They show a small weight loss of epoxide unit at low temperature.

In ionic liquid incorporated polyurethane films, [bmim]PF₆ demonstrated a partially miscible characteristic with polyisoprene based polyurethanes. Incorporation is limited at 10%wt. in non-epoxidized polyurethane and 30%wt in 80%epoxidized films. Therefore, T_g of films is not modified by incorporating [bmim]PF₆. On the other hand, [thtdp]Cl is miscible with these polyurethanes. T_g of [thtdp]Cl incorporated films decrease as proportion of ionic liquid in films increase. It reflects that [thtdp]Cl has plasticizing effect on films.

Thermal stability of non-epoxidized films is not different as ionic liquid was incorporated or not, while epoxidized polyurethanes show two degradation peaks of soft segments. This caused by C-O cleavage activation by ionic liquid cation at epoxide units.

The conductivity of ionic liquid incorporated based polyurethanes can be enhanced by increasing proportion of ionic liquid in films. Polyurethane films, both non-epoxidized and epoxidized films, without ionic liquid give the conductivity in order 10⁻¹⁴-10⁻¹⁵ S/cm. With 30%wt [bmim]PF₆ and 59%wt [thtdp]Cl incorporation in 80% epoxidized polyurethane, the conductivity increase to be 4.15×10⁻⁹ S/cm and 3.70 × 10⁻⁸ S/cm respectively. However, the percentage of ionic liquid incorporation can be limited by miscibility in [bmim]PF₆ incorporation and film weakness at high [thtdp]Cl incorporation.

Epoxidation permits to increase the ionic liquid incorporation proportions, for sample, in 80% epoxidized polyurethane films, up to 30%wt of [bmim]PF₆ and 60%wt. of [thtdp]Cl

can be incorporated. The proportion of ionic liquid incorporation can be increased as percentages of epoxidation increase.

However, in [bmim]PF₆ incorporated films, conductivity of non-epoxidized films is higher than that of epoxidized film at the same percentage of incorporation. This is caused by decreasing of chain mobility in epoxidized polyurethane as shown in increasing of T_g restricting ion mobility in the polymer matrix. In contrast, the conductivity of epoxidized films is higher than those of non-epoxidized films in [thtdp]Cl incorporated films because the combination effect of an increasing of ion carrier caused by epoxide group and of chain mobility from plasticizing effect of [thtdp]Cl, enhances ion transport in polymer films.

In situ polymerization of aniline on polyurethane films using (NH₄)₂S₂O₈/HCl as oxidant was performed. SEM characterization presents that the formation of PANI on PU is an irregular morphology, there are both large and small grain.

Furthermore, preliminary study polymerization of conducting monomer on polyurethanes films by electrochemical technique allows us to prepare the precise located site of PANI on polyurethane film both using dichloromethane and aqueous medium. The formation of conducting polymer on polyurethane films was confirmed by optical microscopic image and doping-dedoping curves. PANI/PU composite is stable in potential window -1V to +0,6V in Bu₄NBF₄/dichoromethane solution and -0.2V to +0,6 V in acid medium.

From study electrochemical polymerization of thin film on ITO plate shows the formation of PANI in bulk polyurethane.

The electrochemical polymerization of EDOT and pyrrole on polyurethane film in LiClO₄ electrolyte solution, conducting polymers prefers to deposits at electrode surface.

References

1. T.C Wen, H.H. Kuo, A. Gopalan, *Macromolecules* 34 (2001) 2958.
2. H.L. Wang, H. M. Kao, Digar, T.C. Wen, *Macromolecules* 34 (2001) 529.
3. A. Pattanayak, S.C. Jana, *Polymer* 46 (2005) 5183.
4. C.S. Kim, B.H. Kim, K. Kim, *J. Power Sources* 84 (1999) 12.
5. J.D. van Haumen, J.R. Stevns, *Macromolecules* 28 (1995) 4268.
6. C.C Chen, W.J. Liang, P.L. Kuo, *J. Polym. Sci., Polymer Chem.* 40 (2002) 486.
7. L. Hong, L.Y. Shi, X. Z. Tang, *Macromolecules* 36 (2003) 4989.
8. B. Singh, S.S. Sekhon, *Chemical Physics Lett.* 414 (2005) 34.
9. A. Lewandowski, A. Swiderska, *Solid State Ionics*, 169 (2004), 21.
10. E. Marwanta, T. Mizumo, N. Nakamura, H. Ohno, *Polymer* 46 (2005) 3795.
11. N. Kebir, *Elaboration de nouveaux polyuréthanes à partir de cis-1,4-oligoisoprènes hétérocarbonyltéléchéliques issus de la dégradation contrôlée du cis-1,4-polyisoprène de haute masse. Etude de leurs propriétés mécaniques, thermiques et biocides, thèse de l'Université du Maine, Le Mans, 2005.*
12. M. Qi, G. Wu, M. Shu, Y. Liu, *Radiation Physics and Chemistry* 77 (2008) 1248.
13. Z. Wirpsza, *Polyurethanes: Chemistry, Technology and Applications*, Ellis Horwood Limited, New York, 1993.
14. Y. Chu, H. Deng, J. Cheng, *J. Org. Chem.* 72 (2007) 7790.
15. T.L. Amyes, S.T. Diver, J.P. Richard, F.M. Rivas, K. Toth, *J. Am. Chem. Soc.* 126 (2004) 4366.
16. M.-H. Yang, G.-B. Yan, Y.-F. Zheng, *Tetrahedron Lett.* 49 (2008) 6471.
17. L.-W. Xu, L. Li, C.-G. Xia, P.-Q. Zhao, *Tetrahedron Lett.* 45 (2004) 2435.
18. <http://www.bekktech.com/dwnlds/MembraneConductivityInformation.pdf>, 7 october 2008.
19. N.J. Pinto, A.A. Acosta, G.P. Sinha, F.M. Aliev, *Synth. Met.* 113 (2007) 77.
20. P. Pissis, A. Kyritsis, G. Georgoussis, V.V. Shilov, V.V. Shevchenko, *Solid State Ionics* 136-137 (2000) 255.
21. W. Klinklai, S. Kawahara, E. Marwanta, T. Mizumo, Y. Isono, H. Ohno, *Solid State Ionics* 177(2006) 3251.
22. P. Pissis, A. Kyritsis, *Solid State Ionics* 97 (1997) 105.
23. Y. Cao, P. Smith, A.J. Heeger, *Synth. Met.* 48 (1992) 91.

24. K. Fatyeyeva, Elaboration and investigation of conducting polymer composites based on polyaniline and polyamide, thesis of Université du Maine, Le Mans, 2005.
25. A. Pud, N. Ogurtsov, A. Korzhenko, G. Shapoval, Prog. Polym. Sci. 28 (2003) 1701.
26. G. Louarn, M. Lapkoski, S. Quillard, A. Pron, J.P. Buisson, S. Lefrant, J. Phys. Chem. 100 (1996) 6998.
27. M. Lapkowski, K. Berrada, S. Quillard, G. Louarn, S. Lefrant, A. Pron, Macromolecules 28 (1995) 1233.
28. L. Wen, N.M. Kocherginsky, Synth. Met. 106 (1999) 19.
29. F. Lux, Polymer 35 (1994) 2915.
30. K.S. Ho, K.H. Hsieh, S.K. Huang, T.H. Hsieh, Synth. Met. 107 (1999) 65.
31. T.L.A. Campos, D.F. Kerting, C.A. Ferreira, Surf. Coating Tech. 122 (1999) 3.
32. S. Mu, J. Kan, Electrochim. Acta, 41 (1996) 1593.
33. Y. W. Chen-Yang, J. L. Li, T. L. Wu, W. S. Wang, T. F. Hon, Electrochim. Acta 49 (2004) 2031.
34. X. Jiang, L. Zhang, S. Dong, Electrochem. Commun. 8 (2006) 1137.
35. C. Cougnon, C. Gauier, J.-F. Pilard E. Raoult, J. Rault-Berthelot, Electrochem. Commun. 8 (2006) 143.
36. D. Shan, S. Mu, Synth. Met. 126 (2002) 225.
37. W.-S. Huang, B.D. Humphrey, A.G. MacDiarmid, J. Chem. Soc., Faraday Trans. I 82 (1986) 2385.
38. W.W. Focke, G.E. Wnek, Y. Wei, J. Phys. Chem. 91 (1987) 5813.

*Chapter4- Synthesis and properties of
polyurethane using chain extender with
pyrrole side group*

4.1. Introduction

Molecular imprinting is an approach to create affinity site for molecules of interest in synthetic materials [1-4]. It is a useful technique for the preparation of synthetic polymers with the molecular recognition properties where binding sites specific for template molecular are formed during polymerization process. Molecularly imprinted polymers are used in several applications such as chromatography [1], solid phase extraction [3], catalysis [4] and sensor [2].

Molecularly imprinted conducting polymers, such as polypyrrole, have merited great interest because of their selectivity and the ease of their preparation; particularly through electropolymerization [1]. Ebarvia et al. [5] synthesized a piezoelectric caffeine sensor by molecularly imprinting method. Caffeine-imprinted polymer was prepared using galvanostatic electropolymerization of pyrrole monomer directly onto a gold-coated quartz crystal used as working electrode in presence of caffeine. Caffeine molecules were entrapped in the matrix of polymer film, and were removed by subsequent washing with water, leaving behind pores capable of recognizing the target analyt molecule. The sensor exhibited a linear relationship between the frequency shift and the \ln of caffeine concentration, good sensitivity and repeatability.

Lee [6] and Huang [7] have synthesized chiral and conductive adsorbent and nano wire for chiral separation of amino acid mixture by molecular imprinting technique. Resin or nano wire surface was modified by polypyrrole coating. By applying a potential difference to the conductive column, racemic amino acids are separated according to their charge characteristic and chiral recognition.

Creation of affinity site through imprinting on the surface of commonly and mechanically strong polymer such as polyurethane, polystyrene is interesting; especially these types of polymers can easily be moulded into any form and are extensively used in the design of biomedical devices. Studies have shown that thin layer of conjugated polymers can be coated virtually on any surfaces using chemical or electro polymerization [8-12]. Sreenivasan have developed the method to identify salicylic acid (SA) using modified polyurethane film. The surface of polyurethane was modified by coating a thin layer of polyaniline. Affinity site for salicylic acid was created in the coated layer by non-covalent imprinting method. The imprint layer adsorbed SA five times more compared to the non-imprinted surface [12].

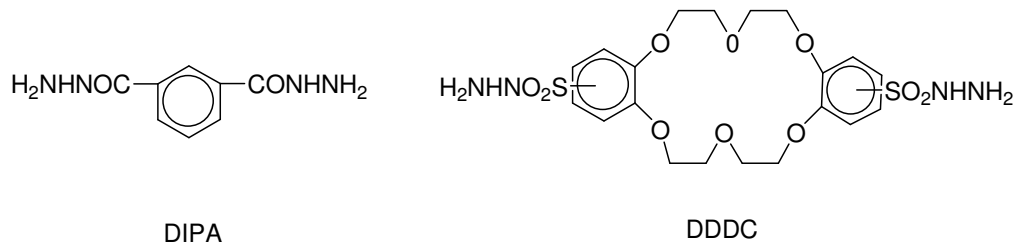
Insulin sensor was prepared by stamping insulin molecule on polyurethane prepolymer surface. With this surface-imprinted polyurethane, Lieberzeit et al. [13] succeeded in directly measuring insulin in aqueous solution.

In order to prepare conducting site on/in the polyurethane film, the previous attempt, we have prepared polyaniline and polypyrrole spots on the polyurethane containing the monomer using the cyclic voltammetric technique. We found that the polypyrrole prefers to deposit at the surface of electrode. From this result, we assumed that if pyrrole ring was incorporated in the structure of the polyurethane as chain extender and if the polymerization of Py unit is previously induced, polypyrrole will be inside the polyurethane films. The electrochemical polymerization of pyrrole derivative monomers has been reported by Lallemand et al. [14]. Therefore, in this work, we have synthesized the derivative of pyrrole which contained diol functional group for using as chain extender in the polyurethane synthesis.

Normally, chain extenders are used to extend the length of hard segment and increase the hydrogen bond and molecular weight of the polyurethane. Commonly commercial chain extenders included 1,4-butanediol (BD), 1,3-propanediol (PD), ethylene diamine(ED), ethylene glycol (EG) and hexanediol (HD) [15,16].

By introducing the chain extender with the different bulkiness as well as rigidity, it may provide the change in the phase mixing, hard segment structure of polymer. Bae et al. [17] studied the effect of linear and non-linear chain extenders to the dynamic mechanical properties of polyurethanes. They found that the use of non-linear chain extenders result in higher glass transition temperature compare with 1,4-butanediol.

Pissis et al. [19,20] have studied the influence of chain extenders on the properties of polyurethane. The degree of microphase separation increases due to dilution of dihydrazide of isophthalic acid (DIPA) and/or blocking of chain extender with crown ether-containing hydrazides. By dielectric study, a sample with dihydrazide of disulfonyl-dibenzo-18-crown-6 (DDDC) as chain extender shows the higher dc conductivity compared with sample without one.



In addition, Araujo and Pasa [18] used the renewable source, biopitch, as chain extender in polyurethanes based on hydroxyl-terminated polybutadiene. It was shown that the biopitch was introduced into the hard segments of polyurethane. The thermal stability of material decreased with addition of pitch. However, a chain extender containing conducting monomer is not reported.

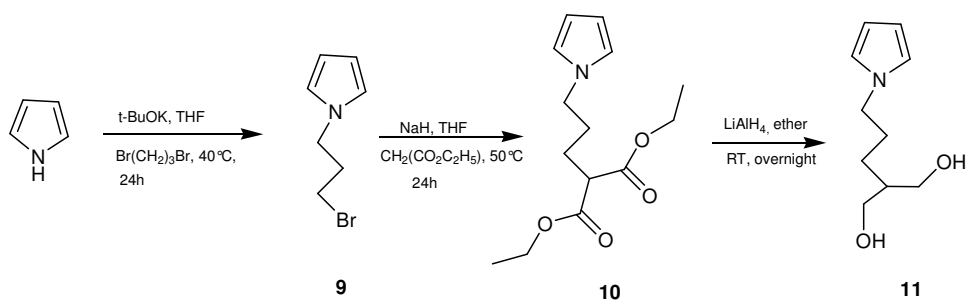
In this chapter, firstly, we have synthesis the new type chain extender containing pyrrole (Py) group by N-alkylation of pyrrole and then diester group displacement was carried out. Finally, the reduction of diester group to hydroxyl group was done. The products were characterized by Fourier Transform Infrared Spectroscopy (FTIR), Nuclear Magnetic Resonance spectroscopy (^1H -, ^{13}C - NMR), Mass spectroscopy (MS) and elemental analysis. The new chain extender has the main chain structure same as the common chain extender, 1,3-propanediol, except it has pyrrole unit as side group.

Secondly, the diol compound with pyrrole side group was used as chain extender in the preparation of polyurethane films. Glass transition temperature and degradation temperature of films containing different percentage of chain extender was characterized by Differential Scanning Calorimetry (DSC) and Thermal gravimetric analysis (TGA) respectively.

Lastly, we have polymerized the pyrrole unit on the polyurethane films by electrochemical method.

4.2. Synthesis and characterization of new chain extender with pyrrole side group

The synthesis of pyrrole (Py) derivative was carried out according to procedure as shown in Scheme 4.1 that modified from method described by Lallemand [14] and Quiroz [21].



Scheme 4.1 The synthesis route of 2-(3-(1H-pyrrol-1-yl)propyl)propane-1,3-diol **11**.

The N-alkylation of pyrrole (Py) with 1,3-dibromopropane was performed using potassium tert-butyrate to provide 1-(3-bromopropyl)-1*H*-pyrrole, **9**. Then, formation of diethyl 2-(3-(1*H*-pyrrol-1-yl)propyl)malonate **10** from compound **9** was achieved by displacement with sodium diethylmalonate, obtained in situ from diethyl malonate and sodium hydride. Finally, compound **10** was reduced by lithium aluminium hydride, yielding 2-(3-(1*H*-pyrrol-1-yl)propyl)propane-1,3-diol **11**.

4.2.1. Synthesis of 1-(3-bromopropyl)-1*H*-pyrrole **9**

The potassium pyrrole salt was formed by the reaction of pyrrole with potassium tert-butyrate in anhydrous THF solution at 0°C under inert atmosphere and 1,3-dibromopropane was then dropwised into reaction solution at the same temperature. The reaction solution was stirred at 40°C overnight; the crude product obtained is dark brown liquid. After purification by column chromatography, we obtained the red-brown liquid. Finally, 1-(3-bromopropyl)-1*H*-pyrrole **9** final product was characterized by ¹H- and ¹³C-NMR and FTIR spectroscopy.

From ¹H-NMR spectrum (Fig 4.1), protons in the pyrrole ring appear at the chemical shifts 6.67 and 6.16 as the triplet peaks. The signal triplet at 4.07 is corresponding to two protons adjacent to Py ring. Triplet and multiplet peaks at 3.30 and 2.24 are correspond to protons near Br group and two protons next to CH₂Br, respectively. By ¹³C-NMR characterization (Fig 4.2), signals of carbons in pyrrole ring appear at 107.35 and 109.56 ppm. Signals at 46.00 and 29.18 ppm correspond to carbon next to Py ring and near Br group in bromopropyl unit.

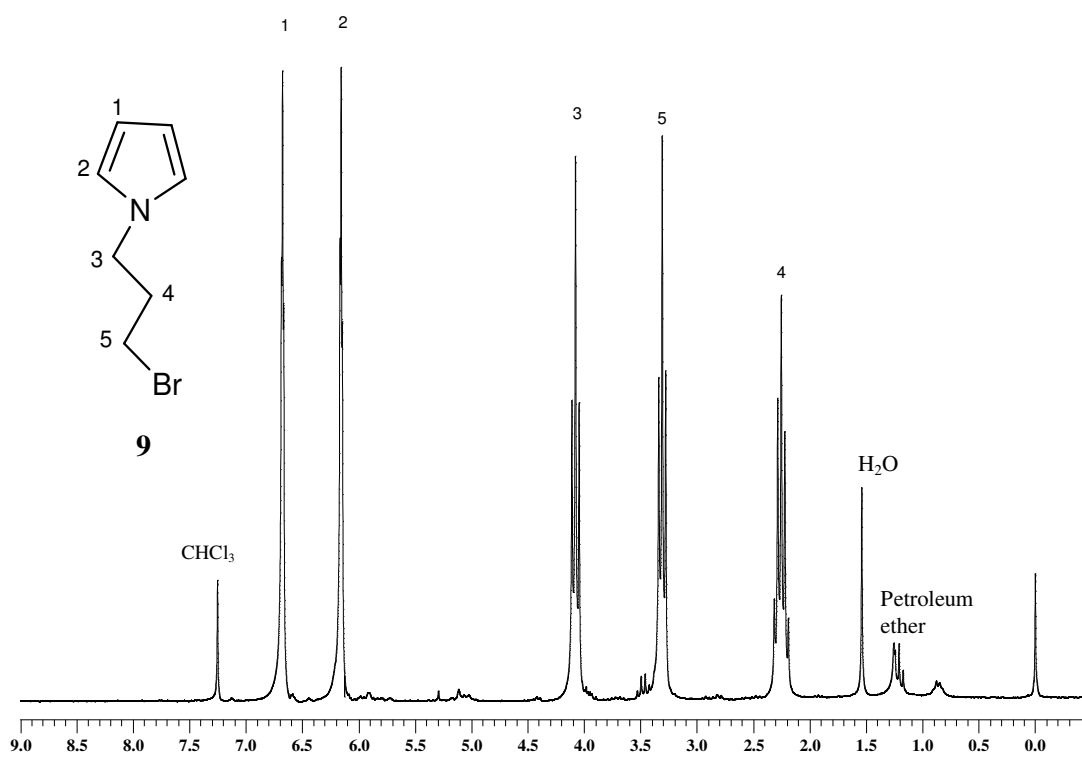


Fig 4.1 ¹H-NMR spectrum of 1-(3-bromopropyl)-1H-pyrrole 9.

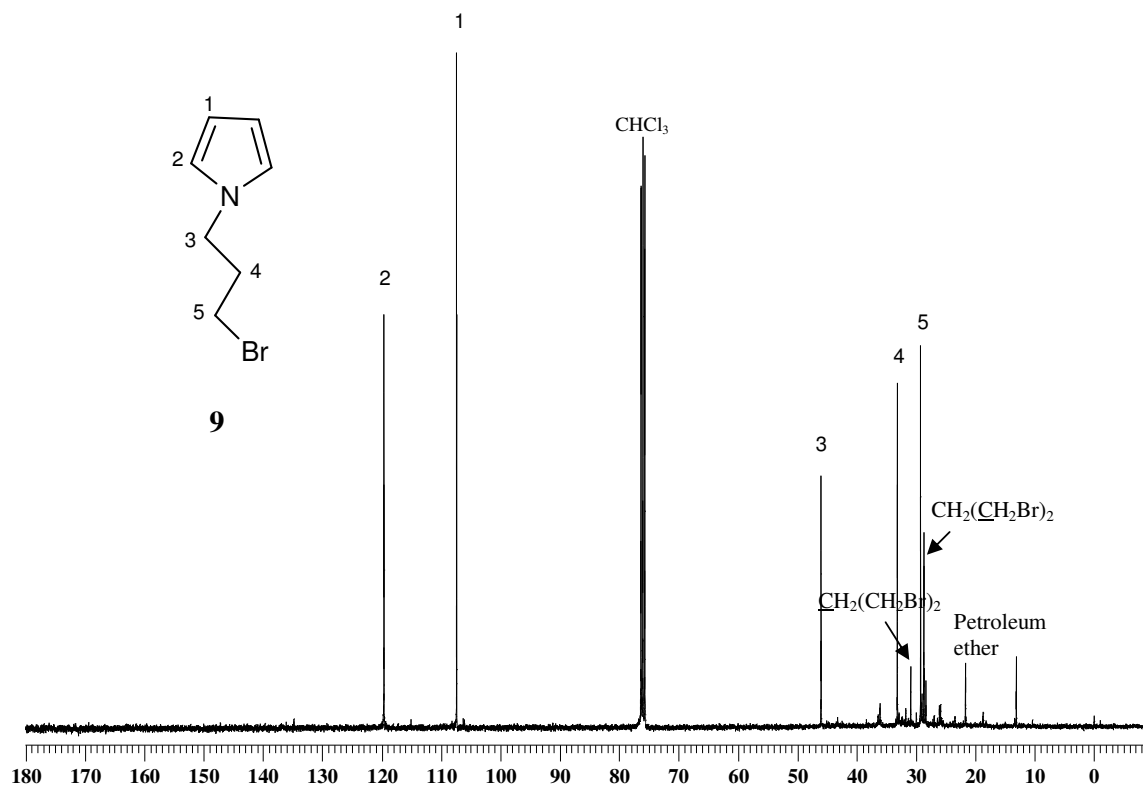


Fig 4.2 ¹³C-NMR spectrum of 1-(3-bromopropyl)-1H-pyrrole 9.

Remaining trace of starting reagent 1,3-dibromopropane is detected by peaks at 28.73 ppm and 30.97 ppm corresponding to methylic group next to CH₂Br and Br, respectively.

FTIR spectrum (appendix 3.1) shows peaks of pyrrole ring at 1500, 1440 and 1100-1050 cm⁻¹ corresponding to C=C, C-C and C-N stretching respectively. The peak at 2900-2700 shows the presence of CH₂ units and a peak of the stretching of C-Br bond appears at 600-500 cm⁻¹.

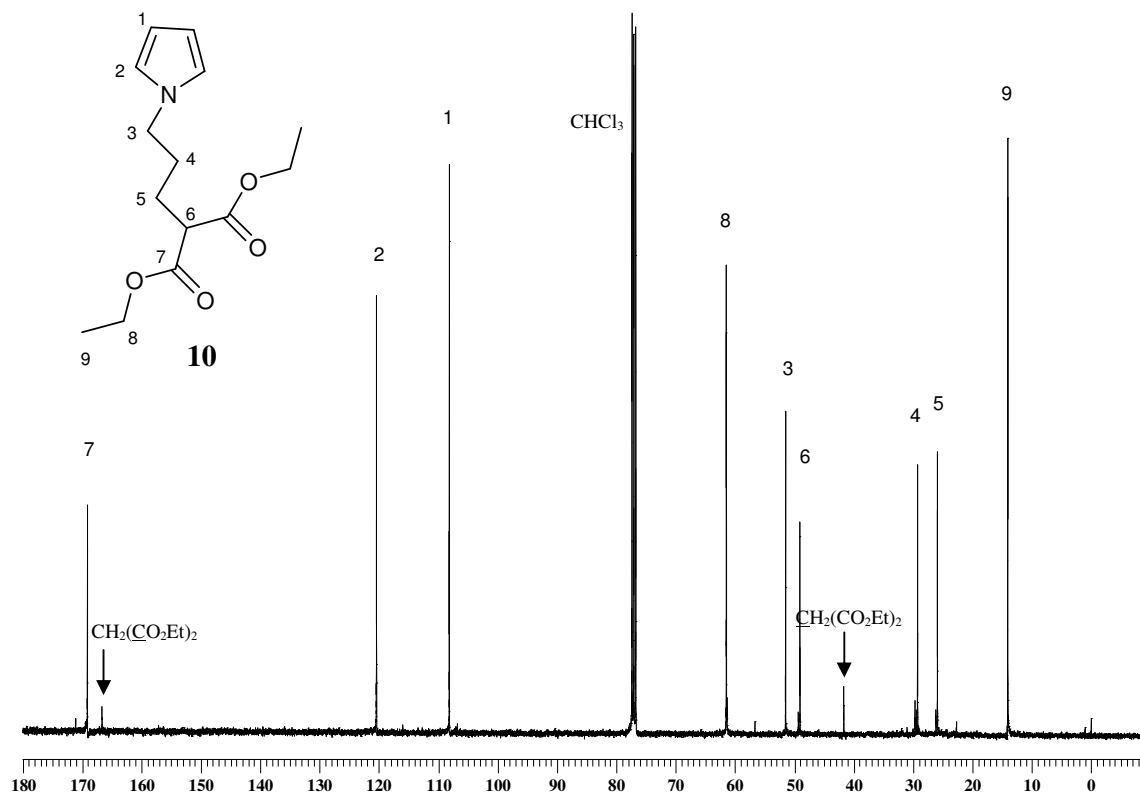
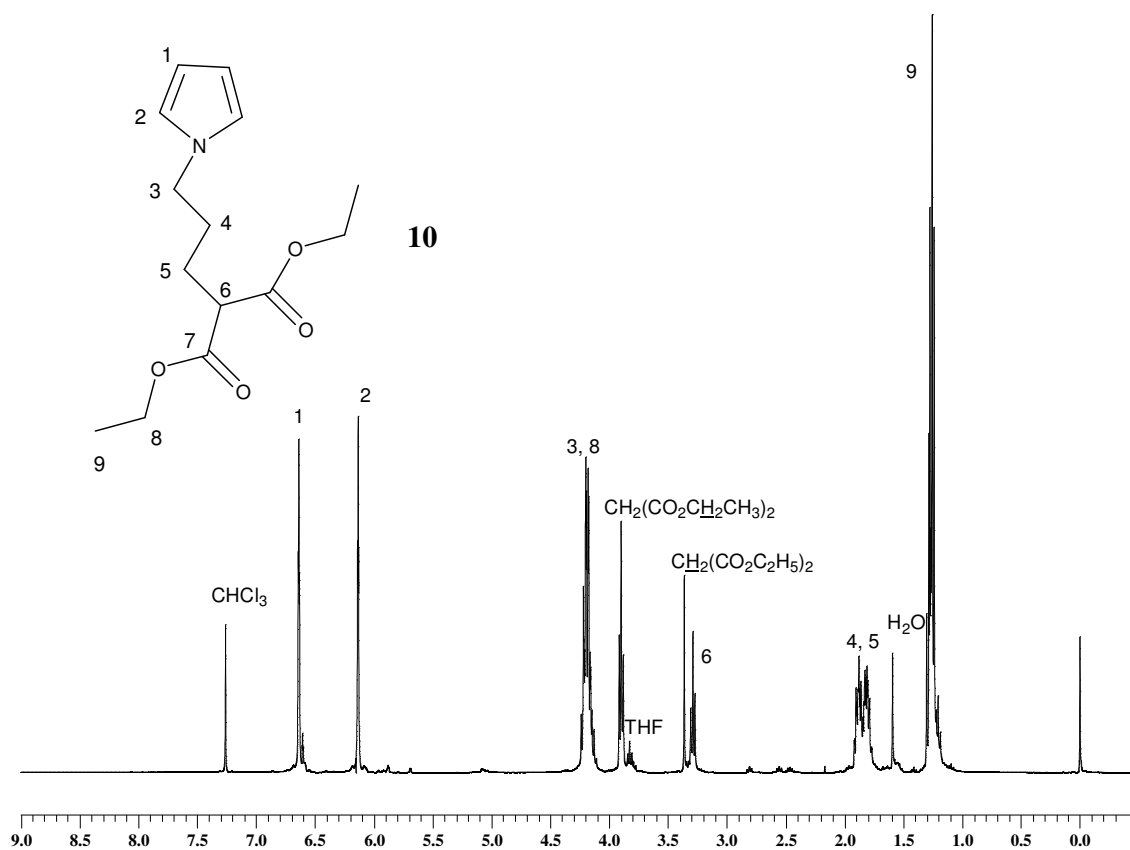
4.2.2. Synthesis of diethyl 2-(3-(1*H*-pyrrol-1-yl)propyl)malonate 10

The reaction of 1-pyrrol-3-bromopropane **9** and diethyl malonate salt was performed by dropwise adding compound **9** into the reaction solution of diethyl malonate and sodium hydride. The displacement of diethyl malonate group at the bromide group occurred. The crude product is purified by column chromatography. The final product is bright yellow liquid with yielding 61%.

By ¹H-NMR characterization (Fig 4.3), we observed the disappearance of signal at 2.24 ppm, corresponding to the protons of CH₂ next to Br group. In addition, there are multiplet signals at 4.17-4.22 ppm that correspond to methylene proton near Py ring and ester group. The signals at 3.29 and 1.28 ppm correspond to the methylenic and methylic protons of diethyl malonate unit. From ¹³C-NMR spectrum, we found carbons signals of diethyl malonate group at 169.11 (C=O), 61.51 (OCH₂CH₃) and 14.07 ppm (CH₂CH₃) (Fig 4.4).

There are remaining of diethyl malonate as shown in ¹H-NMR, peaks at 3.36 and 3.90 ppm correspond to methylic and methylenic protons. A signal at 41.68 and 166.75 ppm in ¹³C-NMR show the presence of methylic carbon and carbonyl group of diethyl malonate compound.

In FTIR spectrum (Appendix 3.1), we observed the disappearance of peak at 500-600 cm⁻¹ that corresponds to C-Br bond stretching, and the appearance of peak C=O stretching at 1730 cm⁻¹.



4.2.3. Synthesis of 2-(3-(1*H*-pyrrol-1-yl)propyl)propane-1,3-diol **11**

The reduction of compound **10** was realized by using LiAlH_4 as reduction agent in ether solution under inert atmosphere. The reaction solution was washed with distilled water and solvent was evaporated. A dark brown liquid was obtained as crude product.

From $^1\text{H-NMR}$ spectroscopy (Fig 4.5), the peak of hydroxyl proton is observed at 2.49 ppm and disappearance of signal at 3.29 ppm of CH in diethyl malonate group is established. Moreover, the complex signal at 3.6-3.8 ppm of the two conformations of protons at CH_2OH (position 7 and 8) caused by chiral carbon. From $^{13}\text{C-NMR}$ analysis (Fig 4.6), the disappearance of C=O at 169.11 ppm and appearance of carbon next to hydroxyl group at 63.99 ppm are observed.

In FTIR spectrum (Appendix 3.1), there is broad peak of O-H stretching at 3300 cm^{-1} . The stretching deformation peak of carbonyl group at 1730 cm^{-1} disappeared.

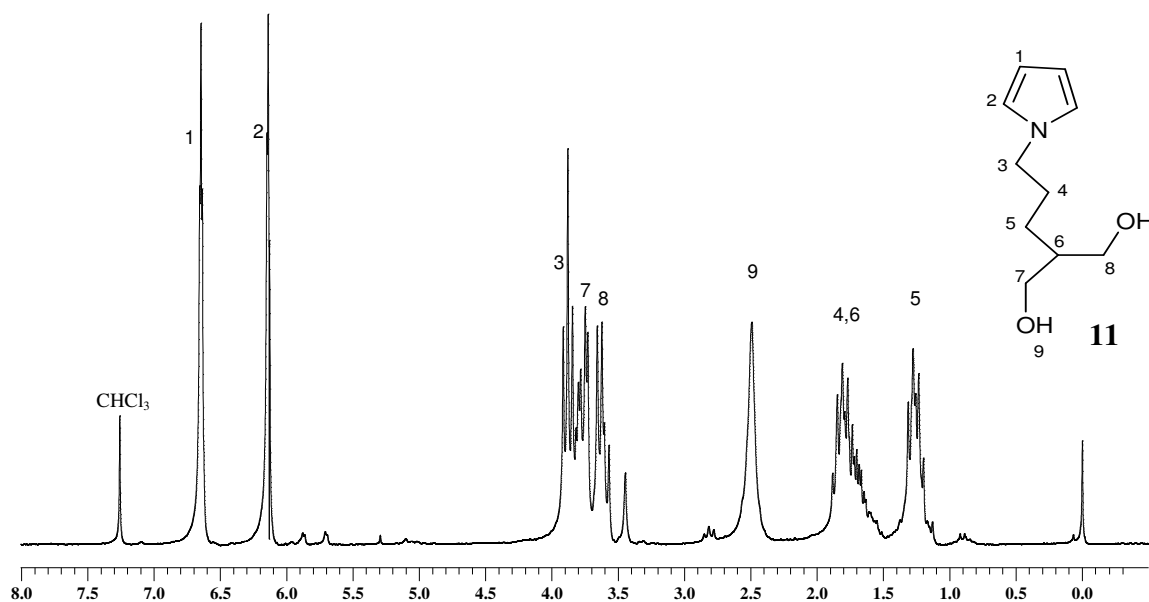


Fig 4.5 $^1\text{H-NMR}$ spectrum of 2-(3-(1*H*-pyrrol-1-yl)propyl)propane-1,3-diol **11**.

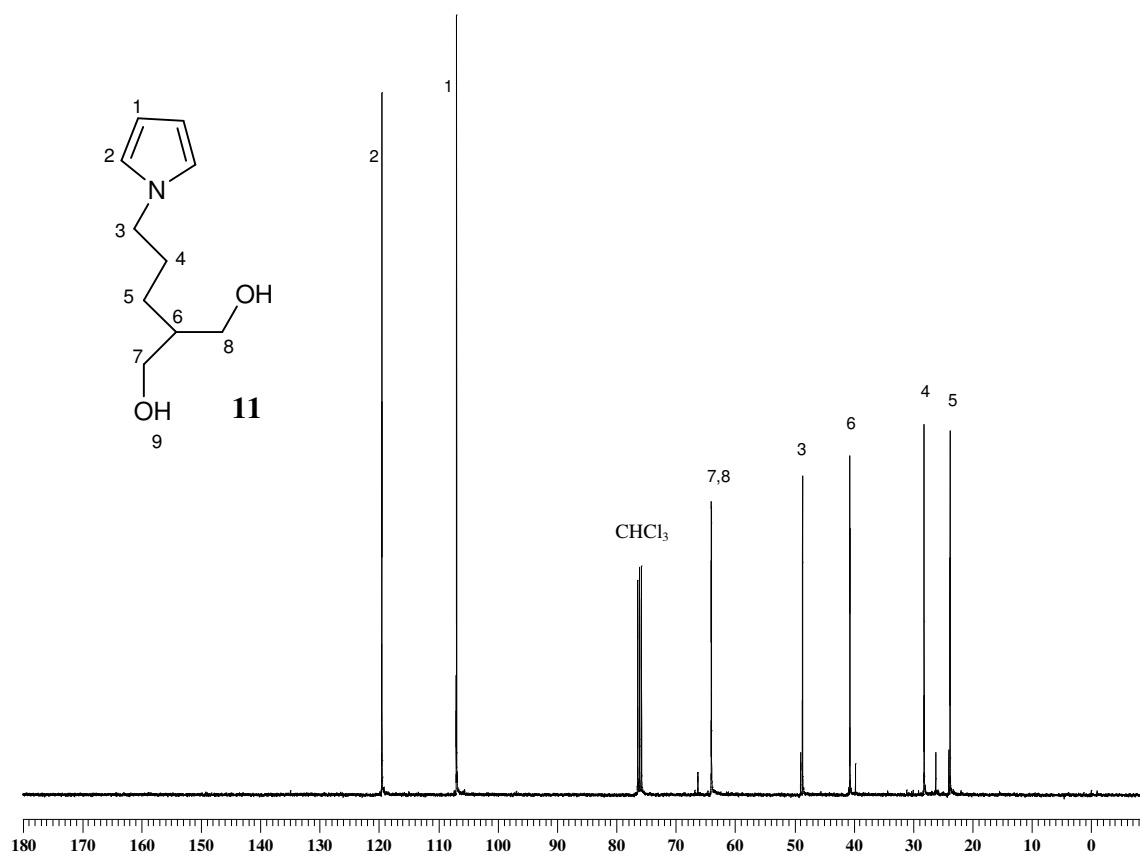
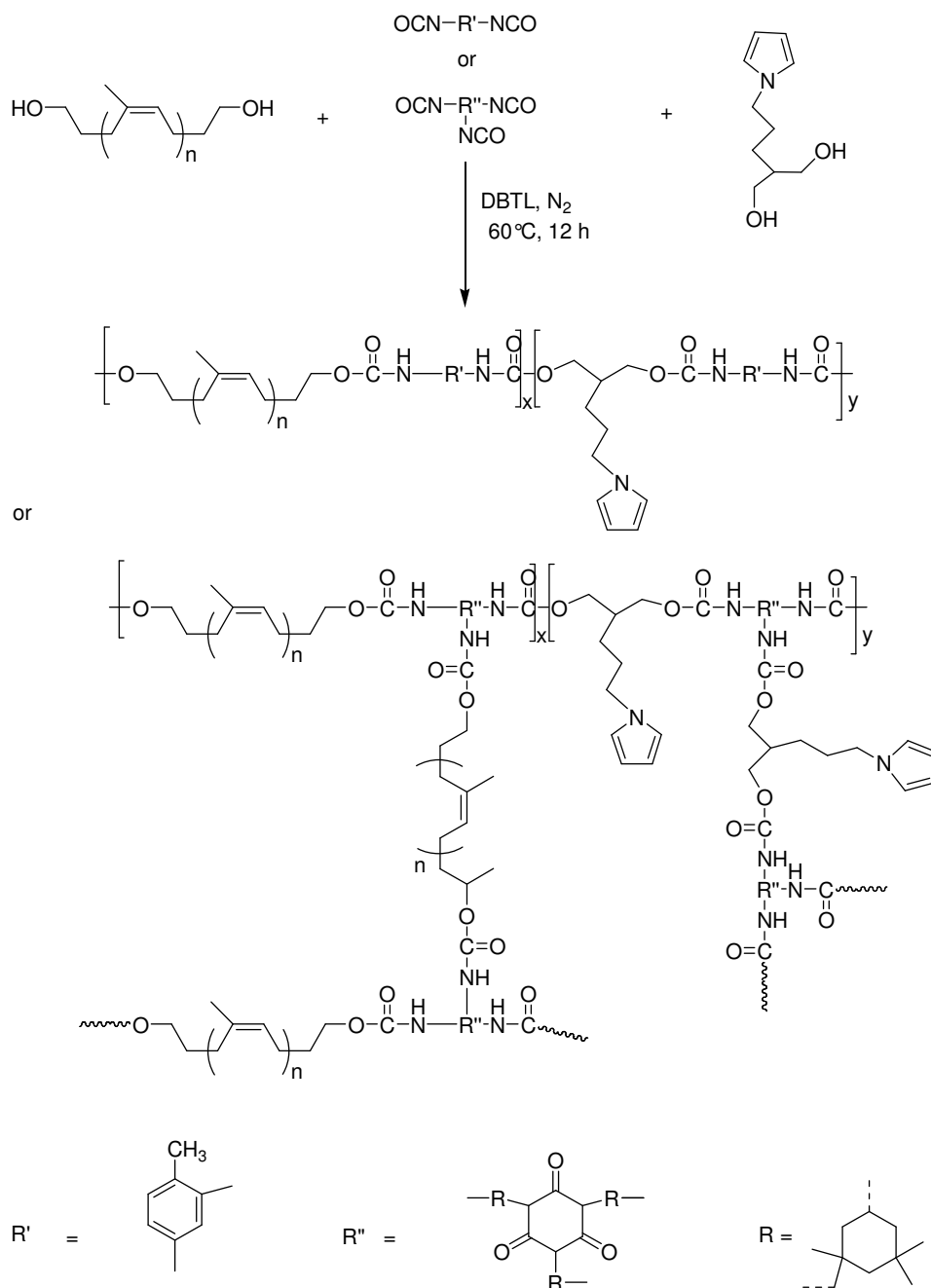


Fig 4.6 ^{13}C -NMR spectrum of 2-(3-(1*H*-pyrrol-1-yl)propyl)propane-1,3-diol **11**.

4.3. Synthesis and properties of polyurethanes using 2-(3-(1*H*-pyrrol-1-yl)propyl)propane-1,3-diol as chain extender

Linear and crosslinked polyurethane from hydroxytelechelic *cis*-1,4-polyisoprene ($\overline{M}_n = 1000$ and 2000) with different proportions of pyrrole derivative chain extender were prepared by one shot method and cast in mould following the procedure described by Kebir et al. [22, 23]. Films were characterized with FTIR, DSC and TGA.



Scheme 4.2 The synthesis of polyurethane using pyrrole derivative as chain extended.

4.3.1. Linear polyurethane with different amounts of chain extender

Linear PUs from hydroxytelechelic cis-1,4-polyisoprene with \overline{M}_n (NMR) about 2000 and 1000 g/mol were synthesized with TDI and different amounts of chain extender (2-(3-(1H-pyrrol-1-yl)propyl)propane-1,3-diol **11**, named KC27).

At 10% chain extender (LPU(2000)10), we didn't see any difference in the FTIR spectrum of PUs with and without chain extender, while at 20% KC27 (LPU(2000)20) and 30% KC27 (LPU(2000)30), a new peak at 727 cm^{-1} which corresponds to pyrrole ring vibration in KC27 is observed.

For linear PUs from hydroxytelechelic cis-1,4-polyisoprene having \overline{M}_n 1000 g/mol, at 20% KC27 (LPU(1000)20) and 40% KC27 (LPU(1000)40), there is a new peak at 725 cm^{-1} and the intensity of this peak increases as amount of KC27 in PU films increases. FTIR spectrums are shown in appendix.

4.3.1.1. Thermal properties of linear polyurethanes with chain extender

- **Differential Scanning Calorimetry (DSC)**

Composition, glass transition temperature and appearance of linear polyurethanes prepared by one shot method from hydroxytelechelic cis-1,4-polyisoprene with \overline{M}_n about 2000 and 1000 g/mol and different proportions of chain extender are summarized in Table 4.1.

Table 4.1 Composition, appearance and glass transition temperature of linear polyurethanes (\overline{M}_n PI \approx 2000 and 1000 g/mol) with different percentages of chain extender.

Polymer code	Chain extender (% by mol)	hard segment (%)	Appearance	T _g (°C)
LPU(2000)0	0	10.2	Yellow, soft ,transparent	-56
LPU(2000)10	10.8	12.1	Yellow, soft ,transparent	-58
LPU(2000)20	22.1	14.7	Yellow, soft ,transparent	-58
LPU(2000)30	27.4	16.0	Yellow, soft ,transparent	-58
LPU(2000)40	33 .2	17.5	Brown, soft ,transparent	-59
LPU(1000)0	0	17.7	Yellow, soft, transparent	-54
LPU(1000)20	20.1	23.7	Brown, soft, transparent	-47
LPU(1000)40	39.9	32.2	Brown, soft, transparent	-51

% hard segment = (wt.TDI+wt.KC27/ total wt.) \times 100

The DSC analysis of linear polyurethanes from hydroxytelechelic cis-1,4-polyisoprene with both \overline{M}_n of PI block gave one well-defined T_g. The soft segment T_g was observed around -58°C in polyurethane with \overline{M}_n of PI block about 2000 g/mol. There is no significant

difference from T_g of polyurethane without chain extender. The hard segment is probably too short compared with the soft segment, therefore, there is not much effect to T_g value of polymer films.

In polyurethane with \overline{M}_n of PI block about 1000 g/mol, T_g is a little higher in film with chain extender because of increasing in proportion of hard segments. However, at high percentage of chain extender, T_g of film decreases. This may be caused by the obstruction of Py ring to hydrogen bonding in hard segments blocks; hence the interactions between chains are weaker. It leads to decreasing of T_g of polymer.

- **Thermal gravimetric analysis (TGA)**

TGA and DTG curves of polyurethanes with \overline{M}_n of PI block 1000 and 2000 g/mol were analyzed comparatively (Fig 4.7-4.10) for verification of degradation step of polymers. The analysis showed two decomposition steps of samples corresponding to the two present phases. The first step (140-320°C) is attributed to the degradation of the hard segments and the second step (320-490°C) is related to the degradation of soft segments from polyisoprene block. This shows the phase separation in the polymer. The maximum rate degradation temperature (T_{max}) and weight loss in each step are shown in Table 4.2.

Table 4.2 Thermal degradation data of linear polyurethanes (\overline{M}_n PI \approx 2000 and 1000 g/mol) with different percentages of chain extender.

Polymer code	Thermal degradation step			
	1st Step		2nd Step	
	T_{max} (°C)	wt. loss (%)	T_{max} (°C)	wt. loss (%)
LPU(2000)0	377	98.1	-	-
LPU(2000)10	292	20.6	378	77.8
LPU(2000)20	296	22.1	377	74.3
LPU(2000)30	295	23.7	378	73.6
LPU(2000)40	293	24.4	379	73.0
LPU(1000)0	278	31.8	376	67.0
LPU(1000)20	298	35.8	383	62.2
LPU(1000)40	299	41.6	380	56.0

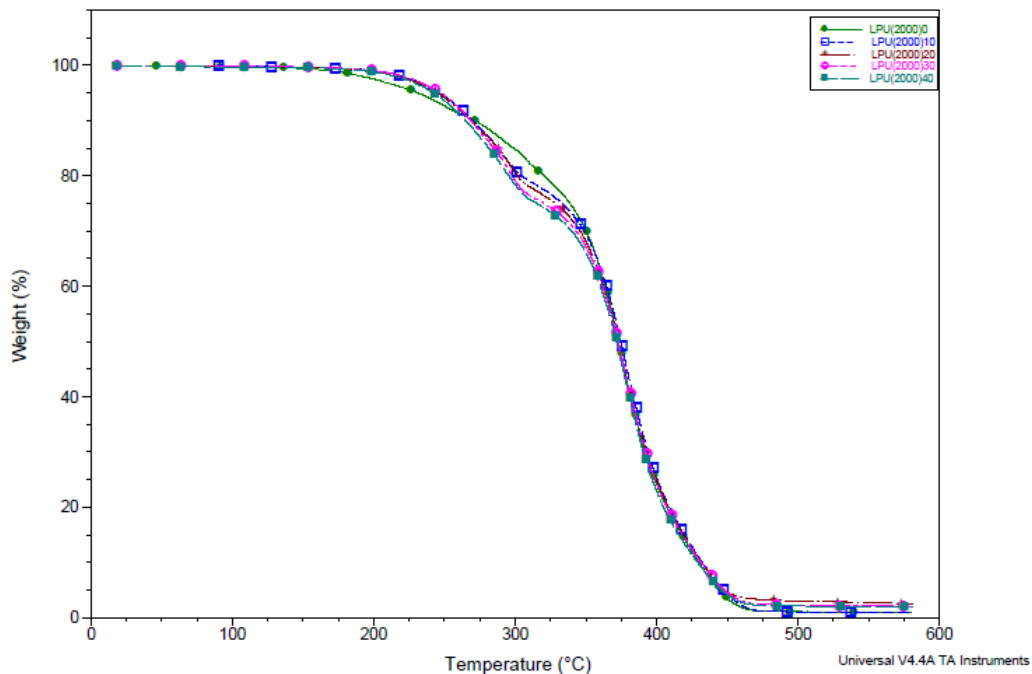


Fig 4.7 TGA thermograms of linear polyurethanes (\overline{M}_n PI \approx 2000 g/mol) with different percentages of chain extender.

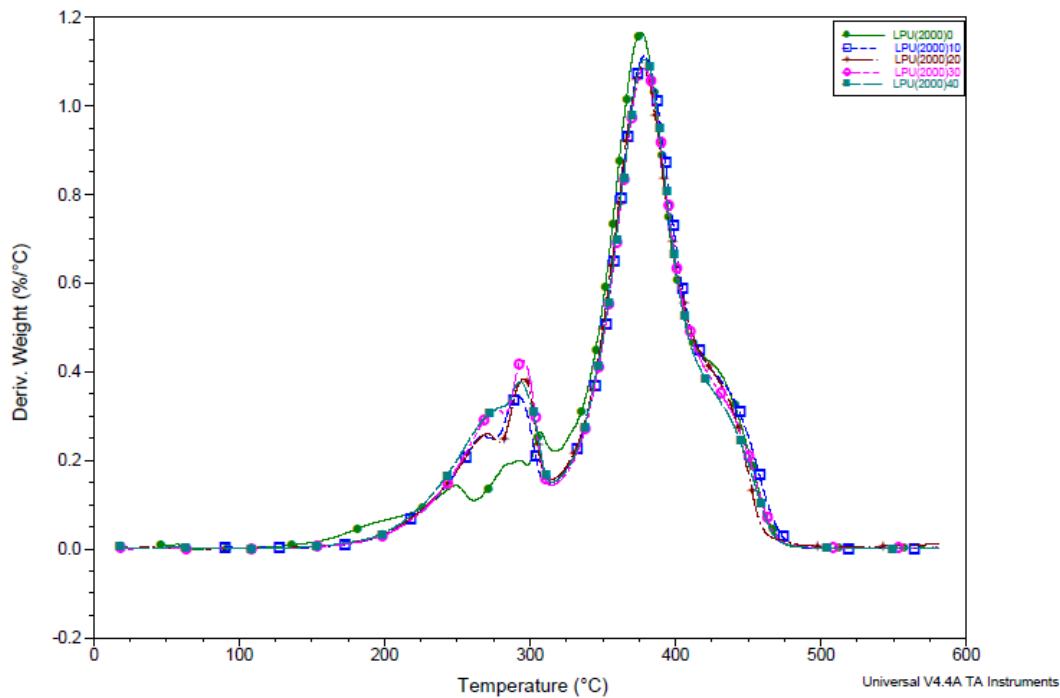


Fig 4.8 DTG curves of linear polyurethanes (\overline{M}_n PI \approx 2000 g/mol) with different percentages of chain extender.

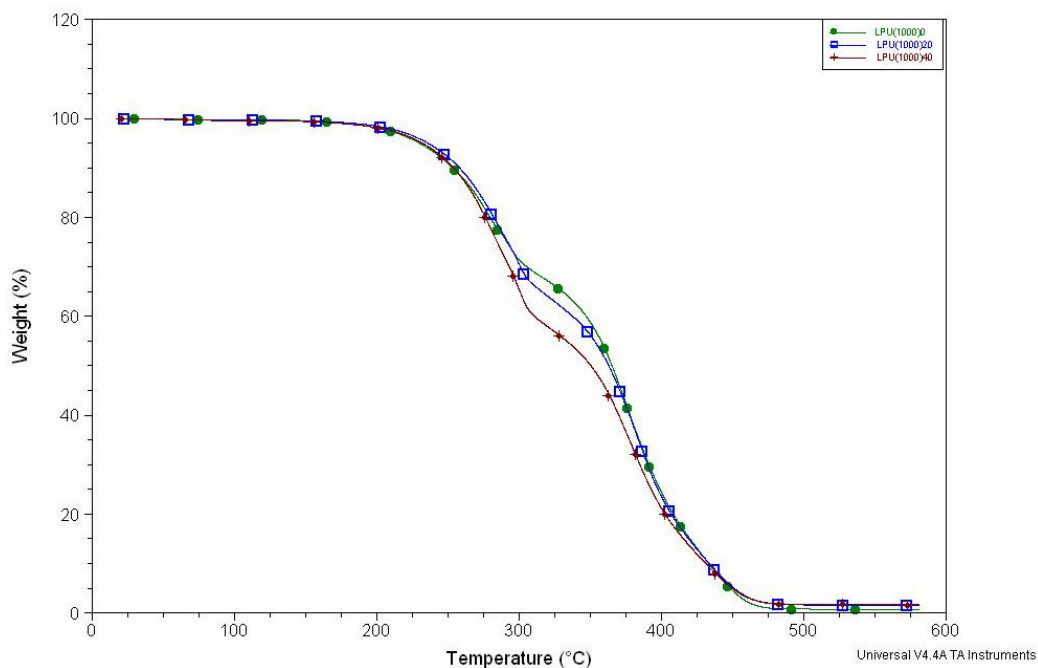


Fig 4.9 TGA thermograms of linear polyurethanes (\overline{M}_n PI \approx 1000 g/mol) with different percentages of chain extender.

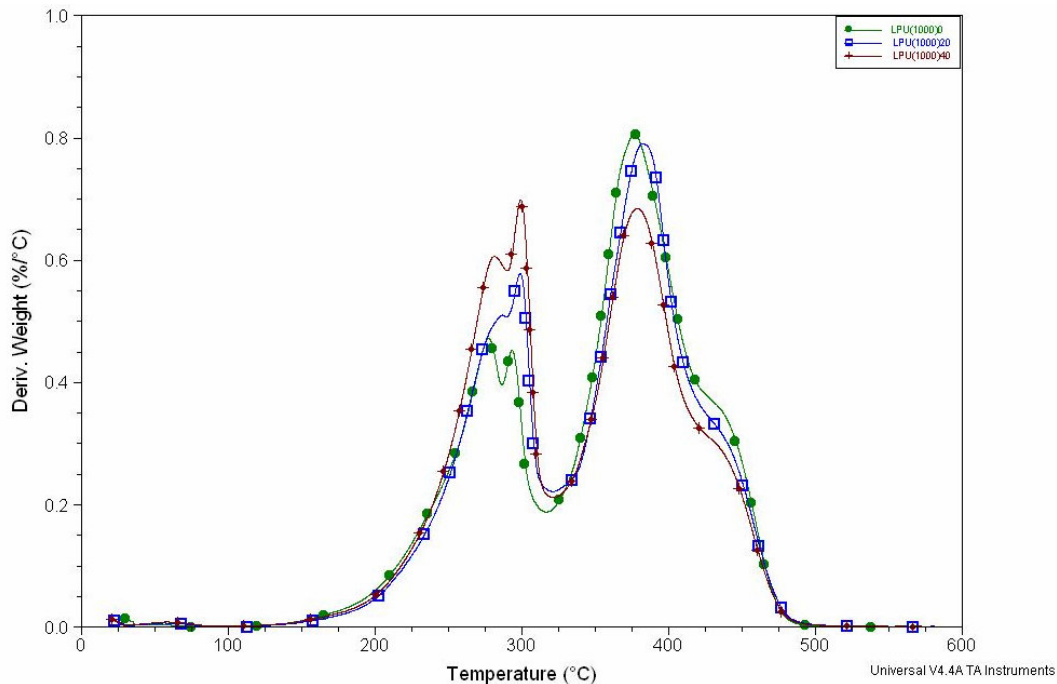


Fig 4.10 DTG curves of linear polyurethanes (\overline{M}_n PI \approx 1000 g/mol) with different percentages of chain extender.

The TGA allows us to observe a quantitative relationship between the proportion of the chain extender used in the formulation and the weight loss of hard segments suggesting that the chain extender degradation is located at this step of degradation.

The relationship of the weight loss in first step with the proportion of hard segments is shown in Fig 4.11. The weight loss increases as the proportion of hard segments in the polymer structure increases in both molecular weights of polyisoprene unit. In the polyurethane with short polyisoprene blocks, the phase separation is clearer. T_{max} values show that the presence of chain extender in the polyurethane formulation does not change the thermal stability of the films.

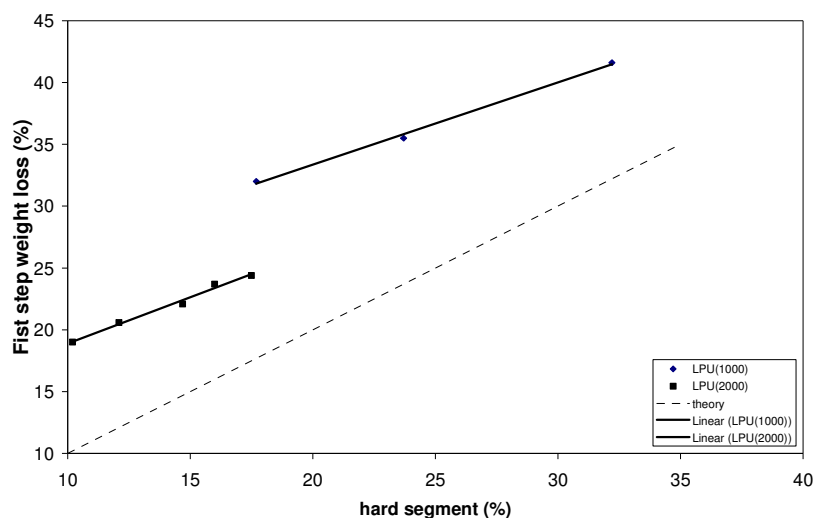


Fig 4.11 The relationship between proportions of hard segments and first step weight loss of linear polyurethane films with different percentages of chain extender.

4.3.2. Crosslinked polyurethanes with different amounts of chain extender.

Crosslinked PUs were synthesized with \overline{M}_n of PI block about 2000 g/mol and 1000 g/mol, triisocyanate I-IPDI, and different amounts of chain extender KC27.

For the crosslinked PU with \overline{M}_n of PI block about 2000 g/mol at 10% (CLPU(2000)10) and 20% KC27 (CLPU(2000)20) the peaks of KC27 unit are not observed, while at 40% (CLPU(2000)40), there is a new peak at 723 cm^{-1} compare with film without KC27 and intensity of peak at 1040 cm^{-1} increases.

For the crosslinked PU from hydroxytelechelic cis-1,4-polyisoprene with \overline{M}_n about 1000 g/mol, at 30 % (CLPU(1000)30) and 40% KC27 (CLPU(1000)40), a new peak at 723 cm^{-1} is also observed and intensity of the peak at 1030 cm^{-1} increases. FTIR spectrums are shown in appendix 3.2.

4.3.2.1. Thermal properties of crosslinked polyurethanes with chain extender

- **Differential Scanning Calorimetry (DSC)**

The composition of crosslinked polyurethane films included appearance and glass transition temperature are shown in Table 4.3. Crosslinked films are more transparent compared with the linear ones. As higher percentages of chain extender and hard segment are, as less flexible films are.

Table 4.3 Composition, appearance and glass transition temperature of crosslinked polyurethanes (\overline{M}_n PI \approx 2000 and 1000) with different percentages of chain extender.

Polymer code	Chain extender (% by mol)	hard segment (%)	Appearance	T _g (°C)
CLPU(2000)0	0	22.5	Yellow, soft, transparent	-55
CLPU(2000)10	9.8	25.9	Yellow, soft, transparent	-53
CLPU(2000)20	18.2	26.6	Yellow, soft, transparent	-53
CLPU(2000)40	39.9	38.2	Yellow, soft, transparent	-56
CLPU(2000)60	60.0	49.0	Brown, stiff, transparent	-61
CLPU(1000)0	0	39.5	Yellow, soft, transparent	-44
CLPU(1000)20	30.5	49.6	Brown, stiff, transparent	-
CLPU(1000)40	40.0	53.6	Brown, stiff, transparent	-

% hard segment = (wt. I-IPDI+wt. KC27/ total wt.) \times 100

T_g of crosslinked PU (\overline{M}_n PI \approx 2000 g/mol) films does almost not varied with the increase of chain extender between 20 to 40 % by mol. While at the amount of chain extender 60% by mol, T_g of film decrease slightly. The pyrrole rings may have a steric effect in order to decrease the interactions between the chains. Therefore, less energy is needed for chain mobility.

When used soft segment is shorter, PU from hydroxytelechelic PI with \overline{M}_n (NMR) about 1000 g/mol, films are hard and T_g can't be defined.

- **Thermal gravimetric analysis (TGA)**

TGA curves are given in Fig 4.12 and 4.13. For well defining the degradation events, DTG curves in Fig 4.14 and 4.15 are analyzed comparatively. Thermal gravimetric analysis of crosslinked polyurethanes shows a one thermal degradation step. This shows the phase mixing of network structure. Hard segments act as crosslinker between soft segments. At low content of chain extender and high molecular weight of polyisoprene block crosslinked polyurethanes, we observe a one complete decomposition step. In the other hand, at higher chain extender content or low molecular polyisoprene block, DTG curves show the hard segment block decomposition of triisocyanate and chain extender before the main degradation of crosslinked structure. The maximum degradation rate temperature and weight loss is shown in Table 4.4.

Table 4.4 Thermal degradation data of crosslinked polyurethanes (\overline{M}_n PI \approx 2000 and 1000) with different percentages of chain extender.

Polymer code	Thermal degradation	
	T_{\max} (°C)	wt. loss (%)
CLPU(2000)0	374	98.7
CLPU(2000)10	379	98.5
CLPU(2000)20	379	98.7
CLPU(2000)40	378	98.4
CLPU(2000)60	375	97.9
CLPU(1000)0	374	97.3
CLPU(1000)30	371	97.4
CLPU(1000)40	361	96.9

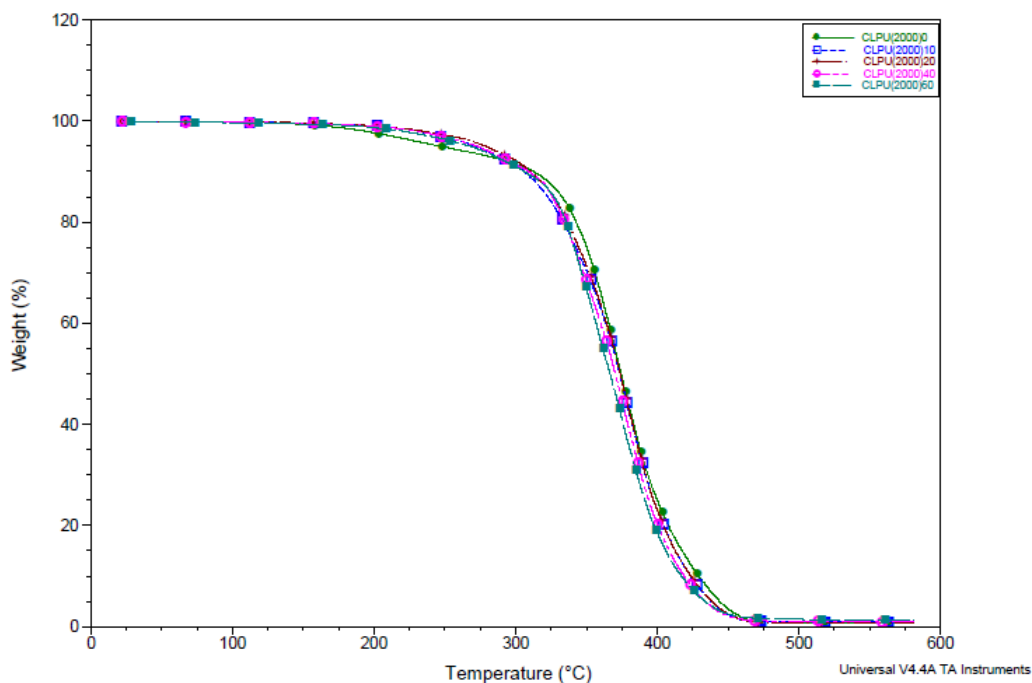


Fig 4.12 TGA thermograms of crosslinked polyurethanes (\overline{M}_n PI \approx 2000g/mol) with different percentages of chain extender.

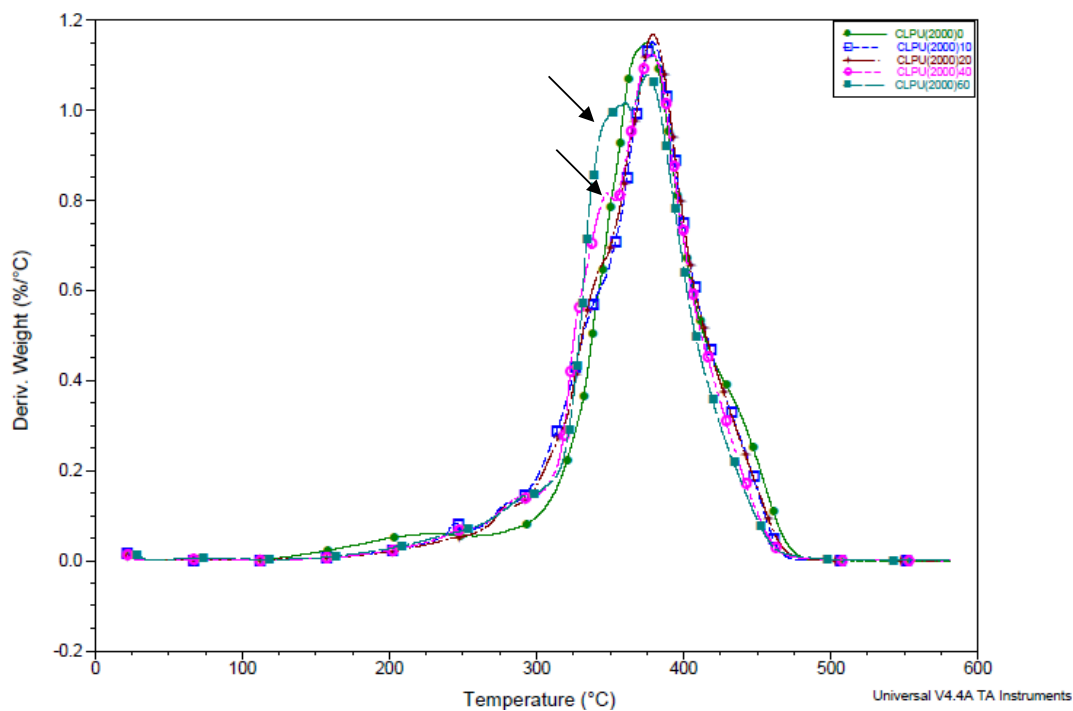


Fig 4.13 DTG curves of crosslinked polyurethanes (\overline{M}_n PI \approx 2000 g/mol) with different percentages of chain extender.

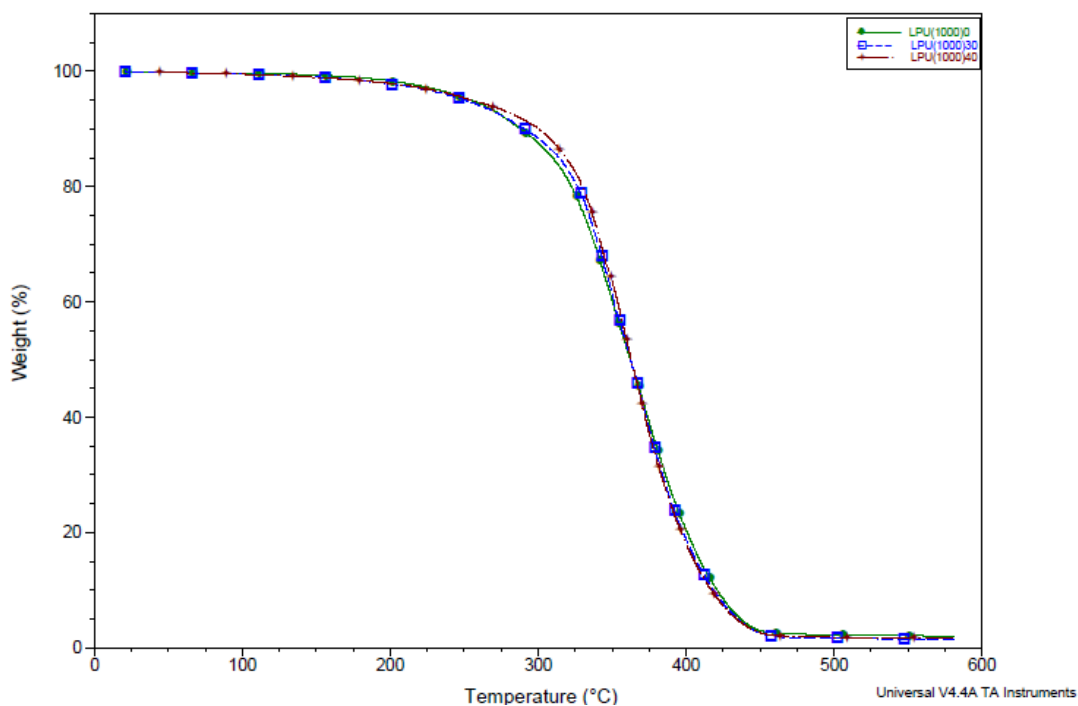


Fig 4.14 TGA thermograms of crosslinked polyurethanes (\overline{M}_n PI \approx 2000g/mol) with different percentages of chain extender.

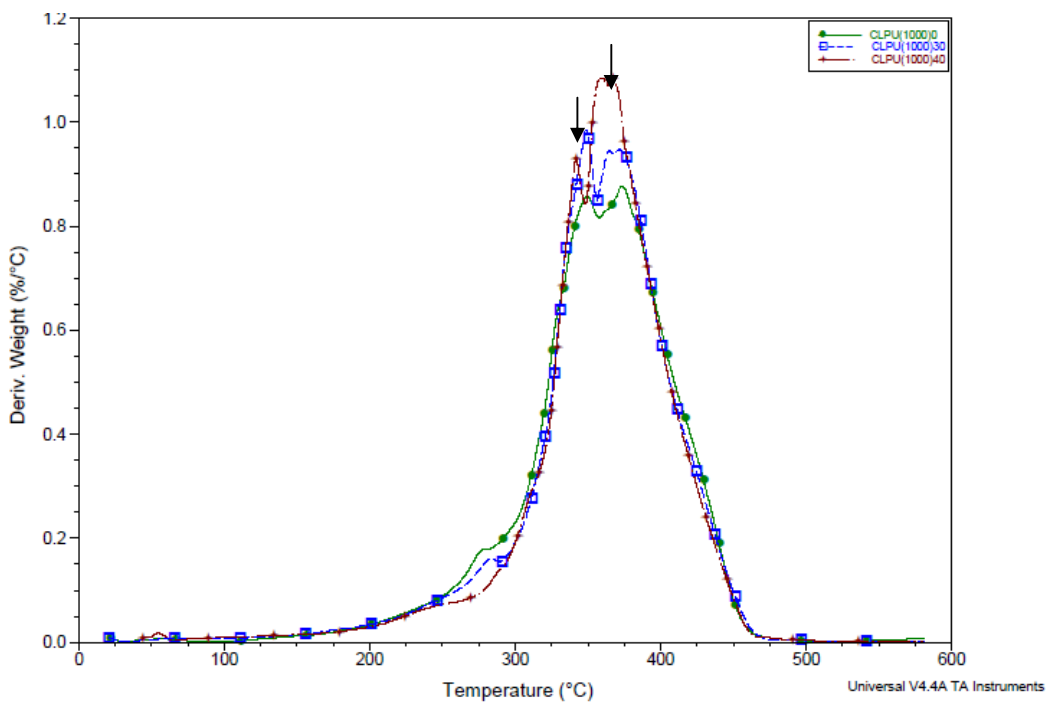


Fig 4.15 DTG curves of crosslinked polyurethanes (\overline{M}_n PI \approx 1000 g/mol) with different percentages of chain extender.

4.4. Electrochemical polymerization of pyrrole on polyurethane films.

The electropolymerization of pyrrole in polyurethane containing pyrrole derivative chain extender were performed by cyclic voltammetry technique in the potential range required for polymerization of pyrrole (-0.5 V to +1.3 V vs. SCE) [19] at sweep rate of 100mV/s in 0.5 M LiClO₄ electrolyte solution. The cyclic voltammograms (CVs) were recorded on glassy carbon electrode (2mm diameter).

4.4.1. Electrochemical polymerization of pyrrole on pyrrole-swollen polyurethane films containing chain extender.

In the first approach, we swelled PU film in the Py monomer and then performed polymerization. CLPU(1000)40 film was swelled in pyrrole monomer for 10 mins, Py at surface was removed by rinsing with distilled water and wiping with filtered paper. Film containing 38% wt. Py was installed in the electrochemical cell consisting of three electrodes. The potential from -0.5 to +1.3 V were cyclized to carry out the polymerization of Py. The cyclic voltammogram is shown in Fig 4.16.

Oxidation peaks located at +0.5 V and +1.1 V (termed B_{ox} and A_{ox}), are ascribed to the oxidation of PPy and Py monomer. The reduction peak centred at -0.3 V. and termed B_{red}, corresponds to the reduction of oxidized PPy chains leading to PPy in this neutral state. The B_{ox}/B_{red} system corresponds to the p-doping and dedoping processes of PPy. The increasing of doping peak of PPy (B_{ox}) about 20 μA per cycle allows appreciating the growth of the PPy film. Besides the conducting surface of the electrode, the conducting surface from PPy formation can also induces the polymerization of monomers. Therefore, more PPy is formed, more conducting surface increases and more Py can be polymerized, that shown in the increasing of oxidation current at +1.1 V in each sweep.

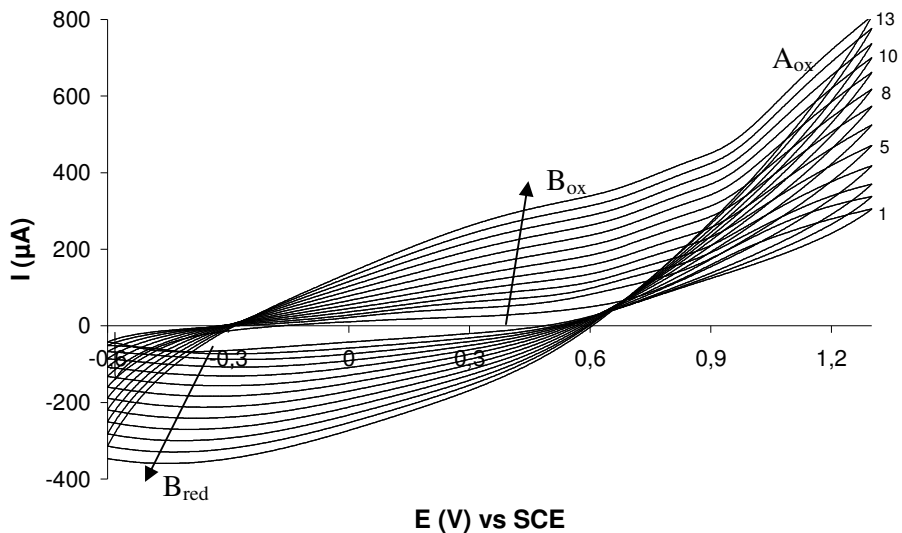


Fig 4.16 Cyclic voltammogram of 38% pyrrole incorporated CLPU(1000)40 film in 0.5 M LiClO_4 recorded on glassy carbon ($\varnothing = 2$ mm). Scan rate 100 mV/s, where A_{ox} , B_{ox} and B_{red} represent oxidation peak of Py, oxidation and reduction peak of PPy, respectively.

The doping-dedoping curves of PPy film are showed in the Fig 4.17. It reflects the oxidation and reduction of the polymer (PPy) inducing counter ion transfer in and out of film. Such feature attests that there is PPy on the PU film. Moreover, when the electrode is removed from the film surface, a dark spot is observed on the PU film as shown in Fig 4.18.

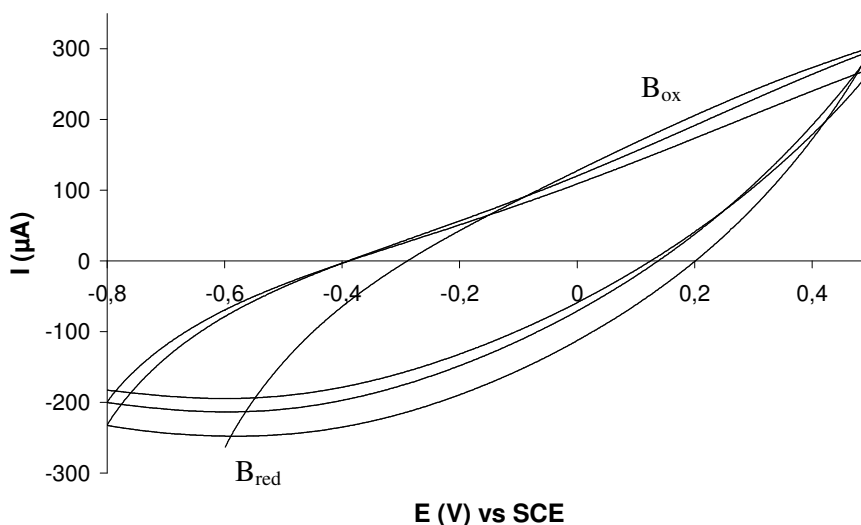


Fig 4.17 Cyclic voltammogram of PPy on 38% Py incorporated polyurethane film containing 40% KC27 in 0.5 M LiClO_4 recorded on glassy carbon ($\varnothing = 2$ mm). Scan rate 100 mV/s.

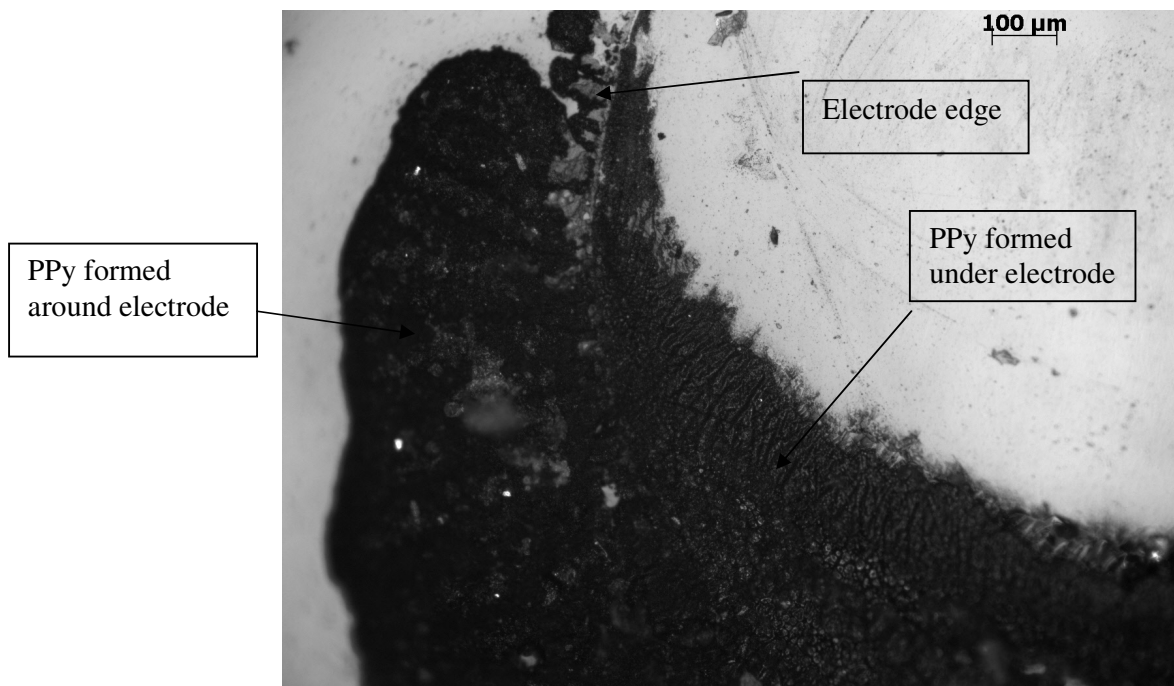
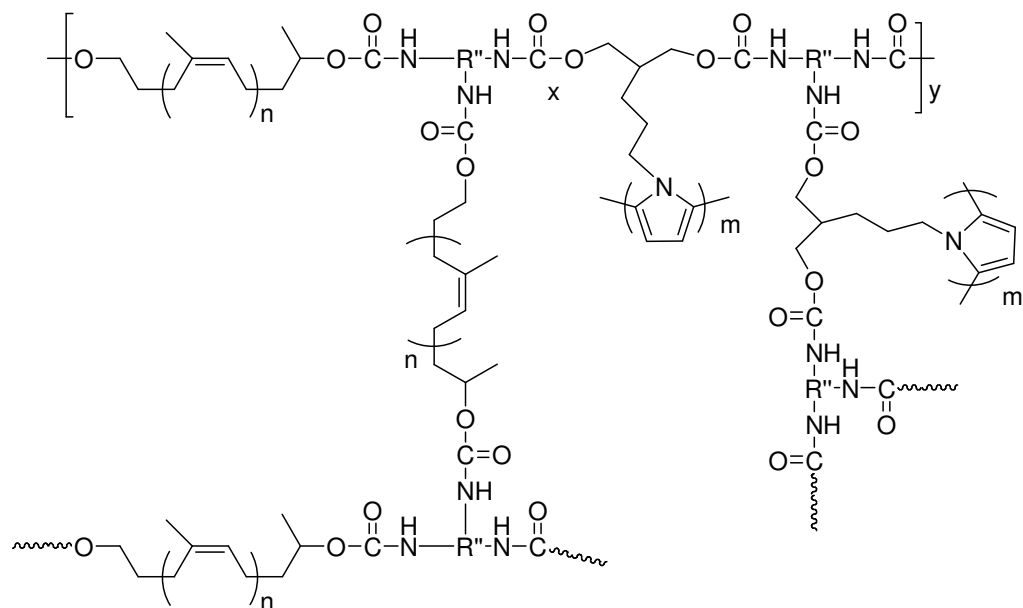


Fig 4.18 Optical microscope image of CLPU(1000)40+PPy film after electropolymerization.

From optical microscopic image of CLPU(1000)40 film after polymerization, we observed the PPy formation on some part of the electrode position and around electrode position. Because the bottom of electrochemical cell is not flat, the electrode was not well applied on film, only some part of film contacts with electrode. When potential was applied, Py in film that contacts with electrode was polymerized, hence, we saw PPy formation only on some part of electrode. The formed PPy under electrode then induced Py monomer around electrode to polymerize. From this reason, we saw also formation of PPy around the electrode position.

Nevertheless, when the glassy carbon electrode is removed from the PU surface, the PPy formed in this case remains on the film (It was not peeled off when we took off electrode). We expect that there is the polymerization of Py unit in the structure of polyurethane film as shown in Scheme 4.3.



Scheme 4.3 The supposed structure of PU/PPy composite.

4.4.2. Electrochemical polymerization of pyrrole on polyurethane films containing chain extender.

A crosslinked polyurethane with 20% (CLPU(2000)20) and 40% mol chain extender (CLPU(1000)40) were installed in an electrochemical cell consisting of three electrodes. Typical cyclic voltammogram recorded for a Py derivative chain extended polyurethane film is shown in Fig 4.19. The oxidation of Py start from +0.9 V vs. SCE (A_{ox}). It must be noted that the current peak ascribed to the oxidation of pyrrole units covalently linked to the PU chains decreases as the potential is cyclized. This decrease of current attests to the consumption of Py in the film. In each cycle, Py are polymerized to form PPy, hence, the concentration of Py in the film decreases. This leads to the decreasing of the oxidation peak of Py.

In addition, after the first sweep, we observe the oxidation peak at +0.2 V (B_{ox}) and reduction peak at +0.1 V (B_{red}) that correlate well with the formation of PPy. Therefore, it shows that there are PPy formed in polyurethane film. The increasing of this oxidation current and decreasing of reduction current in each cycle shows the growth of PPy in the polyurethane film.

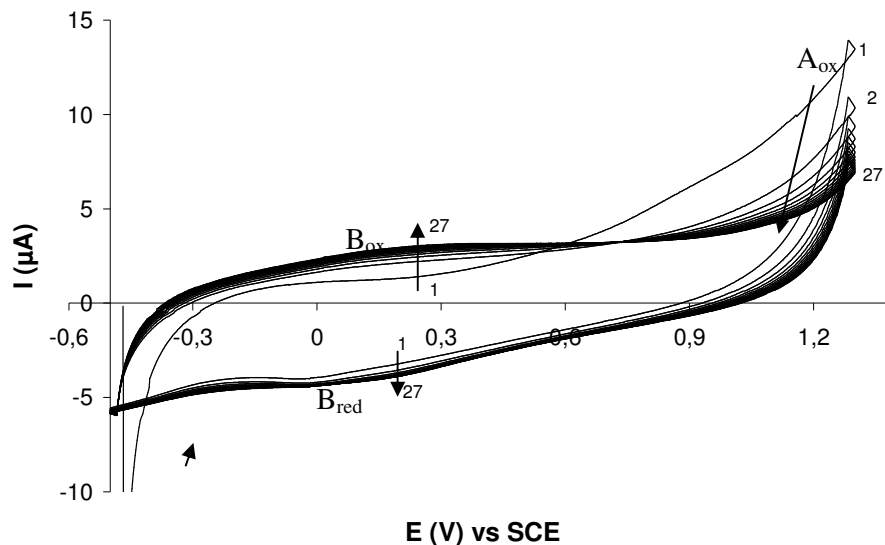


Fig 4.19 Cyclic voltammogram of pyrrole in CLPU(2000)40 film in 0.5 M LiClO₄ recorded on glassy carbon ($\varnothing = 2$ mm). Scan rate 100 mV/s.

The typical doping and dedoping cyclic voltammogram (CV) recorded for PPy films ranging from -0.2 to +0.5 V is shown in Fig 4.20. Fig 4.20a is the doping-dedoping curve of PPy in CLPU(2000)40 film while Fig 4.20b serves as a blank experiment showing a cyclic voltammogram obtained with a CLPU(2000)40 film prior that the electropolymerization of pyrrole units was accomplished. This confirms the formation of PPy in the film. In each cycle of potential, the voltammogram are the same in accordance with the stability of PPy film in the solution over this potential range.

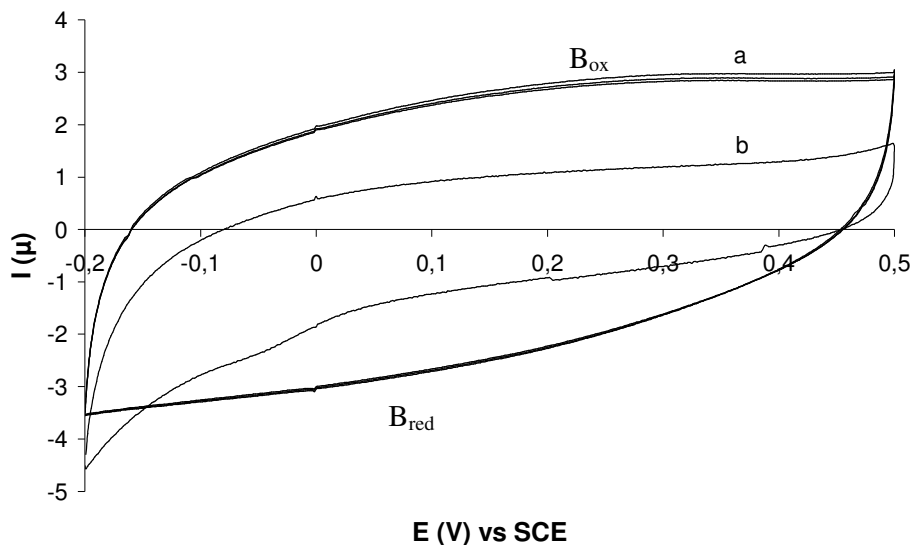


Fig 4.20 Cyclic voltammogram of a) PPy on CLPU(2000)40 film; b) CLPU(2000)40, in 0.5 M LiClO₄ recorded on glassy carbon ($\varnothing = 2$ mm). Sweep rate: 100 mV/s.

We have also performed the electropolymerization of Py in film containing shorter soft segment blocks, CLPU(1000)40. The cyclic voltammogram is shown in Fig 4.21. The oxidation current in the first cycle is higher compared with the cyclic voltammogram of CLPU(2000)40 that corresponds to higher concentration of Py in film. In addition, the oxidation peak and reduction peak of PPy at +0.2 and +0.1V are higher than in CLPU(2000)40 which indicates also higher PPy formation in this PU film.

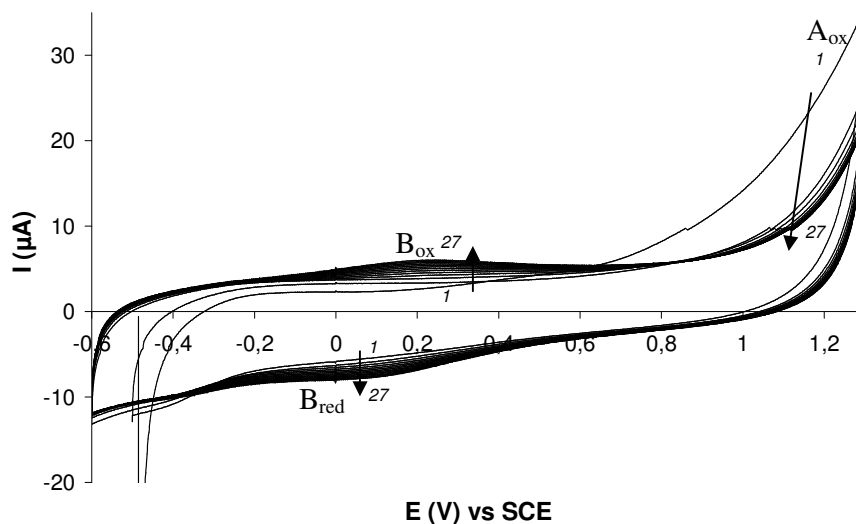


Fig 4.21 Cyclic voltammogram of pyrrole in CLPU(1000)40 film in 0.5 M LiClO₄ recorded on glassy carbon ($\varnothing = 2$ mm). Scan rate 100 mV/s.

Doping and dedoping cyclic voltammogram of CLPU(1000)40 film containing PPy compared with CV of a film without PPy showing in Fig 4.22, confirms the formation of PPy. The cyclic voltammogram shows the stability of PPy film in 0.5 M LiClO₄ solution over the -0.2 to +0.5 V range. The image of PPy on polyurethane film after polymerization is shown in Fig 4.23. We observe the thin spot of PPy on PU film.

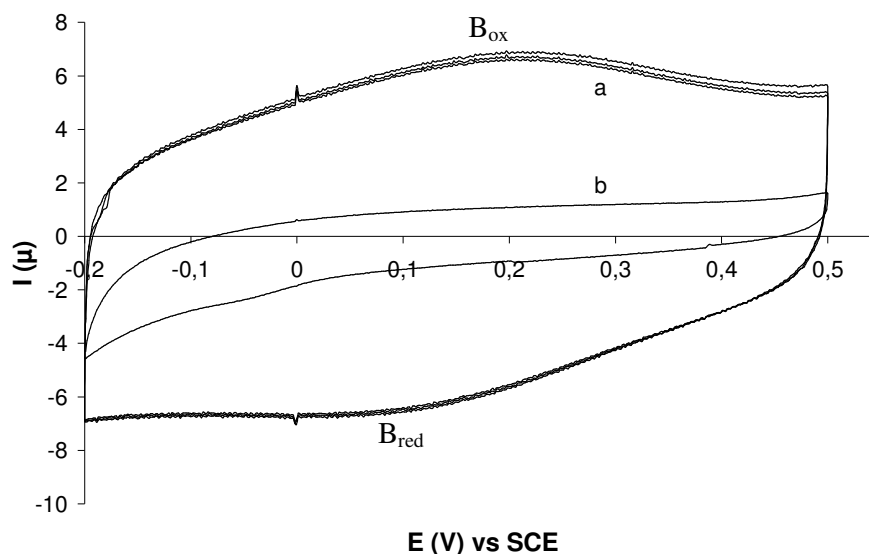


Fig 4.22 Cyclic voltammogram of a) PPy on CLPU(1000)40 film; b) CLPU(1000)40, in 0.5 M LiClO₄ recorded on glassy carbon ($\varnothing = 2$ mm). Scan rate 100 mV/s.

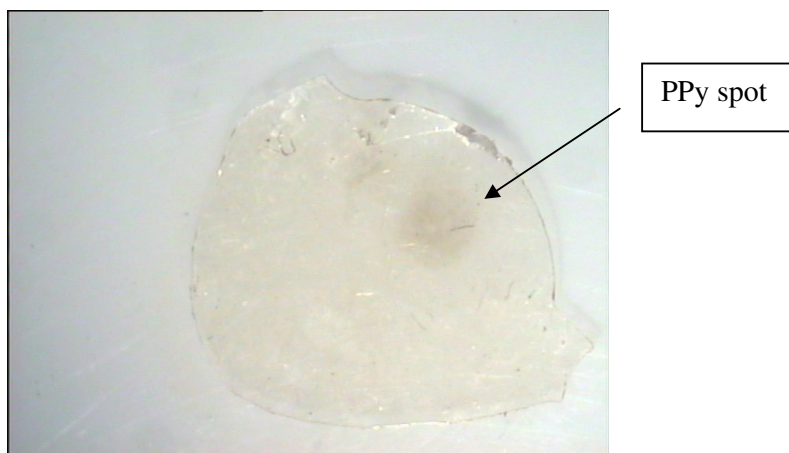


Fig 4.23 Optical microscope image of PPy on CLPU(1000)40 film after electrochemical polymerization.

4.5. Conclusion

In this chapter, we have synthesized a new chain extender containing pyrrole unit. This type of chain extender can be not only used to increase the hard segment of polyurethane but also further polymerized to form the conducting polymer on/in the polyurethane film. Thermal properties of polyurethane with new type of chain extender were studied and electropolymerization of the Py unit in polyurethane was performed.

The pyrrole derivative chain extender, 2-(3-(1*H*-pyrrol-1-yl)propyl)propane-1,3-diol, can be successfully synthesized by classic reaction. N-alkylation of pyrrole with the 1,3-dibromopropane was done, following with the displacement of the bromide end group with diethyl malonate. Finally, the reduction of diethyl malonate was carried out to obtain a dihydroxy group. The characterization in each step confirms the structure of the product obtained.

The polyurethanes using this type chain extender were prepared from two molecular weights hydroxytelechelic *cis*-1,4-polyisoprene, 1000 and 2000 g/mol, and two kinds' diisocyanate, TDI and I-IPDI. By differential scanning calorimetric characterization of films, only one glass transition temperature (T_g) was observed in all percentage of chain extender. T_g of linear and crosslinked polyurethanes with \overline{M}_n of soft segments about 2000 g/mol did not vary with the percentage of the chain extender because the soft segments are much longer than hard segments, therefore, the increasing of hard segments has no effect on T_g of films. On the other hand, in the linear polyurethane with \overline{M}_n of PI block about 1000 g/mol, T_g is more sensitive to the amount of chain extender. In the crosslinked one, at the high percentage of chain extender, T_g can not be defined. Because soft segments are shorter, the increasing of hard segments has more effect to physical properties of film.

From thermal stability characterization, linear polyurethanes show a two steps degradation which reflects to phase separation of soft and hard segments. The phase separation in films with chain extender is clearer than in film without chain extender. While crosslinked polyurethanes show a one step degradation of phase mixing. However, when the soft segments are shorter or at high percentage of chain extender, the degradation of hard segments of triisocyanate and chain extender becomes observed as shoulder in DTA curve. Nevertheless, T_{max} of polyurethane films are not different, even at the 60% mol of chain extender. It means that pyrrole derivative chain extender do not change the global thermal stability of polyurethane films.

The electropolymerization of pyrrole unit in the polyurethane structure in aqueous solution shows the possibility to prepare the conducting composite using polyurethane as matrix polymer. The cyclic voltammetry of electropolymerization of Py and doping-dedoping curve of PPy recorded on glassy carbon confirms the formation of PPy on polyurethane films.

References

1. J.C.C. Yu, E.P.C. Lai, *Reactive & Functional Polymers* 66 (2006) 702.
2. S.Y. Feng, E.P.C. Lai, E. Dabek-Zlotorzynska, S. Sadehi, *J. Chromatogr. A* 1027 (1-2) (2004) 155.
3. X. Zhu, J. Yang, Q. Su, J. Cai, Y. Gao, *J. Chromatogr. A* 1092 (2005) 161.
4. G. Wuff, *Chem. Rev.* 102 (2002) 1.
5. B.S Ebarvia, S. Cabanilla, F. Seville III, *Talanta* 66 (2005) 145.
6. H. Lee, J. Hong, *J. Chromatogr. A* 868 (2000) 189.
7. J. Huang, Z. Wei, J. Chen, *Sens. Actuators B* 134 (2008) 573.
8. A. Boyls, E.M. Genies, M. Lapkowski, *Synth. Met.* 28 (1989) C769.
9. L.Y. Chaing, L. Y. Wang, C;S. Kuo, J.G. Lin, C.Y. Huang, *Synth. Met* 84 (1997) 721.
10. E. Ruckenstein, Y. Sun, *Synth. Met.* 75 (1995) 79.
11. X. Bi, Q. Pei, *Synth. Met.* 22 (1987) 145.
12. K. Sreenivasan, *Anal. Chim. Acta* 583 (2007) 284.
13. P.A. Lieberzeit, A. Afzal, D. Podlipna, S. Krassing, H. Blumenstock, F.L. Dickert, *Sens. Actuators B* 126 (2007)153.
14. F. Lallemand, D. Auguste, C. Amato, L. Hevesi, J. Delhalle, Z. Mekhalif, *Electrochimica Acta* 52 (2007) 4334.
15. N.M.K. Lamba, K. A. Woodhouse, *Polyurethane in biomedical applications*, CRC Press, Florida, 1998.
16. G. Woods, *The ICI polyurethane book*, 2nd ed., ICI Polyurethane and John Wiley & Sons, Netherlands, 1990.
17. J.Y. Bae, D.J. Chung J. H. An, *J. Mater. Sci.* 34 (1999) 2523.
18. R. C. S. Araujo, V. M. D. Pasa, *J. Appl. Polym. Sci.* 88 (2003) 759.
19. P. Pissis, A. Kanapitsas, Y.V. Savelyev, E.R. Akhranovich, E.G. Privalko, V.P. Privalko, *Polymer* 39 (1998) 3431.
20. Y.V. Savelyev, E.R. Akhranovich, A.P. Grekov, E.G. Privalko, V .V. Korskanov, V.I Shtompel, V.P. Privalko, P. Pissis, A. Kanapitsas, *Polymer* 39 (1998) 3431.

21. T. Quiroz, D. Corona, A. Covarruvias, J.G. Avila-Zarraga, M. R-Ortega, *Tetrahedron Lett.* 48 (2007) 1571.
22. N. Kebir, G. Morandi, I. Campistron, A. Laguerre, J.-F. Pilard, *Polymer* 46 (2005) 6844.
23. N. Kebir, I. Campistron, A. Laguerre, J.-F. Pilard, C. Bunel, J.-P. Couvercelle, C. Gondard, *Polymer* 46 (2005) 6869.
24. L.M. Martins, J.C. Lacroix, K.I. Chane-Ching, A. Adenier, L.M. Abrantes, P.C. Lacaze, J. *Electroanal. Chem.* 587 (2006) 67-78.

General conclusion

In this study, new conducting composites of polyisoprene based polyurethanes were prepared through well defined conducting polymer imprinting on the polyurethane surface.

In order to use the renewable source material, in this work, hydroxyl telechelic cis-1,4-polyisoprene obtained by chain-end carbonyltelechelic cis-1,4-oligoisoprene (CTPI) reduction was chosen to be used as the precursor for polyurethane synthesis. Various chain modifications (hydrogenation and different percentages of epoxidation) allow to prepare different precursors for polyurethane synthesis.

The study of ionic liquid incorporation in polyurethane allows us to conclude that the miscibility of ionic liquid with such a polymer is influenced by the microstructure of ionic liquid. Thus hydrocarbon chain consisting [thtdp]Cl presents higher miscibility with polyisoprene based polyurethane than [bmim]PF₆, and acts as plasticizer. Decreasing of T_g together with increasing proportion of [thtdp]Cl in films is observed, while T_g of polyurethanes was not modified as incorporated with [bmim]PF₆ due to its partial miscibility with the host polymer. Moreover, an ionic liquid migration to the surface was demonstrated over 10%wt of [bmim]PF₆ incorporation. The amount of ionic liquid can be increased when polyurethane films were epoxidized. However, polymers thermal stability decreases as incorporated ionic liquid increases due to cationic epoxide units degradation.

The conductivity of ionic liquid polyurethanes increases as the proportion of incorporated ionic liquid increases. For example, in 80% epoxidized films, conductivity increases from 10⁻¹⁴-10⁻¹⁵ S/cm to 10⁻⁹ S/cm with 30%wt [bmim]PF₆ and to 10⁻⁸ S/cm with 59%wt [thtdp]Cl incorporation. However, amount of ionic liquid incorporation depends on miscibility in the case of [bmim]PF₆, and mechanical properties fail as using [thtdp]Cl ionic liquid. Similar results were obtained from [bmim]PF₆ incorporated polyureas synthesized from butylaminotelechelic cis-1,4-polyisoprene and TDI and I-IPDI. Indeed lower conductivity was observed by comparison with previous coatings though a higher thermal stability was demonstrated.

In addition, composites of polyurethane and conducting polymer were also prepared in this work. The precise imprinting of conductive polyaniline on polyurethane film can be performed by electrochemical polymerization. Thus a dark green polyaniline spot on polyurethane film was observed by microscopy. By SEM analysis of polyurethane/polyaniline

composite prepared in organic medium, there is no surface roughness evolution between polyurethane film and the spot site. This indicated that polyaniline may be formed inside polyurethane film. Moreover, the electropolymerization of thin film on ITO plate demonstrates that preparation of conducting polymer in bulk polyurethane can be performed.

Electropolymerization of Pyrrole and EDOT were also attempted, leading to a thin conducting polymer deposits at the electrode surface. In order to get a good imprinting in the polyurethane bulk, specific 2-(3-(1*H*-pyrrol-1-yl)propyl)propane-1,3-diol chain extender was used during polyurethane synthesis. It was found that global thermal properties of polyurethane films are not modified by the presence of this kind of chain extender. Electrochemical polymerization of pyrrole in the polyurethane bulk was then performed as confirmed by the study of the polypyrrole doping and dedoping processes.

Finally, with the concept of molecular imprinting polymer, perspective work which can be further done is synthesis of chain extenders containing special side groups, such as organic molecules recognition groups. By using these kinds of chain extenders in polyurethane synthesis, polyurethane films containing specific groups will be obtained and it can be used in sensor applications for detection or separation of bioorganic molecules.

Experimental Part

1. Chemical products

1.1. Polymer:

Cis-1,4-polyisoprene (80% cis, $\overline{M}_w = 800,000$, Acros Organics)

1.2. Monomers:

- Aniline (C₆H₇N, Aldrich, AR grade)
- Pyrrole (C₄H₅N, 99%, Acros Organics) was distilled under inert atmosphere and kept in refrigerator.
- 3,4-ethylene dioxythiophene (EDOT, C₆H₆O₂S, Aldrich)

1.3. Solvents

Dichloromethane (CH₂Cl₂), chloroform (CHCl₃), methanol (CH₃OH), ethanol (CH₃CH₂OH), ethyl acetate (CH₃CH₂CO₂CH₃), acetone (CH₃COCH₃), water (H₂O) were used after distillation. Tetrahydrofuran was used after distillation under nitrogen atmosphere in presence of Na/benzophenone.

1.4. Reagents

Reagents following were distilled before use:

- 1,3-dibromopropane (C₃H₆Br₂, pur, Serlabo)
- Triethylamine (C₆H₁₅N, Aldrich)

Reagents following were used without further purification:

- *meta*-chloroperbenzoic acid, *m*-CPBA (C₇H₅ClO₃, 77%, Aldrich)
- Sodium borohydride (NaBH₄, 99%, Acros Organics)
- Periodic acid (H₅IO₆, Acros Organics, 99+%)
- Palladium on activated carbon (10 %, Acros Organics)
- Butylamine (C₄H₉NH₂, 99%, Janssen Chimica)
- Sodium triacetoxyborohydride (C₆H₁₀BNaO₆), 97%, Acros Organics)
- Methanesulfonyl chloride or mesyl chloride (CH₃ClO₂S, 99.5%, Acros Organics)
- Acetic acid (CH₃COOH, glacial, Acros Organics)
- Toluene-2,4-diisocyanate, TDI (C₉H₆N₂O₂, 80%, Janssen Chimica)

- Dibutyltin dilaurate, DBTL ($[\text{CH}_3(\text{CH}_2)_{10}\text{CO}_2]_2\text{Sn}[(\text{CH}_2)_3\text{CH}_3]_2$, 95%, Aldrich)
- Isocyanurate of isophone diisocyanate, I-IPDI (VESTANAT[®] 1890/100, Degussa-Hüls, $\overline{M}_n = 825$ g/mol, 16% NCO (w/w), \overline{f}_w (NCO) = 3.43)
- 1-butyl- 3-methylimidazolium hexafluorophosphate ($\text{C}_8\text{H}_{15}\text{F}_6\text{N}_2\text{P}$, Fluka)
- trihexyltetradecylphosphonium chloride ($\text{C}_{32}\text{H}_{68}\text{ClP}$, Fluka)
- Hydrochloric acid (HCl, 37%, Aldrich,)
- Ammonium persulfate ($(\text{NH}_4)_2\text{S}_2\text{O}_8$, 98+%, Acros Organics)
- Diethyl malonate ($\text{CH}_2(\text{CO}_2\text{C}_2\text{H}_5)_2$, 99%, Avocado)
- Sodium hydride (NaH, 95%, Aldrich)
- Lithium aluminum hydride (LiAlH_4 , 95%, Aldrich)
- Tetrabutylammonium tetrafluoroborate (Bu_4NBF_4 , $\geq 99.0\%$, Fluka)
- Potassium tert-butyrate ($\text{C}_4\text{H}_9\text{OK}$, 95%, Acros Organic)
- Lithium perchlorate (LiClO_4 , 99%, Acros Organic)

1.5. Other reagents

- Potassium carbonate (K_2CO_3 , 97%, Prolabo)
- Sodium hydroxide (NaOH, Acros Organics)
- Sodium chloride (NaCl)
- Sodium bicarbonate (NaHCO_3 , Prolabo)
- Sodium thiosulfate ($\text{Na}_2\text{S}_2\text{O}_3$, 98.5%, Acros Organics)
- Magnesium sulfate (MgSO_4 , Fisher Chemicals, 99.7%)
- Silica gel size 40-63 μm (SiO_2)

2. Materials and instruments

2.1. Nuclear Magnetic Resonance (NMR)

NMR spectra were recorded on Bruker 400 Fourier Transform spectrometer at 400.13 MHz for ^1H NMR and at 100.62 MHz for ^{13}C NMR. Chemical shifts are reported in part per million (ppm) down field from the singlet peak of tetramethylsilane (TMS) using as internal reference.

2.2. Size Exclusive Chromatography (SEC)

Number average molecular weight, weight average molecular weight and polydispersity of different samples were measured by Size Exclusive Chromatography on system equipped with Spectra SYSTEM AS1000 autosampler, with a guard column (Polymer Laboratories, PL gel 5 μm Guard, 50x7.5mm) followed by two columns (Polymer Laboratories; 2 PL gel 5 μm MIXED-D columns, 2x300x7.5 mm) and two detectors of SpectraSYSTEM RI-150 and Spectra SYSTEM UV 2000. Tetrahydrofuran was used as eluent with flow rate 1mL/min at 35°C. Polystyrene standards (580-483 x 10³ g/mol) were used to calibrate the SEC. Polystyrene standardized weights, named PS eq., were corrected by the Benoit factor, $\overline{M}_{nSEC} PI = 0.67 \times \overline{M}_{nSEC} PS$.

2.3. Fourier Transform Infrared spectroscopy (FTIR)

IR spectra were recorded on a FTIR Spectrophotometer (Nicolet AVATAR), equipped with a diamond ATR device (attenuated total reflection). Spectra were obtained from 100 scans (solid mode) and 50 scans (liquid mode) between 4000 and 500 cm^{-1} .

The transmission mode was also used to characterize liquid samples by placing sample between two pellets of KBr.

2.4. Differential Scanning Calorimetry (DSC)

Thermal transition of samples was measured by DSC Q100 (TA Instrument) Differential Scanning Calorimeter equipped with the cooling system that temperature can be decrease to -90°C. Samples were put in the aluminium capsule and empty capsule was used as inert reference. The sample and reference are enclosed in the same furnace. The sample and reference crucible are linked by good heat-flow path. The difference in energy required to maintain them at nearly identical temperature is provided by the heat change in the sample.

The calibration in temperature and energy was carried out with a standard Indium :

$$T_f = 156.6^\circ\text{C}$$

$$\Delta H_f = 28.45 \text{ J/g}$$

All experiments were carried out under nitrogen atmosphere at flow rate 50 mL/min with weight of sample 5 to 10 mg. Two scans from -85 to 150°C were performed with a heating and cooling rate of 10°C/min. The condition of the experiment is:

- Isothermal at -85°C during 1 min
- Heating from -85°C to 150°C with the heating rate 10°C/min
- Cooling from 150°C to -85°C with cooling rate 10°C/min
- Reheating from -85°C to 150°C with heating rate 10°C/min

2.5. Thermogravimetric analysis (TGA)

With thermogravimetric analysis (TGA) the mass of the sample is recorded continuously while the temperature is increased at the constant rate. Weight loss occurs when volatiles absorbed by the polymer are driven off and at higher temperature when degradation of the polymer occurs with the formation of volatile products¹.

Thermal degradation of polyurethane films was measured by TGA Q500 (TA Instrument). The instrument is composed of a high-precision balance with a platinum pan that is placed in a small furnace with a thermocouple to accurately give the temperature.

All experiments were done under nitrogen atmosphere at the flow rate 90 mL/min with sample weight 15 to 20 mg. Samples were heated from room temperature to 600°C with rate 10°C/min. and the weight loss was recorded.

2.6. Dielectric relaxation spectroscopy (DRS)

Dielectric spectroscopy (sometimes called impedance spectroscopy) measures the dielectric properties of a medium as a function of frequency². It is based on the interaction of an external field with the electric dipole moment of the sample, often expressed by permittivity.

The method of DRS allows investigating the conductivity mechanism on the basis of measurements of dielectric parameters of the conducting polymers³.

The application of electric field provokes the fluctuation of electrical polarization and this leads to the electrical displacement. The displacement depends on the material polarization. Dielectric polarization arises due to the existence of atomic and molecular forces, and appears whenever charges in a material are somewhat displaced with respect to one another under influence of an electric field⁴.

Dielectric permittivity measurements were performed using Novocontrol broadband dielectric spectrometer (Novocontrol GmbH, Germany) (Fig 1) in wide frequency (0.1 Hz to 1 GHz) and temperature (173 to 423 K) ranges. The spectrometer consists in the following parts:

- Impedance analyzer SOLARTRON SI 12690
- Impedance analyzer HP 4291A
- Dielectric converter NOVOCONTROL
- Temperature controller NOVOCONTROL Quatro cryosystem
- Cryostat
- Sample cell

In our study, we measured at the low frequency, 0.1 Hz up to 10 MHz; a SALARTON SI 1260 analyzer combined with a broadband dielectric converter allows impedance and dielectric measurements.

The polymer film was put between two round parallel golden electrodes as shown in Fig 2.

The dielectric analysis was chosen to calculate dielectric parameters (dielectric constant, imaginary and real permittivity, conductivity, relaxation time, etc). Processing the experiment dielectric spectra was made by mean of WinFit 2.4(1996) software GmbH (Germany).

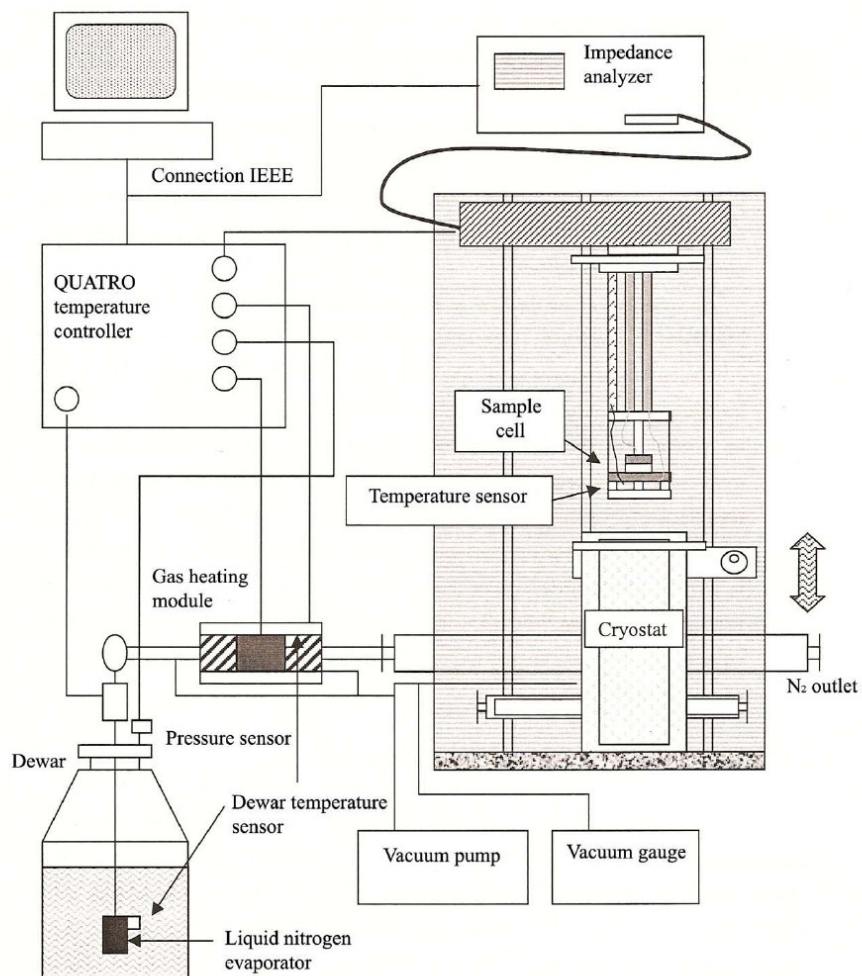


Fig 1 Schematic representation of the dielectric spectrometer⁵.



Fig 2 Sample cell for dielectric measurements.

2.7. Thickness measurement of polyurethane thin film.

Thickness measurements of PU film on ITO plate were carried out by spectral interferometry in white light. The interferograms were recorded with RAMAN T400 in micro-Raman configuration with X50 objective lens. The optical thickness, $n \times e$, was determined from the numerical analysis of profile of interferogram curve. The thickness was then deduced from optical index value.

For PU, $n = 1.575 + 8725 \times \sigma^{-2}$, where σ is wavenumber (nm^{-1})

2.8. Potentiostat/Galvanostat

Electrochemical experiments were performed in three-electrodes cell constituted by a platinum disk ($\varnothing = 1 \text{ mm}$) or glassy carbon ($\varnothing = 2 \text{ mm}$) as working electrode, platinum wire as counter electrode and a silver wire immersed in a 0.1 M AgNO_3 acetonitrile solution or a saturated calomel used as reference electrode as shown in Fig 3. The cell was connected to VMP PAR model VMP2/Z-40 Potentiostat/Galvanostat (Priceton Applied Research) monitored by ECLab software.

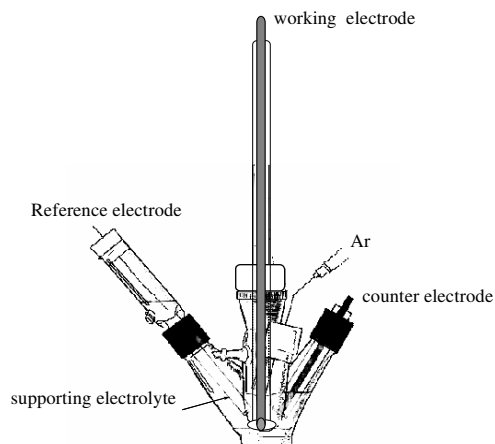


Fig 3 A single-compartment three-electrode cell.

3. Synthesis of precursors of polyurethane.

3.1. Controlled degradation of cis-1,4-polyisoprene 1

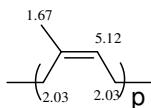
This reaction was done in 2 steps; the reaction of epoxidation of carbon-carbon double bond followed by a step of oxidative cleavage. The oxidation is promoted by periodic acid.

3.1.1. Synthesis of epoxidized cis-1,4-polyisoprene (EPI) 2

Cis-1,4-polyisoprene was purified by dissolving in dichloromethane (20 g PI in 500 mL CH₂Cl₂) and then precipitated in methanol 800 mL.

Characterization :

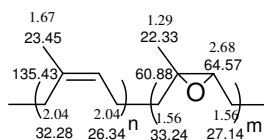
¹H NMR



For the synthesis of epoxidized cis-1,4-polyisoprene, *m*-CPBA 3.60 g (16.1 mmol, 5%epoxidation) in 150mL of CH₂Cl₂ were dropwised into a solution of cis-1,4-polyisoprene 21.77 g (316.4 mmol) in 450 mL of CH₂Cl₂ in a jacketed reactor cooled at 0°C. The reaction was performed for 6 h. Then the reaction solution was washed with saturated NaHCO₃ and NaCl aqueous solution, respectively. The epoxidized cis-1,4-polyisoprene was precipitated in 800 mL ethanol and dried under vacuum until constant weight. Yield = 93-97%

Characterization :

¹H and ¹³C NMR:



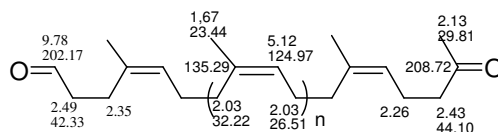
FTIR : $\nu_{C=CH_2} = 3035 \text{ cm}^{-1}$, $\nu_{CH_2,CH_3} = 2900-2730 \text{ cm}^{-1}$, $\nu_{C=C} = 1664 \text{ cm}^{-1}$,
 $\nu_{CH_2,CH_3,cis-1,4-isoprene} = 1440, 1375 \text{ cm}^{-1}$, $\delta_{=C-H} = 834 \text{ cm}^{-1}$, $\delta_{C-O(epoxide)} = 870 \text{ cm}^{-1}$.

3.1.2. Synthesis of carbonyltelechelic cis-1,4-polyisoprene (CTPI) 3

Purified epoxidized cis-1,4-polyisoprene (EPI) 22.32 g (338.9 mmol) was dissolved in 400 mL of THF and periodic acid 4.13 g (18.1mmol) in 10 mL of THF was dropwised in a jacketed reactor at 30°C (reaction time : 6 h). The solution was filtered and solvent was then evaporated. After that, product was dissolved in CH₂Cl₂ (200 mL) and washed with saturated NaHCO₃ and Na₂S₂O₃ aqueous solutions. The organic phase was collected and dried over MgSO₄. The solution was filtered and solvent was evaporated to obtain the yellow viscous liquid. The product was dried under vacuum at 40°C until constant weight. Yield = 88-94%

Characterization :

¹H and ¹³C NMR:



FTIR : $\nu_{C=CH_2} = 3035 \text{ cm}^{-1}$, $\nu_{CH_2,CH_3} = 2900-2730 \text{ cm}^{-1}$, $\nu_{C=O} = 1720 \text{ cm}^{-1}$, $\nu_{C=C} = 1664 \text{ cm}^{-1}$,
 $\nu_{CH_2,CH_3, \text{cis-1,4-isoprene}} = 1440, 1375 \text{ cm}^{-1}$, $\delta_{C-H} = 834 \text{ cm}^{-1}$

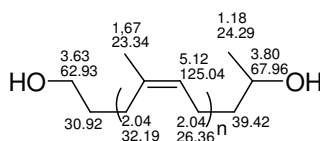
SEC : $\overline{M}_n = 1690 \text{ g/mol}$, $I_p = 1.9$.

3.2. Synthesis of hydroxytelechelic cis-1,4-polyisoprene (HTPI) 4

Sodium borohydride 1.93 g (51.1 mmol) in 10 mL THF was charged into a three-necked round bottom flask equipped with a condenser. Carbonyltelechelic cis-1,4-polyisoprene (CTPI) 8.00 g (4.62 mmol) in 40 mL THF was dropwised into the round bottom flask. Then the reaction was performed at 60°C for 6 h. The reaction solution was cooled down to room temperature. 20g of ice in THF 30 mL was then dropwised into solution. After that, solution was washed with saturated NaCl aqueous solution. The organic phase was collected and dried over MgSO₄. The solution was filtered and solvent was evaporated to obtain light yellow viscous liquid with yielding 89-95 %.

Characterization :

^1H and ^{13}C NMR:



FTIR : $\nu_{\text{OH}} = 3350 \text{ cm}^{-1}$, $\nu_{\text{C}=\text{CH}_2} = 3035 \text{ cm}^{-1}$, $\nu_{\text{CH}_2, \text{CH}_3} = 2900\text{-}2730 \text{ cm}^{-1}$, $\nu_{\text{C}=\text{C}} = 1664 \text{ cm}^{-1}$,
 $\nu_{\text{CH}_2, \text{CH}_3, \text{cis-1,4-isoprene}} = 1440, 1375 \text{ cm}^{-1}$, $\delta_{\text{C}-\text{H}} = 834 \text{ cm}^{-1}$.

Peak $\nu_{\text{C}=\text{O}}$ at 1720 cm^{-1} is disappeared.

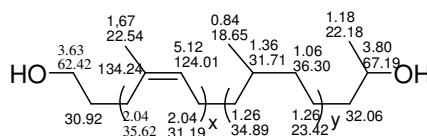
SEC : $\overline{M}_n = 1900 \text{ g/mol}$, $I_p = 1.7$.

3.3. Synthesis of hydrogenated hydroxytelechelic cis-1,4-polyisoprene (HHTPI) 5

Hydroxytelechelic cis-1,4-polyisoprene (HTPI) 1.22 g (0.76 mmol) and palladium (10% on carbon) 791 mg were dissolved in 60 mL of ethyl acetate. Then, solution was introduced to hydrogenation device and shaken under 4.2 bars of hydrogen pressure at room temperature. After shaking for 24 h., pressure dropped to 3.4 bars. The reaction mixture was filtered to remove the catalyst. The solvent was removed under reduced pressure to give light yellow viscous liquid with yielding 67% (hydrogenation 83%).

Characterization :

^1H and ^{13}C NMR:



FTIR : $\nu_{OH} = 3350 \text{ cm}^{-1}$, $\nu_{CH_2,CH_3} = 2900-2730 \text{ cm}^{-1}$, $\nu_{CH_2,CH_3, \text{cis-1,4-isoprene}} = 1440, 1375 \text{ cm}^{-1}$.

Peak of ethylenic double bond, ν_{-CH_2} (3035 cm^{-1}), $\nu_{C=C}$ (1664 cm^{-1}) and δ_{-C-H} (834 cm^{-1}) are disappeared.

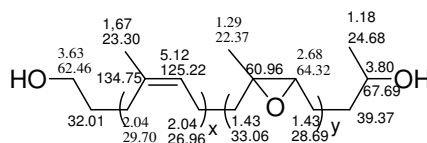
SEC : $\overline{M}_n = 1800 \text{ g/mol}$, $I_p = 1.8$.

3.4. Synthesis of epoxidized hydroxytelechelic cis-1,4-polyisoprene (EHTPI) 6

Hydroxytelechelic cis-1,4-polyisoprene (HTPI) 6.00 g (3.3 mmol) was dissolved with 15 mL of CH_2Cl_2 in three-necked round bottom flask. Subsequently, 0.3 M *m*-CPBA (13.88 g, 80% epoxidized, 9.89g, 58% epoxidized or 6.10 g, 30 % epoxidized) in CH_2Cl_2 solution was added dropwise into the reaction solution at 0°C and solution was stirred at this temperature for 3 h. The solution was filtered and washed with saturated NaHCO_3 aqueous solution two times. Then, solution was dried with MgSO_4 . Finally, the solvent was evaporate under reduced pressure and dried under vacuum until weight constant. Yield was 89%.

Characterization :

^1H and ^{13}C NMR:



FTIR : $\nu_{OH} = 3350 \text{ cm}^{-1}$, $\nu_{CH_2,CH_3} = 2900-2730 \text{ cm}^{-1}$, $\nu_{CH_2,CH_3, \text{cis-1,4-isoprene}} = 1440, 1375 \text{ cm}^{-1}$,
 $\nu_{C-O(\text{epoxide})} = 870 \text{ cm}^{-1}$.

Decreasing of peaks at 3035 cm^{-1} (ν_{-CH_2}), 1664 cm^{-1} ($\nu_{C=C}$) and 834 cm^{-1} (δ_{-C-H}) as percentage of epoxidation increases.

SEC : EHTPI (30%), $\overline{M}_n = 2190 \text{ g/mol}$, $I_p = 2.0$.

EHTPI (58%), $\overline{M}_n = 2210 \text{ g/mol}$, $I_p = 2.0$.

EHTPI (80%), $\overline{M}_n = 2220 \text{ g/mol}$, $I_p = 2.0$.

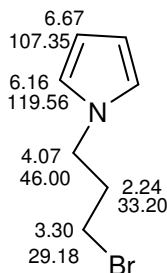
3.5. Synthesis of pyrrole derivative chain extender

3.5.1. Synthesis of 1-(3-bromopropyl)-1H-pyrrole 9

Potassium tert-butyrate 8.45 g (71.6 mmol) was dissolved in anhydrous THF 30 mL under inert atmosphere in three-necked round bottom flask equipped with a condenser. The solution was stirred at room temperature for 30 min. Then, pyrrole 4.0 mL (57.6 mmol) in 10 mL anhydrous THF solution was slowly injected into the reaction solution at 0°C and the solution was stirred at this temperature for 1 h. After that, 20 mL of 1,3-bromopropane (197 mmol) in 5 mL of anhydrous THF was slowly added into solution at 0°C. The solution was stirred at 0°C for 1 h and 40°C for 24 h. The solution was added with 50 mL of ether and then washed with distilled water three times. The aqueous phase was extracted again with CH₂Cl₂. Organic phase was collected and dried with MgSO₄. The solvent was removed under reduced pressure. Crude product was purified with column chromatography (silica gel, Petroleum ether: diethyl ether = 98:2). The final product is red-brown liquid. Yield was 40%

Characterization :

¹H and ¹³C NMR:



FTIR: $\nu_{CH_2} = 2900-2700 \text{ cm}^{-1}$, $\nu_{C=C} = 1500 \text{ cm}^{-1}$, $\nu_{C-C} = 1440 \text{ cm}^{-1}$, $\nu_{C-N(tert)} = 1370$,
 $\nu_{C-N(py)} = 1100-1050 \text{ cm}^{-1}$, $\nu_{C-Br} = 565 \text{ cm}^{-1}$.

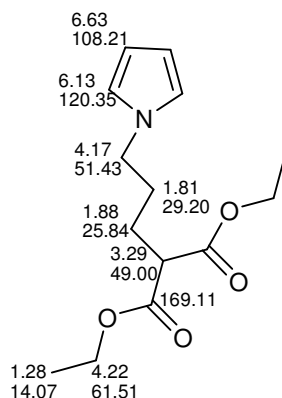
3.5.2. Synthesis of diethyl 2-(3-(1H-pyrrol-1-yl)propyl)malonate 10

Sodium hydride 0.22 g (8.73 mmol) was dissolved with 15 mL of anhydrous THF in three-necked round bottom flask fitted with a condenser under nitrogen atmosphere. The solution was stirred at room temperature for 30 min, and solution of diethylmalonate 0.60 mL (6.58 mmol) in 10 mL of anhydrous THF was then added slowly into the reaction solution. The

solution was stirred at this temperature for 1 h. After that, solution of 1-pyrrole-3-bromopropane 0.95 g (5.06 mmol) in anhydrous THF was slowly added dropwise into the reaction solution and then solution was stirred at room temperature for 1 h and 50°C for 24 h. The reaction solution was cooled down to the room temperature and ether 30 mL was added into solution. The reaction solution was washed with 5 mL of distilled water 3 times and saturated NaCl aqueous solution one time. Aqueous phase was extracted with CH₂Cl₂ 2-3 times. The organic phase was dried with MgSO₄ and the solvent was evaporated under reduced pressure; dark brown liquid crude product was obtained. Then, it was purified by column chromatography (silica gel, cyclohexane : diethyl ether = 6:4). The solvent was evaporated; brown liquid was obtained with yielding 66%.

Characterization :

¹H and ¹³C NMR:



MS (m/z): 268.

Elemental analysis: Calculated : %C = 62.9, %H = 7.9%, %N = 5.2, %O = 23.9;

Found : %C = 61.9, %H = 7.6%, %N = 4.9, %O = 24.2.

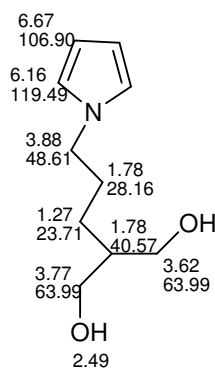
FTIR : $\nu_{CH_2} = 2900-2700\text{ cm}^{-1}$, $\nu_{C=O} = 1730\text{ cm}^{-1}$, $\nu_{C=C} = 1500\text{ cm}^{-1}$, $\nu_{C-C} = 1440\text{ cm}^{-1}$,
 $\nu_{C-N(tert)} = 1370$, $\nu_{C-O} = 1222-1157\text{ cm}^{-1}$, $\nu_{C-N,py} = 1100-1050\text{ cm}^{-1}$.

3.5.3. Synthesis of 2-(3-(1*H*-pyrrol-1-yl)propyl)propane-1,3-diol 11

LiAlH₄ 0.66 g (16.60 mmol) was dissolved with 25 mL of ether in three-necked round bottom flask equipped with a condenser under nitrogen atmosphere. The solution was flushed with N₂ atmosphere for 15 mins. 1-pyrrole-3-diethylmalonate 0.86 g (3.22 mmol) solution in 25 mL ether was injected slowly into reaction solution at room temperature. Then, solution was stirred overnight at this temperature. The remaining LiAlH₄ was hydrolyzed by added water slowly into solution. Then, the reaction solution was washed with saturated NaCl aqueous solution five times. Aqueous phase was extracted two times with CH₂Cl₂. All organic phases were collected and dried over MgSO₄. Solvent was evaporated under reduced pressure, dark brown liquid was obtained. Finally, product was dried in vacuum oven until weight constant. Yield was 61%.

Characterization :

¹H and ¹³C NMR



MS (m/z) : 184.

Elemental analysis: Calculated : %C = 65.5, %H = 9.3%, %N = 7.6, %O = 17.5;

Found : %C = 64.3, %H = 9.2%, %N = 7.5, %O = 17.7.

FTIR : $\nu_{O-H} = 3300 \text{ cm}^{-1}$, $\nu_{CH_2} = 2900-2700 \text{ cm}^{-1}$, $\nu_{C=C} = 1500 \text{ cm}^{-1}$, $\nu_{C-C} = 1440 \text{ cm}^{-1}$,
 $\nu_{C-N(tert)} = 1370$, $\nu_{C-N,Py} = 1100-1050 \text{ cm}^{-1}$, $\nu_{C-O-H} = 1064-1037 \text{ cm}^{-1}$

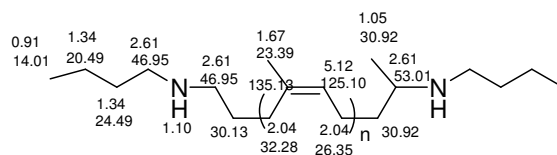
4. Synthesis of precursors for polyureas

4.1. Synthesis of butylaminotelechelic cis-1,4-polyisoprene (PINH) 7

Carbonyltelechelic cis-1,4-polyisoprene 5.0 g (2.77 mmol) was dissolved in 20 mL distilled CH_2Cl_2 in a three-necked round bottom flask equipped with a condenser. Distilled butylamine 0.65 mL (6.58 mmol) in CH_2Cl_2 was injected into the reaction solution under nitrogen atmosphere at room temperature. Sodium triacetoxyborohydride 1.91 g (9.02 mmol) in 75 mL of CH_2Cl_2 and acetic acid 160 μL (2.77 mmol) were then injected into solution. The reaction solution was refluxed under nitrogen atmosphere for 24 h. Then the reaction was washed with 1 N NaOH solution. The aqueous phase was extracted again with ether. Organic phase was dried with MgSO_4 . Solvent was evaporated and light yellow viscous liquid was obtained with yielding 89%

Characterization :

^1H and ^{13}C NMR :



FTIR : $\nu_{\text{CH}_2, \text{CH}_3} = 2900\text{-}2730 \text{ cm}^{-1}$, $\nu_{\text{C}=\text{C}} = 1664 \text{ cm}^{-1}$, $\nu_{\text{CH}_2, \text{CH}_3, \text{cis-1,4-isoprene}} = 1440, 1375 \text{ cm}^{-1}$,
 $\delta_{\text{C-H}} = 834 \text{ cm}^{-1}$.

$\nu_{\text{C=O}} = 1720 \text{ cm}^{-1}$ is disappeared and ν_{NH} is not detected.

SEC: $\overline{M}_n = 1600 \text{ g/mol}$, $I_p = 1.9$.

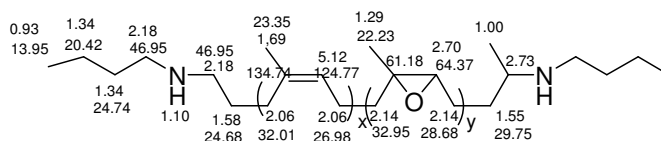
4.2. Synthesis of epoxidized butylaminotelechelic cis-1,4-polyisoprene (EPINH) 8

Butylaminotelechelic cis-1,4-polyisoprene ($\overline{M}_n = 2000 \text{ g/mol}$) 2.07 g dissolved in 15 mL of CH_2Cl_2 was charged into a three-necked round bottom flask fitted with a condenser. *m*-CPBA 3.52 g (16 mmol, 50% epoxidized) in CH_2Cl_2 was then slowly dropwisely into reaction

solution at 0°C. The solution was stirred at this temperature for 4 h. After that, solution was filtered and washed with saturated NaHCO₃ aqueous solution two times. The organic phase was collected and dried with MgSO₄. Solvent was evaporated under reduced pressure. Brown viscous liquid was then dried under vacuum until constant weight. Yield = 82%.

Characterization:

¹H and ¹³C NMR



FTIR : $\nu_{CH_2,CH_3} = 2900-2730\text{ cm}^{-1}$, $\nu_{C=C} = 1664\text{ cm}^{-1}$, $\nu_{CH_2,CH_3,cis-1,4-isoprene} = 1440, 1375\text{ cm}^{-1}$,
 $\delta_{C-H} = 834\text{ cm}^{-1}$, $\nu_{C-O(epoxide)} = 870\text{ cm}^{-1}$.

SEC : $\overline{M}_n = 1430\text{ g/mol}$, $I_p = 2.9$.

5. Preparation of polyurethane films

5.1. Synthesis of polyurethane without chain extender

5.1.1. Synthesis of polyurethane standing films

Polyurethane films were prepared according to the procedure previously described by Kebir et al.^{6,7}. 0.5 g of hydroxytelechelic cis-1,4-polyisoprene ($\overline{M}_n = 2100\text{ g/mol}$) was dissolved in dried THF (0.1g/mL). DBTL and diisocyanate were then added into the solution with ratio of [DBTL]/[OH] = 0.045 and [NCO]/[OH] = 1.2. After stirring for few minutes, the solution was poured into mould and put in desiccator under nitrogen atmosphere for 2 hours and in oven at 60°C for 12 hours.

5.1.2. Preparation of ionic liquid incorporated polyurethane films

An hydroxytelechelic cis-1,4-polyisoprene, or epoxidized hydroxytelechelic cis-1,4-polyisoprene, and different amount of ionic liquid were dissolved in dried THF (0.1 g/mL). DBTL and diisocyanates were added into solution according to previously described method.

The solution was cast in mould and keeps under inert atmosphere for 2 h and dried in oven at 60°C for 12 h.

Films were rinsed with a little amount of acetone to removed non-incorporated ionic liquid. Acetone was evaporated and the amount of incorporated ionic liquid was then calculated.

5.1.3. Preparation of polyurethane coated electrode

An hydroxytelechelic cis-1,4-polyisoprene (or epoxidized hydroxytelechelic cis-1,4-polyisoprene), DBTL and diisocyanate solution prepared according to previous procedure was dropped onto a Pt electrode and put in desiccator under N₂ atmosphere for 2 hours and in oven at 60°C for 12 hours. Finally, films were completely dried in vacuum oven at 50°C overnight.

5.1.4. Preparation of linear polyurethane thin films on ITO plate

In order to form PANI in bulk PU film, PU thin films on ITO plate were prepared by spin coating technique. Solution of hydroxytelechelic cis-1,4-polyisoprene, DBTL and TDI was done according to previously described procedure and solution was then dropped on ITO plate and spin with speed 2000 rpm for 20 seconds. ITO plate was kept under nitrogen atmosphere during 2 hours and then at 60°C for 12 hours.

5.2. Synthesis of polyurethane standing films with chain extender, (2-(3-(1*H*-pyrrol-1-yl)propyl)propane-1,3-diol)

Polyurethane films were synthesized according to method previously described. Different proportion of hydroxytelechelic cis-1,4-polyisoprene and 2-(3-(1*H*-pyrrol-1-yl)propyl)propane-1,3-diol (chain extender) were dissolved in dried THF with the concentration 0.1 g/mL. Then, DBTL was added with [DBTL]/[OH] = 0.045. After that, diisocyanates was added into the solution with [NCO]/[OH] = 1.2. After stirring for few minutes, the solution was pour into mould and put in desiccators under nitrogen atmosphere for 2-3 h and at 60°C overnight.

6. Chemical polymerization of aniline on polyurethane films

Polyurethane films was swelled in aniline monomer for 10 minutes, the excess monomer at surface was rinsed with hexane and wiped with filtered papers. The amount of aniline incorporation was calculated in term swelling degree, α , from weight of film before and after swelling⁵.

$$\alpha = \frac{m - m_0}{m_0} \times 100$$

where m and m_0 are the weight of swelled and non-swelled, respectively.

The swelled polyurethane films then place in the cell (Fig 4) and the cell was filled with oxidant solution, 0.1 M $(\text{NH}_4)_2\text{S}_2\text{O}_8$ in 1.0 M HCl. The reaction was let progress for 20 minutes. Film changes to be green. The solution was taken off from mould and washed with distilled water many times. Film was put in hexane overnight to eliminate remaining monomer. Finally composite film was dried under vacuum until constant weight.



Fig 4 Home-made cell used for obtained one-side surface composite films.

7. Electrochemical experiments

7.1. Electropolymerization of aniline on PU films coated Pt electrode in CH₂Cl₂ solution

Polyurethane coated electrode was immersed in CH₂Cl₂ solution of 0.2 M Bu₄NBF₄. Then, aniline 10 μL was added into solution. Polymerization of aniline on PU film was performed by cyclic voltammetry technique at potential -1 V to +1 V at sweep rate 20mV/s.

7.2. Electropolymerization of aniline on PU standing films in CH₂Cl₂ solution

PU standing film (thickness, $e = 150 \mu\text{m}$) was placed in a reactor containing 10 mL of 0.2 M Bu₄NBF₄ in CH₂Cl₂ solution, then electrode was tightly applied on the elastomeric film. Then, aniline 10 μL was added into the solution ($c = 10 \text{ mM}$), and the electropolymerization of aniline was performed as previously described.

7.3. Electropolymerization of aniline on PU standing films in acid solution

PU standing film was swelled in pure aniline for 10 minutes. The swollen film was placed in the reactor with 1 M HCl and pressed with electrode tightly (surface of electrode well contact with film). Electropolymerization was performed by cyclic potential flow in range 0 to +1.0 V.

7.4. Electropolymerization of aniline on linear PU thin films in acid solution

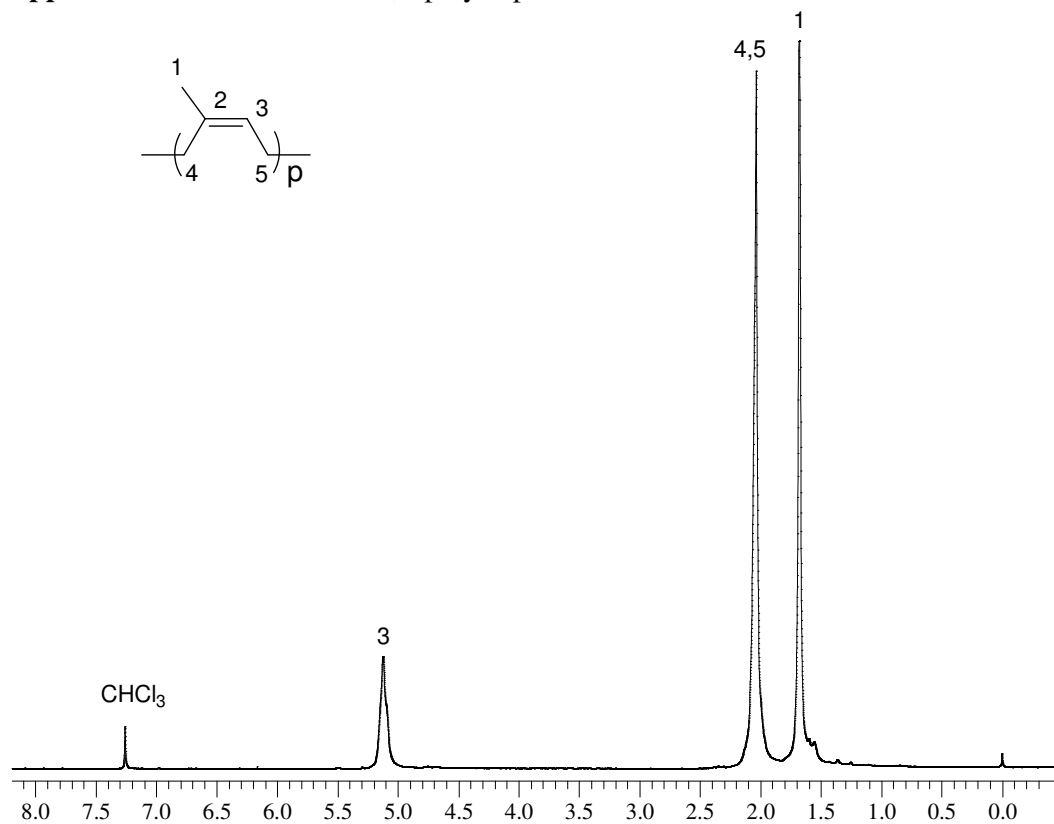
PU thin film on ITO plate (thickness, $e = 1.73 \mu\text{m}$) was installed in a reactor containing 1.0 M HCl. The Pt electrode was applied on film and electropolymerization was performed as previously described.

7.5. Electropolymerization of pyrrole (Py) and 3,4-ethylene dioxythiophene (EDOT) in aqueous solution

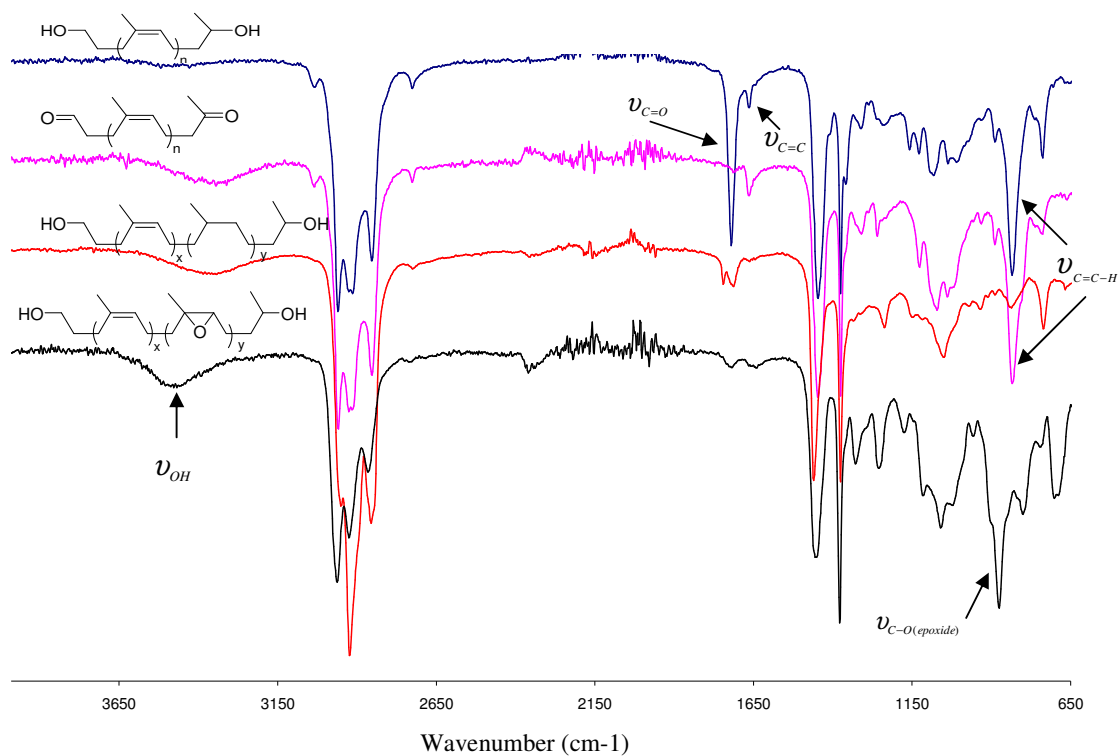
PU standing film with monomer incorporation was put in an electrochemical cell filled with 5 mL of 0.5 M LiClO₄. An electrode was applied tightly on the film. The electropolymerization by cyclic voltammetric technique was performed in the same procedure as aniline in potential range -1.0 V to +1.0 V.

1. Campbell, J.R. White, Polymer Characterization; physical techniques, Chapman and Hall, London, 1989.
2. http://en.wikipedia.org/wiki/Dielectric_spectroscopy, 30 September 2008.
3. N. J. Pinto, P. D. Shah, P. K. Kahol, B. J. McCormick, Solid state communication 97 (1996) 1029.
4. A.K. Jonscher, Dielectric relaxation in solids, Chelsea Dielectrics Press, London, 1983.
5. K. Fatyeyeva, Elaboration and investigation of conducting polymer composites based on polyaniline and polyamide, thesis of Université du Maine, Le Mans , 2005.
6. N. Kebir, G. Morandi, I. Campistron, A. Laguerre, J.-F. Pilard, Polymer 46 (2005) 6844.
7. N. Kebir, I. Campistron, A. Laguerre, J.-F. Pilard, C. Bunel, J.-P. Couvercelle, C. Gondard, Polymer 46 (2005) 6869.

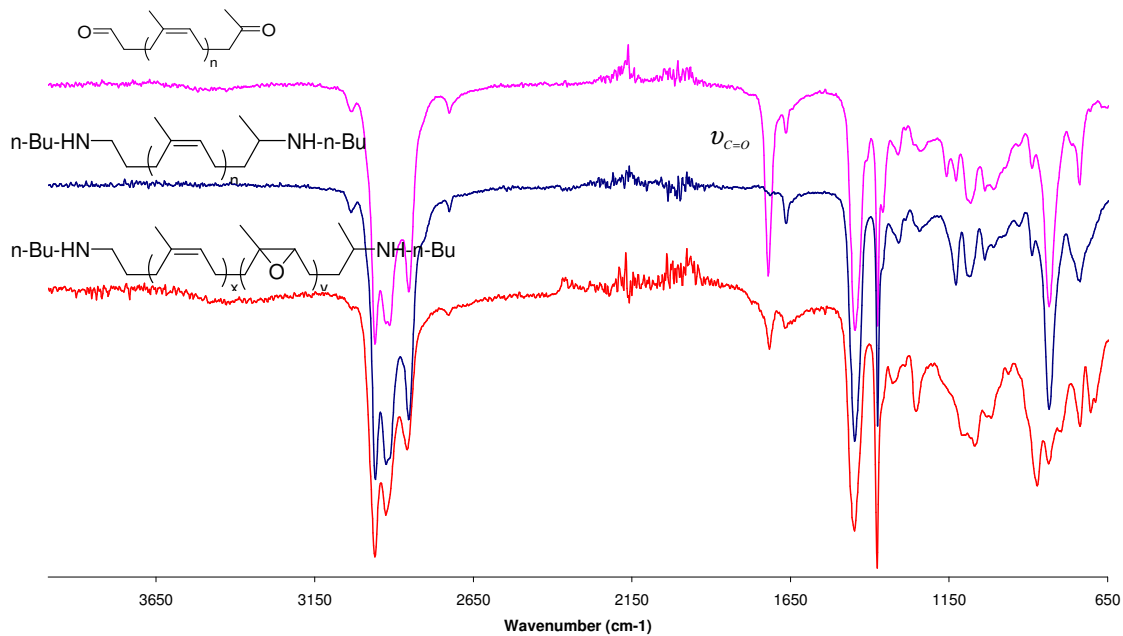
Appendix

Appendix 1.1 ^1H NMR of cis-1,4-polyisoprene

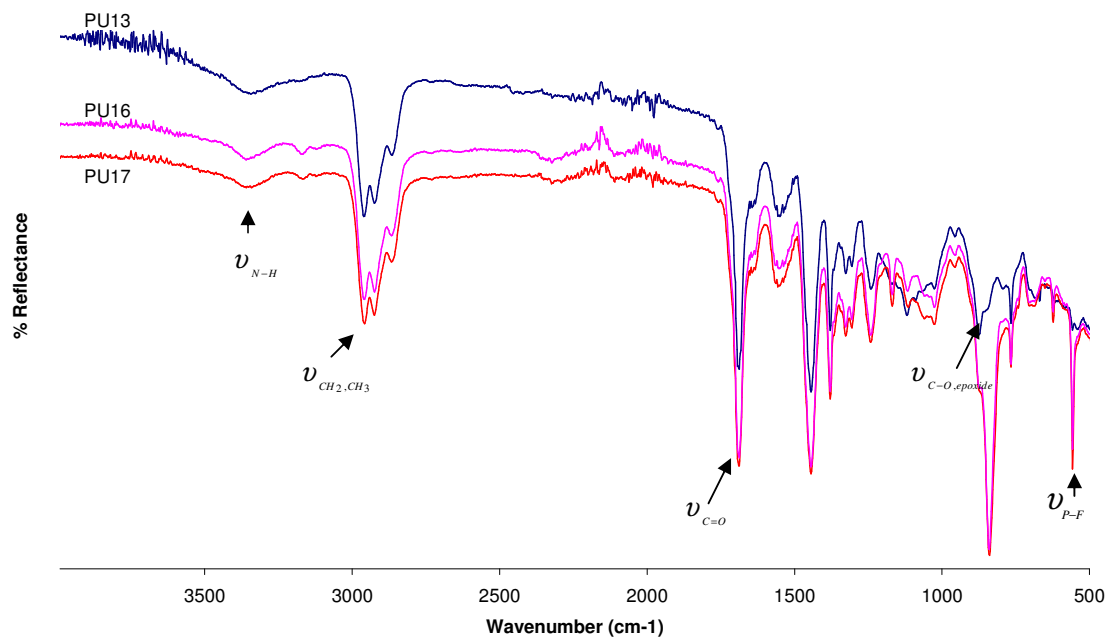
Appendix 1.2 FTIR spectra of carbonyltelechelic cis-1,4-polyisoprene(CTPI), hydroxytelechelic cis-1,4-polyisoprene (HTPI), hydrogenated hydroxytelechelic cis-1,4-polyisoprene (HHTPI) and epoxidized hydroxytelechelic cis-1,4-polyisoprene (EHTPI).



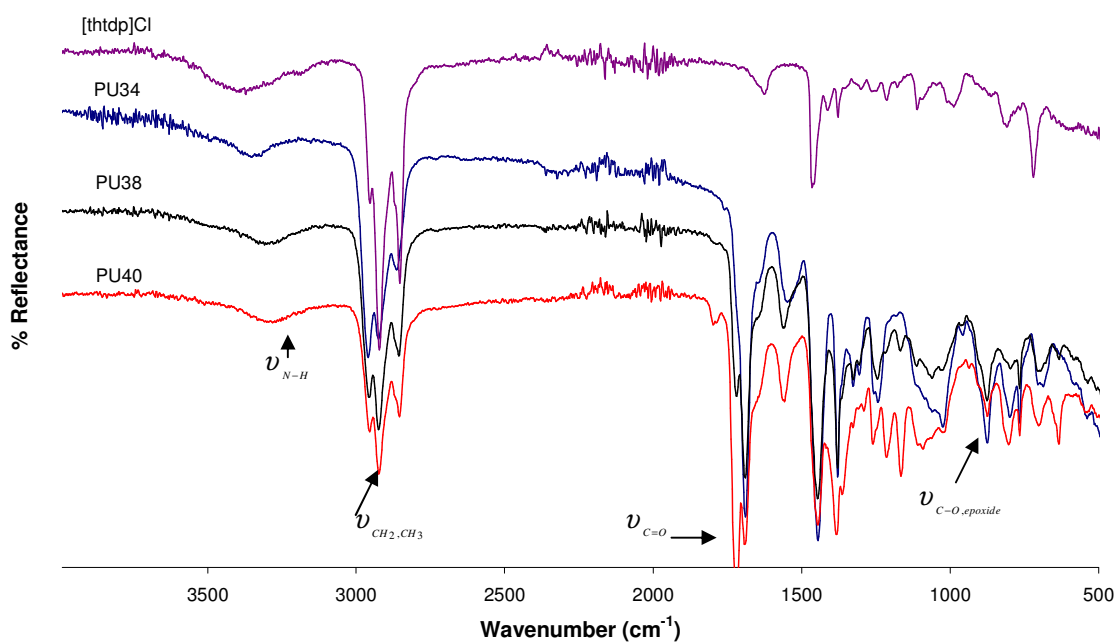
Appendix 1.3 FTIR of butylaminotelechelic and epoxidized butylaminotelechelic cis-1,4-polyisoprene (PINH and EPINH).



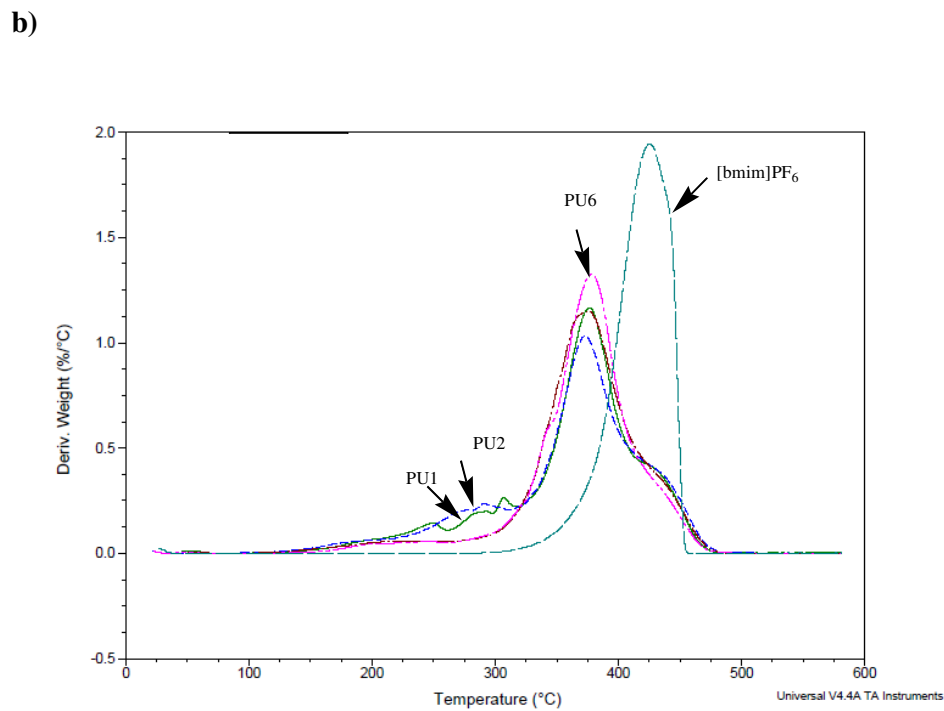
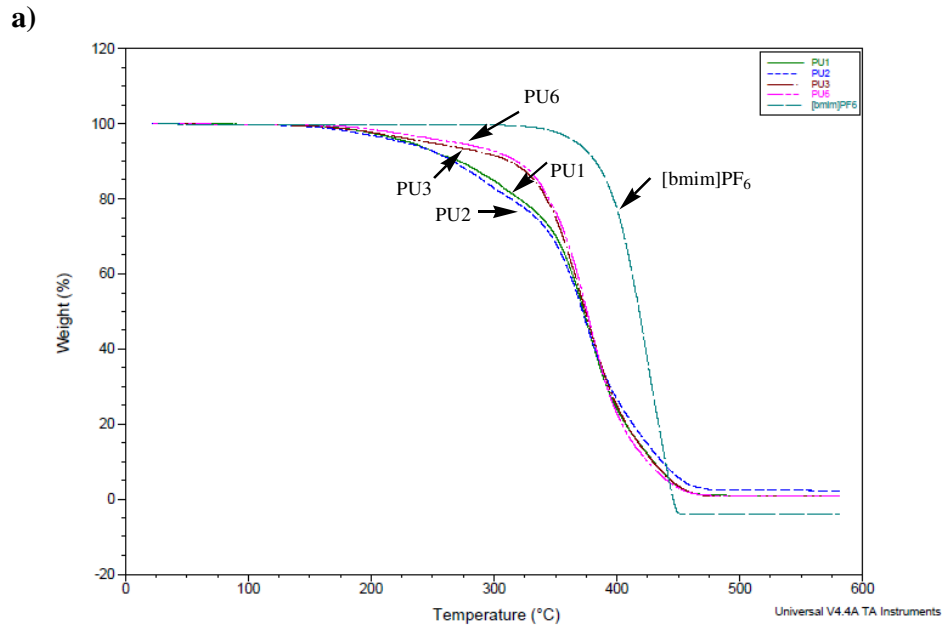
Appendix 2.1 FTIR spectra of crosslinked 80% epoxidized polyurethane with 27% (PU16), 30% (PU17) and without [bmim]PF₆ (PU13).



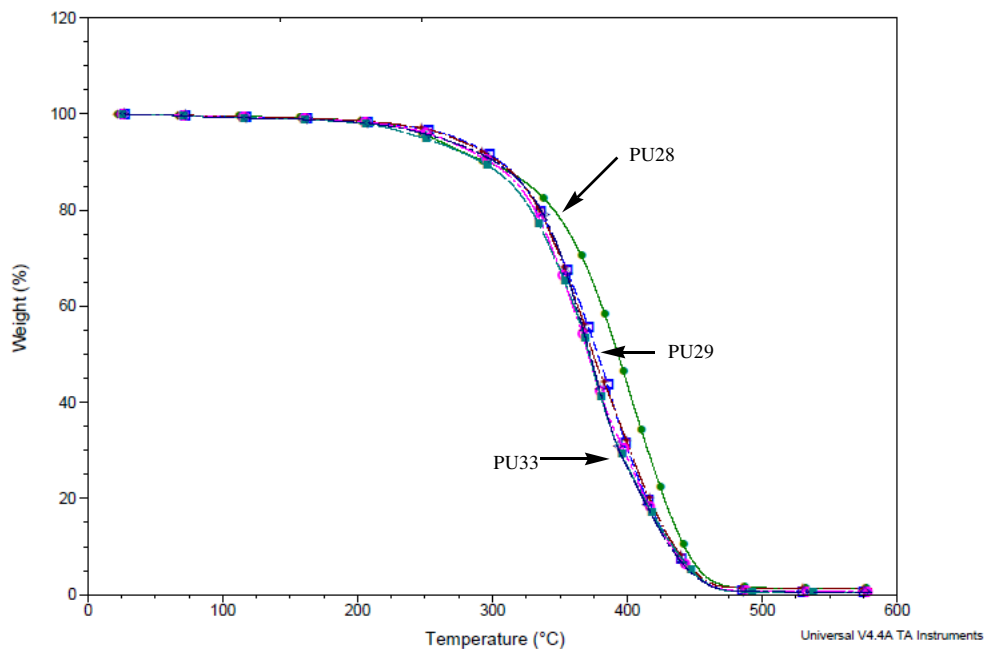
Appendix 2.2 FTIR of [thtdp]Cl, crosslinked 80% epoxidized polyurethane without [thtdp]Cl (PU34), 32% wt. [thtdp]Cl (PU38), 50% wt. [thtdp]Cl (PU40).



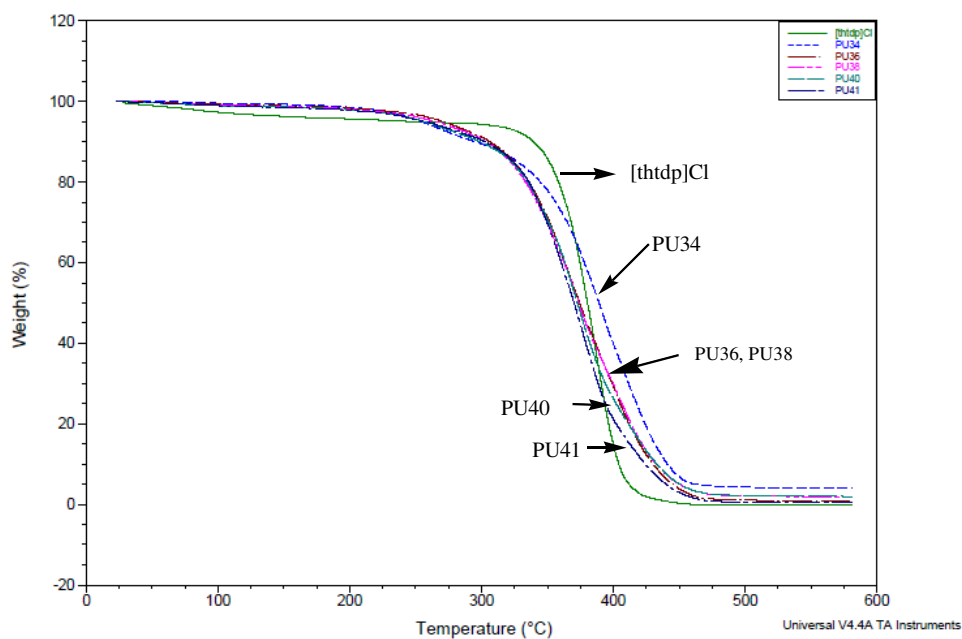
Appendix 2.3 a) TGA thermogram; b) DTG curves of linear polyurethane with 10%wt (PU2); without [bmim]PF₆ (PU1), crosslink polyurethane with 10%wt (PU6) and without [bmim]PF₆ (PU3).



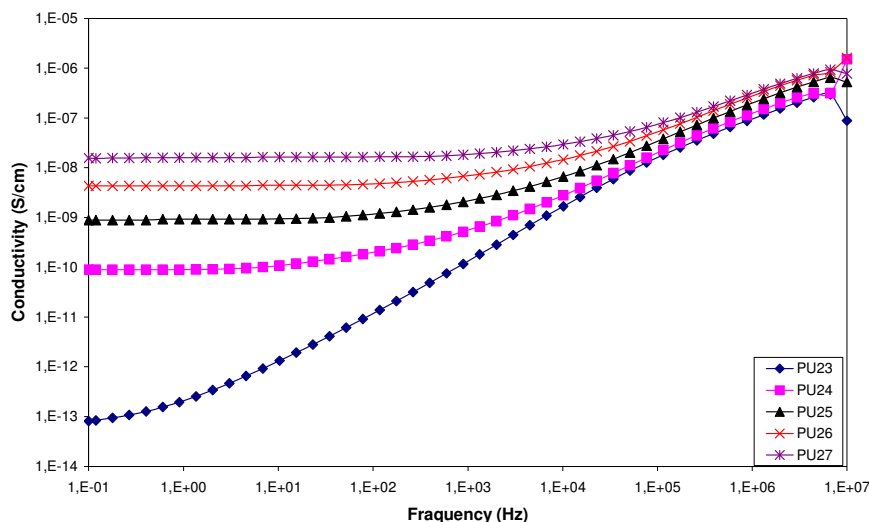
Appendix 2.4 TGA thermogram of crosslinked 58% epoxidized polyurethane with 10%wt (PU29), 18% wt (PU30), 28%wt (PU31), 35% (PU32), 43%wt (PU33) and without [thtdp]Cl (PU28).



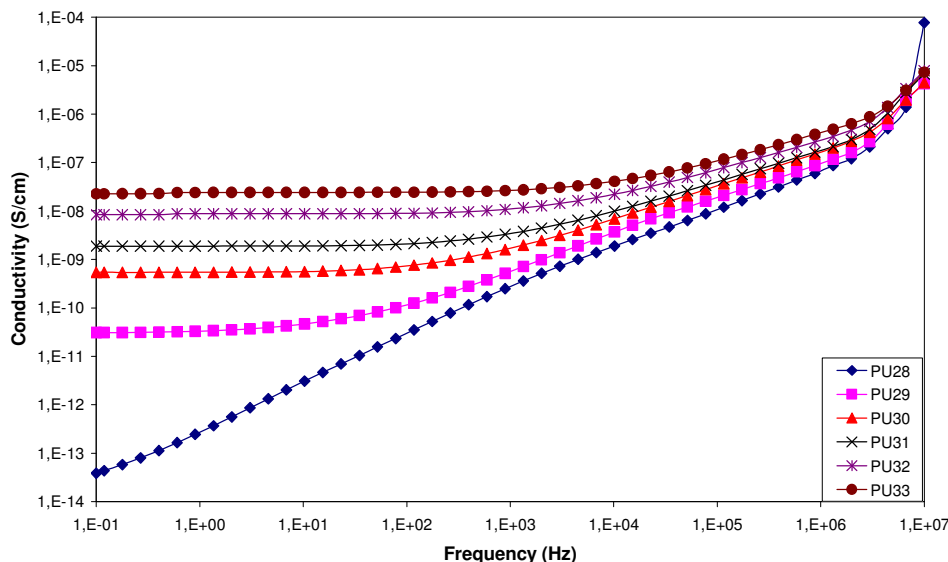
Appendix 2.5 TGA thermogram of crosslinked 80% epoxidized polyurethane with 18% wt (PU36), 32%wt (PU38), 50% (PU40), 59%wt (PU41) and without [thtdp]Cl (PU34).



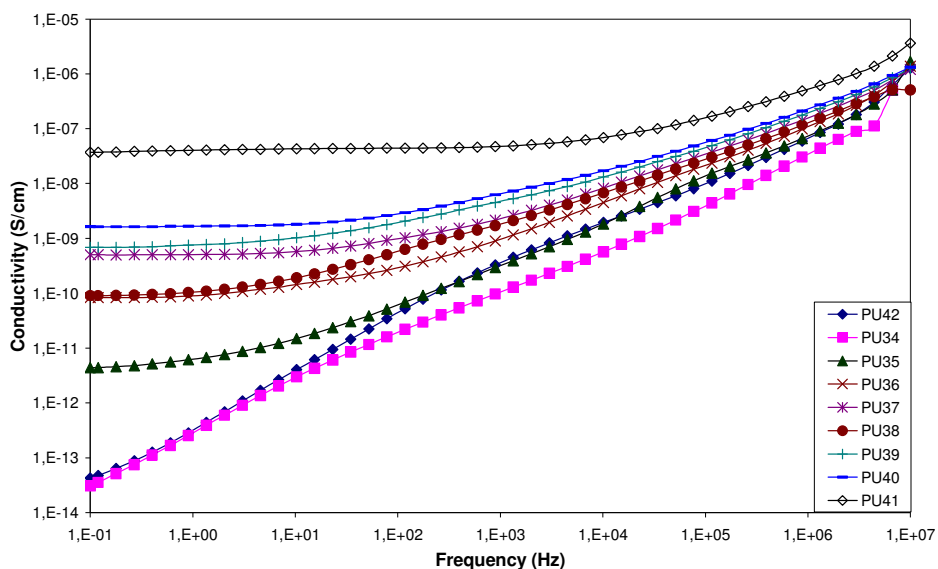
Appendix 2.6 Frequency dependence of conductivity of crosslinked 30% epoxidized polyurethane films with 0%wt (PU23), 11% wt. (PU24), 20% wt (PU25), 30%wt. (PU26) and 36% wt. (PU27) [thtdp]Cl at room temperature.



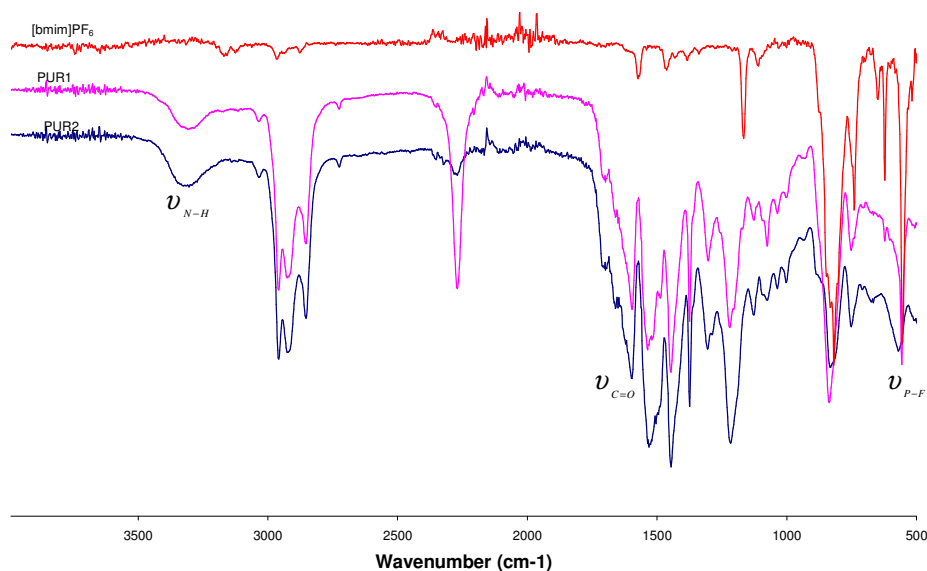
Appendix 2.7 Frequency dependence of conductivity of crosslinked 58% epoxidized polyurethane films with 0%wt (PU28), 10% wt. (PU29), 18% wt (PU30), 28%wt. (PU31), 35%wt. (PU32) and 43% wt. (PU33) [thtdp]Cl at room temperature.



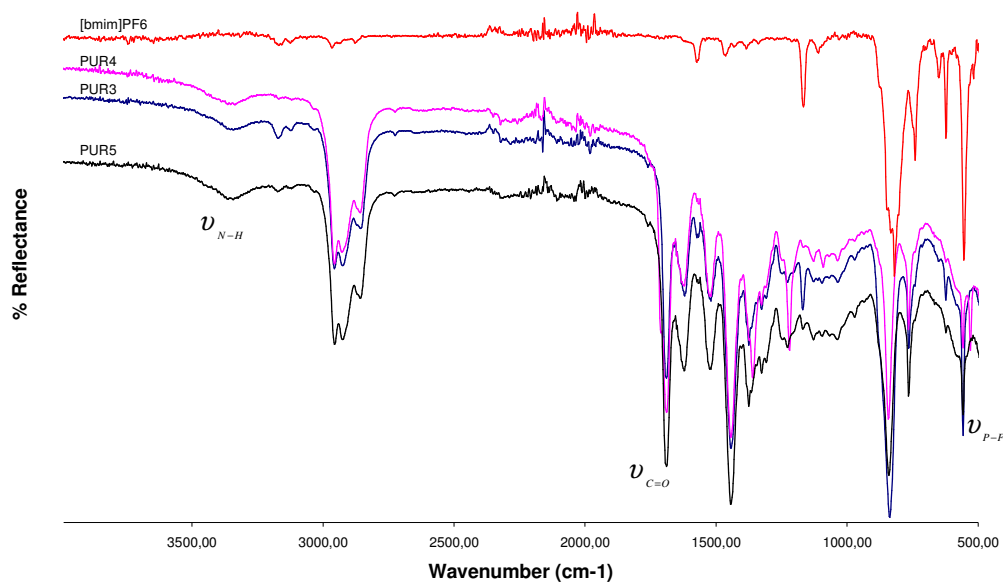
Appendix 2.8 Frequency dependence of conductivity of crosslinked 80% epoxidized polyurethane films with 0%wt (PU34), 9% wt. (PU35), 18% wt (PU36), 23%wt. (PU37), 32%wt. (PU38), 47%wt. (PU39), 50%wt (PU40), 59% wt. (PU41) [thtdp]Cl and .linear 80% epoxidized without [thtdp]Cl (PU42) at room temperature.



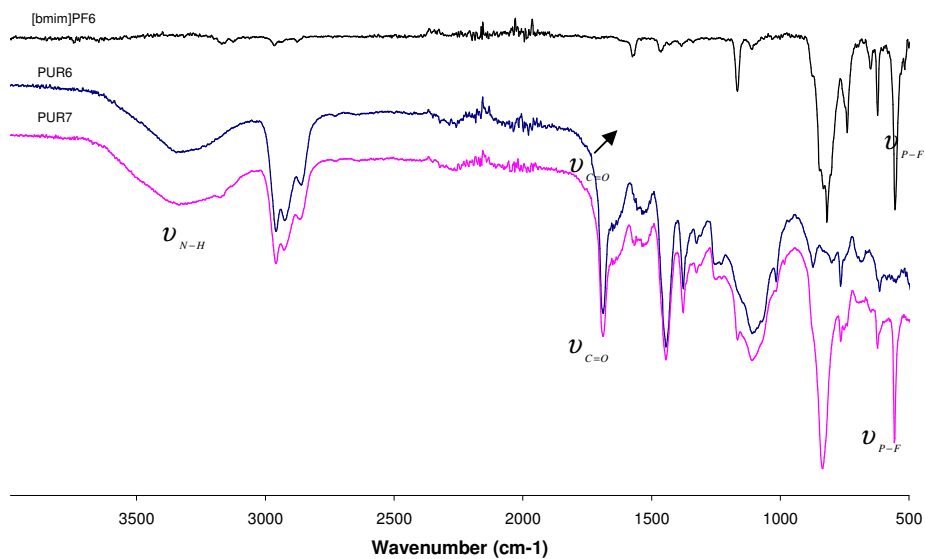
Appendix 2.9 FTIR spectrum using ATR mode of linear polyureas without ionic liquid (PUR1) and 10% wt [bmim]PF₆ (PUR2).



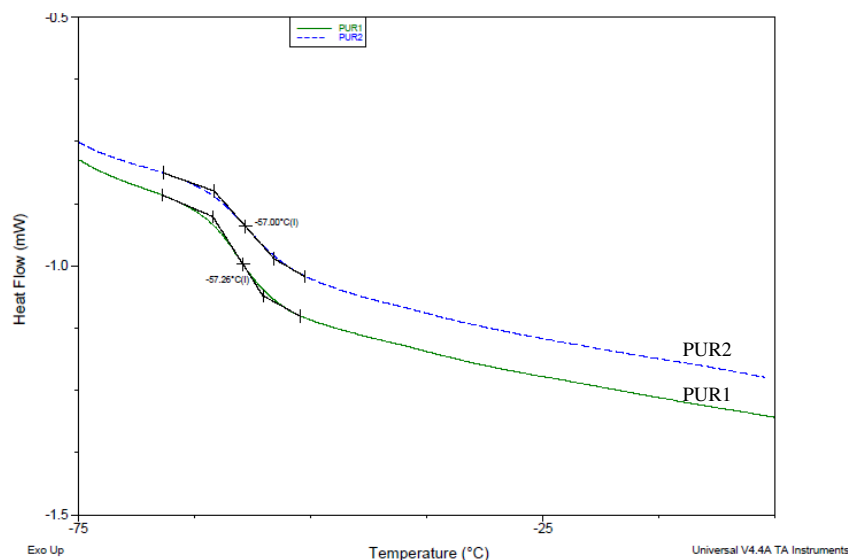
Appendix 2.10 FTIR spectrum using ATR mode of crosslinked non-epoxidized polyureas with 10%wt. (PUR3), 20% wt. (PUR4) and 25%wt. of [bmim]PF₆ (PUR5).



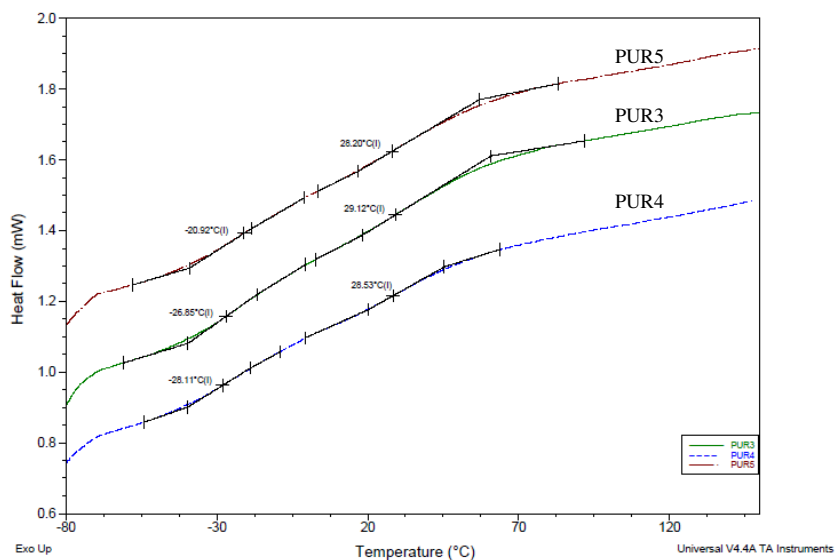
Appendix 2.11 FTIR spectrum using ATR mode of crosslinked epoxidized polyurea with 0%wt. (PUR6) and 20% wt. (PUR7).



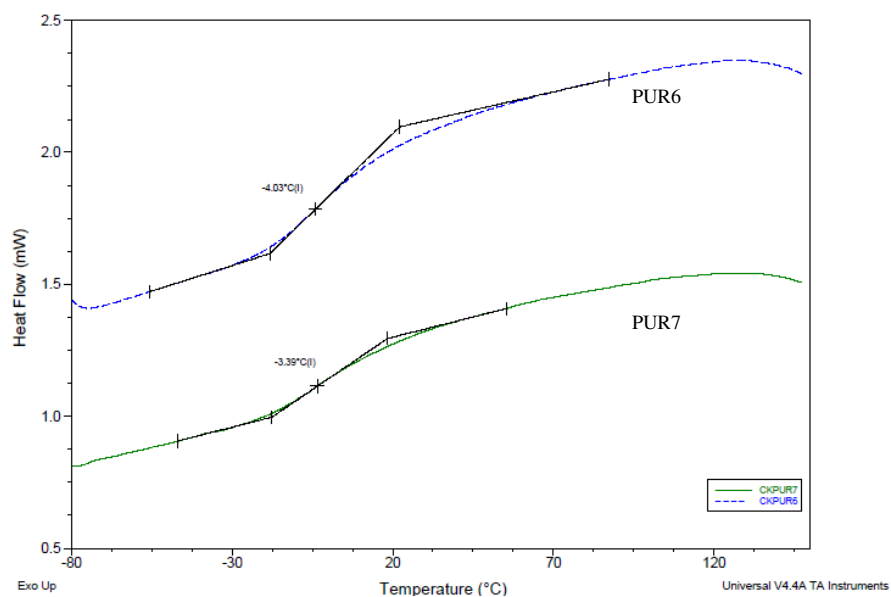
Appendix 2.12 DSC thermograms of linear non-epoxidized polyureas with 0% wt. (PUR1) and 10%wt. of [bmim]PF₆ (PUR2).



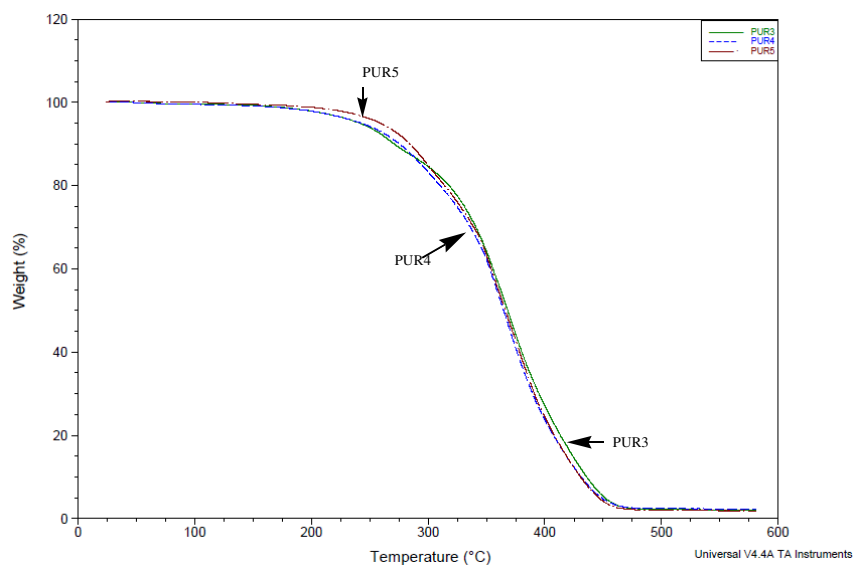
Appendix 2.13 DSC thermograms of crosslinked non-epoxidized polyureas with 10% wt. (PUR3), 20%wt. (PUR4) and 25%wt. [bmim]PF₆ (PUR5).



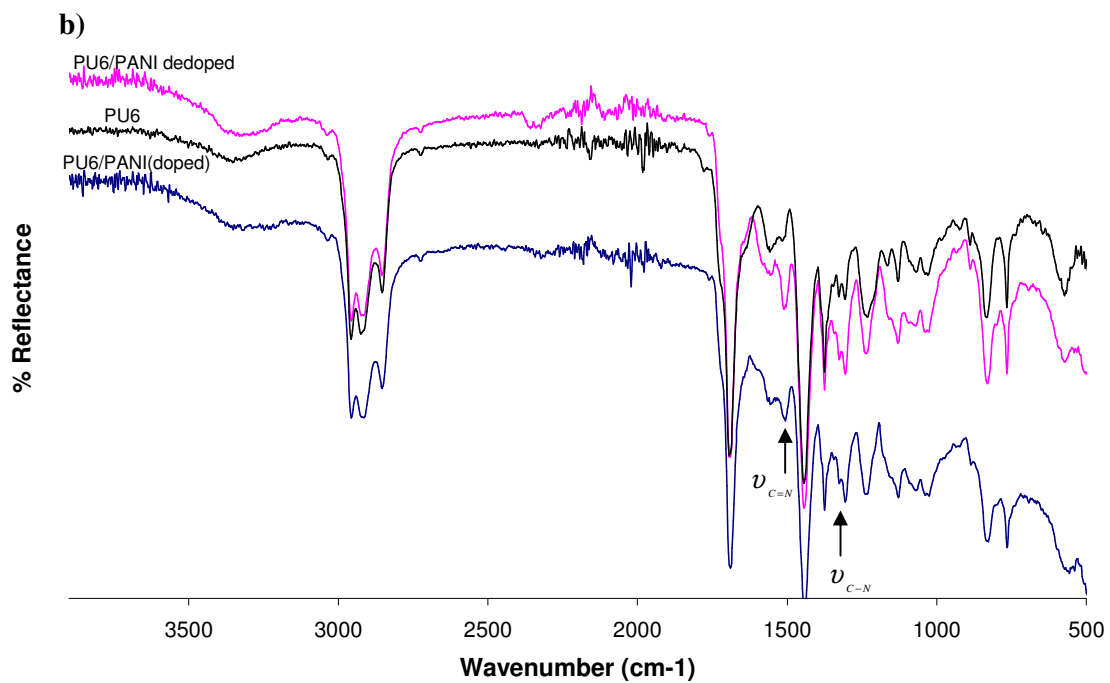
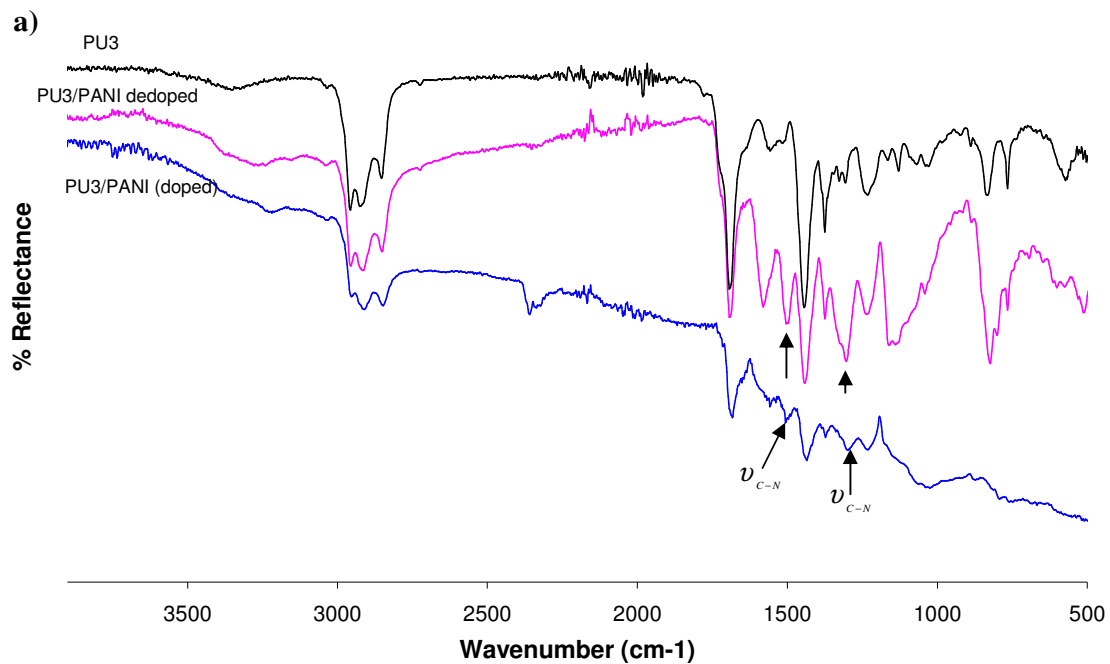
Appendix 2.14 DSC thermograms of crosslinked 54% epoxidized polyureas with 0% wt. (PUR6) and 20%wt. [bmim]PF₆ (PUR7).



Appendix 2.15 TGA thermograms of crosslinked non-epoxidized polyurea film with 10%wt (PUR3), 20%wt 5PUR4) and 25%wt. [bmim]PF₆ (PUR5).

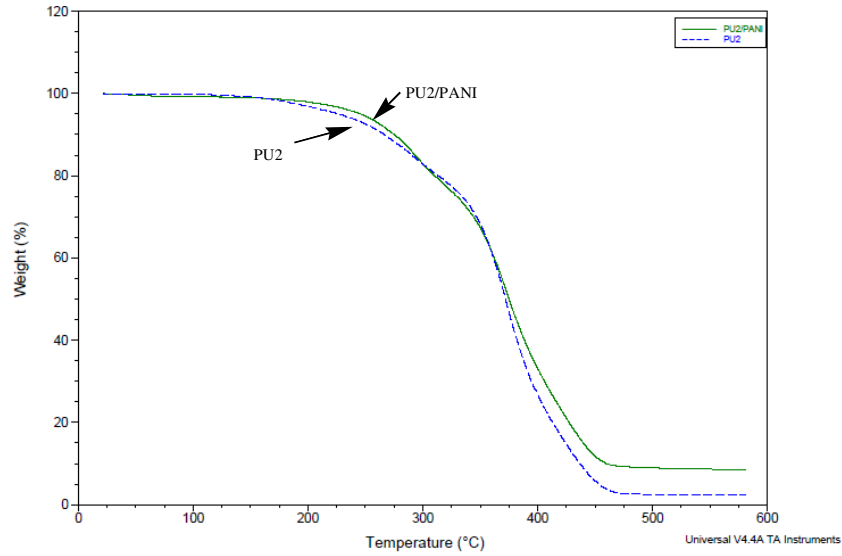


Appendix 2.16 FTIR of crosslinked PU/PANI composites; a) without (PU3/PANI) and b) with 10% wt [bmim]PF₆ (PU6/PANI).

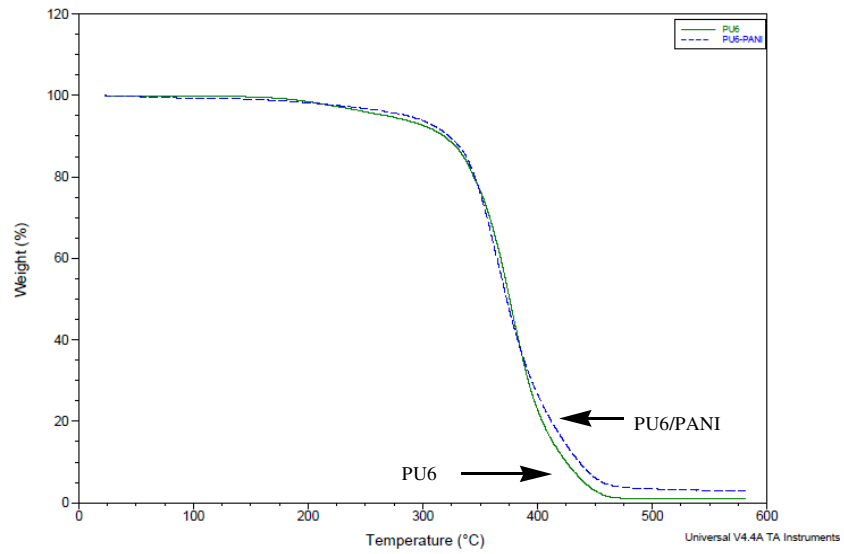


Appendix 2.17 TGA thermogram of PU/PANI composite with bmim]PF₆; a) linear (PU2/PANI); b) crosslinked (PU6/PANI).

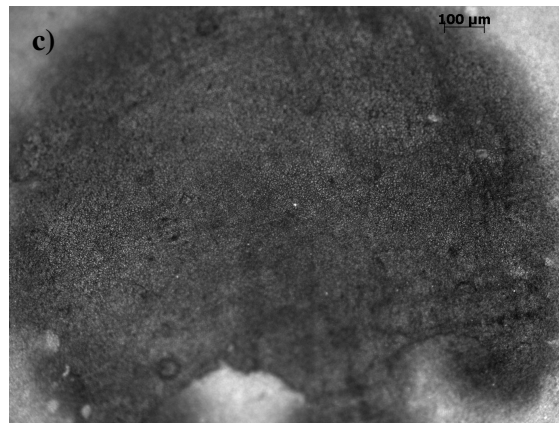
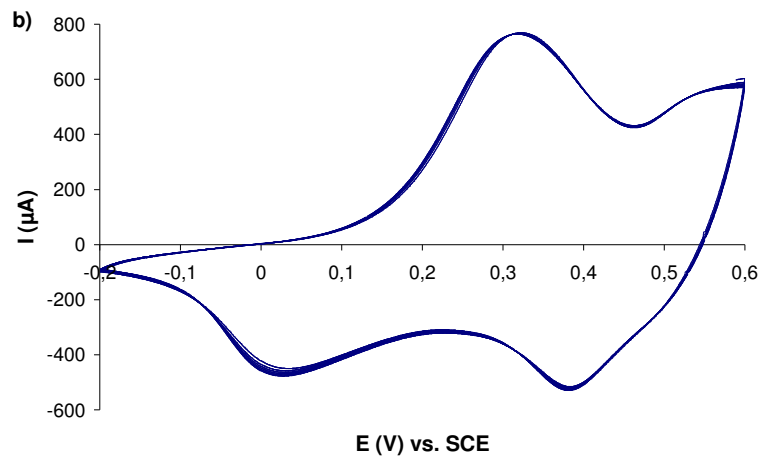
a)



b)

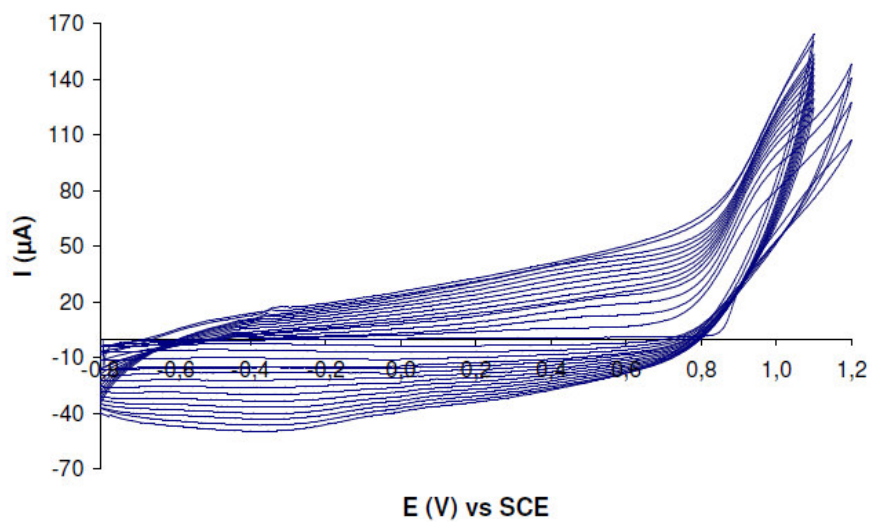


Appendix 2.18 Electropolymerization of PANI on linear hydrogenated PU film in 1.0 M HCl recorded on Pt electrode ($\varnothing = 1$ mm); a) Cyclic voltammograms of polymerization with scan rate 50 mV/s; b) Doped and dedoped curves of PANI on hydrogenated PU film with scan rate 50 mV/s, c) Optical microscopic image of PANI on PU film.

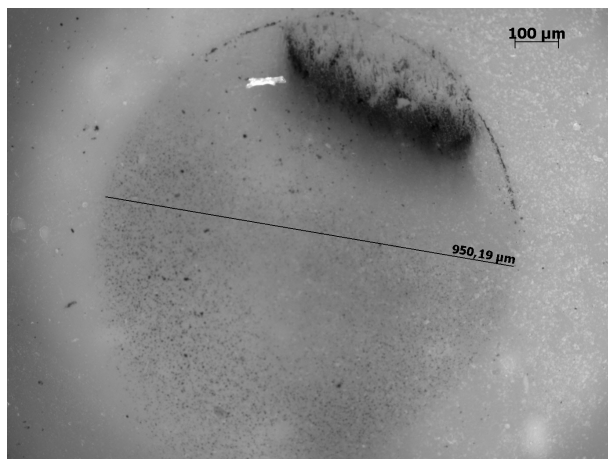


Appendix 2.19 a) Cyclic voltammogram of 35 % EDOT incorporated in linear PU film (PU1) in 0.5 M LiClO₄ recorded on Pt electrode ($\varnothing = 1$ mm). Scan rate of 50 mV/s; b) Optical microscopic image of film after electropolymerization.

a)

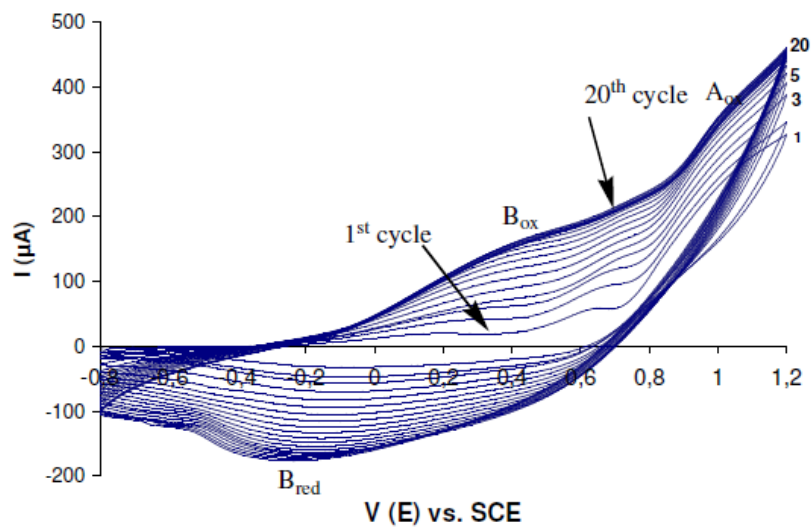


b)

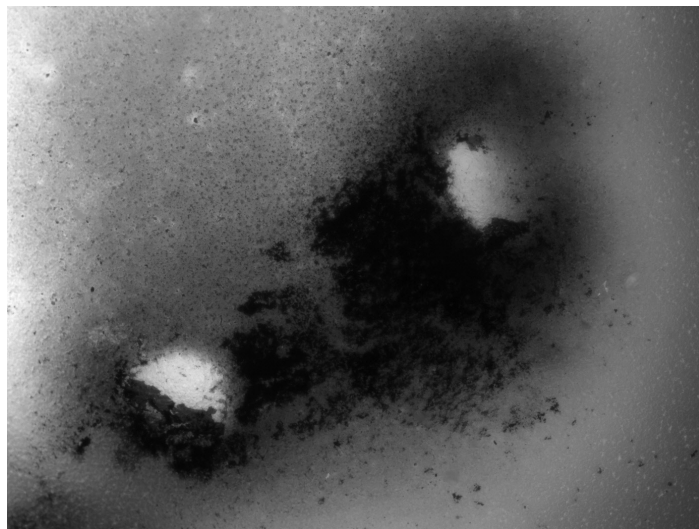


Appendix 2.20 a) Cyclic voltammogram of 35 % Py incorporated in linear PU film (PU1) in 0.5 M LiClO₄ recorded on Pt electrode ($\varnothing = 1$ mm). Scan rate of 50 mV/s; b) Optical microscopic image of film after electropolymerization.

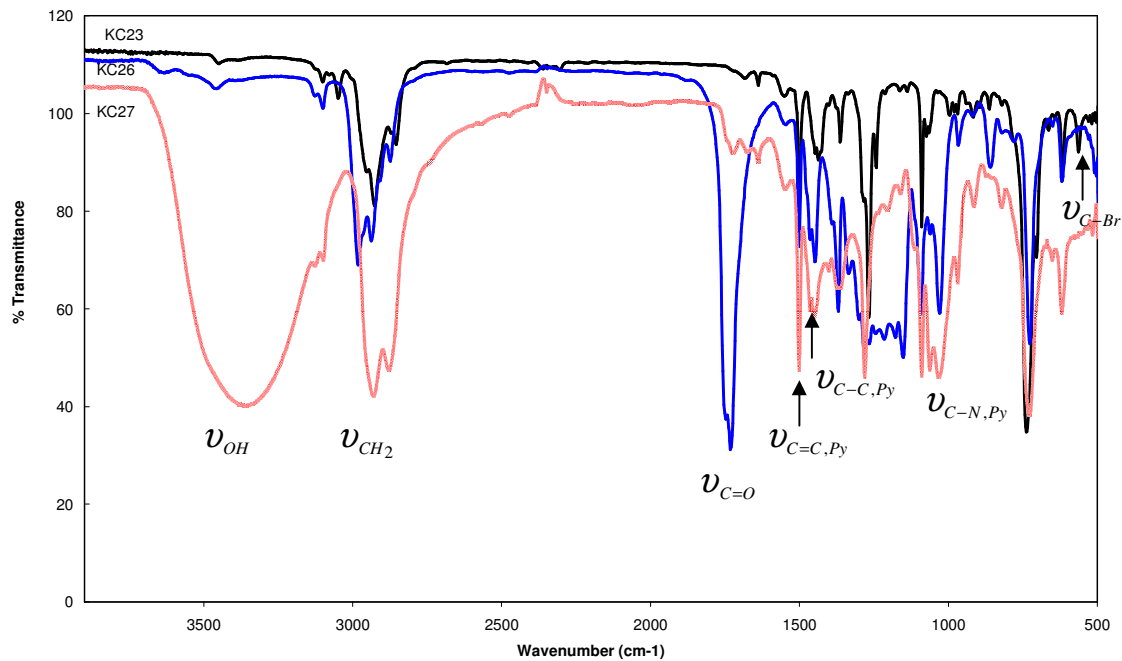
a)



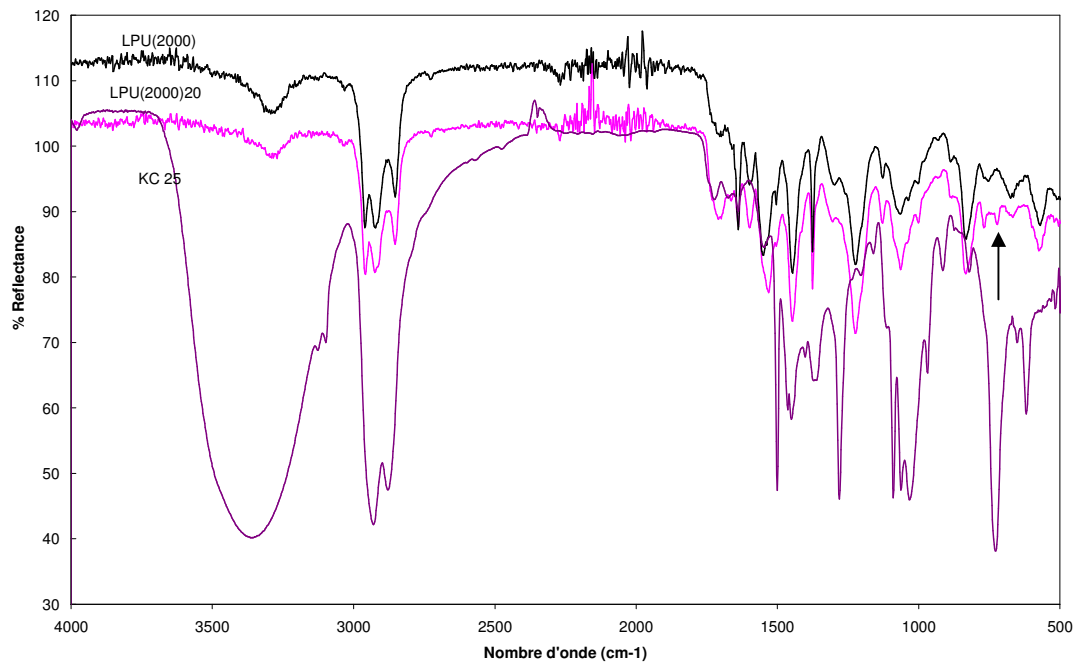
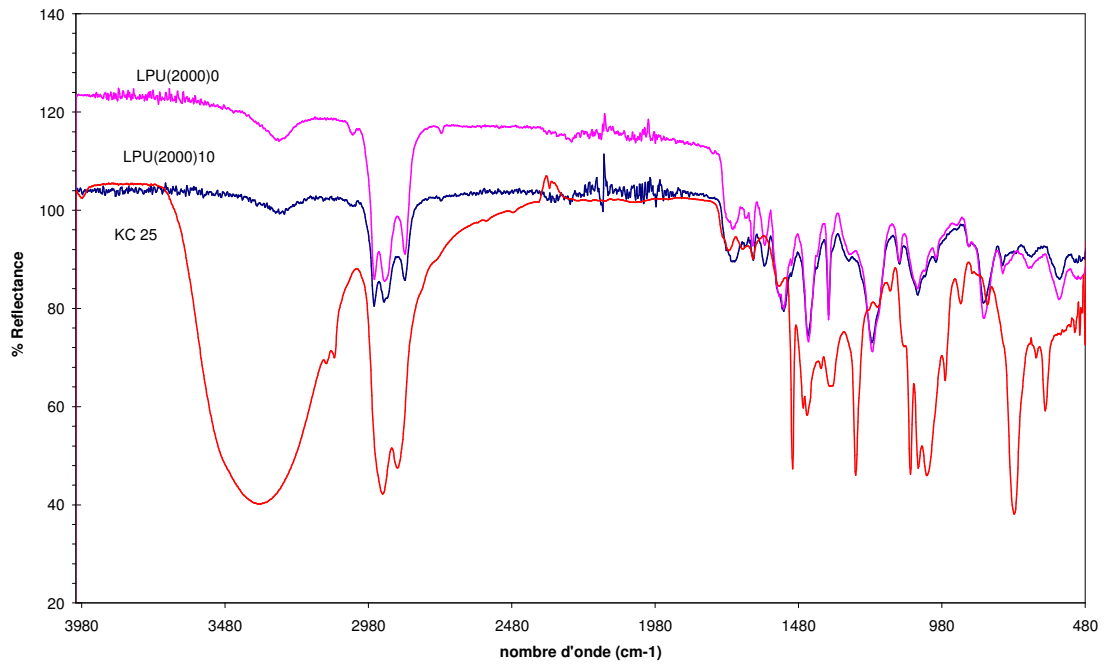
b)



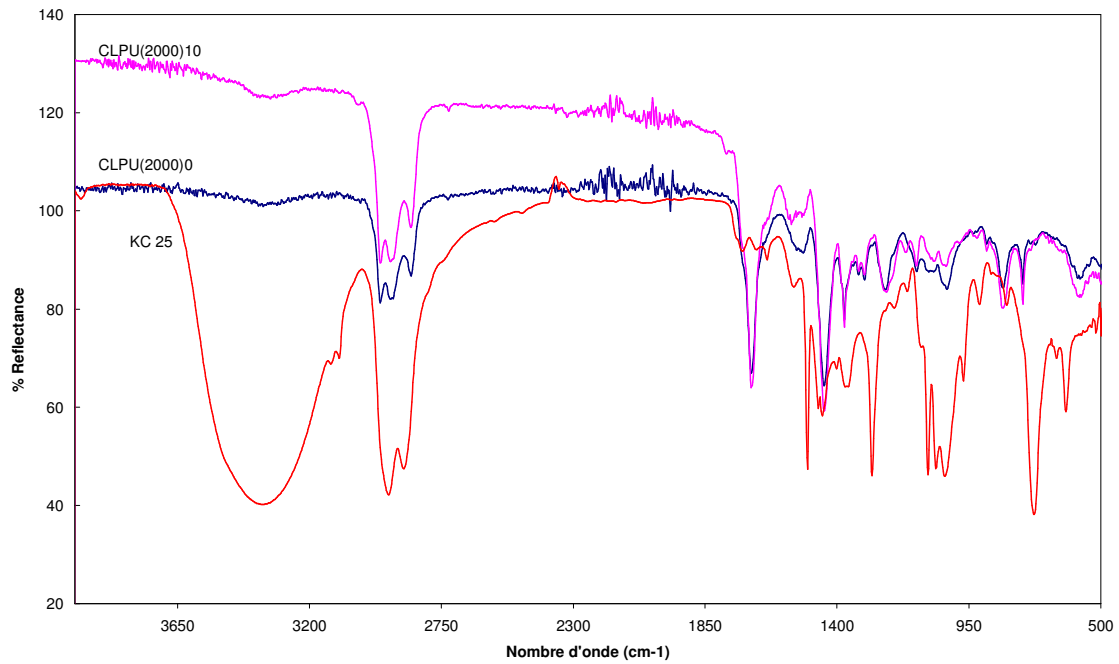
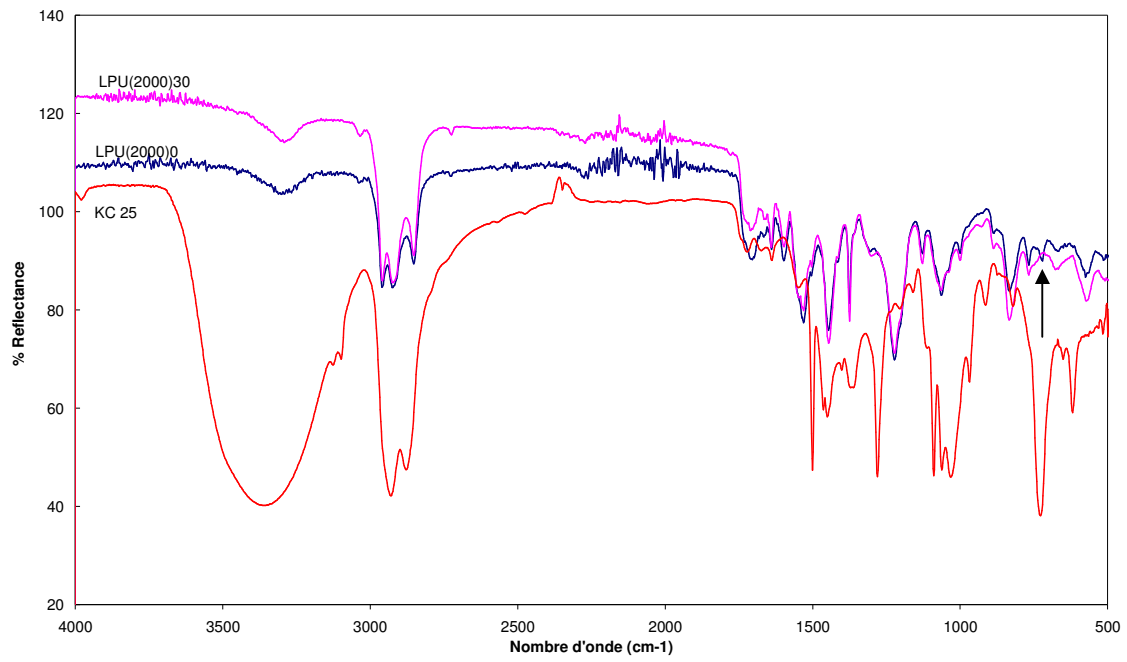
Appendix 3.1 FTIR spectrum of 1-(3-bromopropyl)-1*H*-pyrrole **9** (KC23), diethyl 2-(3-(1*H*-pyrrol-1-yl)propyl)malonate **10** (KC26) and 2-(3-(1*H*-pyrrol-1-yl)propyl)propane-1,3-diol **11** (KC27) using transmission mode.



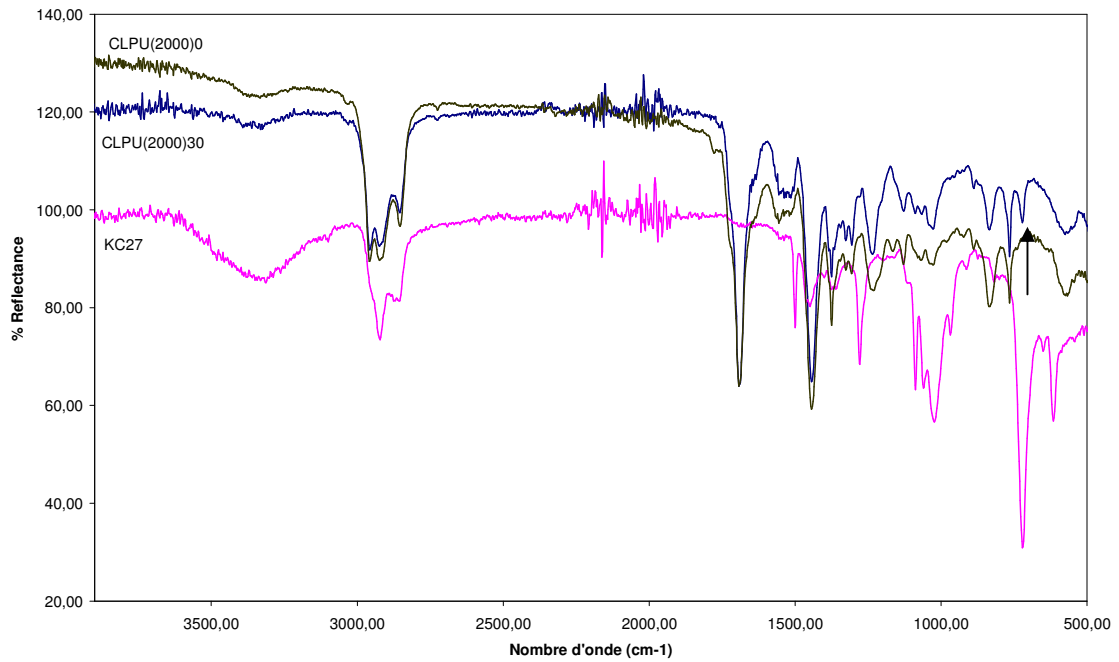
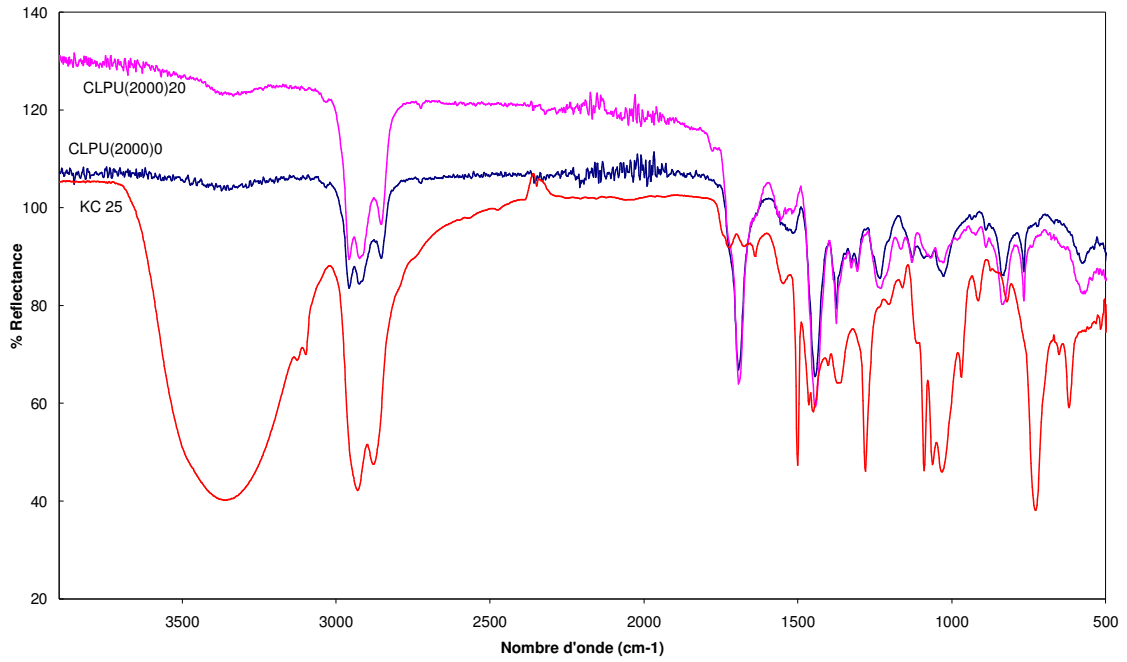
Appendix 3.2 FTIR spectrum of linear and crosslinked polyurethanes (\overline{M}_n PI \approx 1000 and 2000) with the different percentages of chain extender compared with a polyurethane without chain extender using ATR mode.



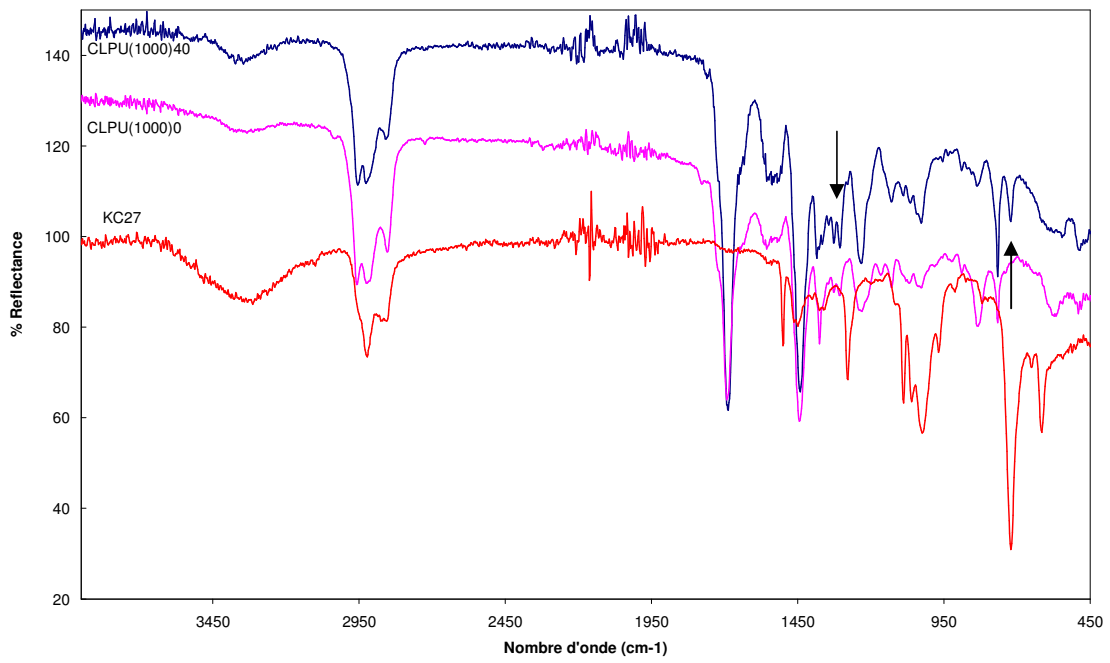
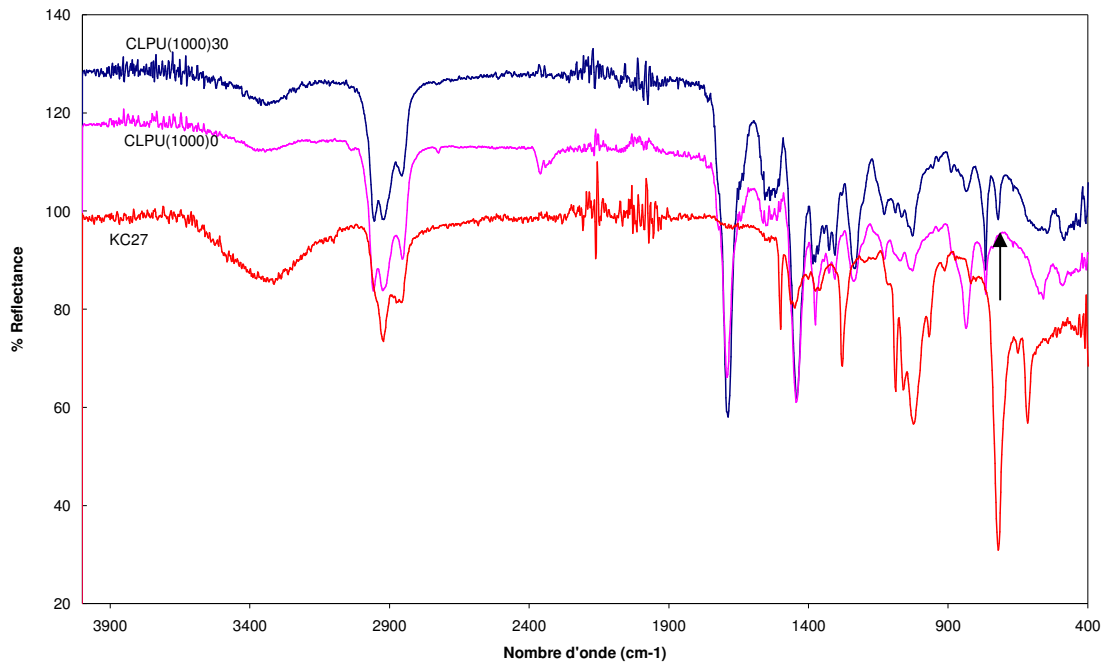
Appendix 3.2 (cont.)



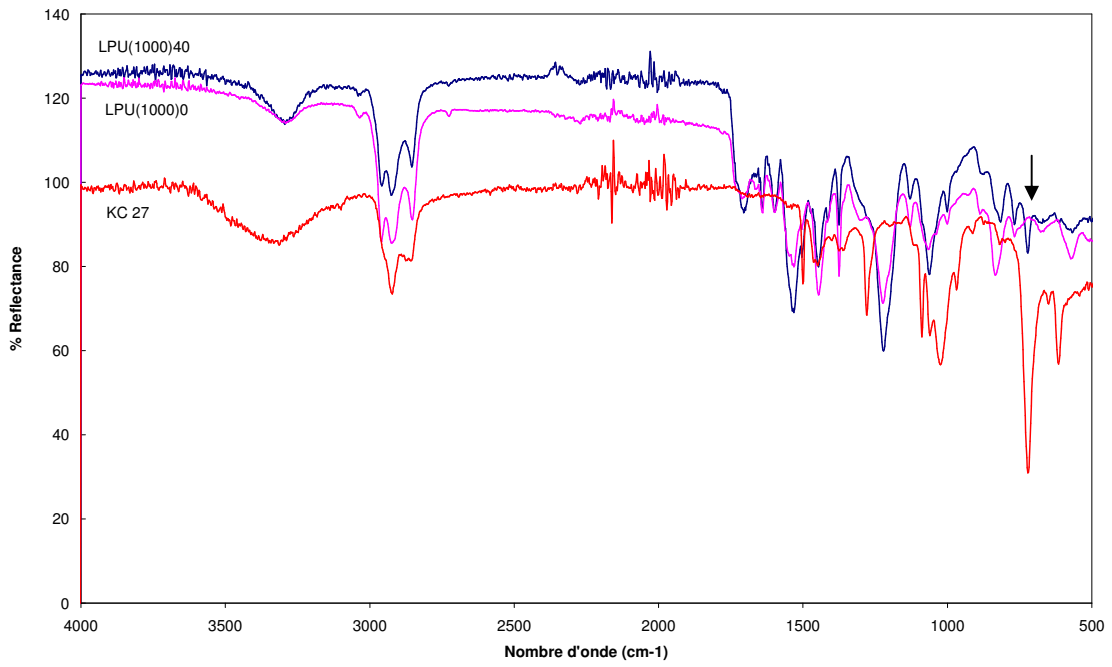
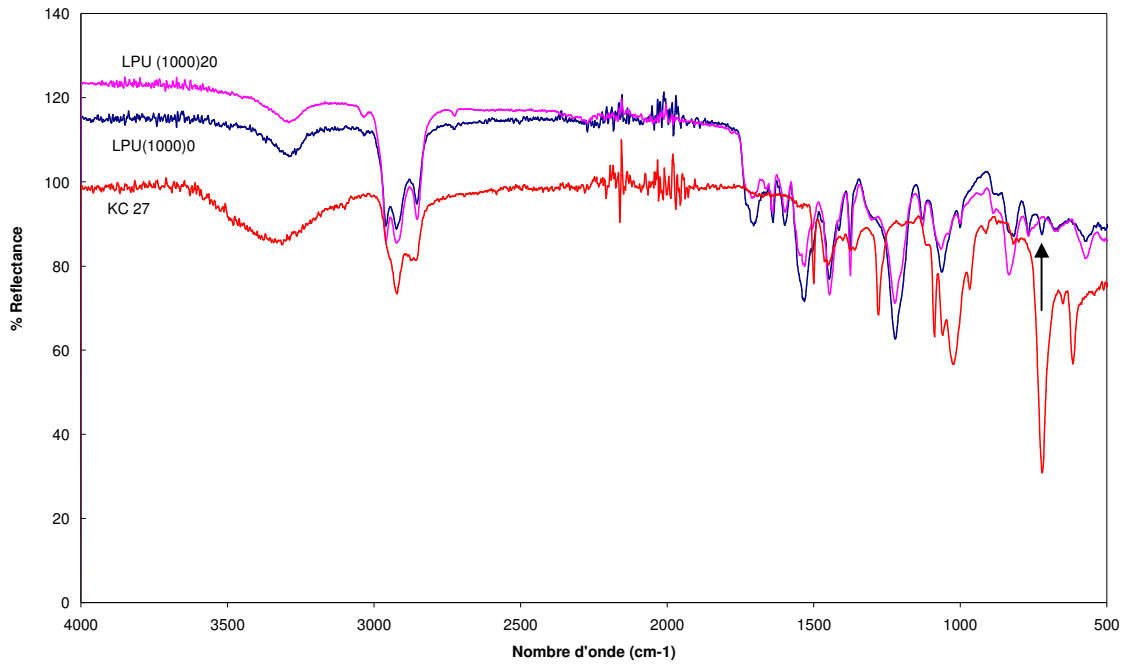
Appendix 3.2 (cont.)



Appendix 3.2 (cont.)

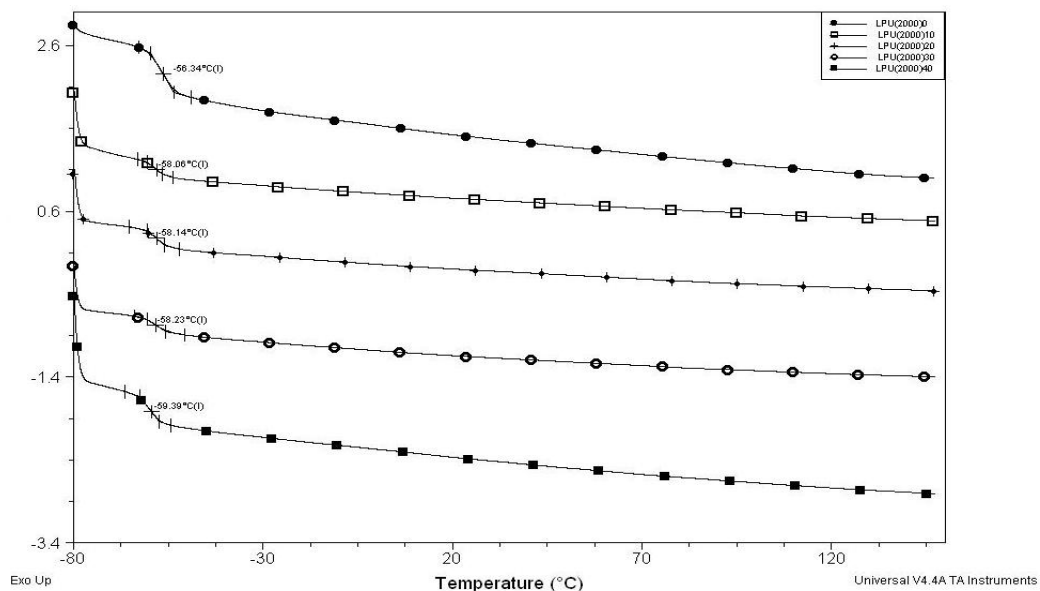


Appendix 3.2 (cont.)

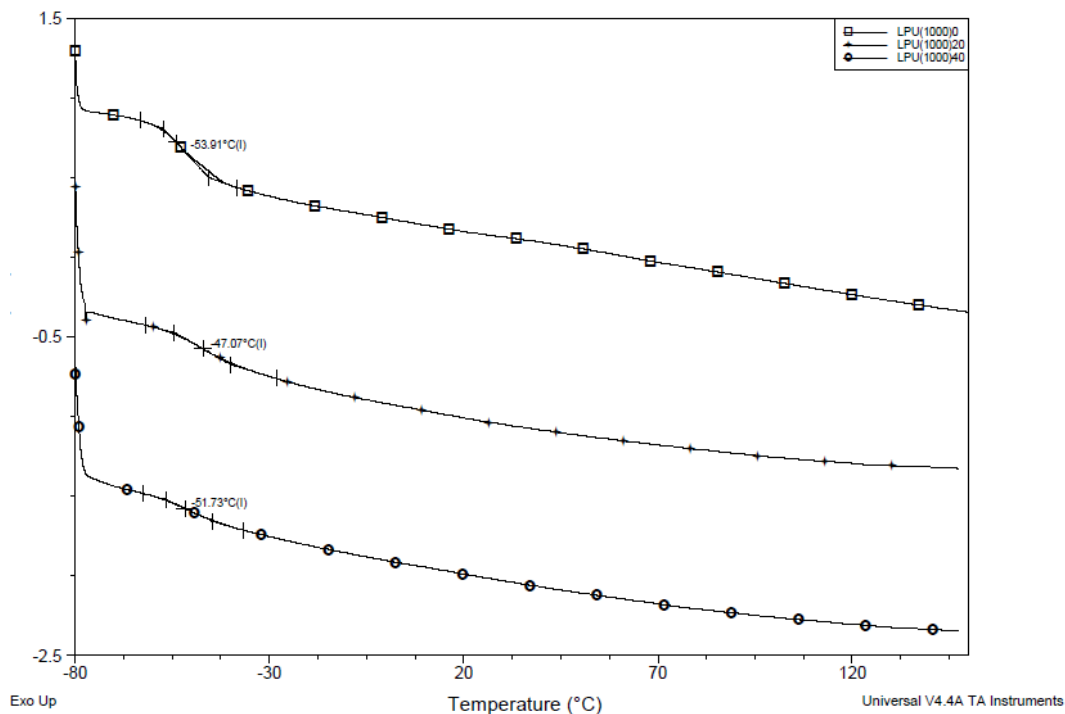


*KC 25 and KC27 is the same structure; FTIR, KC25 using transmission mode.

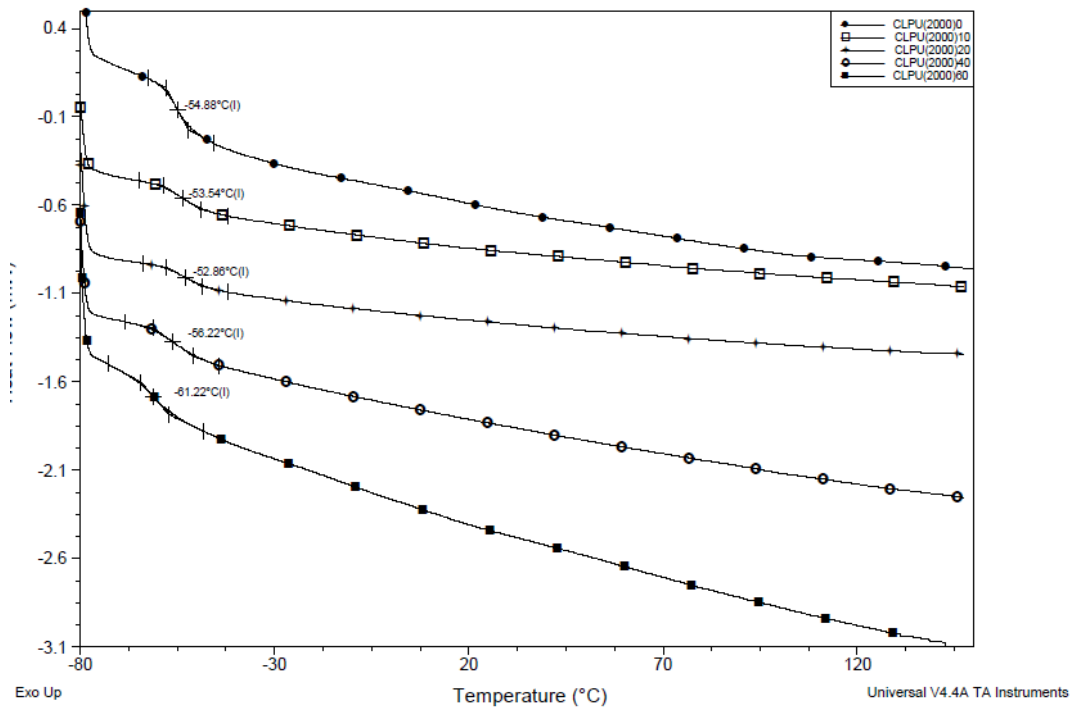
Appendix 3.3 DSC thermograms of linear polyurethanes (\overline{M}_n PI \approx 2000 g/mol) with different percentages of chain extender.



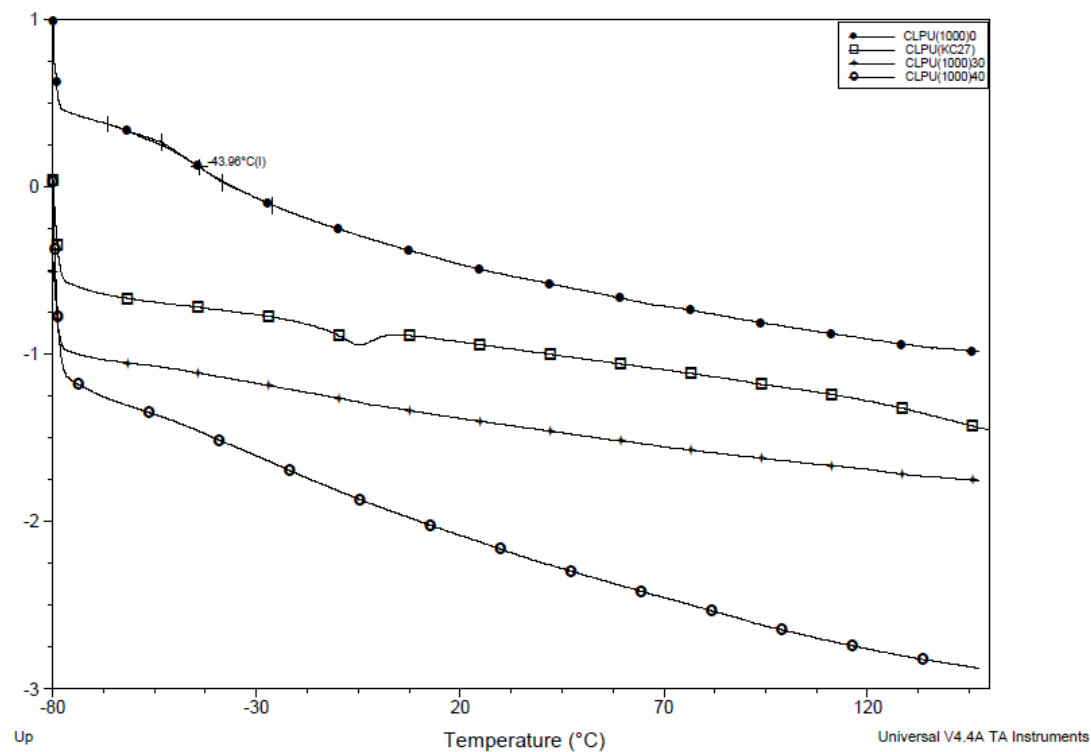
Appendix 3.4 DSC thermograms of linear polyurethanes (\overline{M}_n PI \approx 1000 g/mol) with different percentages of chain extender.



Appendix 3.5 DSC thermograms of crosslinked polyurethanes (\overline{M}_n PI \approx 2000 g/mol) with different percentages of chain extender.



Appendix 3.6 DSC thermograms of crosslinked polyurethanes (\overline{M}_n PI \approx 1000 g/mol) with different percentages of chain extender.



Elaboration of electronic conductor composite materials; study of physical and electrical properties.

Abstract:

The hydroxytelechelic oligoisoprene was synthesized according to well-controlled degradation procedure which has been recently developed in our laboratory, followed by the reduction of carbonyltelechelic cis-1,4-polyisoprene (CTPI) into hydroxytelechelic cis-1,4-polyisoprene (HTPI). Telechelic oligomers were characterized by FTIR, ^1H -, ^{13}C -NMR and SEC. Linear and crosslinked polyurethane films were synthesized from hydroxytelechelic cis-1,4-polyisoprene and diisocyanates or triisocyanates using dibutyltin dilaurate as catalyst. The modification of main chain by epoxidation or hydrogenation allows us to modify the properties of films.

In this work, we have studied the possibility to use these kinds of polyurethanes as the polyelectrolyte matrix. The incorporation of ionic liquids, 1-butyl-3-methylimidazolium hexafluorophosphate and trihexyltetradecylphosphonium chloride, in polymer films was done and the conductivity of films was measured by dielectric relaxation spectroscopy. The presence of epoxidation in the main chain of polyurethane allows us to incorporate more amount of ionic liquid in film. Type of ionic liquid has an effect on the compatibility and properties of polyurethane films. The thermal properties of films were determined by DSC and TGA.

Moreover, the polyurethane films were used as supporting matrix in an electropolymerization of a conducting polymer. By this method, we can prepare the precise polyaniline spot according to the electrode on the polyurethane film support.

In addition, new type chain extender containing pyrrole monomer unit was synthesized. Its structure was confirmed by NMR, mass spectroscopy and elemental analysis. Polyurethanes using this pyrrole derivative chain extender were prepared and the thermal properties were investigated. Finally, the electropolymerization of pyrrole unit in polyurethane structure was performed.

Keywords :

Cis-1,4-polyisoprene, telechelic oligomers, polyurethane, thermal properties, ionic liquids, conductivity, electropolymerization, polyaniline, pyrrole derivative chain extender.